Doctoral theses at NTNU, 2016:185

Clara Good

Photovoltaic-thermal systems for zero emission residential buildings

ISBN 978-82-326-1708-1 (printed ver.)
ISBN 978-82-326-1709-8 (electronic ver.)
ISSN 1503-8181

NTNU
Norwegian University of
Science and Technology

NTNU
Norwegian University of
Science and Technology
Thesis for the Degree of
Philosophiae Doctor
Faculty of Architecture and Fine Art
Department of Architectural Design, History and
Technology

Doctoral theses at NTNU, 2016:185

NTNU
Norwegian University of
Science and Technology

Clara Good

Photovoltaic-thermal systems for zero emission residential buildings

Thesis for the Degree of Philosophiae Doctor

Trondheim, June 2016

Norwegian University of Science and Technology
Faculty of Architecture and Fine Art
Department of Architectural Design, History and Technology

NTNU
Norwegian University of
Science and Technology

NTNU
Norwegian University of Science and Technology

Thesis for the Degree of Philosophiae Doctor

Faculty of Architecture and Fine Art
Department of Architectural Design, History and Technology

ISBN 978-82-326-1708-1 (printed ver.)
ISBN 978-82-326-1709-8 (electronic ver.)
ISSN 1503-8181

Doctoral theses at NTNU, 2016:185

Printed by NTNU Grafisk senter

Summary

This thesis concerns the use of solar energy in energy efficient buildings. More precisely, the topic is photovoltaic-thermal (PV/T) solar energy systems, and how these can be used to provide renewable energy in zero emission buildings. PV/T modules are a hybrid between photovoltaic (PV) modules and solar thermal collectors, and therefore generate electricity and thermal energy simultaneously. The objective of the thesis was to investigate the potential of PV/T systems to minimize the life cycle greenhouse gas emissions of a residential building.

The building sector accounts for around one third of the global energy use and about half of the electricity use, and is therefore a key area to focus on in the effort to mitigate climate change and to create more sustainable societies in the future. The environmental impact of buildings need to be lowered by reducing the energy demand during construction and operation, but also by replacing polluting energy sources with renewable ones. The European Union has demanded of its member states that all new buildings shall be nearly zero energy buildings by 2020.

Solar energy is well-suited to use in buildings, and can supply electricity, lighting, heating, and cooling. Once installed, a solar energy system supplies energy without pollution, is silent, have few or no moving parts, and can also be integrated into the building itself. In order to do investigate how PV/T systems can best be used in buildings to minimize life cycle emissions, the systems have been studied both in terms of energy performance and in terms of greenhouse gas emissions.

The main research method in this thesis has been simulation of solar energy systems in buildings. Using simulations, PV/T systems have been compared to other solar energy systems with separate PV modules and solar thermal collectors. The simulation studies were performed in the simulation programs Polysun and PVsyst, and were based on commercial solar energy products available on the current market. The use of heat pumps, air-source and ground-source, in combination with solar energy systems was also studied.

Two case buildings, the ZEB residential concept and the Living Lab, have been used in the simulation studies. The buildings are two of the pilot buildings of the Norwegian Research Centre for Zero Emission Buildings (the ZEB Centre). Both buildings are single family residential buildings located in Central or Southern Norway, and are designed to meet the Norwegian passive house requirements.

The embodied emissions of the solar energy systems were determined using elements of life cycle assessments (LCA). A review of previous research found few studies of the environmental impact of PV/T modules, especially using industrially produced modules. The embodied emissions of such a PV/T module was therefore determined in this thesis, based on a combination of data from databases and information from module producers. The embodied emissions of the case buildings and the other solar energy systems studied were determined using a combination of databases and previously published research in the ZEB Centre.

The results show that PV/T systems can be a good renewable energy solution for energy efficient buildings, but that their performance is highly dependent on how the system is designed and what control strategies are used. The simulations showed that the systems with PV/T modules typically had higher primary output per unit area than the systems with separate PV modules and solar energy collectors, but that this also depended on how the solar energy systems were designed. However, due to a higher use of electricity to run e.g. circulation pumps, the energy balance of the whole building was not improved compared to systems with separate solar technologies.

The thermal output of PV/T systems are typically of a lower temperature than that of solar thermal collectors, and the technology should therefore be used in energy systems where low temperature heat is valuable. The combination of PV/T modules and ground source heat pumps showed potential to increase the efficiency of a building's energy system compared to other solar energy technologies, especially when PV/T modules were installed on the source side of the heat pump. However, the studies also showed that it is a complex task to design such as system, and the energy demand required to operate it can easily be higher than the gains. No clear benefit from cooling of PV/T modules were found in the simulations in this thesis.

In terms of emissions, no benefit of PV/T modules was found in the case studies. The generic PV/T module which was modelled had around 30% higher embodied emissions than a comparable PV module, and the increase in energy output from the PV/T module was not high enough to allow for this. It was in general found to be quite difficult to reach a net zero emission balance for a building, at least if embodied emissions of materials were included. A large solar energy installation was necessary to reach a balance, which sometimes resulted in non-optimal system designs. Nearly zero emission buildings, or zero emission neighbourhoods, might be a more feasible goal for new buildings.

Even though all of the studied solar energy systems were found to be the source of a high share of the total embodied emissions of a building, they also contributed to a large reduction in greenhouse gas emissions over their lifetime. That is, solar energy installations, PV/T systems included, contribute to reduced emissions also in a Scandinavian climate.

Acknowledgements

This PhD project has been performed within the Joint Research Centre (JRC) on Sustainable Energy between NTNU and Shanghai Jiao Tong University (SJTU) in China. I would like to thank the JRC for giving me this opportunity and supporting me throughout my project. I was also fortunate to be given the opportunity to visit SJTU on two occasions: once during the 2013 summer school on sustainable energy and once as a visiting PhD candidate. I would like to thank our Chinese colleagues Yanjun Dai, Tianshu Ge, Yong Li, and Rushu Wang for their help along the way. A special thanks to Jinfeng Chen, without whom I probably would not even have survived the first week on campus in Shanghai.

I would also like to thank the Research Centre on Zero Emission Buildings (the ZEB Centre) for giving me continuous support during my whole PhD project, both scientifically and financially. A significant part of my research builds on previous research in the ZEB Centre, and my research would not have been possible without this valuable resource. I have also had the pleasure of working with some of the excellent researchers in the ZEB Centre.

There are many people without whom this thesis would never have been finished. First and foremost, I want to thank Anne Grete Hestnes for her constant support, help, and encouragement. You have let me do things my own way, but always kept me from losing focus, and I have been very lucky to have you as my supervisor. Thank you also to my co-supervisors Annemie Wyckmans, for introducing me to the international research community, and Inger Andresen, for always keeping me on the right track.

I would like to thank Torhildur Kristjansdottir for the many interesting discussions and for guiding me through the LCA jungle, Laurent Georges for helping me with the Polyun model, and Igor Sartori for sharing his expertise on zero emission buildings. Thank you also to my other co-authors: Aoife Houlihan Wiberg, Reidun Dahl Schlanbusch, Marianne Inman, Gabriele Lobaccaro, Siri Hårklau, Francesco Goia, and Jinfeng Chen. It has been a pleasure working with you, and I hope to get the chance again in the future.

Johan Ahlgren at Energiförbättring Väst AB deserves a special mention for taking the time to show me the PV/T installations in Sweden.

I would also like to thank all my colleagues at NTNU and the ZEB Centre. A special thank you to Brit Gullvåg, Katrine Peck Sze Lim, and Maja Todoroska for taking care of anything and everything. I also want to thank all the PhD candidates from the 8th floor lunch room for making the workdays so much more fun, I will miss you all!

Last but not least, I want to thank my family and friends for helping and supporting me along the way. Finally, thank you Tobias, my love and best friend, for all your help and encouragement (and criticism). I could not have done it without you.

Contents

List of figures

List of tables

Nomenclature and abbreviations

Nomenclature

a_1	W/m^2K	first order heat transfer coefficient
a_2	W/m^2K^2	second order heat transfer coefficient
A_c	m^2	collector gross area
A_{fl}	m^2	heated floor area
A_{PV}	m^2	PV module area
C_p	J/kg K	specific heat capacity of heat transfer medium
E_{net}	kWh	annual net energy
E_{exp}	kWh	exported energy
E_{del}	kWh	delivered energy
$E_{exp,tmp}$	kWh	temporary exported and later reimported energy
E_{load}	kWh	annual energy load
E_{gen}	kWh	annual energy generation
FF	-	fill factor
f_{GHG}	kg CO_2	greenhouse gas emission factor
f_{grid}	-	grid interaction index
f_{load}	-	load match index
f_P	-	primary energy factor
F_R	-	collector heat removal factor
G	W/m^2	irradiance
$GWP100a$	$kgCO_{2eq}$	global warming potential at 100 years
GHG_{net}	$kgCO_{2eq}$	annual net greenhouse gas emissions
I_{sc}	A	short circuit current
P	W	power
P_{max}	W	power at maximum power point (of PV cell or module)
Q	kWh	thermal energy
$\dot{Q}$	W	thermal power
SPF	-	seasonal performance factor of a heat pump
SPF_{sys}	-	seasonal performance factor of an energy system
T_a	°C	ambient temperature
T_i	°C	collector inlet temperature
T_m	°C	mean collector temperature
T_o	°C	collector outlet temperature
U_L	W/m^2K	collector heat loss coefficient
V_{oc}	V	open circuit voltage
α	-	absorptance
τ	-	transmittance

Subscripts for energy balance calculations, in addition to the nomenclature listed above.

del	delivered
el	electricity
exp	exported
gen	generated
grid	to/from the grid
i	energy carrier i
load	load
net	net
th	thermal
tmp	temporary exported and later reimported
u	useful

Abbreviations

AM	air mass (spectrum)
CAD	computer aided design
COP	coefficient of performance
DHW	domestic hot water
EPBD	Energy Performance of Buildings Directive
GHG	greenhouse gas
GPBT	greenhouse gas payback time
GROI	greenhouse gas return on investment
GWP	global warming potential
IEA	International Energy Agency
IPCC	Intergovernmental Panel on Climate Change
SF	solar fraction
SPF	seasonal performance factor
STC	standard test conditions
ZEB	zero energy building or zero emission building
The ZEB Centre	The Norwegian Research Centre on Zero Emission Buildings

Chapter 1: Introduction

1.1 Introduction

This thesis concerns the use of solar energy in energy efficient buildings. More precisely, the topic is photovoltaic-thermal (PV/T) solar energy systems, and how these can be used to provide renewable energy in zero emission buildings.

PV/T modules are a hybrid between photovoltaic (PV) modules, which generate electricity, and solar thermal collectors, which generate heat. PV/T modules therefore generate energy in two forms (electricity and thermal energy) simultaneously. As a result of this, the planning and installation of such systems can be more complex than that of separate PV or solar thermal systems. Even though a PV/T module is a hybrid of two technologies, the combined characteristics are different from that of the two parts. It therefore needs to be treated as a complete technology in itself, and practices or principles that apply to the separate technologies cannot be used directly when working with the design of PV/T systems.

There are several types of PV/T modules and systems, but the focus of the work presented in this thesis is flat-plate PV/T modules with a liquid heat transfer medium. This type of PV/T technology is the one that is most similar to standard PV modules and flat plate solar collectors used today. The objective of the thesis has not been to develop new technologies or solutions, but to evaluate how existing technology can be used in the most efficient way. The decision to focus on flat plate PV/T is based on the maturity of this technology relative to other PV/T technologies, and its similarity to existing solar energy systems in Europe.

The specific focus of the work presented in this thesis is the use of PV/T technology in zero emission buildings. In such a building, a zero emission balance is reached between greenhouse gas emissions that are associated with the construction, operation, and demolition of the building on one side, and on the other side greenhouse gas emissions that are avoided by the use of locally generated renewable energy instead of more polluting forms of energy. In order to calculate the emission balance, it is necessary to perform a detailed analysis of the environmental impact of the building, including the materials and construction as well as the use phase. In this thesis, the focus is on greenhouse gas emissions, measured in carbon dioxide equivalents (CO_{2eq}).

In addition to the analysis of the building itself, or rather as a part of it, it is necessary to perform an environmental impact analysis of the energy system. Solar energy systems, in particular those using silicon solar cells, are relatively energy-demanding to produce, and therefore have a high environmental impact in terms of embodied emissions. There is a quite large number of extensive studies of the environmental impact of PV technology. However, the environmental impact of PV/T technology has been the focus of few studies so far, and those that do exist are mostly concerned with laboratory or custom-made systems.

The building sector accounts for around one third of the global energy use, and about half of the electricity use. It is also responsible for around a third of the global greenhouse gas

emissions [1]. The Intergovernmental Panel on Climate Change (IPCC) has now established beyond all doubt that greenhouse gas emissions caused by human activities are the main driver for climate change [2]. The building sector is consequently a key area to focus on in the ongoing effort to mitigate climate change, and to create more sustainable societies in the future.

Two paths need to be followed in order to reduce the environmental impact of the building sector: reducing the energy demand in construction and operation of buildings, and replacing polluting energy sources with renewable energy sources. On a European level, the European Union (EU) has put pressure on its member states to transform the building sector. In its recast of the Energy Performance of Buildings Directive (EPBD), the EU has directed its member states to ensure that by 2020, all new buildings shall be *nearly* zero energy buildings [3]. A nearly zero energy building is described as:

"a building that has a very high energy performance, [---]. The nearly zero or very low amount of energy required should be covered to a very significant extent by energy from renewable sources, including energy from renewable sources produced on-site or nearby"

The EU member states and associated countries are commissioned to establish their own definitions of a nearly zero energy building, as well as plans for how to reach the target. In Norway, which is an associated country to the EU, the energy performance of buildings is regulated through the Technical Building Regulations (Byggteknisk forskrift, TEK) [4]. In the latest update of the regulations (TEK10, 12.11.2015) the energy efficiency requirement is at passive house level, and is set to be further tightened until a nearly zero energy building level is reached by 2020 [5].

Solar energy is well-suited to use in buildings. Passive solar energy provides lighting and heating through windows and the building envelope. Active solar energy systems can supply electricity, heating, and cooling to buildings. Once installed, a solar energy system will supply energy without any pollution and requires minimal maintenance. In addition, solar energy systems are silent, have few or no moving parts, and can be fully integrated into the building itself.

Buildings require electricity, heating, and sometimes cooling. In buildings with ambitious energy targets, solar thermal and photovoltaic installations may need to "compete for" the available space on the buildings' roofs and façades. Since both electricity and heat is generated in a PV/T module, it is a technology which is particularly interesting for building use. Another argument that is used in favour of PV/T modules is architectural uniformity of PV/T modules compared to using PV modules and solar thermal collectors side by side. The possibility of a reduction in the use of materials is also sometimes mentioned as a benefit of PV/T modules, and the validity of this statement is the topic of Chapter 6 in this thesis.

Earlier studies have shown that the emissions associated with materials and construction, the so called embodied emissions, make up around half of the total emissions of an energy efficient building [6]. The studies also showed that solar energy system, in particular solar cells, can account for around a third of the embodied emissions [6-8]. It is therefore of great importance

to try to reduce the environmental burden of solar energy systems through design and material choices, but also to make sure that existing systems perform well and get proper maintenance.

1.2 Research design

1.2.1 Research questions

The focus of the work presented in this thesis has been to investigate whether or not PV/T systems are a good solution for providing renewable energy to zero emissions buildings, and in that case how the systems should be designed. The objective is described by one main research question and three sub-questions.

Main research question: *What is the potential of PV/T systems to minimize the life cycle greenhouse gas emissions of a residential building?*

Sub-questions:

a) How should PV/T technology be used in buildings to achieve high energy output and good load coverage?
b) How does the energy performance of PV/T systems compare to that of separate PV and solar thermal systems?
c) How does the environmental impact of PV/T systems compare to that of separate PV and solar thermal systems?

Sub-question a) deals with how PV/T systems should be designed to reach their full potential, and how PV/T can be combined with other technologies. A large part of the focus in this thesis is set on the combination of PV/T modules and heat pumps of different types. System design with a focus on Northern European climate is also discussed. Load coverage refers to the match between the availability of and demand for energy.

Sub-question b) relates to the question of whether it is better, from an energy perspective, to use the hybrid technology or the two constituent technologies separately. There are a number of different options within all three technologies (PV, solar thermal and PV/T), as well as countless ways of designing a system. In addition, the energy performance, especially of thermal systems, requires that the load profile is taken into account. For these reasons, this question is not covered in its full extent in this thesis, but studied by way of case studies. The limitations on the analysis are described in the next section.

Sub-question c) focuses on the environmental impact of solar energy technologies. As mentioned in the introduction, the possibility of saving materials (and thereby reducing embodied emissions) is mentioned as a benefit of the hybrid PV/T technology compared to the two separate technologies. Similar benefits are also mentioned for building integration of solar energy systems. One of the objectives of this thesis is to analyse and quantify the environmental impact of different solar energy systems in buildings, in order to establish whether there are possible environmental benefits.

1.2.2 Limitations

PV/T technology and energy efficient buildings are both large research topics in their own right. In order to limit the work to the timeframe of a PhD project, the following limitations are introduced:

1. Only flat plate PV/T technology with liquid heat transfer is studied.
2. Only small residential buildings in Scandinavian climate are studied.
3. The environmental impact is assessed only through greenhouse gas emissions, using the global warming potential at 100 years (GWP100), as defined by IPCC [9].
4. Economic analyses are not included.

1.2.3 Structure of the thesis

This thesis is divided into seven main chapters:

Chapter 1: Introduction
Chapter 2: Background
Chapter 3: PV/T technology and applications
Chapter 4: Design of PV/T systems
Chapter 5: Energy performance of PV/T systems in buildings
Chapter 6: Environmental impact of PV/T systems
Chapter 7: Conclusions

Chapter 1 (the present chapter) introduces the topic, the research questions, and the research method.

Chapter 2 starts with an introduction to solar energy technology in general. This is followed by a brief description of the development of energy efficient buildings, as well as an overview of different concepts and calculation methods. The use of solar energy in buildings is also discussed in this chapter. Furthermore, the concept of life cycle assessments (LCA) is introduced in this chapter.

Chapter 3 provides an overview of previous research on PV/T technology, and the different types of PV/T modules. Applications of PV/T technology is also discussed, with a special focus on buildings. This chapter also includes a brief overview of the PV/T market.

In Chapter 4, an attempt is made to answer research question a), by evaluating how PV/T systems should be designed. The chapter also deals with how PV/T modules can be combined with other energy sources, in particular with heat pumps.

Research question b) is the focus of Chapter 5, where the energy performance of PV/T modules is studied. PV/T systems are compared to systems with separate PV modules and solar thermal collectors for two Norwegian residential case buildings.

Chapter 6 focuses on research question c). The embodied energy and emissions of PV/T modules and systems are evaluated and compared to that of PV modules and solar collectors. In addition, the influence of system design on the emission balance of a building is studied.

The thesis is concluded by Chapter 7, with a summary of the results, conclusions, and suggestions for further work.

1.2.4 Papers

The main part of this thesis is based on research which has been published at conferences and in scientific journal publications. The papers are presented in full in Appendix B, and summarized below.

Paper I

Good, C., Chen, J., Dai, Y., & Hestnes, A. G. (2015). *Hybrid Photovoltaic-thermal Systems in Buildings – A Review.* Presented at SHC Conference 2014 in Beijing and published in Energy Procedia

Paper I provides an overview of how PV/T installations have been used in buildings. It is based on a review of scientific literature, case studies, and direct communication with module manufacturers. Paper I is the basis for Section 3.2 of this thesis.

Paper II

Good, C., Andresen, I., & Hestnes, A. G. (2015*). Solar energy for net zero energy buildings – A comparison between solar thermal, PV and photovoltaic–thermal (PV/T) systems.* Presented at CISBAT 2015, Lausanne, Switzerland and published in Solar Energy.

Paper II presents a simulation study of different types of solar energy systems on a case building (the ZEB residential concept). The objective of the study was to compare the energy performance of PV/T systems with that of systems with PV modules and solar thermal collectors. Paper II is the basis for Section 5.2 of the thesis.

Paper III

Good, C. (2013). *Influence of system lifetime on environmental impact assessments of photovoltaic systems in buildings.* Presented at the Young Researcher Forum at CESB13, Prague.

Paper III is focused on the environmental impact of PV modules, in particular how it is influenced by the assumptions regarding module lifetime. The paper also discusses how and why PV modules fail, and how this has been studied. The results from this paper are not specifically referred to in the thesis, but have been used as part of the background material for Chapter 6.

Paper IV

Good, C. (2016*). Environmental impact assessments of hybrid photovoltaic–thermal (PV/T) systems – A review*. Published in Renewable and Sustainable Energy Reviews.

Paper IV is a review of previous research on the environmental impact of PV/T modules and systems. The results from the review are presented in Section 6.1.2 and used as a background for the rest of the work in Chapter 6.

Paper V

Good, C., Kristjansdottir, T. F., Houlihan Wiberg, A., Georges, L., & Hestnes, A. G. (2015). *Influence of PV technology and system design on the emission balance of a net zero emission building concept.* Published in Solar Energy and previously presented at Eurosun 2014, Aix-les-Bains, France, with the title "A comparative study of different PV installations for a Norwegian net zero emission building concept."

Paper V presents a study of how the design of a PV system influences the emission balance of the building on which it is installed, using the ZEB residential concept as a case. The objective was to find the best compromise between low embodied emissions and high energy output, that is, how a PV system should be designed to have the highest possible positive environmental impact. The work in this paper is presented in Section 6.3.

Paper VI

Kristjansdottir, T.F., Good, C., Inman, M.R., Dahl Schlanbusch, R., Andresen, I (2016). *Embodied greenhouse gas emissions from PV systems in Norwegian residential Zero Emission Pilot Buildings.* Published in Solar Energy.

Paper VI presents a study of the embodied emissions of three different PV systems on three of the ZEB Centre's pilot buildings. Significant attention is given to the parts of the system other than the PV modules themselves (the so-called BOS), and the results show that the choice of components for the BOS has a large influence on the system's environmental impact. My contribution to this paper has been mostly related to energy simulations, but also to the discussion and general structure of the study. The work presented in this paper has been used as background and input to the analyses in Section 5.3 and Section 6.4, which are focused on one of the three case buildings presented in the paper (the Living Lab).

The research presented in Section 5.3, Section 6.2, and Section 6.4 is not yet published. Papers based on this research will be submitted for publications after the submission of the thesis.

1.3 Research methods

1.3.1 Literature review

Literature review was used to investigate the state of the art of PV/T technology, as well as the use of PV/T systems in buildings. This review is presented in Paper I, and discussed further in Chapter 3. In addition to scientific publications, the review relied on case studies from PV/T producers and installers, as well as direct communication with companies.

A literature review was also conducted as a background for the calculations of the environmental impact of PV/T modules. This review is presented in Paper IV and discussed in Chapter 6.

1.3.2 Case study

A large part of the work presented in this thesis is based on case studies of two of the pilot buildings of the Norwegian Research Centre on Zero Emission Buildings (the ZEB Centre). The two cases are the ZEB residential concept building and the Living Lab. The case buildings

are described in Section 5.2 and Section 5.3. Both buildings are small detached houses, new constructions and located in similar climate in Central and Southern Norway. An important difference between the two cases is that the ZEB residential concept is only a model of a building, while the Living Lab is an actual, constructed building. In addition, the ZEB residential concept has a significantly larger floor area than the Living Lab (160 m^2 compared to 102 m^2).

Benefits of using cases studies include that the energy systems can be studied with predetermined boundary conditions, and that the results of the studies can be related to a real case. A particular benefit of using two of the ZEB Centre's pilot buildings is that they have been (and will be) the subject of several other studies, which means that there is a significant amount of data to build on. Important earlier studies of the two case buildings, that the present analyses build on, are energy performance analyses [6, 10] and environmental impact assessments [11, 12].

A disadvantage of using case studies is that the results have limited validity for other cases, especially buildings that are not similar to the presented cases. This study does not include a wide variety of cases or building types, and it is therefore not possible to draw any statistical conclusions based on the results of only two studies.

As mentioned in Section 1.2.2, the focus of the thesis is only on small residential buildings. In Norway, 72% of dwellings[1] are in small houses with four or fewer dwellings. There is, however, a large difference between the urban and rural regions; in the three largest Norwegian cities (Oslo, Bergen, and Trondheim), below 30% of the inhabitants live in detached houses. There is also an increase in the number of dwellings in blocks of flats. In the whole country, 65% of the detached buildings has a floor space between 80 m^2 and 200 m^2, although there are large regional differences. [13] Considering these statistics, the two case buildings are representative for a large share of the Norwegian building stock. Both the case buildings are also located in Central and Southern Norway, similarly to 90% of the existing dwellings in the country, and to 88% of the detached houses.

Both the two case buildings are new building projects, representing the current state of the art in both building technology and building regulations in Norway. Statistical data for the last 15 years show that the increase in the number of small houses with one to two dwellings has generally been less than 1% per year [13]. New buildings clearly represent a small fraction of the building stock. However, since this is thesis focused on how to use solar energy systems in the best possible way, the use of new constructions without any restraints regarding systems design is considered to be appropriate. It is, however, worth pointing out that refurbishment of existing buildings is very important in order to reduce the energy consumption of the building stock, in Norway as well as in the rest of Europe. The results from the case studies in this thesis can also be applied to the installation of solar energy systems in existing buildings.

[1] A dwelling is here defined as a conventional dwelling with at least one room and kitchen, while a building refers to a physical built structure. A building can contain several dwellings.

1.3.3 Energy simulations

The work presented in this thesis relies to a large extent on simulations of energy performance of solar energy systems as well as of the two case buildings.

1.3.3.1 Polysun

The simulation program Polysun from Vela Solaris [14] has been used for the energy performance simulations in Paper II, which is described in Section 5.2, and also in Section 5.3 and Section 6.4. Polysun is a dynamic simulation tool for thermal and electric solar energy solutions systems, as well as for various hydronic systems such as heat pumps and district heating.

Polysun includes an extensive model database of systems and commercial products, including PV/T modules. The choice of Polysun above other simulation tools was partly based on the existence of this database. Many published simulation studies of solar thermal and PV/T systems use the simulation program TRNSYS [15], which was also initially considered for this thesis. TRNSYS is a simulation tool for transient simulations and mostly used to assess the performance of thermal and electrical energy systems. It is also possible make detailed simulations of a building, and to connect it to a CAD model. The main reason that Polysun was chosen for the simulations in this thesis was the ease and reliability with which PV/T modules could be modelled and simulated. There are several types (models) for PV/T modules in TRNSYS, but they require information which is not commonly available from commercial producers. The models in Polysun are based on parameters that are defined according to European and American standards, and therefore found in producer datasheets.

Polysun calculates the energy output of PV modules using the Beyer model [16]. In this model, the energy output of a PV module is calculated based on the following inputs [17]:

- 3 efficiency readings for the module at different irradiance
- 3 efficiency readings for the inverter with different loads
- The installed power
- The module's temperature coefficient

An efficiency curve can be created from these inputs, and the energy output at any combination of irradiance and temperature is calculated.

The solar thermal performance is calculated in Polysun according to the European standard EN ISO 9806[2] [18]. The main input parameters are the absorber area, efficiency rate parameters (as specified in the standard), the IAM (incidence angle modifier) values KCH1 and KCH2, and the specific heat capacity of the collector. The efficiency rate parameters are different for covered and uncovered collectors, where the latter type requires one additional parameter related to wind dependent losses. [17]

[2] EN ISO 9806:2013 supersedes EN 12975-2:2006, which is referred to in the Polysun User Manual.

The electric and thermal simulations of PV/T modules in Polysun are performed with a combination of the two methods described above. Covered as well as uncovered collectors can be modelled.

According to Vela Solaris, results of the PV/T simulations have been compared to measured values from Meyer Burger in Switzerland and a project is also started with Fraunhofer ISE and Solarzentrum Allgäu Germany. So far the simulated values are found to be close to the measured ones, but slightly underestimating the energy output (thermal and electric). This is possibly due to the use of one module temperature for the whole module independent of the module layout. [19]

The building simulations in Polysun are not very detailed. Polysun includes two main options for simulating the heating and cooling need of a building: it can either be simulated based on a number of parameters (such as area, U-value, and ventilation rate), or based on the annual power or energy demand. In both cases, an hourly heating profile is created based on the local weather data. The second method is used in both the two case studies analysed here. Data of the annual heating demand is sourced from previous publications. Since the analyses in the thesis have focused on the solar energy systems, and not the buildings, the use of this simplified method for building simulation is considered acceptable. In addition, the results of the simulations of different buildings are not compared to each other, but only to other versions of the same building.

The energy demand for domestic hot water (DHW) and electricity is analysed in a similar way, namely by using a total annual value which is scaled by a profile. A DHW profile for a single family residential building and a residential electricity profile (both internal in Polysun) were used in the simulation of case building 1, while DHW and electricity profiles from the Norwegian standard NS 3031 [20] was used for case building 2. The use of different profiles is due to a development in the research methodology during the course of the project. The values from NS 3031 are considered to be more appropriate for Norwegian conditions.

The load profiles for heating as well as electricity are of importance for the end result. The domestic hot water profile, and to a lesser extent the space heating profile, determine whether solar thermal energy is needed or not, which in turn influences the energy yield of the system. If there is no present need for space heating or domestic hot water, and the storage tank is fully charged, solar heating from the collectors cannot be utilized and is “lost”. The electricity load profiles determine whether the electricity output from the solar energy systems is used directly or exported. The electricity profile is of importance in the calculations of net energy demand, if the delivered/exported balance calculations are used (see Section 2.2.1). The profiles are also of importance if different weighting factors are used for exported and delivered electricity, or if the weighting factors vary with time. The latter was outside of the scope of this thesis.

The shading analysis is a weakness in Polysun. Shading can only be modelled in a two-dimensional way, composed of a horizon line and shading from simple objects. The program also includes a function for “row-to-row” shading of modules. In this function, however, all rows in a system – also the front row – are given the same shading profile. In the case of the

Living Lab, this means that both parts of the roof will be simulated with the same shading profile (see Section 5.3). Shading of solar energy systems is further discussed in Chapter 4.

1.3.3.2 PVsyst

Papers V and VI are concerned only with electricity output from PV modules, and no thermal output. The simulation tool PVsyst [21], which is dedicated to simulations of PV systems, is used in the analyses in these papers. The simulations in PVsyst are focused only on PV system, and no thermal components can be simulated. It is possible to simulate both grid-connected and stand-alone PV systems. The simulation results can be given in monthly, daily and hourly data.

The PV simulations in PVsyst are more detailed than those in Polysun, and are based on a theoretical model rather than curve fitting from measured values. Measured values are, however, also used in the PV model in PVsyst to model actual modules. PVsyst uses the one-diode model developed by Shockley and described by for example Duffie and Beckman [22]. An adjusted version of the model is used to simulate thin film solar cells. In addition to the irradiance and temperature, this model takes into account the series and shunt resistance of the solar cells, the photocurrent, the inverse saturation current, and the diode quality factor. [23]

PVsyst is one of the most commonly used simulation programs for analyses of PV systems. The program also includes a very large database of PV modules and inverters, and data can be easily imported from the PV industry database in Photon magazine for up to date information. The program also makes it easy to import meteorological data from different sources. PVsyst does not include building simulations, but an electricity use profile can be included in the simulations in order to study grid interaction or load match.

The shading calculations in PVsyst are superior to those in Polysun. In PVsyst, it is possible to model complex 3D scenes, composed of a horizon line and near shadings, where the effect on different surfaces can be modelled throughout the year. It is therefore no problem to model systems with multiple orientations. The program also makes it possible to evaluate the impact of shading on PV systems with different string layouts.

1.3.3.3 Uncertainties

The result of the simulations should ideally have been compared with measured data in order to validate the results. However, since the first case study is not constructed and the second one just recently completed it has not been possible to compare the results of the case studies. This applies both to the energy performance of the building and to the solar energy installations. There are so far no installations of PV/T systems in Norway to which the results could have been compared.

Another weakness is the quality of solar irradiation data in Norway. Solar resource data is commonly based on different combinations of satellite data and ground measurements. The satellite data is usually from geostationary satellites (in orbit above the equator) which have lower accuracy at high latitudes [24]. Meteonorm data, which is used in the simulations in this thesis, is based on a combination of satellite data and three ground stations in Norway (Bergen, Bodø and Tromsø) [24]. Data for any location other than these three is interpolated. At higher latitudes Meteonorm data is reported to have uncertainty levels up to 10% [25].

1.3.4 Comparative analysis

A main part of the research has been conducted through comparative analysis of different technologies on the two case buildings. This method was chosen early because of the way PV/T was developed and is often described: as a hybrid of two other technologies, namely photovoltaic (solar cells) and solar thermal, which could be installed *instead of* these technologies. A natural question was therefore to ask: is PV/T better than the system it would replace? The answer to this question is of importance for example to architects and engineers in the planning stages of a new building project, or for a building owner considering a refurbishment. The systems are here only compared to other systems on the same building, that is, there is not comparison between the two buildings.

In hindsight, the focus on comparative analysis might have been an impediment to some aspects of the study. This is due to two factors in particular. Firstly, that PV/T would not always replace another solar technology, which raises the question of what the comparison should actually focus on. An increasingly common approach is to install PV/T in combination with a ground source heat pump, in which case the alternative might have been to install the heat pump only, the heat pump in combination with solar thermal collectors, or other renewable or non-renewable energy systems. Secondly, that the effort to design comparable systems to analyse sometimes result in sub-optimisations, for example of dimensioning or orientation. In addition, it is not obvious where to draw the system boundary in a comparison between a PV system and a PV/T system, since the latter also require some hydronic components, which would not be required in the former.

Comparative analyses in different forms are, however, often found in previously published research on PV/T systems. The performance of PV/T systems are often compared to PV and solar thermal systems, or only PV systems [26-30]. The combination of PV/T modules and ground source heat pumps are compared to systems with only ground source heat pumps, direct grid electricity, or ground source heat pumps and other solar technologies [31-35]. Comparative analyses are also used to evaluate the environmental impact of PV/T modules, where they are compared to PV modules, direct use of grid electricity, or gas boilers [36-39]. Building on previous research, it therefore seemed sensible to employ a comparative analysis also in this thesis. As mentioned, a comparative approach will also be of importance in building design processes, where the choice of energy systems will be based on comparative analyses of energy performance, economy, and possibly environmental issues.

Two different dimensioning approaches were used in the analyses in this thesis. In the first case study (ZEB residential concept), the roof area was set as the boundary condition for the installation. Both covered and uncovered PV/T modules were used. The relative area of the thermal components in the different systems was varied in order to achieve the same thermal solar fraction during summer. In the second case (the Living Lab), which is an actual building, the compared systems were based on the existing installation. The compared solar energy systems in this case study were allowed to differ in size since this made most sense considering the architectural design of the particular building. Only uncovered PV/T modules, which are relatively similar to PV modules, were used in this case study. Since uncovered PV/T modules favour the electricity output over the thermal output, the PV/T system was restricted to the area

of the original PV system. The difference between covered and uncovered PV modules are explained further in Section 3.1.2.

In the building simulations, the focus has not been on the building, but rather on the way the solar energy systems perform in combination with the building. It was therefore considered acceptable to use simplified building models for the simulation of space heating demand, and to use standardised values for lighting and domestic hot water demand. The important factor was that the building model was kept the same in the compared systems.

1.3.5 Environmental impact analysis

The environmental impact analysis of the PV/T modules are here evaluated using life cycle assessments (LCA). A single issue impact assessment method is used in this thesis, focusing only on global warming potential at 100 years (GWP100a) as described by the Intergovernmental Panel on Climate Change (IPCC)[9]. Global warming potential is measured in carbon dioxide equivalents (CO_{2eq}) per functional unit. The LCA methodology is described in more detail in Section 2.3.

The analysis is performed using the LCA tool Simapro 8.0 [40] . Simapro is the world's leading LCA tool and can be used to collect, analyse, and monitor data on products and services. The analysis of the environmental impact of the PV/T modules in this thesis is based on data from the Ecoinvent database v. 3.1 [41] in combination with information from two PV/T manufacturers. It is one of the most comprehensive and well documented databases, and includes a broad range of processes. LCA tools and databases are described further in Section 2.3.3 and Section 2.3.4. The data collection is described together with the case studies Chapter 6.

Chapter 2: Background and theory

2.1 Solar energy

2.1.1 The solar resource

The sun is an abundant renewable energy resource, which is freely available on most places on Earth. In fact, the sun is the ultimate energy source behind most other renewable sources, including wind power, hydropower and bioenergy. Even fossil fuels can be said to be stored solar energy. From the point of view of life on Earth, the sun is an infinite source of energy; astronomers estimate its lifetime to 5 billion years from now.

The amount of solar radiation that hits the surface of the Earth every year is far larger than the global energy demand. In one hour, the Earth receives more energy in the form of solar radiation than the total global energy demand for a year [42]. The solar resource is shown in Figure 1, compared to other renewable and finite energy resources [43]. It should be noted that the renewable resources is shown as annual capacities, while the total amount is shown for the finite resources. The annual global energy demand is shown in the same figure.

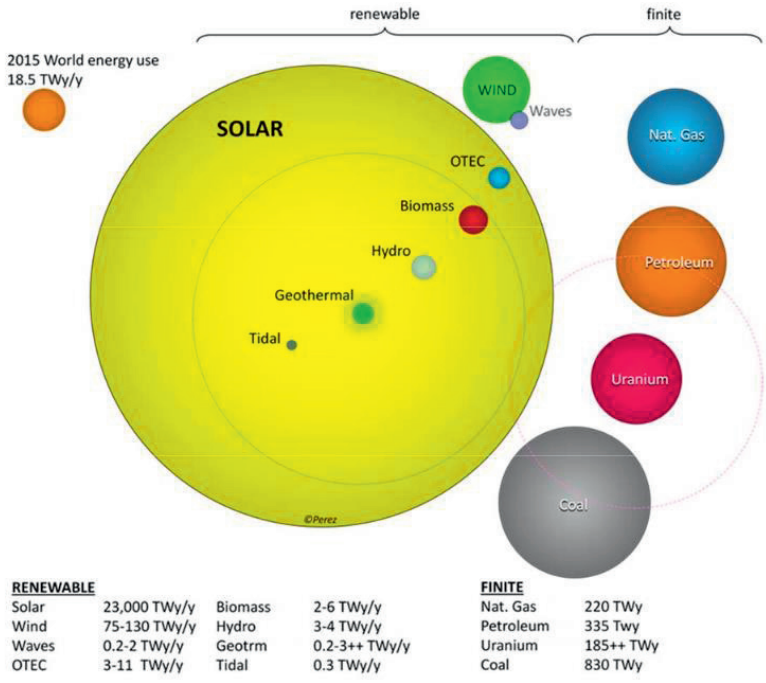

Figure 1. The global energy reserves [43]. (OTEC refers to ocean thermal energy conversion.)

Solar radiation is available everywhere on Earth, although at different levels. The radiation is highest close to the equator, but the difference between locations largely depend on the local weather conditions. When the radiation at different locations is compared, it is not uncommon

that the value on a horizontal surface is given. This can be misleading, especially for locations at high latitudes, since horizontal is far from the optimal installation angle for solar energy systems.

Figure 2 shows a map of the global irradiation on an optimally inclined surface [44]. It shows that the radiation on an optimally inclined surface in most of Northern Europe is around 800-1100 kWh/m^2 per year. Comparing this to the much higher radiation at the equator, it may seem that solar energy utilization is not appropriate this far north. However, until just a few years ago, the largest market for PV installations was actually Germany, which now has been surpassed by China [45]. Germany still has 21% of the world's total installed PV power [45], and a level of irradiation that is relatively similar to that in parts of Scandinavia.

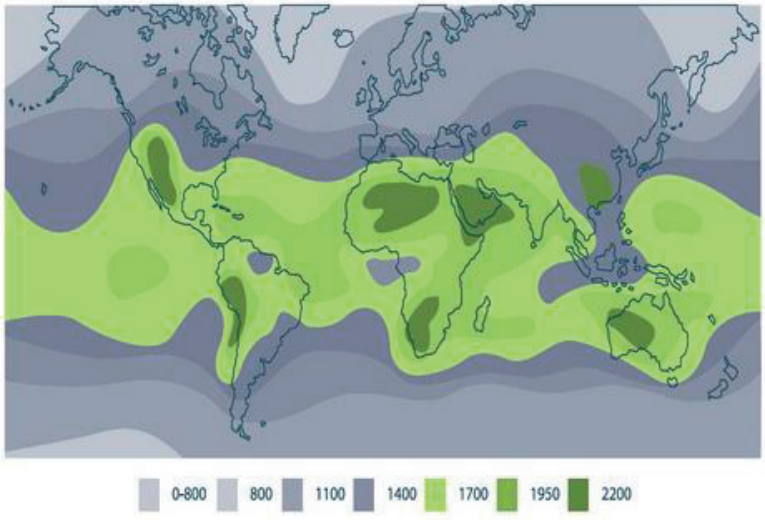

Figure 2. The annual global solar radiation on an optimally inclined surface, measured in kWh/m^2. Figure from Multiconsult [44].

The largest challenge of solar energy utilization in Northern regions is arguably not the amount of radiation, but rather the large differences between the many hours of sunlight in summer and the short days in winter at high latitudes. The annual variations are also mismatched with the energy demand of a typical residential building, which requires most energy for heating and lighting during winter.

The varying sun path over the year also means that the optimal angle can vary significantly between summer and winter. As an example, the optimal tilt angle for a PV system in Oslo in Southern Norway is around 40° if the annual output should be maximised. However, if the system is designed for high output during the summer months, the best angle is around 30°. If the system is instead designed for winter yield, the optimal angle would be approaching 70°.

2.1.2 Passive and active solar energy

Solar energy utilization is generally divided into passive and active type. All buildings use passive solar heating to some degree when solar radiation is transmitted through windows and

glazing, and the radiation is absorbed by floors, walls or furniture. The utilization of passive solar energy can be significantly improved by careful design of the building and by use of thermally "heavy" materials, such as stone or concrete, which absorb and store solar radiation. In Norway, passive heating supplies around 10% of the annual energy demand for space heating [46].

Active utilization of solar energy includes the use of photovoltaic (PV) and solar thermal systems, or, as will be explored in this thesis, photovoltaic-thermal systems. In a PV module, the absorbed solar radiation is converted to electricity. A solar thermal collector absorbs solar radiation and converts it to heat, which can be used for example for preparation of domestic hot water (DHW) or space heating. PV/T modules are a combination of PV modules and solar thermal collectors, and are described in Chapter 3. There are also several methods available for utilizing solar energy for cooling, and solar thermal energy to generate electricity, but these technologies are outside of the scope of this thesis.

2.1.3 PV modules

Photovoltaic (PV) cells, or solar cells, convert solar radiation to electricity. Most solar cells are made up of two semi-conductor materials, forming a so-called p-n junction. When radiation is absorbed by the solar cell, a voltage is created across the p-n junction due to the movement of electrons and holes (the absence of electrons). This is known as the photovoltaic effect. If the two sides of the p-n junction are connected, a current is generated in the external circuit. [47]

Crystalline silicon solar cells are by far the most common technology today, accounting for more than 90% of the market [45]. Crystalline silicon solar cells are made from thin wafers (nowadays typically around 160-200 µm) of either monocrystalline (mono-Si) or polycrystalline (poly-Si) silicon. These are mature and robust technologies, and the efficiency of commercially available modules is in the range 15-22%.

The production of silicon solar cells is energy-intensive. The most energy demanding step is the production of high-purity silicon, so-called solar grade silicon. Since poly-Si cells have somewhat lower demands on purity, the production is slightly less energy demanding than that of mono-Si cells. Poly-Si cells are also typically of lower efficiency, and have a somewhat lower cost.

The other large technology group is thin film solar cells. These can be made of different materials or composites, but have the common feature of being made of thin films (1-2 µm) [48]. Technology developments and increased efficiency have made thin film modules a viable alternative to crystalline silicon modules, even though the efficiencies are still typically lower. The most common materials are amorphous silicon (α-Si), CdTe (Cadmium Telluride), and CIS/CIGS (Cadmium Indium (Gallium) Selenide). Efficiencies of commercial modules range from 5-13% [49]. The production of thin film modules is significantly less energy demanding than the production of crystalline silicon solar modules.

In addition to the technologies mentioned above, there are also several new developments in solar cell technology, including dye-sensitized solar cells (Grätzel cells), tandem and multi-

junction solar cells, quantum dot solar cells, and the use of new materials such as perovskites and nanomaterials. These technologies are still more or less at a laboratory stage.

A standard crystalline silicon solar cell of 156 mm x 156 mm generates a voltage of around 0.5 V and a power of less than 5 W [48]. PV modules are therefore composed of a number of series- and parallel-connected solar cells to increase the output voltage. Common module nominal power output today range from around 100 W_p to over 300 W_p (Watt peak, see Section 2.1.3.1) [48]. The cells are encapsulated and laminated together with a glass pane for structural stability. The module also typically has an aluminium frame, although frameless modules are increasingly common, especially in modules intended for building integration. A typical module structure is shown in Figure 3.

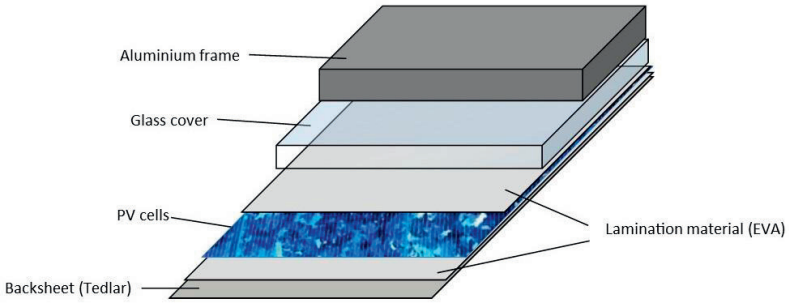

Figure 3. Structure of a crystalline silicon solar module (not to scale).

The structure of a thin film module is a little different from crystalline solar modules. Thin film solar technology does not require cells to be a certain shape or size, but consists of several thin layers of deposited material. Physical or chemical deposition methods are used to create thin layers on a substrate of e.g. glass or metal [48]. The cells and connection between them are created as the thin film is deposited. Thin film modules can be produced on different substrates and can be made flexible or semi-transparent.

2.1.3.1 Performance of PV modules

The instantaneous efficiency η of a PV module is defined as the ratio of the maximum power output P_{max} (W) output to the irradiance[3] G (W/m^2) and the area of the module A_{PV} (m^2), as shown in Equation (1).

$$\eta = \frac{P_{max}}{G \cdot A_{PV}} \qquad (1)$$

The maximum power, P_{max}, is calculated according to Equation (2), where I_{sc} (A) is the short circuit current, V_{oc} (V) the open circuit voltage and FF (-) the fill factor. The fill factor is the

[3] The definitions from Duffie and Beckman [22] are used in the text: irradiance G (W/m^2) refers to the rate of energy on a unit area, and irradiation I (Wh/m^2 or the SI unit J/m^2) refers to the energy on a unit area during a specified time. I is found by integration of G. Insolation refers to irradiation specifically from the sun.

ratio between the maximum power output and the product of I_{sc} and V_{oc}. [47]. Typical fill factors vary from 0.5 to 0.82 [48].

$$P_{max} = I_{sc} \cdot V_{oc} \cdot FF \quad (2)$$

The nominal performance of PV modules is measured under so-called Standard Test Conditions (STC), which means 1000 W/m^2 radiation, AM1.5 spectrum, and 25°C cell temperature. These are conditions that rarely occur during real operation. The radiation that is not converted to electricity is partly reflected by the front glass and partly converted into heat in the module. A module under 1000 W/m^2 irradiation is therefore typically significantly warmer than 25°C [47]. The rating of a PV module is given in Watt peak (W_p), which is the power output from the module at STC. The efficiency given in datasheets is the value for STC.

The module performance at the Nominal Operating Cell Temperature (NOCT), which is sometimes given by producers, represents a more typical situation. NOCT is defined as the temperature of the cells at 800 W/m^2 irradiation, ambient temperature of 20°C, wind velocity of 1 m/s, and an open back side (which influences heat loss from ventilation). Typical NOCT values are in the range 33-58°C [47].

The efficiency of a PV module decreases with increasing temperature, primarily because of decreasing voltage [47]. A module with a higher cell temperature than at STC will therefore have a lower power output than rated. For a crystalline silicon solar cell, the temperature coefficient is around -0.5%/°C [50]. The efficiency of thin film solar cells are not as affected by temperature as that of crystalline silicon solar cells.

2.1.3.2 PV systems

In PV systems, or arrays, PV modules are connected in series into module strings. In addition to the PV modules themselves, a PV system requires some auxiliary components which are commonly referred to as Balance of System (BOS). For stand-alone systems (systems not connected to the grid) BOS typically includes cabling, a charge controller, and a battery. For grid-connected systems, which are the primary focus of this thesis, BOS includes at least cabling and an inverter. Some grid-connected systems also include battery storage, usually to be able control when energy is imported and exported to the grid and to increase the self-consumption of energy. In some cases, an electric car can be used as energy storage. Sensors can also be included to monitor energy performance and environmental conditions.

PV modules generate DC (direct current) electricity. The inverter converts the DC from the PV modules to AC (alternating current) to match the grid. Inverters also include safety features that prevent the PV system from exporting power when the grid is down, for example during maintenance.

The energy performance of a PV system is referred to as the performance ratio (PR) and is defined as the ratio between the actual energy output and the output of a "perfect" system at the same irradiation. The PR is influenced by e.g. shading or soiling, reduced efficiency due to module temperature, losses in cabling, and the efficiency of the inverter. For a well-designed

PV system, the performance ratio should be over 80%. [51] Typical PR values for systems in Germany are nowadays in the range 80-90%, compared to around 70% in the 1990s [45].

Two relatively new types of products on the market are micro-inverters and power optimisers. Instead of using one inverter for one or a few strings of modules, these systems convert the power output of each module individually. The advantage is that the performance of each individual module can be optimised, and the energy output of the string is no longer limited by the weakest performing module. Such systems are less affected by shading and can also include modules with different orientations.

In Scandinavia, an optimally inclined PV system can be expected to have an annual output of around 80-150 kWh/m^2 [52], or 750-950 kWh/kW$_p$ [53].

2.1.4 Solar thermal collectors

In a solar thermal collector, the absorbed solar radiation is converted to heat. The heat is extracted by a heat transfer medium that flows across the absorber. The heat transfer medium is typically water or glycol-mixed water, but sometimes also air. Collectors with liquid heat transfer media is the focus of this thesis. There are several different types of solar thermal collectors, for example flat plate, vacuum tube, and parabolic through collectors.

A flat plate solar thermal collector (Figure 4, left) consists of an absorber, which absorbs the solar radiation, and insulation to reduce the thermal losses to the surroundings. In its simplest form, an absorber is simply a black or dark surface. However, modern, spectrally selective absorbers are designed to absorb as much as possible of the short wave solar radiation, while emitting as little heat as possible. Most collectors also have a glass cover, which transmits the solar radiation but reflects back the long wave heat radiation emitted from the absorber, thereby increasing the collector temperature and efficiency. The cover also protects from wind and cooling by the surroundings. Uncovered collectors are typically used for less demanding applications such as swimming pool heating.

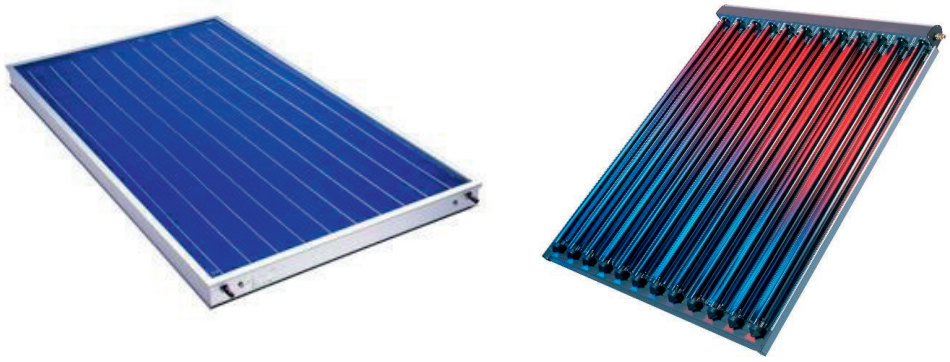

Figure 4. A flat plate solar thermal collector (left) and a vacuum tube collector (right). Photo © Wagner & Co, Cölbe and European Solar Thermal Industry Federation (ESTIF).

In a vacuum tube collector (Figure 4, right), the absorber in each glass tube is insulated by the surrounding vacuum. Vacuum tube collectors are more efficient than flat plate collectors and can reach higher output temperatures.

Worldwide, vacuum tube collectors account 54% of the market, while in the EU countries flat plate collectors account for 86% of the market (values from 2008 and 2009) [52]. Vacuum tube systems with integrated water storage are common in warmer countries, and especially in China. These systems are often thermosiphon systems, where the fluid is naturally circulated in the pipes due to the lower density of the heated fluid. Vacuum tube systems are not as common as flat plate collectors in building integrated applications.

2.1.4.1 Performance of solar collectors

The amount of energy that can be harvested from solar collectors depends on the design and operation of the complete system, such as the flow rate and temperature of the incoming heat transfer medium, and not only on the efficiency of the collector.

The instantaneous efficiency η of a collector is defined as the useful energy output divided by the incoming radiation, according to Equation (3), where $\dot{Q}_u$ (W) is the rate of useful energy gain, G (W/m^2) is the solar irradiance, and A_C (m^2) is the gross collector area [22].

$$\eta = \frac{\dot{Q}_u}{G \cdot A_C} \qquad (3)$$

The efficiency of three types of solar collectors (uncovered flat plate, covered flat plate, and vacuum tube) versus the temperature difference between the collectors and the ambient is shown in Figure 5. The warmer the collector gets (i.e. the higher the temperature difference to the ambient), the higher are the heat losses to the surroundings and the lower the efficiency. The highest efficiency is reached when the inflow temperature of the heat transfer medium is as low as possible.

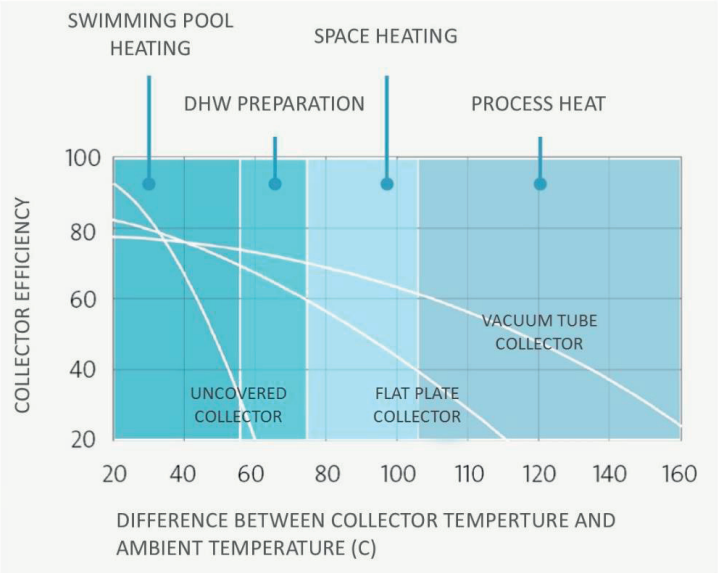

Figure 5. Solar collector efficiency versus the temperature difference between collector and the ambient, shown for different irradiation levels. Figure from [54] .

The thermal output of a solar thermal collector is given by Equation (4) [22].

$$\dot{Q}_u = A_c F_R [G(\tau\alpha) - U_L(T_i - T_a)] \qquad (4)$$

F_R	collector heat removal factor (-)
G	irradiance (W/m^2)
$\tau\alpha$	transmittance absorptance product (-)
U_L	collector heat loss coefficient (W/m^{2}K)
T_i	inlet temperature (°C)
T_a	ambient temperature (°C)

The transmittance absorptance product ($\tau\alpha$) describes how much of the incoming radiation is actually absorbed by the collector, and is the product of the transmittance, τ, of the cover and the absorptance, α, of the absorber. The collector heat loss coefficient (U_L) describes how much of the energy that is lost to the surroundings through the top, bottom, and edges of the collector.

The heat removal factor F_R is a complex factor that relates the actual useful energy gain of the collector to the gain if the whole collector surface would be at the fluid inlet temperature [22]. It is defined according to Equation (5).

$$F_R = \frac{\dot{m} C_p (T_o - T_i)}{A_C [G(\tau\alpha) - U_L(T_i - T_a)]} \qquad (5)$$

$\dot{m}$	mass flow rate of heat transfer medium (kg/s)
C_p	specific heat capacity of heat transfer medium (J/kg K)
T_o	collector output temperature (°C)

The calculation of energy output from a solar collector over a whole year is a complex process, and calculation or simulation tools are often used.

In product datasheets, the potential thermal output of a solar collector is sometimes given as the zero-loss efficiency η_0 and the thermal loss factors. The zero-loss efficiency is the efficiency when the temperature of the heat transfer fluid is the same temperature as the ambient, that is, when there is no thermal loss from the collector to the surroundings (the values where the curves crosses the y-axis in Figure 5). In addition to the optical efficiency, the first and second order heat loss coefficients a_1 (W/m^{2}K) and a_2 (W/m^{2}K^2) should be given. Given these factors, the thermal power output $\dot{Q}$ of a collector is calculated according to Equation (6) [18]. The mean collector temperature T_m (°C) is used instead of the input and output temperatures as in the previous equation.

$$\dot{Q} = A_c\eta_0 - \frac{a_1 \cdot (T_m - T_a)}{G} - \frac{a_2 \cdot (T_m - T_a)^2}{G} \qquad (6)$$

The zero-loss efficiency of good quality flat plate modules is usually above 80% and the first order heat coefficient below 3.5 W/m^{2}K [55]. A modern flat plate collector mounted at optimal orientation can be expected to give an annual output of 300-500 kWh/m^2 in a Northern European climate [56].

2.1.4.2 Solar thermal systems

Solar thermal systems typically consists of the collectors, a thermal storage tank, a piping system, and a control system. Several components are necessary in the piping system, such as pumps, valves, expansion vessels, and controllers. The principle of a solar thermal system for DHW preparation is shown in Figure 6.

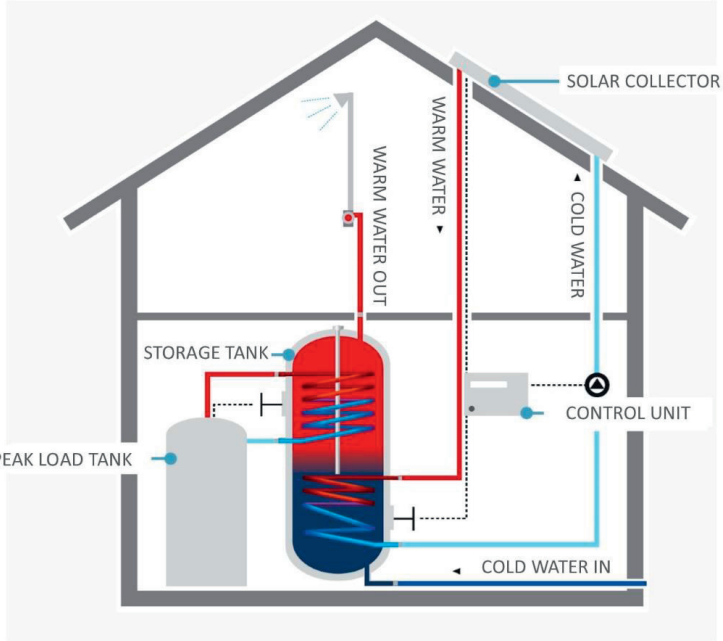

Figure 6. The principle drawing of a solar thermal system for DHW preparation (not to scale). Figure from [54].

A backup heater, such as an electric immersion heater, is also usually installed in DHW systems to ensure an uninterrupted supply of hot water even at times of low solar radiation and to avoid the risk of legionella growth. Legionella is a bacterium which can cause serious respiratory illness, and which grows quickly in water between 30°C and 45°C [55]. The bacteria die at 50°C or above, and DHW storages are therefore typically heated to high temperatures at regular intervals to avoid bacterial growth. Legionella is not a problem if a heat exchanger is used to heat the DHW, and where DHW is not stored.

There are several different ways of connecting the collectors to the storage tank, depending on the intended use of heat, what type of heat transfer medium is used, and the type of tank. A system that will only be used for DHW preparation can be relatively simple. If water is used in the collectors, the circuit can be connected directly to the tank (direct system). If a glycol-water mix is used in the collectors, the collector circuit is connected to the tank via a heat exchanger (indirect systems).

In a solar combi-system, the solar thermal collectors supply heat for DHW as well as for space heating, in combination with one or more auxiliary energy sources. Common auxiliary energy sources are bioenergy (for example pellet boilers), heat pumps, gas, or electricity.

It is common to use a stratified tank to improve the system performance. Stratification means that there is a temperature gradient in the tank, where the water in the tank is coldest in the bottom to warmest in the top of the tank. In this way, cold water is always available for the solar collector circuit, while hot water is available for use in the building. The space heating

circuit, which requires water of medium temperature, can be connected at the middle of the tank.

Another important parameter to consider when designing the system is the stagnation (or equilibrium) temperature. This is the maximum temperature that can be reached when there is no flow through the collector, for example at times of high irradiation and a full heat storage, or in the case of a power outage. Flat plate collectors can have stagnation temperatures of up to 200°C, and vacuum tube collectors up to 300°C. It is important to make sure that there are sufficient strategies in place to avoid stagnation, or that all components can withstand these temperatures. [55]

In Northern Europe, it is common to dimension the solar thermal system according to the thermal load in the summer, which should be mainly the DHW load. Rule of thumb values for DHW systems are around 2-3 m^2 collector per person, and a storage volume of 50-75 l/m^2 collector area. Such a system can be expected to cover 40-60% of the annual hot water load. For a combi-system, the storage volume can be increased to 75-125 l/m^2 collector. Depending on the building's energy standard, the system can be expected to cover 15-40% of the annual thermal load. [54, 56]

Increasing the system size is not only unnecessary, but can even be damaging to the system since it can lead to overheating during summer. The output of a solar thermal system is only useful when it can be used directly or stored. Over-production may lead to overheating, which can cause damage to the components. One strategy to avoid this is to install the collectors vertically on the façade, which reduces the output during the summer. This is especially suitable at high latitudes, where the sun angle is low. A larger system can then be installed without the problem of summer overheating, and can also cover a greater fraction of the load during the heating season. Design of solar energy systems, especially for northern regions, will be further discussed in Chapter 4.

2.1.5 Solar energy in buildings

Active solar energy utilization has several characteristics that makes it suitable for building use. It is quiet, requires no fuels to operate (except for a small amount of electricity for circulation pumps), and is available more or less everywhere. Solar thermal systems are easily combined with other energy sources, such as bioenergy or heat pumps, in hybrid systems. This thesis focuses on the use of solar energy in residential buildings, but there is also a large potential for solar energy in industrial, commercial, and agricultural buildings, as well as swimming halls, health care institutions etc.

When solar energy systems are installed in new building projects, they should be part of the design from the starting phase. In this way, the orientation of the building, tilt of the roof, and other design factors can be used to optimise the building for solar energy utilisation. Solar installations are also appropriate for already existing buildings, in particular if they are done during a refurbishment. Shading and non-optimal module orientations may, however, be a problem in such cases.

2.1.5.1 Building integration

Building integrated PV systems (BIPV) and building integrated solar thermal systems (BIST) are typically defined as systems that are an integrated part in the building envelope [57]. That is, the solar module or collector replaces another building component, such as façade claddings, roofing materials, or solar shading. It is sometimes differentiated between building integrated systems and building added systems [58], where the latter refers to systems that are added to the building envelope, but does not replace any other building materials. An example of a building integrated (left) and a building added (right) solar thermal system is shown in Figure 7.

Figure 7. A building integrated (left) and a building added (right) solar thermal system. Photos © European Solar Thermal Industry Federation (ESTIF).

A strong argument for building integration of solar energy systems is that the buildings are already there and no additional land is occupied by the installation. Installing solar energy systems on buildings also means that the energy is generated where it is used, which reduces the transmission losses. In the case of solar thermal systems, it is crucial, since the heat from the collectors cannot typically be transported over long distances before it is used [52]. There is, however, a growing number of district heating systems with large scale solar thermal plants, notably in Denmark [59]. Norway's largest solar thermal installation, in Lillestrøm, is also connected to a district heating network [60].

A downside of building integration of PV systems, particularly in roofs and façade is the increased module temperatures due to reduced backside ventilation, which leads to lower module efficiencies. Module ventilation should be considered in the design of the systems. Building integration can also, depending on the specific design of the system, make it more difficult to get access to the system for cleaning and maintenance. Replacement of modules and other components may also be more complicated if the modules are an integrated part of the building.

Integration of active solar energy systems into buildings have several aspects. A solar energy system can be integrated perfectly into the technical system of a building, but not at all integrated architecturally, and vice versa. Architectural integration of solar thermal systems is covered in detail by Munari Probst and Roecker [52]. They point out that the low architectural quality of many of existing building integrated solar thermal systems is a barrier to the widespread use of the technology in buildings.

One possible reason for the lack of focus on architectural integration is suggested to be that solar thermal systems (at least on residential buildings) are typically small roof-mounted installations with limited visibility, and therefore mostly considered to be a technical component. A survey by the authors also confirmed that there was a clear discrepancy between architects on the one hand, and engineers and façade manufacturers on the other, regarding the perceived quality of an integration, where the engineers and façade manufacturers were less demanding regarding the formal integration [52].

According to Munari Probst and Roecker, architectural "integratability" of solar thermal systems depends on the functional, constructive, and formal architectural levels, which all bring their own constraints and possibilities. They found that the lack of formal integratability of existing products was a barrier to full system integration, and suggested a strategy for the development of new, more building-oriented products. Some of the most important factors were found to be multi-functionality, durability, and formal flexibility, where the last point includes flexibility in module shape and size, jointing, colour, and textures and finish.

Three different examples of architectural building integration of solar thermal systems from Scandinavia are shown in Figure 8.

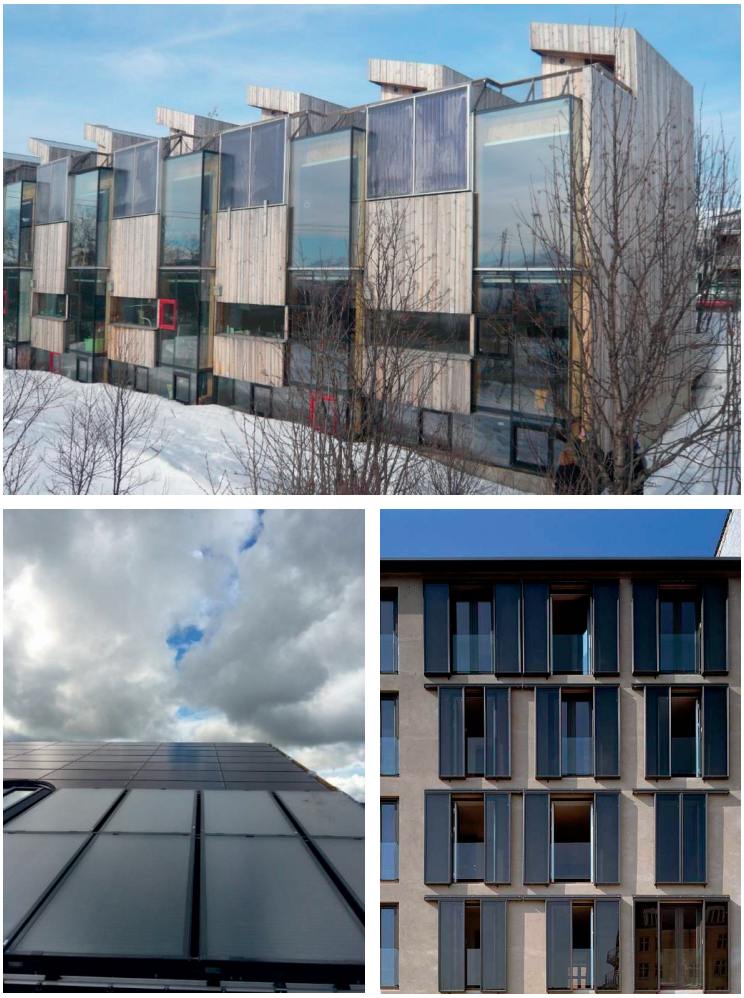

Figure 8. Different approaches to building integration of solar thermal systems. Clockwise from top: Façade integrated flat plate solar collectors in Storelva passive houses in Tromsø, Northern Norway (photo: Solvår Wågø, NTNU/SINTEF Byggforsk), solar thermal collectors used as solar shutters in Copenhagen (photo: CF Møller Architects), roof-added solar thermal collectors at Multikomforthus, Larvik (photo: Harald Amundsen, Brødrene Dahl).

Architectural integration of PV modules was extensively discussed in the doctoral thesis of Klaudia Farkas [57], building partly on the work by Munari Probst and Roecker. Farkas separates between structural integration, where the PV module is integrated into a building component, and conceptual integration, where the solar installation is a part of the whole building design concept. Full building integration requires both structural and conceptual integration. Different approaches to building integration of PV systems are shown in Figure 9.

Figure 9. Different approaches to building integration of PV systems. Clockwise from top left: the Grätzel cell façade at EPFL in Lausanne (photo: Clara Good), building inregrated PV modules at Oseana kunst- og kultursenter in Os (photo: Tove Heggø/Creative Commons), roof integrated PV at Skarpnes zero energy neighbourhood in Arendal (photo: Hans Kristian Sonesen, Skanska), and green façade integrated PV modules on Solsmaragden in Drammen (photo: FUSen AS).

Farkas describes the architectural potential of photovoltaic technology as depending on the possibility of structural integration, the formal flexibility (the availability of different shapes, colours etc.), the product system (availability of components available for mounting etc.), and the availability of dummies (fake modules used for creating a uniform appearance) [57]. More and more products for building integration are being developed, for example modules of different colour, frameless modules, and special roofing products such as solar cell tiles.

2.1.6 Solar energy in Norway

Energy efficient buildings are expected to be the main driver for increased solar energy utilisation in Norway [61]. Installations in Norway are relatively expensive compared to other countries due to the small market. In addition, the cost of electricity from the grid is relatively low (0.12€, compared to the EU average of 0.14€ during 2014 [62]) which means longer payback times. However, PV installations on buildings can be seen as an energy efficiency measure or as a replacement for another building component, and their comparative advantages are therefore not always cost [61].

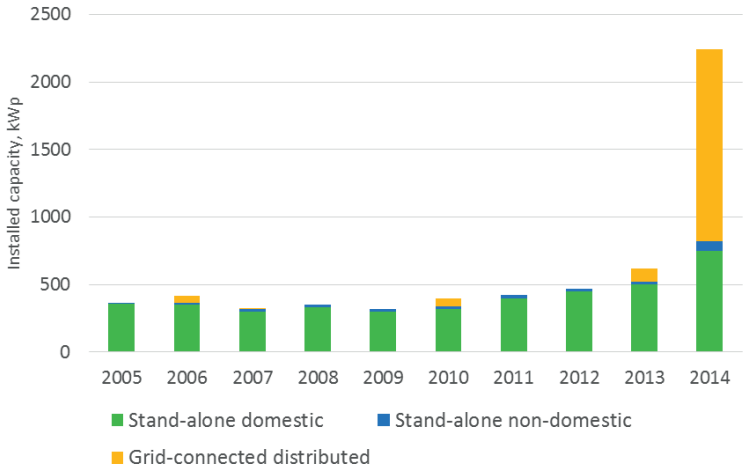

Figure 10. The annual installed PV capacity in Norway [63].

All grid-connected PV installations in Norway are installed on buildings [61]. Historically, off-grid cabins and holiday homes has been the largest market for PV systems in Norway [63]. However, a significant increase in the installed capacity of grid-connected systems took place in 2013 and 2014, when several large-scale installations were completed (Figure 10). These installations were primarily installed on large, non-residential buildings. The total installed PV capacity in Norway (around 13 MW) is still small compared to other countries [61]. Neighbouring Sweden has a total installed capacity of around 80 MW [64], while Germany is approaching 40 GW [61]. Different funding schemes have been of significant importance for the increased PV market in these two countries. Norway has only recently initiated an economic incentive system for PV installations. Since 2015, 35% of the total cost of a PV installation can be refunded, up to 10 000 NOK[4] plus 1 250 NOK per kW_p up to 15 kW_p [65].

As for PV systems, the solar thermal market is also quite limited in Norway. The total installed solar thermal capacity was 30 MW_{th} (megawatt thermal) by the end of 2013. Of these, 90% were glazed flat plate collectors. [66] The total scale of installations were 16 000 m^2, out of which 13 000 m^2 belongs to one single system connected to a district heating network, which was mentioned above [60, 67].

As for PV, energy efficient buildings are expected to drive the market development for solar thermal installations. Domestic combi-systems for DHW and space heating account for 60% of the market in Norway, and the large system in Lillestrøm accounts for another 30% [67]. Installers of domestic solar thermal systems can receive economic support in Norway; 25% of the total cost up to 10 000 NOK plus 200 NOK per m^2 up to 25 m^2 is refunded [68].

[4] At the time of writing 1 NOK was equal to 0.11€.

2.2 Zero energy/emission buildings

2.2.1 Definitions

In simple terms, a net zero energy building (nZEB) is a building where the energy that is used by the building is balanced, or "offset", by renewable energy generated on the building site. If the amount of renewable energy from the building site is equal to or larger than the energy demand, the building has reached a zero energy balance. There are a number of definitions of zero energy buildings, and several ways to calculate the zero energy balance [69]. In most cases, the balance is calculated as the *net* balance over a specific time, normally a year. This means that the building can exchange energy with the grid(s) and thus does not have to be self-sufficient with energy at all times. In the remainder of this text, the term zero energy building should be understood to mean *net* zero energy building.

The European Union has been an important driving force for the development of energy efficient buildings in Europe. According to the energy performance in buildings directive (EPBD) [3], the Union requires of its member states that all new buildings shall be "nearly zero energy buildings" by the end of 2020, and by the end of 2018 for buildings owned and occupied by public authorities. The definition of a nearly zero energy building is left to each member state to develop, but the EPBD (Article 2.2) describes it as:

"[---] a building that has a very high energy performance [---]. The nearly zero or very low amount of energy required should be covered to a very significant extent by energy from renewable sources, including energy from renewable sources produced on-site or nearby."

In September 2015, the U.S. Department of Energy published a report with a common definition for zero energy buildings, including zero energy campuses and zero energy communities [70]. According to this report, a net zero energy building is defined as:

"An energy-efficient building where, on a source energy[5] basis, the actual annual delivered energy is less than or equal to the on-site renewable exported energy"

A comprehensive work towards a definition was also developed by Sartori, et al. [71]. According to their definition, a net zero balance is reached when the weighted supply meets or exceeds the weighted demand. The calculations in this thesis are based on the definition of Sartori, et al., which is also the one used in the Norwegian Research Centre on Zero Emission Buildings (the ZEB Centre).

To reach a net zero energy balance, the first priority should be to decrease the need for delivered energy, and then to meet the remaining demand with on-site renewable energy sources [71]. A graph describing this principle is shown in Figure 11, where a net zero energy balance is reached for any point on or above the net zero balance line. As implied in the graph, the amount of

[5] Source energy is defined as the building energy demand "plus the energy consumed in the extraction, processing and transport of primary fuels such as coal, oil and natural gas; energy losses in thermal combustion in power generation plants; and energy losses in transmission and distribution to the building site." [70]

supplied energy required (the height on the y-axis) is lowered by increasing the energy efficiency of the building (moving left on the x-axis).

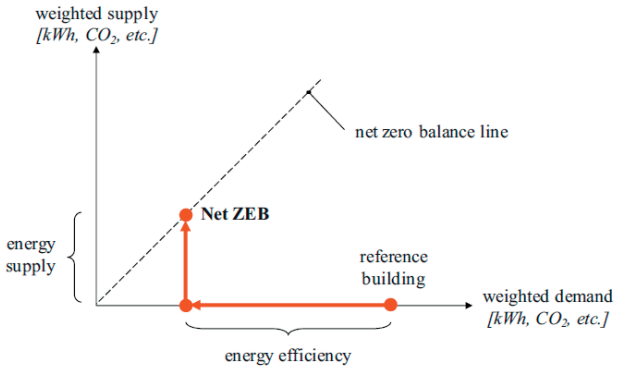

Figure 11. A visualization of the ZEB balance concept. Source: Sartori, et al. [71], used with permission.

The definition of a net zero balance according to Sartori, et al. is straight-forward but requires that a number of other factors are determined, for example the balancing type, the weighting system, and the system boundaries. The meaning of some of these factors are shown in Figure 12. As the figure shows, there are two main balancing types: load/generation and delivered/exported energy. The difference between the two balancing types is that the delivered/exported energy balance takes into account the load match and interaction with the grid, while the load/generation balance completely overlooks this. [71]

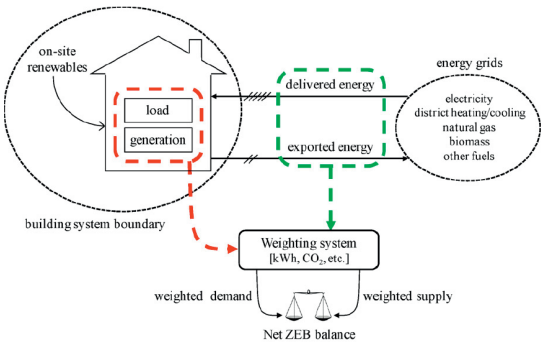

Figure 12. Sketch of the connection between buildings and grids. Source: Sartori, et al. [71], used with permission.

The weighting system converts all energy carriers, such as exported or imported grid electricity, biomass, or district heating, to one common metric [71]. The main difference between a net zero *energy* building and a net zero *emission* building is the weighting system used. In a zero energy building, the common metric is usually primary energy measured in kWh. In a net zero emission building the common metric is greenhouse gas emissions, measured in kg carbon dioxide equivalents (kg CO_{2eq}). The locally generated renewable energy is commonly weighted

according to the emission factor of the energy it replaces (offsets), for example electricity from the grid.

The system boundaries include the physical boundary and the balancing boundary. The physical boundary determines for example whether a renewable energy source can be installed at a distance from the building (e.g. a nearby wind turbine) or only on the building itself (e.g. building integrated PV). The balancing boundary determines which of the loads and energy sources that should be included in the calculation, for example whether to include the use of electric consumer equipment such as computers. Depending on the balancing boundary, the loads can also include energy required for construction and demolition of the building.

The ZEB Centre has expanded the definition of zero emission buildings to include several ambition levels, depending on the included loads [72]. The levels are shown in Figure 13.

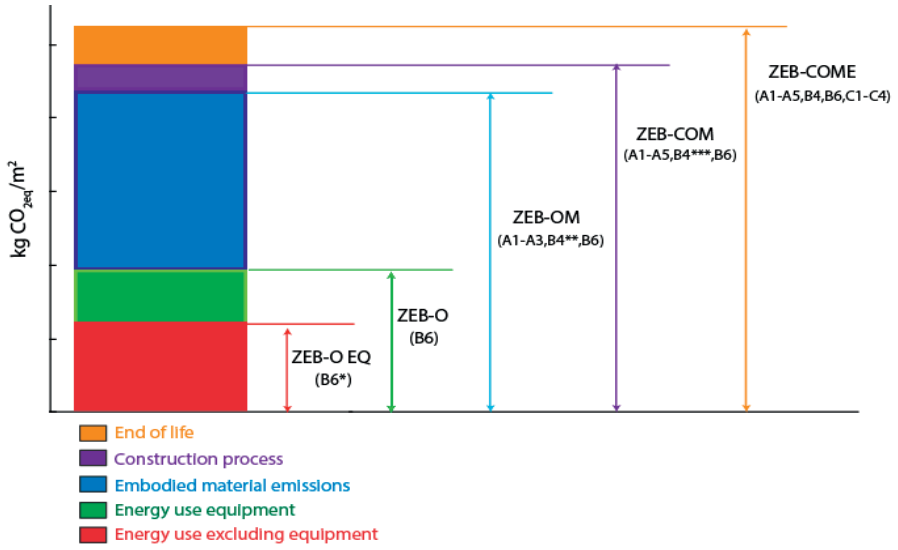

Figure 13. ZEB ambition levels as developed by the ZEB Centre [73].

These ZEB ambition levels will be used for the calculations of both the energy and the emission balance in this thesis. ZEB-O÷EQ, which is the lowest level of ambition, includes energy demand for operation excluding technical equipment, while ZEB-O includes all operational energy. ZEB-OM includes energy for operation and embodied emission/energy of materials. ZEB-COM includes energy for operation, materials and construction of the building, and ZEB-COME also includes end-of-life (i.e. deconstruction or demolition). The highest ambition level is ZEB-COMPLETE, which includes all life cycle phases from cradle to grave. [73] A more detailed description is given in Figure 16. It can be noted that a building with a ZEB-O÷EQ balance would still be a net zero energy building according to the EPBD, which does not require that the consumption from equipment, and in the case of residential buildings not even that from lighting, is included in the balance.

2.2.2 Zero energy/emission balance calculation

The calculation methods used in the case studies in this thesis are based on the definitions by Sartori, et al. [71] and the European standard EN 15603 [74]. In addition, the ambition levels defined by the ZEB Centre [72] were used, also adapted for zero *energy* balance. The zero emission balance is calculated in the same way as the zero energy balance, but using greenhouse gas (GHG)[6] emission factors for weighting.

Two balancing methods are used in the cases studies, but the physical boundary is in both cases set to the building itself. As mentioned above, the load/generation balance is equivalent to the delivered/exported balance with no grid interaction, i.e. where all energy generated on the building is exported and all energy to meet the loads is imported [71].

A general equation for the load/generation balance is shown in Equation (7), based on the references given above. The net zero energy balance is reached if the value of the annual net energy E_{net} is zero or positive, that is, if the generation meets or exceeds the load[7].

$$E_{net} = \sum_i E_{gen,i} f_{gen,i} - \sum_i E_{load,i} f_{load,i} \qquad (7)$$

E_{net}	annual net energy (kWh)
$E_{gen,i}$	generated energy, carrier *i* (kWh)
$f_{gen,i}$	weighting factor (generation) for carrier *i*
E_{loadi}	energy load of carrier *i* (kWh)
$f_{load,i}$	weighting factor (load) for carrier *i*

The energy carriers considered in the case studies in this thesis are electricity and heat. In the case studies in this thesis, the solar heat generation is taken into account as a reduction in the electric loads of the heat pump and electric heater. The load/generation balance can then be calculated using only electricity. This approach is similar to the one used by Dokka, et al. [75]. The load/generation net energy balance is then calculated according to Equation (8).

$$E_{net} = E_{gen,el} f_{gen,el} - E_{load,el} f_{load,el} \qquad (8)$$

$E_{gen,el}$	generated electricity (kWh)
$f_{gen,el}$	weighting factor for generated electricity
$E_{load,el}$	electricity loads (kWh)
$f_{load,el}$	weighting factor for electricity load

The delivered/exported balance is in principle calculated using the same method, as shown in Equation (9). The total source energy from solar radiation, the ambient air, or the ground is not included as an input in the delivered energy, but is calculated as the delivered energy from e.g. solar collector or PV module [74].

[6] From now on, the term "emissions" should be understood as greenhouse gas emissions

[7] The definition of E_{net} in EN15603 is given in the opposite direction, which means that a balance is reached for zero or negative values. The definition used by the ZEB Centre is used in this thesis.

$$E_{net} = \sum_i E_{exp,i} f_{exp,i} - \sum_i E_{del,i} f_{del,i} \quad (9)$$

$E_{exp,i}$ exported energy, carrier *i* (kWh)
$f_{exp,i}$ weighting factor (exported) for carrier *i*
$E_{del,i}$ delivered energy, carrier *i* (kWh)
$f_{del,i}$ weighting factor (delivered) for carrier *i*

As for the first case study, the only imported and exported form of energy is electricity, and Equation (9) can therefore be reduced to Equation (10).

$$E_{net} = E_{exp,el} f_{exp,el} - E_{del,el} f_{del,el} \quad (10)$$

$E_{exp,el}$ exported electricity (kWh)
$f_{exp,el}$ weighting factor for exported electricity
$E_{del,el}$ delivered electricity (kWh)
$F_{del,el}$ weighting factor for delivered electricity

2.2.3 Weighting factors

Weighting factors are used to determine the value of different energy carriers in order to enable a comparison. Examples of weighting methods are primary energy, GHG emissions, and cost, but other political factors can also be used. This thesis will focus on primary energy and GHG emissions.

2.2.3.1 Primary energy

Primary energy is energy in its original form, before it has been converted into other forms of energy. The primary energy factor describes the amount of primary energy that is required to deliver one unit of energy, taking into account all necessary steps including extraction, processing, generation, distribution etc. [20]

If electricity that is delivered from the grid is considered to have the same value as electricity exported to the grid, it is not necessary to use weighing factors to calculate E_{net}. Equation (10) can then be reduced to Equation (11). (Only the exported/delivered balance is shown from now on, but Equation (8) can be simplified in a similar way for the load/generation balance.)

$$E_{net} = E_{exp,el} - E_{del,el} \quad (11)$$

$E_{exp,el}$ exported electricity (kWh)
$E_{exp,el}$ delivered electricity (kWh)

However, weighting factors can be used to differentiate between delivered and exported grid electricity. Such factors are introduced in the preliminary standard prEN 15603[8] [74, 76], where solar energy is converted to primary energy using the primary energy weighting factors (f_P) in Table 1.

[8] This preliminary standard has not yet been approved, and is used here as a source for the primary energy factors only.

Table 1. Primary energy weighting factors (f_p) for solar energy according to prEN 15603 [74]. Grid electricity is included for comparison.

Energy carrier		Non-renewable primary energy factor	Renewable primary energy factor	Total primary energy factor
Delivered				
Grid electricity	$f_{Pdel,el}$	2.3	0.20	2.50
Grid electricity by hydropower plant	$f_{Pdel,el(hydro)}$	0.50	1.00	1.55
Delivered from onsite				
PV electricity delivered from onsite	$f_{Pgen,el(PV)}$	0.00	1.00	1.00
Thermal solar energy delivered from onsite	$f_{Pgen,el(st)}$	0.00	1.00	1.00
Exported				
PV electricity exported to the grid	$f_{Pexp,grid}$	1.60	0.00	1.60
PV electricity temporary exported and reimported later	$f_{Pexp,tmp}$	2.00	0.00	2.00

Primary energy factors indicate the amount of energy that was required to provide one unit of energy in the current form. For the grid electricity, as an example, this means that 2.3 kWh of non-renewable energy was in fact needed to provide 1 kWh of electricity in the grid. The higher the primary energy factor, the more inefficient is the process of supplying the energy.

The weighting factors in Table 1 differentiate between a renewable and a non-renewable component. It is up to the authorities in each country to determine which of the factors are to be used. Only the non-renewable primary energy factor is used in this thesis.

If the primary energy weighting factors in Table 1 are used, Equation (10) can be written as Equation (12).

$$E_{net} = (E_{exp,el,tmp} \cdot f_{P,exp,el,tmp} + \mathrm{E}_{\mathrm{exp,el,grid}} \cdot f_{Pexp,el,grid}) - (E_{gen,el} \cdot f_{Pgen,el} + E_{del,el} \cdot f_{Pdel,el}) \quad (12)$$

$E_{exp,el,tmp}$	annual exported and later reimported electricity (kWh)
$f_{Pexp,el,tmp}$	primary energy factor for exported and later reimported electricity (-)
$E_{exp,el,grid}$	annual surplus electricity exported to grid (kWh)
$f_{Pexp,el,grid}$	primary energy factor for surplus electricity exported to grid (kWh)
$E_{gen,el}$	electricity generated onsite (kWh)
$f_{Pgen,el}$	primary energy factor for electricity delivered from onsite (-)
$E_{del,el}$	electricity delivered from grid (kWh)
$f_{Pdel,el}$	primary energy factor for electricity delivered from grid (-)

Exported and later reimported electricity, $E_{exp,tmp}$, refers to electricity that is exported from the building and later reimported. For example, this could be a surplus of solar electricity generated in the summer, which is reimported to power a heat pump during the winter.

2.2.3.2 Greenhouse gas mission

As mentioned above, the zero emission balance is similar to the zero energy balance, but calculated using GHG emission factors. The net annual emissions GHG_{net} (kg CO_{2eq}) is analogous to the net annual energy E_{net}. Emissions that are avoided due to the use of renewable energy instead of more polluting energy sources are counted as negative, or avoided, emissions.

In the two case studies, where only electricity is imported and exported, the balance Equation (10) can then be written as Equation (13), weighted by emissions.

$$GHG_{net} = E_{exp,el} f_{GHG,exp,el} - E_{del,el} f_{GHG,del,el} \quad (13)$$

GHG_{net}	annual net GHG emissions (kg CO_{2eq})
$f_{GHG,exp,el}$	GHG emission factor for exported electricity (kg CO_{2eq}/kWh)
$f_{GHG,del,el}$	GHG emission factor for delivered electricity (kg CO_{2eq}/kWh).

The factors $f_{GHG,exp,el}$ and $f_{GHG,del,el}$ are the grid emission factors for export and import to the grid and play an important role in the analysis. If delivered and exported electricity to the grid are assumed to have the same GHG emission factor, Equation (13) can be further simplified to Equation (14), where $f_{GHG,sym,el}$ is the symmetric grid emission factor (kg CO_{2eq}/kWh).

$$GHG_{net} = (E_{exp,el} - E_{del,el}) f_{GHG,sym,el} \quad (14)$$

The grid emission factors vary depending on the energy mix in the local grid, where a grid with a high share of renewable energy gives a low emission factor and a grid with a high share of fossil fuels gives a high emission factor.

The current Norwegian electricity grid, which is almost entirely based on hydropower, has a grid emission factor of around 0.04 kg CO_{2eq}/kWh [41]. This can be compared to the current European grid factor, of around 0.36 kg CO_{2eq}/kWh [77]. However, the Norwegian grid is connected to the Nordic and European electricity grid, through both import and export. Much of the Norwegian renewable electricity is also sold to customers in other countries through the European Guarantees of Origin system. According to the Norwegian Water Resources and Energy Directorate (NVE), the grid emission factor of the Norwegian electricity mix has been between 0.307 kg CO_{2eq}/kWh and 0.500 kg CO_{2eq}/kWh during the years 2011-2014 if trading of Guarantees of Origin are taken into account. [78]

In analyses of buildings, it is also necessary to consider the development in the electricity grid during the building's lifetime. In this thesis, the lifetime of the building is assumed to be 60 years, in accordance with values used in previous studies in the ZEB Centre. The lifetime of PV systems is assumed to be 30 years based on the recommendations in the Methodology Guidelines on Life Cycle Assessments of Photovoltaic Electricity [79], in combination with producer warranties. The lifetime of solar thermal systems can be expected to be 20-25 years [80].

Several scenarios for the future grid in Europe were developed in the ZEB Centre by Graabak, et al. [81], and the influence on zero emission buildings was analysed by Georges, et al. [11] in a European and Norwegian context. The development of the specific grid emission factor (kg CO_{2eq}/kWh) in the different scenarios is shown in Figure 14. The most ambitious scenario analysed by Graabak, et al. was the so-called ultra-green scenario, in which it was assumed that emissions of the European grid will be reduced by 90% by 2050 in line with EU long term political goals [82, 83]. The ultra-green scenario represents a combination of a reduced energy demand, increased energy generation from renewables and nuclear, as well as increased transmission capacities [81]. The red scenario is the least ambitious of the scenarios, and includes only low-tech developments of traditional, mostly centralized energy sources [81].

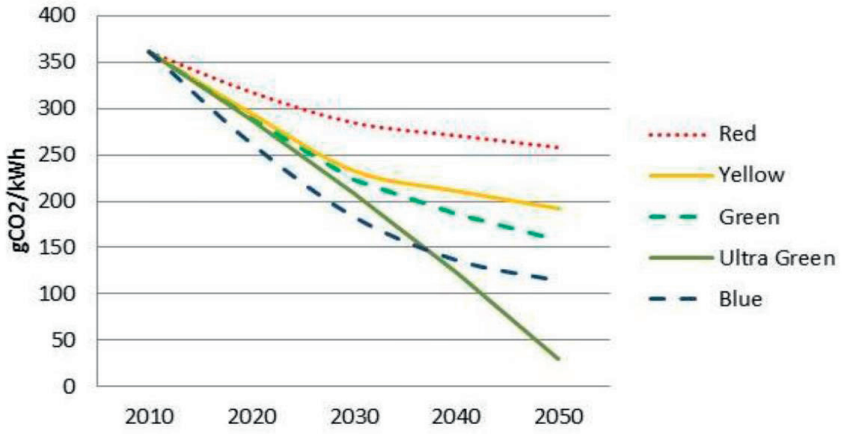

Figure 14. The development of the specific grid emission factor in the different emission scenarios. Figure from [81].

There is currently no standard way of accounting for grid emissions in Norway. The average factor for the ultra-green scenario is the one recommended and commonly used factor in the ZEB Centre for calculating emissions in long term perspective [78]. This grid factor (referred to as the ZEB grid factor in this thesis) starts at the current EU level of 0.361 kg CO_{2eq}/kWh and declines to 0.031 kg CO_{2eq}/kWh by 2050, as shown in Figure 15.

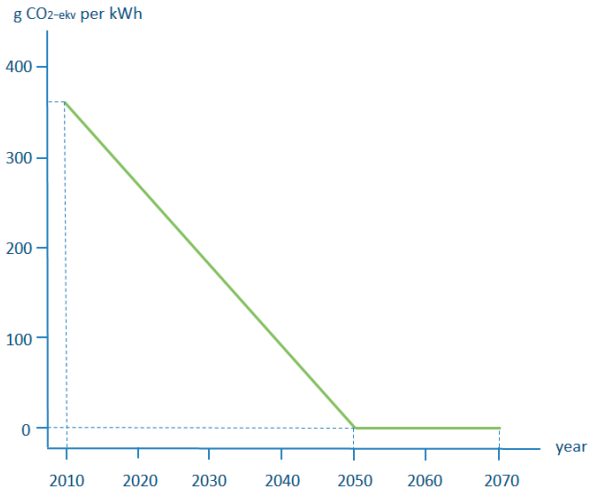

Figure 15. The development of the grid emission factor used in the ZEB Centre. Figure from [72].

Both the current EU grid factor and the ZEB grid factor are used in this thesis, in order to represent the range between a pessimistic "business as usual" scenario and an optimistic outlook on the development of the European electricity grid. The use of the ZEB factor makes it possible to compare analyses within the ZEB Centre. The average over 60 years, the assumed lifetime of new buildings, is 0.132 kg CO_{2eq}/kWh [81]. The average ZEB factor over 30 years is also used in this thesis, since this is the assumed lifetime of a PV/T system. The 30 year ZEB factor is 0.238 kg CO_{2eq}/kWh.

2.2.3.3 Including embodied emissions

Embodied emissions refer to the amount of GHG emissions (regardless of their type and source) emitted during one or more life cycle stages of a given product, other than the ones related to its operation [84]. The embodied emissions are the emissions associated with producing a material or component, and which thereby are "embodied" in the final product.

The emissions are calculated and expressed as CO_2 equivalents (CO_{2eq}). The life cycle stages include production of the materials and components (A1-3), transport to site (A4), construction (A5), maintenance (B1-7) including replacement of new materials over the lifetime of the building (B4), 'end-of-life' of the building (C1-4) and next stage product (D) including reuse, recycling, with labelling of the life cycle stages according to EN 15978 [85]. An overview of the embodied emissions included in the ZEB ambition levels, according to the stages of EN 15978, is shown in Figure 16.

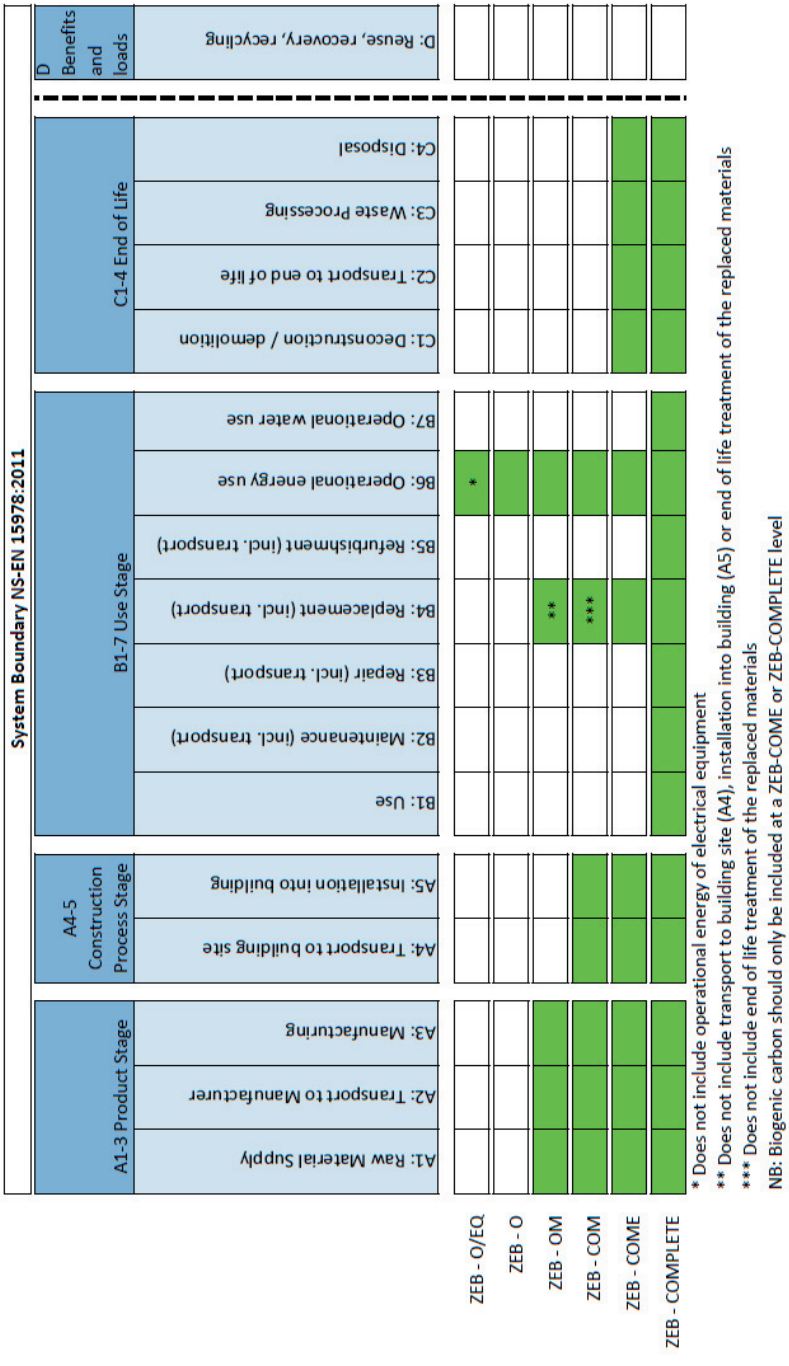

Figure 16. The ZEB ambition levels defined with the life cycle phases defined according to EN 15978. Figure from [73].

The amount of embodied emissions depends on the energy intensity of the production, but also on which energy sources that are used. This, in turn, depends to some extent on where the component was produced, and which means of transport was used. [78] A component with high embodied energy can have relatively low embodied emissions, if it was produced with renewable energy. Embodied emissions can be determined using life cycle assessments, which are discussed in Section 2.3.

Embodied emissions can be included in the net emission balance calculations of a building. In this thesis, the whole lifecycle of the building is considered inside the calculation boundary, that is, embodied emissions are included in the balance calculations. Following the practice used in the ZEB Centre, the embodied emissions are annualized over the building lifetime when included in the calculations [73]. This practice is also followed here, which means that the value of embodied emissions can be added to Equation (13) to give Equation (15), where $GHG_{embodied}$ (kg $CO_{2\,eq}$) are the annualized embodied emissions [78]. The embodied emissions can here be interpreted as an addition to the emissions for delivered energy.

$$GHG_{net} = E_{exp,el} f_{GHG,exp,el} - E_{del,el} f_{GHG,del,el} - GHG_{embodied} \qquad (15)$$

$E_{exp,el}$	exported electricity (kWh)
$f_{GHGexp,el}$	GHG factor for exported electricity (kg CO_{2eq}/kWh)
$E_{del,el}$	delivered electricity (kWh)
$F_{GHG,del,el}$	GHG factor for delivered electricity (kg CO_{2eq}/kWh)
$GHG_{embodied}$	annualized embodied emissions (kg CO_{2eq})

2.2.4 Load match and grid interaction

Given the primary energy factors in Table 1, self-consumption of electricity is considered more valuable than export to the grid. PV electricity that is exported to the grid and later reimported is given a higher primary energy factor than electricity that is only exported to the grid. If this weighting system is used, systems with a high share of self-consumption, i.e. systems with good temporal match between available energy and energy demand, will achieve better balance results (i.e. higher values of E_{net}).

There are a number factors that can be used to assess the match between availability and demand in buildings. An overview of such factors for determination of load match and grid interaction is given in [86]. The load match is a measure of how much of the building energy load that can be covered by local energy generation, while the grid interaction describes to what extent energy is exchanged with the grid(s) [86]. The factors can be calculated over different time periods, from sub-hourly to yearly.

The two factors that are used in this thesis is the load match index and the grid interaction index. A generalized term for the load match index $f_{load,i}$ of energy carrier i is given by Equation (16) [71], where N is the number of data samples, g_i and l_i stand for generation and load of carrier i, and t is the time interval of the analysis. The term in brackets indicates that the load match cannot be higher than 1 (100%).

$$f_{load,i} = \frac{1}{N} \sum_{year} min\left[1, \frac{g_i(t)}{l_i(t)}\right] \quad (16)$$

If only solar energy is considered, the load match index is also referred to as the solar fraction (*SF*), which is a common assessment factor for the dimensioning of solar thermal systems.

The grid interaction index describes the variability of the net grid export during the year [71]. Only the grid interaction with the electricity grid is considered in this thesis. A general equation for the grid interaction index $f_{grid,i}$ for carrier i is given in Equation *(17)*, where STD denotes standard deviation, e_i and d_i are the exported and delivered energy of carrier i respectively, and t is the time interval as before.

$$f_{grid,i} = STD\left(\frac{e_i(t) - d_i(t)}{|\max(e_i(t) - d_i(t))|}\right) \quad (17)$$

The standard deviation is normalized by the absolute value of the maximum difference between exported and delivered electricity for the analysed time period. The grid interaction index does not indicate if there is an energy deficit or a surplus, but describes the variability in the exchange with the grid. A constant value over the analysed period, e.g. a year, results in a low value of the grid interaction index, while large fluctuations result in high values.

Both the load match index and the grid interaction index are sensitive to the time resolution, and large differences can be obtained depending on whether data for hourly, daily, or monthly time intervals are used [71]. It is therefore important to specify over which time period, and with which time interval, the calculations are performed.

2.3 Life cycle assessments

Life cycle assessment, or LCA, is one of several tools available for environmental systems analysis. It is a method of evaluating the environmental impact of a product or service throughout its life cycle. Depending on the scope of the assessment, this may include all processes from the extraction of raw materials ("cradle") to its recycling or disposal ("grave").

Possible applications of LCA are listed in the international standards and include identification of improvement possibilities, decision making, choice of environmental performance indicators, and market claims [87]. An LCA is a study of a whole product system, and not just a few processes. In addition, the results are related to the function of a product, which means that it is an appropriate method for comparison of different products if their function is the same. [88]

LCA is focused on studying technical systems and processes, but also include information about how the technical systems relate to the natural and social systems in which they exist [88]. An LCA can be used to determine the embodied emissions of a product (see Section 2.2.3.3), but a full LCA focuses on more than one impact factor.

Life cycle assessments are used in Chapter 6 of this thesis, and a brief overview of the methodology is given below.

2.3.1 LCA structure

A standardisation of the methodology is described in ISO 14040 [87] and ISO 14044 [89]. According to these standards, an LCA should be divided into the four following steps:

1. Goal and scope definition
2. Life cycle inventory (LCI)
3. Life cycle impact assessment (LCIA)
4. Interpretation

2.3.1.1 Goal and scope definition

The goal and scope definition is an important step, where the objective, choice of functional unit, and boundary conditions of the study are determined. These choices can have a big impact on which data needs to be collected and on how the data collection should be performed.

The goal of the LCA determines how the results are interpreted. The goal formulation should state why the study is performed, the intended use of the results, and to whom the results will be communicated (the target audience) [88]. The goal should be formulated as specifically as possible. The scope of the LCA defines the temporal, geographic and technological system boundaries of the study, as well as the mode of analysis and the level of detail that should be used [90].

The functional unit should be based on the *function* of the studied product or process, and not relate to production or consumption volumes [88]. The functional unit should be described in as much detail as possible, in order to avoid confusion in the interpretation of the results, and should be as close as possible to the end use [90]. For a PV system, as an example, one possible functional unit could be 1 kWh electricity delivered to the consumer.

Reference flows of functionally equivalent products can be determined based on the functional unit [90]. In the PV system example, reference flows could be 1 kWh electricity delivered to the consumer from the grid or from a diesel generator. These reference flows have the same functional unit, but the required infrastructure is very different.

2.3.1.2 Life cycle inventory

Data on processes and materials are gathered in a life cycle inventory (LCI). An LCI should be based on the goal and scope definition and should include the three following steps: construction of a process flow model, data collection for all activities, and a calculation of the required quantities in relation to the functional unit [88].

The flow model is usually given in a flow chart, where all included processes and activities are shown. This includes not only physical materials and products, but also e.g. transport, use, and waste management [88].

The data collection is the most time consuming part of an LCA. Information on inputs and outputs on all included processes and activities described in the flow model needs to be

collected. According to the LCA standard, the data should include information on energy, material, and other physical inputs; products, co-products and waste; emissions to air, water and soil; and other environmental aspects [87]. Descriptive, qualitative data is needed in addition to numerical data [88]. Information on transport routes may also relevant. In addition, it is important to include an assessment of data uncertainty.

The source of the data can be direct measurements, data from production, generic input from databases, official statistics, or a combination. To get specific data, it is often necessary to contact companies, who may not be willing to share information about their production due to confidentiality or other factors. Questionnaires are often used in the communication with companies [91].

The data in an LCI is sometimes divided into foreground data and background data, where foreground data is the detailed information about the specific product or process in question, and background data is the generic data on e.g. common materials, transport, and waste management, which is normally taken from databases [91].

The calculation of required quantities may include normalizing annual values by production volumes and setting up mass balances between inputs and outputs of the activities in the flowchart [88]. This step often includes issues related to allocation of inputs and outputs (see Section 2.3.2). In practice, the calculation often includes large amounts of data and is therefore often solved using some kind of software tool (Section 2.3.4)

2.3.1.3 Life cycle impact assessment

An assessment of the large amount of data in an LCI is performed through life cycle impact assessment (LCIA) methods, where the impacts of the processes are classified and characterised. Optionally, the LCIA may also include normalisation, ranking, grouping, and weighting (not used in this thesis) [91].

An LCIA method is a description of how to classify the inventory results in a set of impact categories that describe environmental impact. Classification means that data from the inventory are sorted according to the environmental impact that they contribute to. A parameter from the inventory may contribute to several impact categories. [88]

Different LCIA methods use different impact categories. Each impact category is described by a category indicator, for example damage to ecosystems, acidification, or global warming potential. The objective of the impact assessment is to turn numerical data from the inventory, e.g. kg carbon dioxide (CO_2) equivalents, into information about a resulting environmental impact, e.g. global warming potential. Some methods only focus on a single issue.

This analysis in this thesis is based on a single-issue impact analysis of the global warming potential at 100 years (GWP100a) as defined by IPCC [9]. The metric GWP is based on the radiative forcing from emissions of different greenhouse gases, for example methane (CH_4) and nitrous oxide (N_2O). Radiative forcing is the net irradiance at Earth's atmosphere, i.e. the balance between energy from the sun and energy emitted from Earth. GWP is expressed in kg CO_2 equivalents (CO_{2eq}), that is, the amount of CO_2 that would cause an equivalent effect.

According to IPCC, GWP is the recommended metric compare future climate impacts of greenhouse gases, and the GWP100a was the basic metric of the Kyoto Protocol. However, its adequacy is also debated, especially related to different time horizons (100, 50 and 20 years are defined). For example, the 100 year timeframe underestimates the impact of greenhouse gases with a shorter lifetime in the atmosphere, such as methane, while the 20 year timeframe does not consider impacts after this time. [9, 92]

Some LCIA methods contain *midpoint* and *endpoint* indicators. The GWP100a indicator used in this thesis is a midpoint indicator. Midpoint indicators are considered to be links in the analysed cause-effect chain, while endpoint indicators describe the effect. Examples of midpoint indicators are ozone depletion potentials, global warming potentials, or photochemical ozone creation potentials. Examples of endpoint indicators are human health impact in terms of disability adjusted life years (DALY), climate change, or ozone depletion. [93]

The endpoint indicators, which are closer to the end or the analysis, are easier to understand and communicate, while midpoint indicators, which are closer to the inventory, have lower uncertainty levels. The choice of indicator should therefore be adapted to the target audience. [91]

2.3.1.4 Interpretation

In the interpretation phase, the results of the LCIA are evaluated based on the objectives determined in the goal and scope phase. The results of the interpretation may be formulated as conclusions or recommendations for decision makers, if this was defined as the goal of the study. However, the interpretation should also reflect the fact that the LCIA is a relative approach that reflects potential, and not actual, impacts. [94] It is recommended to include a sensitivity assessment of the most significant impact factors as part of the interpretation phase.

2.3.2 Attributional and consequential LCA

Product systems often include processes that are linked to each other, for example processes with more than one product, collective waste treatment of several products, or recycling [88]. The question of how divide the loads in such multifunctional processes is called *allocation* and is important in LCA.

The LCA standard states that allocation should be avoided if possible, either by dividing the unit processes into several processes, or by expanding the system boundary [89]. If allocation is necessary, the processes should be divided according to the physical properties if possible. If this is not possible, other allocation methods can be used, such as economic value. It is important that the sum of the physical processes do not add up to more than 100%, i.e. that the same input or output is not accounted for more than once.

The main methods of dealing with the allocation issue result in two main LCA modelling practices: attributional and consequential LCA. In consequential LCA, the issue of multifunctional processes are solved by system expansion. This type of LCA is appropriate in "what if?" studies, i.e. in analyses of the consequences of a change in a system, such as how the environmental impact changes when one product is replaced by another product [91].

Sub-division of processes or allocation is used in attributional LCA, which is the modelling practice used in this thesis. Attributional LCA is appropriate in analyses of the total environmental impact of a product (e.g. carbon footprinting), in localisation of hot spots in the production, or in comparisons of products with the same functional unit [91].

The analyses in this thesis focuses on comparing different products and systems with the same functional unit, and attributional LCA is therefore used. This means that allocation is used as the method for handling linked processes. The allocation database (default) in Ecoinvent is used.

2.3.3 LCI databases

Even in the case of detailed information from companies, some of the data in an LCI is typically collected from databases. This may for example be generic data on raw materials, processes, or whole products. Some databases focus on one particular field, such as a particular raw material or a geographic region, while others are more generic.

The Ecoinvent database [41] is used in this thesis. It is one of the most comprehensive and well documented databases, covers over 10 000 processes, and is maintained in a joint effort between several Swiss institutions [91]. The database is not specialised in a particular field, but covers a broad range of processes and also includes assessment of data uncertainty.

2.3.4 LCA software

The LCA process can be simplified by using software tools for data collection and analysis. Compiling an LCI involves gathering large amounts of data, which needs to be structured and transparent. The LCI is subsequently analysed using different sets of impact factors. An LCA software can be very helpful in the process of collecting, structuring, and analysing the data, and can also contain direct links to LCI databases.

Simapro from PRé Consultants [40] is used in this thesis. According to the developers, Simapro can be used for life cycle assessment, sustainability reporting, carbon and water footprinting, product design, and generating environmental product declarations (EPDs). The software is useful for collecting and structuring data and also incorporates the Ecoinvent database (v2 and v3) which was described above. The software also includes information on a large number of impact assessment methods, and the LCIA and data communication is much simplified.

2.3.5 Uncertainties and weaknesses of LCA

Performing an LCA is a complex task which is associated with a large number of uncertainties. Although they are not always taken into account, uncertainties can have a large impact on the result of the LCA. In addition, it should be pointed out that an LCA does not give an absolute result, but only relative answers. The answer also depends on how the question was asked. The goal and scope definition is therefore an important part of the LCA, as it establishes why the study is performed, and what the boundaries and limitations are. As a consequence of these factors, two different LCAs cannot be directly compared to each other.

According to Ayres [95], there are two recurring problems in LCA: Firstly, the use of incompatible units, e.g. energy and mass, and secondly, the widespread use of generic, average, or theoretical data. Finnveden, et al. [96] divide the uncertainties according to their source and type. The main sources of uncertainty are the data, the choices made by the LCA practitioner, and the relations. The data can for example be variable due to time or external conditions, be miss-specified, incomplete, or simply erroneous. The choices may be inconsistent with the goal and scope, or even between alternative processes in the same analysis. Relations may be incomplete, wrong, or incorrectly implemented in the software. Another criticism of LCA is that it does not properly address impacts related to e.g. land use, including impacts on biodiversity, and resource aspects, including freshwater resources [96].

One way of reducing the impact of uncertainties is to create regulations, guidelines, or recommendations for how an LCA in a specific field of context should be performed. However, Finnveden, et al. warns that recommendations can sometimes be in conflict with science, leading to more confusion, and caution is recommended. Today, LCA methodology is detailed in ISO standards (as described in Section 2.3.1) and there are also guidelines for specific types of LCA. The use of guidelines in this thesis is discussed in Section 6.1.3.2.

It is also possible to quantify the uncertainty using statistical methods. In some databases, for example in the Ecoinvent database, most of the data include probability distributions. This makes it possible to calculate a range of probable results, for example using Monte Carlo simulations. This topic is further discussed in Section 6.1.3.7.

Chapter 3: PV/T technology and applications

3.1 PV/T technology

Photovoltaic-thermal (PV/T[9]) technology is a combination, or hybrid, of photovoltaic (PV) and solar thermal technology. While PV modules deliver electricity and solar thermal collectors deliver heat, a PV/T module delivers electricity and heat simultaneously, in the same module.

The basic idea of the PV/T concept is to utilize more of the solar radiation by also harvesting the heat that is generated in PV modules. Since PV cells generally become less efficient with increasing cell temperature, the heat removal has a double benefit: cooling the modules and at the same time making use of the "waste" heat. The concept is also sometimes referred to as solar co-generation or solar CHP (combined heat and power), or tri-generation when solar cooling is included.

A solar cell converts around 10-20% of the incoming solar radiation to electricity; the rest of the radiation is either reflected or converted to heat in the cell. A PV module can reach temperatures of up to 70°C during operation. As described in Section 2.1.3.1, the efficiency of solar cells typically decreases by around 0.5% per °C increase in cell temperature, and overheating can in some cases also cause structural damage to the module.

By cooling the module with air or liquid, the efficiency of the solar cells can be increased. Furthermore, the total efficiency of the module can be drastically increased by also utilizing the energy that is available in the cooling medium. This is the basic concept that led to the development of PV/T technology. [97]

The focus in this thesis has been on current PV/T technology and on products that are available on the market. However, a brief overview of research and development of PV/T is presented in the following sections along with a description of different PV/T concepts.

3.1.1 Review of previous research and development

The PV/T concept is not new, but there has been an increased activity in PV/T research and development since the 1990s. Since the start of the century, a growing number of commercial products have been introduced on the market. Several reviews describing this development have been published in recent years, for example by Zhang et al.[98], Tyagi et al. [99], and Chow et al. [97].

PV/T technology was first proposed as early as in the 1970s [100], also in combination with heat pumps [101], and with concentrating photovoltaics [102]. The work that followed the initial concepts mainly focused on flat plate collectors with air or water cooling [97]. The influence of the module design, such as glazing and of the construction of channels, on performance was studied by several research groups [103]. Examples of different design

[9] Photovoltaic-thermal technology is referred to with several abbreviations in literature, including PV/T, PVT, PV-T, PV-Thermal and solar hybrid. PV/T is used consistently in thesis.

concepts for air and water based systems are shown in Figure 17. Different materials were also tested, such as the polymeric PV/T module developed by Sandnes and Rekstad [104].

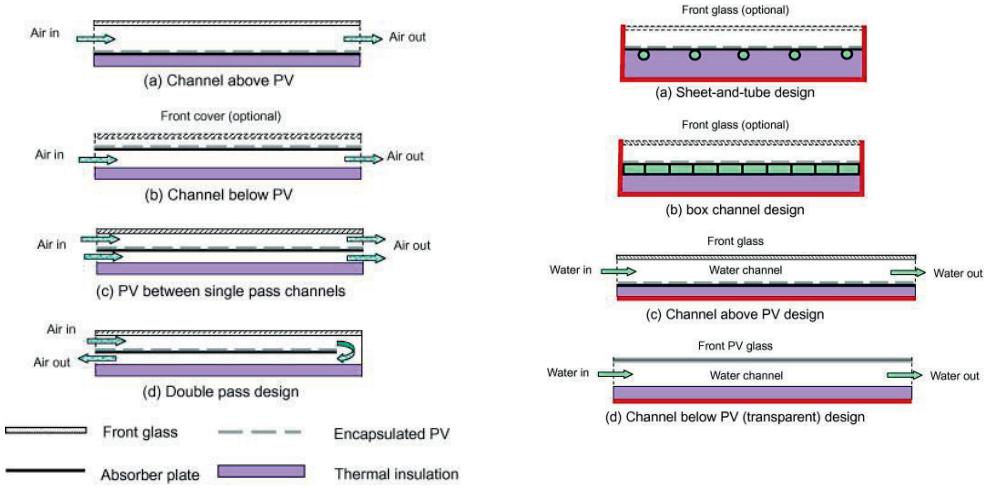

Figure 17. Cross-section of some common designs for PV/T-air (left) and PV/T-liquid (right). Reprinted from Chow, et al. [97]. Copyright (2016), with permission from Elsevier.

Several research groups also focused on creating numerical models to evaluate the performance of PV/T modules and systems, for example , Sopian, et al. [103], and Zondag, et al. [105]. Many research groups have also used simulation programs, notably TRNSYS, in their analyses. Several TRNSYS models of PV/T modules have been created for example by Collins [106], who also made an overview of existing models, and Stegmann, et al. [107].

A large number of experimental studies have been performed. For example by Tripanagnostopoulos, et al. [108], who tested several configurations of air and water PV/T modules, also including reflectors to improve the performance; Chow, et al. [109], who studied a façade-integrated system in Hong Kong; Corbin and Zhai [110], who studied a PV/T concept for building integration; and Dupeyrat, et al. [111] who measured the performance of covered PV/T prototype in several operation modes, achieving performance values close to those of equivalent PV modules and solar collectors.

A comprehensive overview of different aspects of PV/T technology was published by Michael, et al. [112]. They studied the advantages and drawbacks of e.g. different solar cell technologies, material choices, designs, and applications, and also outlined areas in need of more research. The thermal performance of materials, reliability studies, and introduction of nanotechnology were some of the proposed future research areas.

Zondag, et al. [113] made a theoretical study of nine different PV/T concepts to establish the expected performance, and also tested one concept experimentally. They studied the impact of glazing and absorber design on the thermal and electrical efficiency. They found that a single cover sheet-and-tube was the most promising concept for DHW systems, but that uncovered collectors with heat pumps had potential for low-temperature applications.

Fortuin, et al. [114] carried out a study of PV/T development from a more conceptual point of view, and also outlined the future research needs. They focused especially on collector insulation and stagnation protection, and collected results from performance tests of several prototypes. One of the tested PV/T prototypes had a thermal performance in line with a good solar thermal collector.

More recent studies also focus on the application of PV/T technology, especially for electricity supply, heating, and cooling of buildings. Bazilian, et al. [115] made a general overview of the potential for PV/T technology in the built environment, and also calculated the economic payback time of several types of installations. Glazed PV/T collectors for swimming pool heating were found to have the shortest payback time. The authors also pointed out the potential of PV/T façades, which could provide electricity, hot water, as well as architectural uniformity compared to separate PV and solar thermal installations.

Building projects including PV/T modules have been studied by among others Mei, et al. [116], who performed a study of the ventilated PV façade at Mataró Library; Athienitis, et al. [117], who studied a prototype of a building integrated transpired PV/T collector; and Kazanci, et al. [29], who evaluated the PV/T system on the Danish Solar Decathlon building from 2012.

A few international projects on PV/T technology have been carried out. In 2005, the International Energy Agency Solar Heating and Cooling Programme (IEA SHC) initiated Task 35 – PV/Thermal Solar Systems, which was dedicated to increase the understanding of the concept and contribute to the development of a commercial market and international performance standards [118]. Among other things, the project compiled an overview of PV/T systems and projects (used as a reference document for the overview in Section 3.2), issued recommendations for characterization and monitoring of PV/T systems, and performed and international market survey.

In 2006, the report "PVT roadmap – A European guide for the development and market introduction of PV-Thermal technology" was published by the PVT Forum, which was a part of the EU project PV Catapult, in an effort to gather the scattered research community [119]. This report described the state of the art, market situation, and market potential for PV/T technology in Europe, with the aim to "identify promising markets for PVT and to identify the economical, policy, legislative, and technical bottlenecks".

The residential market for space heating and domestic hot water preparation was seen as the most promising in the short and medium term, including both single-family and multi-family houses. The building sector, with actors such as real estate managers, housing cooperatives, and energy companies, was expected to be a market driver in the early stage. The combination of PV/T and heat pumps was also seen as a promising application. On the other hand, the lack of standardisation and certification as well as unclear funding schemes was already then identified as a barrier to further market development. [119]

3.1.2 Types of PV/T

A number of different PV/T concepts has been developed over the years, and the concepts are so different that is makes little sense to discuss "PV/T systems" without further specification of

technology or application. It has been pointed out that a more precise terminology is needed in order to characterize the different PV/T systems, not least with regard to standardisation, certification and funding schemes [120].

A general distinction can be made between PV/T technologies that use air as a heat transfer medium, and technologies that use a liquid heat transfer medium. (From now on, air and liquid based PV/T concepts will be referred to as PV/T-air and PV/T-liquid in the text.) Furthermore, PV/T concepts are constructed based on combinations of different PV technologies, such as crystalline or thin film PV, and different solar thermal technologies, such as flat plate collectors, evacuated tube collectors, or concentrating collectors.

There are also some concepts that are sometimes referred to as PV/T systems, but that do not utilize specific PV/T technology. These are for example installations where heat from a ventilated PV façade is used in building ventilation systems, or where PV cells and thermal collectors are installed side by side. Side by side systems will not be discussed here.

Flat plate collectors with air or liquid heat transfer appear to be the most commonly studied type in literature, and it is also the technology used in the greatest number of installed systems today. One reason is probably their similarity to PV modules and flat plate solar thermal collectors.

A brief overview of different PV/T types are given in the following sections, based on the PV/T types identified in the PV/T roadmap [119]: PV/T-liquid, PV/T-air, ventilated PV, and concentrating PV/T. A few examples of commercially available products is also given. The overview in this thesis is mostly focused on the European market, since this is also the focus area of the building analysis. A few Chinese producers were found during the market review, but it has been difficult to obtain further details on e.g. module performance, production, or installed systems.

3.1.2.1 PV/T with liquid heat transfer

A distinction is generally made between covered and uncovered PV/T modules (sometimes referred to as glazed and unglazed). The nomenclature is in this case somewhat confusing, since both types are actually covered by a protective glass sheet like the one used for PV modules. The covered or glazed PV/T modules have an additional transparent cover at a distance from the absorber surface for thermal insulation.

Uncovered, or unglazed, PV/T modules are similar to PV modules with some form of attached heat exchanger, e.g. tubes or a flat plate. The modules can be uninsulated or insulated to reduce heat loss from the back and edges, but the electricity output is prioritized over the thermal output.

Covered, or glazed, modules are more similar to solar thermal collectors with PV cells added on top. The PV cells may be added on the front glass or below it, and may be spaced to form a semi-transparent surface. The glazing reduces the thermal losses and these types of modules therefore generate higher temperatures and larger annual thermal yields than uncovered modules, at the expense of the electric output.

As mentioned in Section 1.2.2, the focus of this thesis is flat plate PV/T modules with a liquid heat transfer medium. The reason for this limitation is technology maturity and similarity to existing systems. Flat plate PV/T with liquid heat transfer was found to be the most mature PV/T technology with the highest number of market available products, at least in Europe, which is the focus of this study [120]. In addition, it bears the greatest similarity to existing solar energy installations in Europe, which are mostly PV modules and flat plate solar collectors (see Section 2.1.6). It is also easily combined with hydronic heating systems, which offer energy source flexibility. This is regarded as an important quality for future building energy systems in Norway.

One of the oldest producers in the market is the solar thermal company Turkish Solimpeks, who started their production of PV/T in the early 2000s. They produce two versions of their collector Volther: one prioritising thermal output (PowerTherm) and one prioritising electric output (PowerVolt).

The French producer Dualsun is one of the few on the market who specialise only in PV/T modules and do not also produce PV modules or solar thermal collectors. Their unglazed Wave (formerly Hybrid) was also the first module to be certified with the Solar Keymark for PV/T modules.

Other products on the market include Wiosun PV-Therm from German Solarzentrum Allgäu and the Hybrid from the Swiss producer Meyer Burger.

3.1.2.2 PV/T with air heat transfer and ventilated PV

A PV/T-air system is a relatively simple construction that can be realised with conventional PV modules, although specialised products also exist. An air gap is usually provided behind PV installations to ensure proper ventilation and cooling of the modules. Making active use of this heated air in such a ventilated PV system turns it into a PV/T system.

PV/T-air collectors are generally designed for direct use in the ventilation system of a building, but can also be used for hot water preparation if an air/water heat exchanger is included. However, the efficiency is generally lower than with a PV/T-liquid system. Other applications may be drying or solar cooling. [119]

SolarWall from Conserval Engineering is an example of a commercially available PV/T air collector. It is available both as a façade module where PV modules are installed on top of transpired solar collectors (shown in Figure 18) or as a ducted module suitable for roof integration [121].

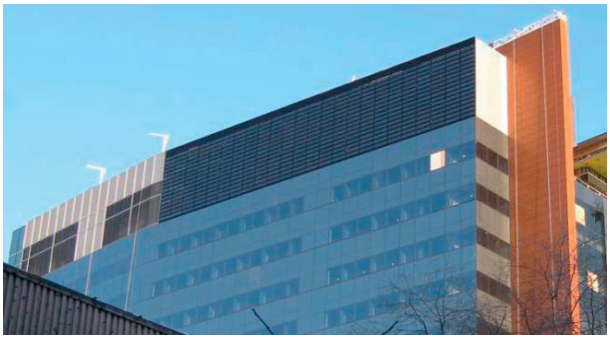

Figure 18. The SolarWall PV/T facade at Concordia University, Montreal. The PV/T system is the dark blue area on the upper part of the façade. Photo courtesy of Conserval Engineering.

3.1.2.3 Concentrating PV/T

In concentrating PV/T (CPVT) collectors, reflective or refractive concentrators are used to focus solar radiation, resulting in high electric efficiencies and high temperatures. A review of the development in CPVT technology was recently published by Sharaf and Orhan [122], who made a general distinction between high-concentrating and low-concentrating PV/T collectors. Low-concentrating CPVT may be appropriate for residential applications, while high-concentration CPVT produces hot water or steam at a significantly higher temperature than flat plate collectors and therefore has a wider range of application areas [122]. Examples of concentrating collector types are parabolic dish collectors, parabolic trough collectors, and linear Fresnel collectors.

Parabolic dish collectors use curved mirrors to focus the radiation onto a small PV cell area and thermal unit. Parabolic trough collectors use curved mirrors and a tubular thermal receiver unit. Fresnel collectors use Fresnel lenses to focus the sunlight onto a thermal collector. Fresnel collectors can be made relatively flat and therefore has potential for use in buildings. Other CPVT systems typically use tracking, but it is not always used in linear Fresnel collectors. [122]

More than 50 experimental and theoretical studies of CPVT were found by Sharaf and Orhan [122], but only six companies with prototypes or actual products. Of these, two were parabolic trough collectors, two were linear Fresnel collectors, and one a parabolic dish collector. (No information was found on the technology of the sixth type.)

Zenith Solar/SunCore produces a high-concentrating CPVT of the dish type with two-axis tracking. The radiation is reflected onto a multi-junction PV cell and heat exchanger. The collectors are claimed to have a combined efficiency of at least 72% and can deliver water with a temperature up to 100°C. According to the producer, the concept works best in hot climates. [123]

Figure 19. Parabolic trough PV/T collector. Photo courtesy of Absolicon [124].

The Swedish company Absolicon (formerly Arontis) was founded in 2007 and makes a parabolic trough PV/T collector, the X10 (Figure 19). The collector delivers electricity and water at up to 75°C. The collector is commercially available and installed in several places in Europe. [124]

Chromasun has developed a compact micro-concentrator unit with linear Fresnel concentration together with the Australian National University. The unit, which is developed for rooftop integration, can reach a maximum output temperature of 200°C. [125]

3.1.2.4 Other PV/T concepts

Several other PV/T concepts have been modelled or tested, but few have so far reached the market. The PV/T module Virtu from Naked Energy is, according to the producers, close to market ready. The module, shown in Figure 20, is a PV/T-liquid module using vacuum tube collector technology. According to the company, the concept has up to 80% combined efficiency and delivers the same energy output in half the area compared to separate PV and solar thermal installations. The output temperature is in the range 40-85°C. Additional benefits are stated to be less shading problems than flat plate collectors as well as reduced soiling and dust collection. [126]

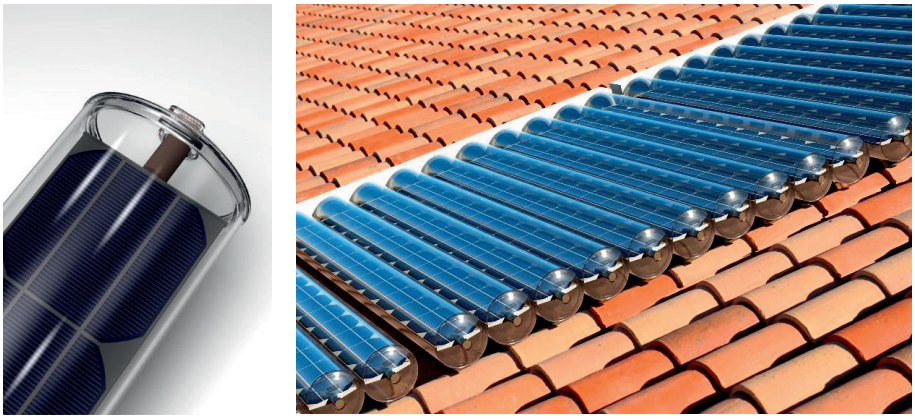

Figure 20. The Virtu vacuum tube PV/T collector. Photo courtesy of Naked Energy.

There has also been efforts to create components for building integration. Anderson et al [127] developed a BIPV/T system for integration into roofs. The system was tested in an outdoor steady state test in New Zealand. A hybrid solar window with water cooled PV cells, tiltable reflectors, and anti-reflection treated glazing was developed by Davidson et al. [128, 129] at Lund University in Sweden. The PV cells are water-cooled, and reflectors provide additional heating of the water pipes. The windows are installed in a low energy single family building in Älvkarleö (60.57N, 17.45E) in Mid-Sweden, shown in Figure 21.

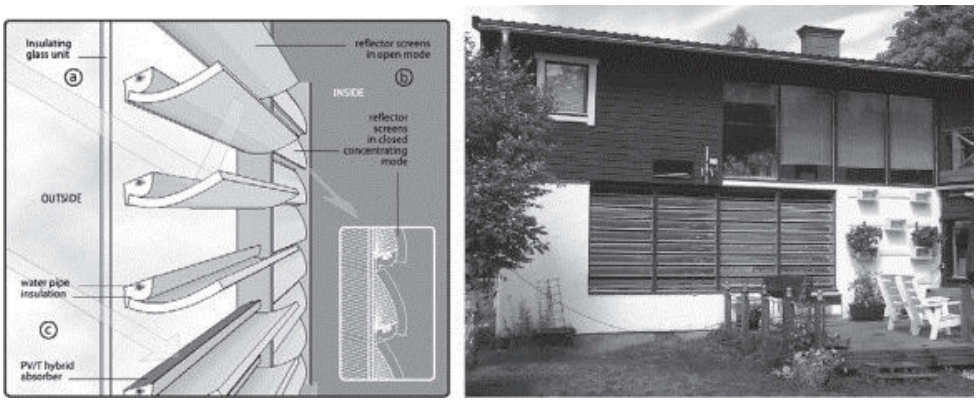

Figure 21. The concept of the hybrid PV/T window (left), and the Swedish pilot installation (right). The PV/T window is located on the lower, white part of the wall. Reprinted from Davidsson, et al. [128]. Copyright (2016), with permission from Elsevier.

3.1.3 The PV/T market

The market for PV/T systems is still very small compared to the markets for pure photovoltaic or solar thermal systems, but an increase in the number of commercially available products can be identified in the last decade. The increased interest in PV/T is probably, at least to a certain extent, driven by the increasing interest in energy efficient buildings worldwide. Stricter energy requirements for buildings, such as the European Commission's goal that all new buildings

shall be “nearly zero energy buildings” by 2020 [19], puts pressure on the building industry to find solutions for on-site renewable energy generation.

The PV/T roadmap (described in Section 3.1.1) identified around 20 developments or market attempts, but only nine commercial actors (three PV/T-air systems, two unglazed PV/T-liquid, one glazed PV/T-liquid, and three concentration PV/T systems). It was concluded that the actual number of installations was small, and with no experience from long term operation. A few of the identified products or producers are still on the market today, while some have disappeared and others have emerged. Several of the developers described in the roadmap had closed or halted development due to technical or material-related problems in the production. [119]

A market survey published in Task 35 in 2007 found ten producers of commercial PV/T products, and six that had gone out of the market [4]. In addition, the study found 25 concepts that were under development.

A recent study in the project PVT-Norm in Germany found 41 producers of PV/T collectors, showing a significant increase in commercially available products [5]. The large majority of these, around 80%, were uncovered PV/T collectors. Even though the PV and solar thermal markets are both dominated by Chinese companies, most of the PV/T producers found in the study were European. It is, however, a testament to the instability of the PV/T market, perhaps to the solar energy market in general, that several of the companies from the review have gone bankrupt or closed down production during the course of writing this thesis.

Task 35 also published a study in which architects, engineers, building owners, and solar dealers in Canada, Germany, Denmark, Sweden, Italy and Spain were interviewed [11]. One conclusion from the survey was that the markets were very country-specific and depended to a large degree on the composition of the existing PV and solar thermal markets. The PV/T market maturity was found to depend mainly on to what degree PV was a part of the earlier market for energy systems.

The type of PV/T systems that was dominating the market were also found to be country-specific. In Canada, the aforementioned Conserval Engineering, who produces transpired solar collectors and PV/T-air systems, was found to be dominating the market with their SolarWall. Sweden has traditionally had a stable market for liquid-based solar thermal collectors, and air-based PV/T systems were regarded with scepticism by the Swedish interviewees, even though the climate in Sweden and Canada is relatively similar. However, the number of PV/T systems installed in Sweden to this date is very small.

China is by far the largest solar thermal market in the world with 86% of the market and 64% of the total installed capacity [12]. Most of the solar thermal systems in China are evacuated tube collectors for water heating, while glazed flat plate collectors dominate in the rest of the world. PV/T-air systems is not at the focus of research and development in China, but more interest is put in PV/T systems for water heating and with direct connection to heat pumps. According to Fang et al [11], it is expected that PV/T hot water systems will become one of the main solar system types in buildings in China.

Favorable government policies and economic incentives are probably the largest drivers for all types of solar installations. However, since a PV/T system delivers both electricity and heat, there may be confusion as to how it should be classified. As mentioned earlier, there is also a lack of adequate terminology to describe PV/T systems, which can also influence the incentives.

The relation between standards and innovation, and the effect on market development, has been analyzed by Kramer and Helmers [21]. They found that the lack of standards and certifications is a strong barrier to market development. It leads to a lack of technical information on the products, restrictions in government incentives, and an uncertainty among consumers. The recent developments in certifications specifically for PV/T products, such as the Solar Keymark [22], can therefore be expected to have a positive influence on the market.

3.1.4 PV/T performance

Since the operation of the thermal and electric parts of the component affect each other, evaluating and communicating the performance of PV/T modules involves some additional difficulties compared to doing the same for separate PV and solar thermal systems. For example, the electric output is influenced by the temperature of the module, which is directly dependent on how the thermal system is operated. While the electric output can be exported to the grid, the thermal output depends strongly on the design and operation of the whole thermal energy system, including user profiles and storage options. It is therefore also difficult to directly compare the performance of different PV/T systems. [119]

Since PV/T modules generate heat and electricity simultaneously it is necessary to use some kind of method to combine or compare the output of the two energy carriers. Several approaches are used in literature, including primary energy, cost savings, exergy, or simple addition [130].

There has recently been developments in the certification and standardisation of PV/T modules. In Europe, the Solar Keymark certification scheme for solar thermal collectors now also include a certification especially for PV/T modules [131]. In this certification procedure, it is stated that the thermal efficiency of the modules should be determined with electrical production under maximum power point (MPP) conditions, i.e. optimal operation. The electrical performance is evaluated under STC conditions as usual.

Some general performance trends of PV/T technology were given in the PV/T roadmap [119]. It was found that the electrical output was in general around 40% of the thermal output, but in terms of primary energy they were approximately equal. Interestingly, it was also found that both the thermal and electrical yield was typically lower than that of separate solar thermal and PV components. However, as they were generated by the same area, the total output per area was still significantly larger. As for all solar energy systems, the influence of the local climate conditions, including irradiation levels, temperature and duration of the heating season, are of great importance.

Due to the lack of standardisation, there has been no standard way of communicating the performance of PV/T modules. In a product data sheet, separate electric and thermal efficiencies are usually given. However, a combined efficiency, i.e. an addition of the thermal and electric efficiency, is sometimes used in performance descriptions. A combined efficiency does not take

into account the temperature of the thermal output, nor the different energetic value of electricity and heat. Some performance claims of selected manufacturers are given below.

Conserval engineering claims that their PV/T-air system SolarWall reduces the temperature of the PV cells by 10-20°C, which leads to an increased electrical output of 5-10%. The heat generation in the SolarWall system is reported to be three times that of the electrical output, and the total efficiency above 50%. The output is claimed to be 100 W/m^2 electricity and 200-300 W/m^2 thermal energy. [121]

Dualsun states that the cooling of the PV cells in their Wave module can increase the efficiency of up to 15%, and that an installation can generate 2-4 times more energy than a standard PV installation. The modules are also stated to generate around 85% heat and 15% electricity. The thermal performance was measured to 549 W_{th}, and the maximum temperature up to 74.4°C. [132]

Wiosun claims that it is possible to momentarily increase the electrical efficiency of the PV-Therm modules by up to 30%. The rated thermal performance (at η_0) is 698 W_{th}, and the maximum temperature 75°C [133].

The performance of the Hybrid module from Meyer Burger has been measured in the project Suurstoffi in Switzerland (see section 3.2.3). According to measurements, the electricity output was increased by 10% annually compared to PV modules, and up to 20% during summer [134]. The measurements are reported to correspond well to simulations.

This thesis is focused on flat plate PV/T-liquid modules. Performance values for some of the market-available modules of this type are summarized in Table 2.

Table 2. Performance ratings of selected commercial flat plate PV/T-liquid modules.

Producer	**Module**	**Module type**	**Rated electric power at STC***	**Electrical efficiency at STC***	**Thermal power****	**Thermal zero-loss efficiency η0**	**Stagnation temperature**	**Ref.**
			W_p	%	W_{th}	%	°C	
Dualsun	Wave (formerly Hybrid)	Uncovered flat plate PV/T-liquid	250	15.40		51 (insulated) 55 (uninsulated)	74.4	[132]
Wiosun	PV-Therm (poly-Si)	Uncovered flat plate PV/T-liquid	190-200	17.40-17.80	*At ΔT = 5 K:* 781 (uninsulated) 878 (insulated)	71.50	75.0	[133]
Wiosun	PV-Therm (mono-Si)	Uncovered flat plate PV/T-liquid	195-205	18.43-18.84	*At ΔT = 5 K:* 781 (uninsulated) 878 (insulated)	71.50	75.0	[133]
Solimpeks	Volther PowerTherm	Covered flat plate PV/T-liquid	180	Not given	*Peak power:* 690	Not given	134	[135]
Solimpeks	Volther PowerVolt	Uncovered flat plate PV/T-liquid	200	Not given	*Peak power:* 629	Not given	101	[135]
Meyer Burger	Hybrid	Uncovered flat plate PV/T-liquid	285	17.4	*Output at T0:* 900	60	80	[136]
PA-ID GmbH	2Power	Uncovered flat plate PV/T-liquid	260	Not given	*Peak power:* 719 (at STC) 557 (at NOCT)	Not given	85	[137]

**Standard test conditions, see Section 2.1.3.1.*
***The thermal power is given in several different ways by the producers.*

3.2 PV/T systems in buildings

PV/T technology is an interesting technology for building application for several reasons. In general, buildings require heating as well as electricity, and sometimes cooling, all of which can be provided by a PV/T system. Building integrated PV systems are especially prone to overheating due to the limited possibilities for backside ventilation, and cooling of the modules therefore becomes particularly interesting. PV/T modules can also provide architectural uniformity compared to PV and solar thermal systems installed side by side. In projects with ambitious energy targets, different solar energy installations may start to "compete" for the limited available area on e.g. roofs and façades. A hybrid system makes it possible to generate solar electricity and heating from the same area.

Due to the large variety of PV/T technologies, there is also a large range of possible building applications. An examination of the use of PV/T in buildings is presented in Paper I, and summarised here. The paper is based on a review of relevant scientific publications and projects, as well as communication with PV/T system manufacturers and installers. An evaluation of the suitability for building use, including possibilities for integration, for some of the technologies is also provided in the paper.

Four main types of installations were identified, which included the majority of the installations: ventilated PV installations and air-based PV/T, small scale PV/T-liquid systems, large-scale PV/T-liquid systems with ground source heat pumps, and industrial and non-residential buildings with concentrating PV/T installations.

The increased interest in building integrated solar energy systems was probably of importance for the increased interest in PV/T technology in the 1990s [97]. During the last decade, PV/T installations have developed from largely being custom-built pilot or research projects, to also include a growing number of commercial installations. Due to the rapid development in the solar energy market, a review of installed systems gets outdated quickly. Some additions are therefore made to this text compared to the overview in Paper I.

3.2.1 Ventilated PV and PV/T-air systems

According to the Chow et al., PV/T-air systems were more readily used in buildings in Europe and North America than PV/T-liquid systems, even though the efficiency of the PV/T-liquid systems is higher. [97] The same tendency was also found in the overview of PV/T projects conducted by IEA SHC Task 35 in 2007: out of 20 systems, only two used liquid heat transfer medium [138].

One reason for the prevalence of air systems may be that they are relatively simple compared to liquid systems. Making use of the excess heating in a ventilated PV system creates a form of PV/T system. One early example of this type of installation is the Mataró Library in Spain, which has a 20 kWp ventilated PV façade with solar air collectors for preheating of the ventilation air [116].

However, there are also commercial PV/T-air products. A large commercial actor is the aforementioned Canadian company Conserval Engineering. The company has several

installations around the world, including a 300m^2 installation at Concordia University in Montreal (Figure 18), rated at 24.5 kW electric and 75 kW thermal power. The installation provides heating to the ventilation system, and the system performance is monitored by the university.

Most PV/T-air systems seem to be installed on larger, non-residential buildings, but there are also PV/T-air systems on residential buildings. One example is the SolarWall installation on the roof of the home/office of architect George Beeler in California, USA, where 22.6 m^2 PV/T modules provide 100% of the annual electricity need and contributes to preheating of the space heating and domestic hot water [139].

3.2.2 Small and medium scale PV/T-liquid systems

In the review presented in Paper I it was found that more of the recent installations used PV/T modules with liquid heat transfer, compared to the dominance of air systems in earlier days. However, the situation appeared to be very country-specific, and sometimes completely dominated by one manufacturer or installer.

While PV/T-air systems may be easier to install, PV/T-liquid systems are more efficient [97]. The use of PV/T-liquid collectors makes it possible to integrate the PV/T system into hydronic heating systems in buildings, which can be adapted to low temperature heat sources. The collectors can be connected to a storage tank and combined with other heat sources, such as different types of heat pumps or biomass boilers. The systems can be used for space heating, DHW preparation, or both. Examples of these types of systems are found in several countries.

In the UK, the number of PV/T installations increased rapidly from 2008 due to the operations of the company Newform Energy, who marketed and installed Solimpeks PV/T modules. Solimpeks modules are also installed in Turkey, France, and Australia [140, 141]. One of the UK installations is Crossway, which was the first certified passive house in the UK (Figure 22).

Figure 22. The Crossway passive house, using flat plate PV/T modules from Solimpeks. Photo: Hawkes Architecture.

According to Newform Energy, who went into administration in the late 2014, they had installed over 300 PV/T installations in the UK [142]. The bankruptcy came close after a subsidy debate in the UK, where it appeared that PV/T customers receiving feed-in tariffs (FiTs) would not eligible for economic support through the Renewable Heat Incentive (RHI) [143].

The French market is currently dominated by the PV/T producer Dualsun, which has around 30[10] monitored installations throughout the country. Most are in the range of 6 to 12 modules (1.5-2 kW_p), but there are also larger installations. The smaller residential systems typically include both flat plate PV/T collectors and regular PV modules. A system of 6 modules and a 300 l storage tank is reported to cover around 65% of the hot water demand for a single family building in Marseille in southern France (Figure 23) [144].

PV/T installations are also used in more spectacular applications, such as the off-grid system at the Arpont shelter in Vanois National park, France (Figure 23). The modules are installed facing from east to west in order to match the energy demand of the shelter, which is mostly during morning and evening. The vertical installation prevents snow from accumulating on the system. [145]

Figure 23. A residential PV/T system in Marseille (left), and the installation at Arpont Shelter (right). Photos courtesy of Dualsun.

The German company Wiosun also has several installations in Europe. According to the company, the market in Switzerland is promising because of the strict regulations regarding building heating, while the German market is more difficult due to particulars in the subsidy schemes [146]. Some examples of building integrated systems exist, such as the residential building with Wiosun modules in Figure 24 (left). A product developed for buildings is shown in Figure 24 (right), where Wiosun modules have been made with brick-red backsheets and frames. [147]

[10] Information from late 2014.

Figure 24. A building integrated PV/T system with Wiosun modules (right) and red PV/T modules by Wiosun. Photo: Wiosun [147]

3.2.3 Large scale PV/T-liquid systems with ground source heat pumps

Several authors conclude that uncovered flat plate PV/T collectors are promising when used in combination with heat pumps [97, 120], perhaps especially in combination ground source heat pumps with bore holes [148, 149]. Several of the smaller systems described in Section 3.2.2 also include heat pumps of different types, although typically not with the ground as the heat source.

Probably the largest system to date is the PV/T system installed in the area Suurstoffi in Rotkreuz-Risch, Switzerland. The second stage of the project was carried out in 2014 and included over 3515 m^2 hybrid PV/T modules from the Swiss company Meyer Burger [150]. The modules are mounted horizontally on the buildings' roofs, as shown in Figure 25. The area is designed with a low temperature heating system, and the thermal output of the PV/T modules is used for regeneration of geothermal boreholes. The system is an implementation of the Low-Exergy building concept introduced by Professor Hansjürg Leibundgut at ETH in Zürich [151]. There are also other large systems in Switzerland, including the 1000 m^2 installation at WBG Oberfeld close to Bern [152].

Figure 25. The Suurstoffi PV/T installation from above. Photo: Simon Büttgenbach/Meyer Burger Group.

In Scandinavia, several relatively large-scale PV/T installations have been installed in Sweden by the company Energiförbättring Väst AB (EFVAB), who markets and installs Wiosun modules. One of the largest installations is Jättens Gömme in the Gothenburg region, where 400 m^2 of unglazed PV/T collectors, 272 kW combined heat pump power, and 28 bore holes provide heating and hot water to 90 apartments. This is a refurbishment project, where PV/T has been used to upgrade an under-dimensioned borehole installation. [148] Norway's first installation, in Bergen in south-west Norway, is still only in the planning phase, but will use a similar concept with uncovered PV/T modules and ground source heat pumps [153].

PV/T and ground source heat pumps have also been studied theoretically by several research groups. The topic will be further examined in Chapter 5 of this thesis.

3.2.4 Concentrating PV/T

Since concentrating PV/T collectors generally provide water of a higher temperature than most flat plate collectors, they are more interesting for industrial and other non-residential projects.

The technology is proven to work in both hot and cold climates. An example from Sweden is shown in Figure 19, where the Swedish manufacturer Absolicon's concentrating PV/T collectors are installed on a local hospital in Härnösand, Sweden. The installation provides electricity, heating, and solar cooling to the operation theatre and the dental clinic [154].

Figure 26. A concentrating PV/T system from Cogenra. Photo: University of Arizona Tech Park.

An example from a hotter climate is the Cogenra installation on a building at the University of Arizona Tech Park (Figure 26), which delivers 191 kW thermal and 36 kW electric power to the building [155].

3.2.5 Conclusion

While the concept of PV/T modules was proposed already in the 1970s, it has not yet reached a widespread use. The early developments focused mainly on design issues, material choices, and performance testing. The research interest increased during the 1990s, possibly due to an increased interest in energy efficient building technology. In the more recent research, many studies also focus on applications of PV/T technology, for example in building energy systems.

A few international projects have been carried out to gather the research community and establish the drivers and barriers for further development, including the IEA SHC Task 35 and PVT Forum. The use of PV/T systems in residential buildings was pointed out as a potential application, and the combination with heat pumps was seen as promising.

In the recent decade or so, the number of installed systems has increased rapidly, and gone from largely custom-made components and pilot projects to commercial installations. During the same time, a shift can be seen from PV/T-air systems to PV/T-liquid systems.

The rapid development and changes in the PV/T market shows that it has still not reached a stable size. The market has also proven to be very sensitive to country-specific subsidy schemes (or lack thereof). Recent developments in testing and certification, such as the introduction of a Solar Keymark certification for PV/T modules, is of importance for further market development.

Chapter 4: Design of PV/T systems

4.1 PV/T system design

A PV/T module is a hybrid of a solar collector and a PV module, but also a complete technology in itself. The design of PV/T systems is in a sense also a combination of design principles from the two separate technologies, but some special considerations are required. The following sections discuss design issues for PV/T systems, based on concepts from PV and solar thermal system design.

4.1.1 Orientation

The orientation of a solar energy system is described by the direction it is facing (the azimuth) and the tilt angle of the modules. The appropriate orientation depends on how the output is to be used. For a grid-connected PV system with no restrictions on grid interaction, the objective is most often to reach as high output as possible over the whole year. The optimal angle for maximum output during the year can be established through geometrical calculations of the sun height and irradiation, and depends on the latitude of the installation. The optimal tilt angle for different locations in Scandinavia, as calculated by PVGIS, is shown in Figure 27.

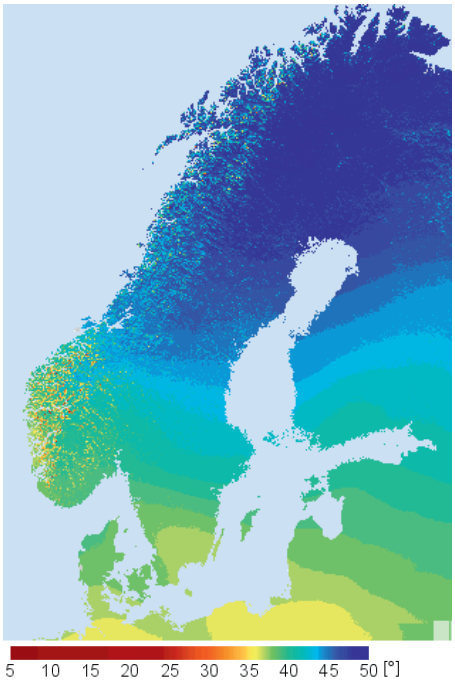

Figure 27. Optimal angle for solar energy installations in Scandinavia. Source: Google Maps (2016) and PVGIS [156].

A distinctive feature of the solar resource at northern latitudes is the large contrast between summer and winter, which was described in Section 2.1.1. This means that the optimal tilt angle

in summer is lower, and the optimal tilt angle in winter is much higher than the one for yearly optimal output. Solar thermal collectors are usually installed at higher tilt angles than PV modules, since the thermal energy output is typically more valuable during spring, autumn and winter, when the sun angle is low. In Scandinavia and other locations at high latitudes, it can also be beneficial to install solar energy systems on façades. For solar thermal systems, this strategy helps avoid overheating during the summer while shifting the output towards spring and autumn, the so-called shoulder seasons. For PV systems, it reduces the peak in the output during summer and midday, which can be beneficial if there are restrictions on grid transfer.

In the case of installations on limited flat areas, such as flat roofs, the high tilt angles at northern latitudes lead to problems with self-shading. There are in practice two alternative installation strategies: the modules can be mounted at a close to optimal tilt angle and spaced with enough distance to avoid shading, or they can be installed at a lower-than-optimal tilt angle, but closer together. In the latter case, the modules may also be installed with two orientations, which increases the number of modules that can be installed. Most of the recent large-scale PV installations in Norway use dual-orientation design, with south/north or east/west facing modules at low tilt angles. This increases the module area that can fit on a flat installation area, such as a roof or field. However, the performance and output of each installed module is decreased, compared to a system at optimal tilt angle.

The required distance d (m) in order to avoid row-to-row shading can be calculated according to Equation (18), where b (m) is the height of the rows , β (°) is the tilt angle of the modules, and γ (°) is the sun height at noon on the "worst case" day, i.e. lowest considered sun height. The sun height is the angle between the horizon and the sun. [157]

$$d = b \cdot \frac{\sin(180° - \beta - \gamma)}{\sin(\gamma)} \qquad (18)$$

As follows from Equation (18), the lower the sun height, the longer the required distance d will be. Calculations for a flat roof in Oslo show that the required distance between rows of PV modules installed at the optimal tilt angle is in the range of 10 m, if the sun height at noon in January (around 7°) is used. However, since only a small fraction of the solar radiation is available in winter, some degree of shading during this time might be tolerated.

The impact of shading on module performance is further discussed in Section 4.1.3. The impact of the tilt angle and orientation on the energy output and emission balance of a PV system is studied in Paper V, and discussed in further detail in Chapter 6.

4.1.2 Dimensioning

The dimensioning of grid-connected PV systems is relatively straight-forward if there are no restraints on grid transfer. In buildings with specific energy targets, the PV system may be dimensioned to cover the annual electricity demand, disregarding the mismatch in generation and load. The grid is used as a buffer, and electricity is exported during times of surplus generation, and imported during times when the demand is higher than the generation.

If there are limitations on grid transfer, the PV system may have to be dimensioned to cover the largest occurring loads, while avoiding excess export to the grid. As an example, the new Norwegian legislation for so-called electricity prosumers (producers and consumers), *Plusskundeordningen*, sets a limit to the power that can be exported to the grid [158]. At other times, the dimensioning of PV systems is simply due to economic or space limitations.

Domestic solar thermal systems should be dimensioned based on the load. In Northern Europe, it is not possible for a solar thermal energy system to meet the whole thermal energy demand over the year (without and extremely large storage), due to the long heating season and limited solar radiation during the colder part of the year. Solar thermal systems are therefore usually dimensioned for the summer load, which includes only DHW. The space heating is of a lower importance, at least for the dimensioning, since the thermal yield is lower during the cold months [56]. The mismatch between energy demand and solar energy availability is shown in Figure 28, exemplified by results for the Living Lab. The solar energy availability peaks during summer, when the energy demand is lowest, and is basically zero during the coldest months.

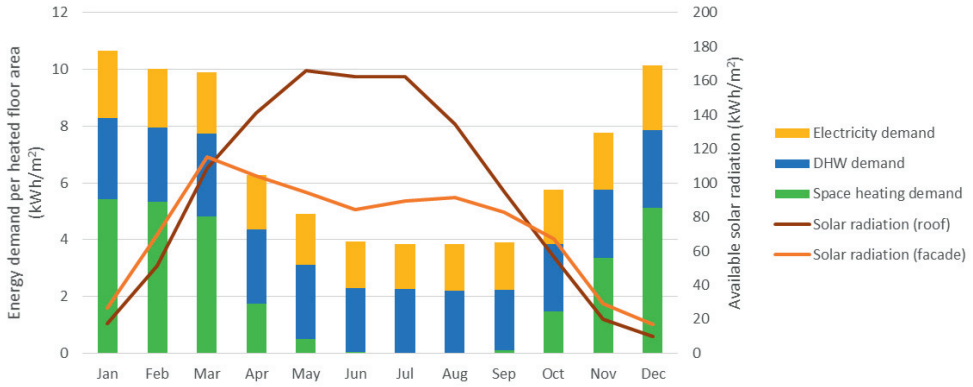

Figure 28. The energy demand versus solar radiation availability for the Living Lab, as simulated in Polysun.

A well-designed solar energy system can cover around 40-60% of the annual DHW demand, or around 15-20% of the combined demand for DHW and space heating [56]. An annual energy yield of 300-700 kWh/m^2 collector area can be expected [54]. Scandinavian rule-of-thumb values for dimensioning solar thermal systems are given in Table 3. The appropriate dimensioning will of course depend on, among other factors, the actual DHW and heating demand, as well as the orientation and type of solar collectors.

Table 3. Rule-of-thumb values for dimensioning solar thermal systems for a single family residential building in Scandinavia [56].

Type of system	Collector area	Storage volume	Solar fraction
DHW only	4-6 m^2	300-500 l	40-60%
DHW and space heating	8-15 m^2	300-1000 l*	15-40%

** Depending on which other heat source(s) are used.*

For a regular residential solar thermal system it is not efficient, economically or technically, to install a larger system to achieve a higher solar fraction, since this will lead to excess energy during the summer. The consequences are overheating, a lower efficiency of the system, and also possible damage to components. As shown in Figure 28, an installation on the façade would have a less pronounced peak during the summer, which reduces the risk of overheating. In this case, the system size can be increased to achieve a higher solar fraction in autumn and spring.

Due to the relatively low output temperatures, the dimensioning of uncovered PV/T systems is similar to the dimensioning of PV systems. The risk of overproduction and overheating during summer is low in Northern European climates. In the case of covered PV/T modules, the dimensioning should be based on the same principles as for solar thermal systems, but the installed area can be increased due to the lower thermal efficiency compared to solar collectors.

4.1.3 Shading and soiling

Shading and soiling of modules is probably one of the major problems for building integrated and building added solar energy systems. Shading can be caused by e.g. chimneys, trees, or neighbouring buildings. It is important to design the system so that shading is avoided, to the extent this is possible.

The major soiling factor in Norway is snow coverage. An example from the Living Lab after snowfall is shown in Figure 29. The tilt angle of the modules is steep enough to allow the snow to slide off, but the shape of the roof stops the snow from sliding off completely. The snow also sticks to the module frames, and in this case frameless modules could have reduced the problem slightly.

Figure 29. ZEB Living Lab after a snowfall in late November 2015. Photo: Clara Good.

There are so far few studies of how much snow and other types of soiling affect solar energy systems, in Norway or elsewhere. The impact of snow can be very site-specific, and local measurements are necessary to get accurate information of the conditions. The new preliminary version of the Norwegian standard NS 3031 [20] includes standardised values for the soiling factor for solar energy modules at different locations and tilt angles in Norway. The values for Oslo and Trondheim are presented in Table 4.

Table 4. Soiling factors for solar energy systems in Oslo and Trondheim, according to prNS 3031 [20].

	Tilt	**Jan**	**Feb**	**Mar**	**Apr**	**May**	**Jun**	**Jul**	**Aug**	**Sep**	**Oct**	**Nov**	**Dec**
Oslo	*0-15°*	60	75	60	2	2	2	2	2	2	2	15	45
Trondheim	*0-15°*	60	75	45	8	2	2	2	2	2	2	15	53
Oslo	*15-25°*	40	50	40	2	2	2	2	2	2	2	10	30
Trondheim	*15-25°*	40	50	30	5	2	2	2	2	2	2	10	35
Oslo	*25-40°*	20	25	20	2	2	2	2	2	2	2	5	15
Trondheim	*25-40°*	20	25	15	3	2	2	2	2	2	2	5	18

Due to the recent publication of prNS 3031 (December 2015) these values are not used in the case studies described in this thesis.

In the case of PV modules, the relationship between the shaded module area and the reduction in energy yield is not proportional. Depending on the type of module and how it is shaded, the reduction in energy output may be very large. Since the modules are built up of strings of cells, the shading of one cell will influence the current of the whole string, which will be reduced to the level of the shaded cell.

The principle is shown in Figure 30 for a thin film module and a crystalline silicon module. The thin film module consists of one string of cells, connected horizontally in the figure. The crystalline silicon module has two strings with bypass diodes. In the left figure, the lower part of the modules is shaded. The power output reduction is around 10% for the thin film module, the same as the shaded area. In the crystalline silicon module, cells in both the two strings are completely shaded, which reduces the output of the module by almost 100%. In the right figure, the power reduction in the thin film module is around 100%, since two cells in the string are completely shaded. Only one string is affected in the crystalline silicon module, and the output is therefore reduced by around 50%. [159] Since modern crystalline silicon PV modules typically have three bypass diodes, the reduction in the right hand shading case would have been around 33% if such modules had been used.

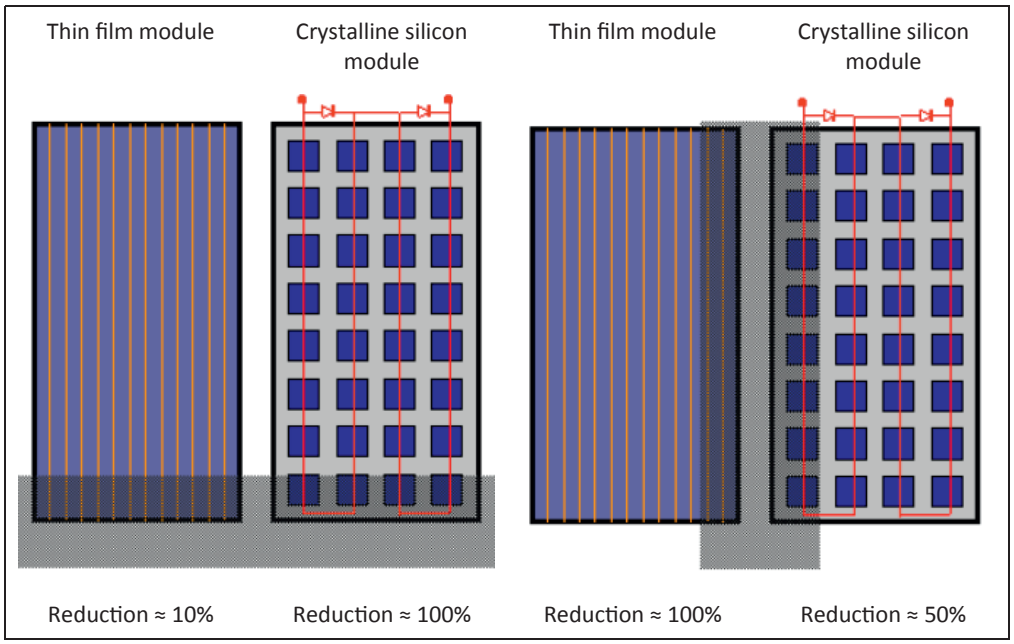

Figure 30. The effects of shading on energy output are shown for two types of modules and two shading cases. Figure from SolEL-programmet [159], used with permission.

Shading and soiling also affects the performance of solar thermal collectors, but in this case the decrease in output is more or less proportional to the shaded area. Since PV/T modules contain solar cells, they are affected in a similar way to PV modules. It is therefore important to avoid shading and soiling as much as possible in the design of PV/T systems.

4.2 PV/T and heat pump systems

4.2.1 Hybrid solar energy systems

Solar energy is a variable energy source. The annual and diurnal variations are regular and predictable, but variations in weather and cloud conditions can create large fluctuations in the energy output of solar energy systems. Such systems therefore need to be combined with other energy sources into hybrid energy systems in order to provide uninterrupted and reliable energy.

Solar thermal collectors can be combined with several types of energy sources, for example wood stoves, pellet burners, and heat pumps. The combination of solar thermal collectors and heat pumps was extensively studied in IEA SHC Task 44 – Solar and Heat Pump Systems [160].

Since electricity can be exchanged with the grid, grid-connected PV systems do not necessarily have to be combined with other energy sources (in addition to the grid) in order to meet the electric as well as the thermal energy demand of a building. Off-grid systems typically use a battery to store energy.

Nowadays, it is becoming more common to use PV modules in combination with heat pumps of different types as an efficient way to provide space heating and/or domestic hot water in buildings. One reason that this solution has gained some ground on solar thermal systems is the massive price reduction of PV systems over the last decades. It is in some cases also easier to install a PV and heat pump system than a solar collector system in existing buildings, at least if air-to-air heat pumps are used, since it does not require additional piping or changes to the building's heating system. Heat pumps can also provide cooling if necessary.

In the PV/T Roadmap, the combination of PV/T and heat pumps for heating and domestic hot water was pointed out as one of the most promising applications in the medium to long term perspective [119]. PV/T systems need to be integrated into the thermal as well as the electric system of the building. The thermal output of PV/T collectors is generally lower than that of solar thermal collectors, and they therefore work best in solutions where low temperature heat is useful. Low temperature hydronic heating systems, e.g. underfloor heating and modern radiators are examples of such systems.

Since PV/T modules provide heating as well as electricity, they are especially suitable to use in combination with heat pumps. The electricity output can be used to operate the heat pump, which provides heating when the solar thermal output is not sufficient. The solar thermal output can also be used as preheating for the source side of the heat pump or charging of the source.

The focus of this thesis is PV/T modules in combination with heat pumps, which are used in both the two case studies. The PV/T modules are combined with an air-to-water heat pump in the first case study (the ZEB residential concept), while a ground source heat pump is used in the second case study (the Living Lab).

4.2.2 Heat pump operation

A heat pump is a device that transports thermal energy from a lower temperature level to a higher temperature level [161]. The process takes place in a closed loop where the heat transfer medium undergoes continuous changes of state between liquid and vapour. The working principle of a compression heat pump is shown in Figure 31.

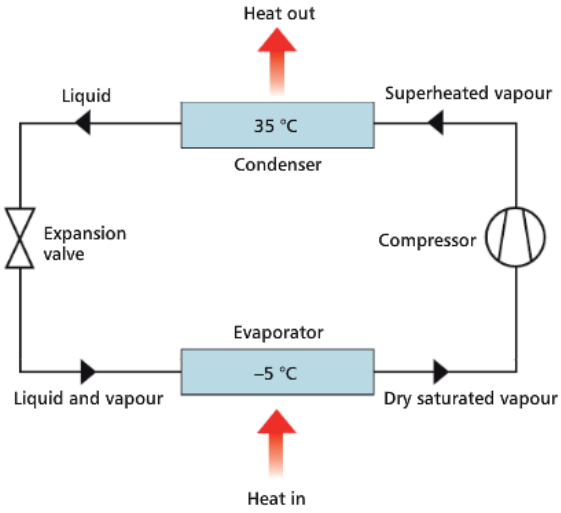

Figure 31. The vapour compression cycle of a heat pump. Figure from CIBSE [162], used with permission.

The refrigerant fluid in the circuit is at a low temperature and pressure when it enters the evaporator. The refrigerant is heated in the evaporator, and thereby provided the latent heat needed to vaporise. The vapour is compressed to a higher pressure by the compressor, which also increases the saturation temperature (boiling point). The vapour is thus condensed, and gives away its latent heat as useful heat in the condenser. The refrigerant passes through the expansion valve, where the pressure is decreased before the cycle can start again. The thermal energy input to the evaporator is collected from the environment, such as the air, the ground, or a body of water. The temperature levels given in Figure 31 are representative for a ground source heat pump system. Electricity is required to drive the process by powering the compressor. [162]

The theoretical efficiency (ε_c) of a heat pump is given by the Carnot cycle, according to Equation (19), where T_{out} (°C) is the temperature of the output side and T_{in} (°C) is the temperature of the input side [161].

$$\varepsilon_c = \frac{T_{out}}{T_{out} - T_{in}} \qquad (19)$$

The actual performance of a heat pump includes several losses, and is described by the coefficient of performance (COP). The COP can be calculated according to Equation (20),

where $P_{delivered}$ (kW) is the thermal power delivered from the heat pump, and P_{input} (kW) is the power input to drive the heat pump [161].

$$COP = \frac{P_{delivered}}{P_{input}} \qquad (20)$$

The COP is an instantaneous value, that varies with the input and output temperatures. It is therefore common to use the average annual performance or the seasonal performance factor (SPF) when assessing their performance over time. The SPF, which is sometimes also referred to as the seasonal COP (SCOP), is the ratio between the total energy input and the total amount of energy delivered. [161] The SPF can also be calculated for the complete heating system and must then include additional energy required by for example circulation pumps. In this thesis, the average coefficient of performance of the heat pump over a given time period is referred to as SPF, and the same factor for the whole system is referred to as SPF_{sys}.

It follows from Equation (19) that the efficiency of a heat pump is increased with a decreasing difference between input and output temperature. The relationship between the output temperature and the COP (for an input temperature that is constant at 0°C) is shown in Figure 32 for a ground source heat pump.

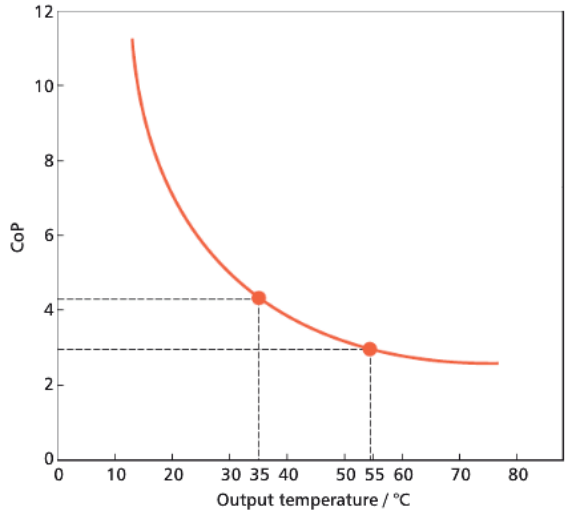

Figure 32. The relationship between output temperature and COP for the example of a ground source heat pump (input temperature is constant at 0°C). Figure from CIBSE [162], used with permission.

In product datasheets, the COP of the heat pump is given based on the source and sink temperatures, and the type of heat source and heat sink. As an example, the COP of an air-to-water heat pump, working with an input temperature of 0°C and an output temperature of 35°C would be noted as A0/W35 (this point is marked in Figure 32). The type of refrigerant in the heat transfer circuit is also of importance, and should be given in the datasheet. [161]

4.2.3 Air source heat pumps

Air source heat pumps use the ambient air to harvest energy. The heat pumps can either be air-to-air or air-to-liquid. Several configuration options exist, including split or compact systems and ducted or ductless systems [161].

The advantage of these systems are that they are relatively cheap and easy to install, since the heat source is available everywhere and requires no ground work or special permissions [161]. Air-to-air heat pumps furthermore require just a simple installation inside the building, while air-to-water heat pumps are connected to new or existing hydronic heating systems.

The disadvantage of using air as heat source is that the COP decreases with decreasing outdoor temperatures, while the heating demand of a building increases. The match between high efficiency and high demand is therefore low. However, there have been large developments in air source heat pump technology during recent years, and air source heat pumps are now also a good alternative for colder regions. The Swedish Energy Agency has tested air-to-air heat pumps in Scandinavian climate, and concluded that the SPF of modern air source heat pumps are in the range 2.8 to 4.1 in the south of Scandinavia and 2.3 to 2.6 in the northern part [163].

4.2.4 Ground source heat pumps

As the name implies, ground source[11] heat pumps use the ground as a heat source for the evaporator. They typically use the low temperature (<30°C) at relatively shallow depths (up to 200 m). [162] The heat stored in the ground is primarily solar heat, but it is also regenerated by rain water. Below 15 m, the ground temperature is typically constant over the year, with a temperature similar to the average air temperature at the site. The ground source temperature in Scandinavia is between 2°C and 9°C. [161]

A major differentiation is made between closed-loop and open-loop systems. Closed-loop systems use heat exchangers to extract heat from the ground, while open-loop systems pump ground water. Open-loop systems require careful consideration of the surroundings, since the circulated water needs to be disposed back into the environment, creating a flow and/or temperature difference. [162]

The analysis in this thesis concerns closed-loop systems. Three closed-loop concepts are shown in Figure 33. Vertical closed-loop heat exchangers are typically referred to as borehole heat exchangers, while the horizontal type is sometimes called surface collectors [162].

[11] "Geothermal heat pumps" is sometimes use as a collective name for heat pumps that harvest energy from the Earth's crust, which is primarily stored solar energy in the ground or aquifers. These should not be confused with high temperature geothermal energy, which is harvested from geologically active sites. [162] "Ground source heat pumps" will be used in this thesis.

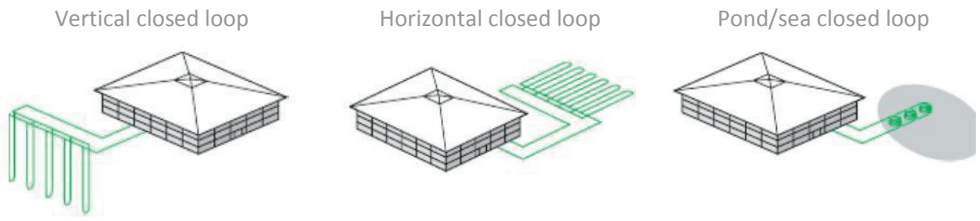

Figure 33. Ground source heat pumps with vertical and horizontal closed loop. Figure from CIBSE [162], used with permission.

Borehole heat exchangers have the advantage of requiring a small surface area, while the installation cost can be high. Horizontal collectors are less expensive to install, but on the other hand occupies a larger area which cannot be built upon [162].

Ground source heat pumps are typically of brine-to-water type, where an anti-freeze medium (brine) is used in the ground to avoid freezing of pipes [161]. The stable ground temperature is advantageous for efficient heat pump operation. Ground source heat pump systems for heating can typically reach SPF_{sys} values between 3.8 and 4.2, but the performance depends to a large extent of the design of the complete heating system [162]. Tests by the Swedish Energy Agency showed SPF_{sys} values between 2.8 and 5.0 for a Scandinavian climate [164].

4.2.5 PV/T and ground source heat pump systems

There are several reasons that PV/T modules and ground source heat pumps would appear to be a good combination, a number of which are mentioned in the previous sections. PV/T systems can be used with ground source heat pumps in several types of system designs. Section 4.2.5.1 presents an overview of previous research, while a few possible system solutions are outlined in Section 4.2.5.2.

4.2.5.1 Previous research

Solar thermal systems and ground source heat pump systems have been studied to quite a large extent. PV/T systems in connection with ground source heat pumps are so far, however, the topic of relatively few studies.

One of the earliest studies of a PV/T system with a ground source heat pump was done by Bakker, et al. [33], who simulated a single family house in the Netherlands with the simulation program TRNSYS. The study found that a PV/T system of 25 m^2 combined with a ground source heat pump had the same output as a system with 26 m^2 PV modules and 7 m^2 collectors and a ground source heat pump. Both systems covered up to 100% of the building's heat demand and almost all of the electricity demand of the heat pump, in addition to keeping the ground at a stable temperature. The costs of the two systems were approximately equal, but the PV/T system had the benefit of taking up a smaller area.

Bertram, et al. [32] combined simulations in TRNSYS with measurements over two years on a 39 m^2 unglazed PV/T system in Frankfurt am Main, Germany. The results showed an annual temperature increase of 3K, which led to a 9% lower electricity consumption due to a higher efficiency of the heat pump. The study also included an extrapolation over 20 years, which

showed that the benefits of the system increased over time compared to a system without PV/T, due to the solar regeneration of the ground. This is especially the case for under-dimensioned boreholes. The additional PV yield was determined to be 4%, which was deemed not to justify the installation alone. However, in some cases, such as building integration (and backside insulation) of the modules, the benefits may be larger.

Ille, et al. [120], made a simulation study in TRNSYS of three typical PV/T systems. In addition, the authors did a market survey of PV/T modules available in Germany. They studied three different system configurations: PV/T and heat pump connected in parallel, PV/T and heat pump connected in series and parallel, and finally PV/T and heat pump in series and parallel with regeneration of a ground source probe. They found that the heat pump in series connection increased the useful thermal output from the PV/T, since the operation of the PV/T modules were determined by the operation of the heat pump and not only by the level of irradiation. The largest share of useful thermal output was therefore in the winter. Only during the summer was there direct charging of the tank. The increase in electric output of the PV/T was found to be less than claimed by many producers. Furthermore, the authors found that regeneration of the bore holes did not contribute to an improved system performance, since the use of pumps consumed more energy than was gained. However, they suggested that the regeneration could increase the performance of systems with under-dimensioned boreholes by preventing the ground from cooling over time.

Entchev, et al. [35] studied a hybrid renewable energy generation system with a ground source heat pump and a PV/T system, designed for load sharing between an office and residential building in Ottawa, Canada. The analysis was made in TRNSYS. The system included heating, cooling, and DHW preparation. They found that the combined ground source heat pump and PV/T system resulted in an energy saving of 58% compared to a conventional system. The use of a solar pre-heat tank connected to the PV/T collectors was found to increase the efficiency of the collectors and thereby of the whole system. Due to the decreased grid-independence, they suggested that it could be an attractive solution for remote areas. Using regeneration of boreholes as thermal storage does not seem to have been studied.

Canelli, et al. [34] studied several cogeneration strategies in Naples, Italy, through simulation in TRNSYS. The energy, CO_2 emissions, and cost reduction from each of the alternatives were studied. In addition to a ground source heat pump connected with a PV/T system, they also studied a case with only ground source heat pump, and a case with fuel cells and ground source heat pump. The PV/T and ground source heat pump showed the best performance, resulting in a primary energy saving of 53.1% and a 52.0% reduction in CO_2 emissions, compared to the reference case. However, the economic analysis showed that the economic payback for the PV/T and ground source heat pump was the longest of the studied systems, with 18.5 years, even though the operational cost of this system was low.

4.2.5.2 System design

The “conventional” way of combining solar thermal systems and heat pumps is by using the heat pump as the backup load for the solar thermal systems during times of low solar

radiation [165]. This type of connection is used with an air-to-water heat pump in the first case study, which is described in Section 5.2. Solar thermal collectors can also be integrated on the source side of the heat pump.

According to Braungardt, et al. [165] there is a growing number of solar thermal and heat pump systems on the market, and they sometimes differ considerably from each other in design. The major differences were found to be the type and sizing of heat sources, the type and configuration of the storage system, the temperature level of the solar thermal component, and the type of incorporation of solar thermal on the source and sink side of the heat pump.

An example of a solar collector and ground source heat pump connected separately to the tank (sometimes referred to as parallel connection) is shown in the top figure in Figure 34. In this case, the solar thermal component and the heat pump work mostly independently of each other, supplying heat to the common storage tank for DHW. In this figure, the space heating circuit is connected directly to the heat pump, but a buffer tank or combined tank can also be used for DHW and space heating.

The lower figure in Figure 34 shows an integrated connection (sometimes referred to as a series connection, or a coupled system) of a solar collector and heat pump. The solar collector can in this case be used as input to the heat pump or injected to the ground. This solution is appropriate for low temperature solar thermal components, such as unglazed solar collectors or PV/T modules. For higher temperature solar components, the collector can also be connected to the storage tank in addition to the heat pump, such as the connection in Figure 35.

The PV/T modules or solar collectors can be connected directly (as in Figure 34) or indirectly to the rest of the energy system. In an indirect connection, for example as the one shown in Figure 35, the output of the solar thermal component goes through a buffer tank before it is used by the heat pump.

Regarding the integration of PV/T systems rather than pure solar thermal collectors with heat pumps, the lower temperature of the former needs to be considered. PV/T modules may not be as appropriate for direct use in domestic hot water preparation as solar collectors, or not during as long a period of the year.

The energetic benefit of solar thermal and ground source heat pump systems depends on the level of irradiation and the climate at the site of the installation. Girard, et al. [31] studied a space heating system for a single family house with solar thermal collectors and ground source heat pumps for 19 European cities at different latitudes. A system with only a ground source heat pump, as well as a system with only electrical radiant heaters, were evaluated as references. The results showed that the solar thermal coupling increased the SPF_{sys} values for all locations, although the increase was significantly larger for southern locations than for northern ones. The greatest difference between the systems with and without solar collectors was found for locations with mild weather and high solar irradiation, such as around the Mediterranean. No similar study for PV/T systems was found.

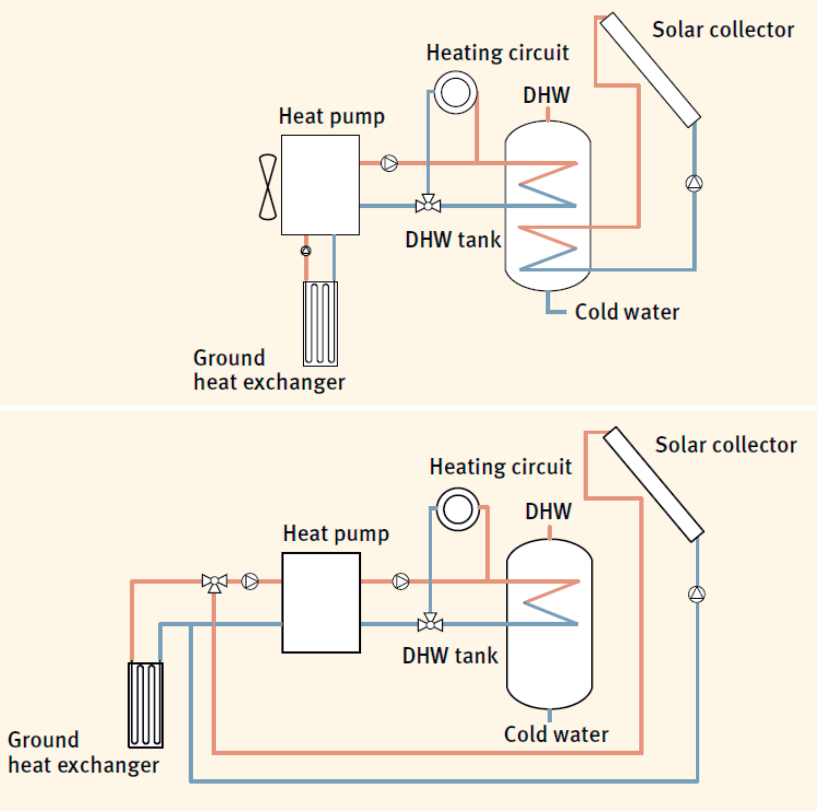

Figure 34. An example of a separate connection of a solar collector and ground source heat pump (top), and an integrated connection where the solar collector assists the borehole or the heat pump (bottom). Figures from Braungardt, et al. [165] © Fraunhofer Institute for Solar Energy Systems ISE.

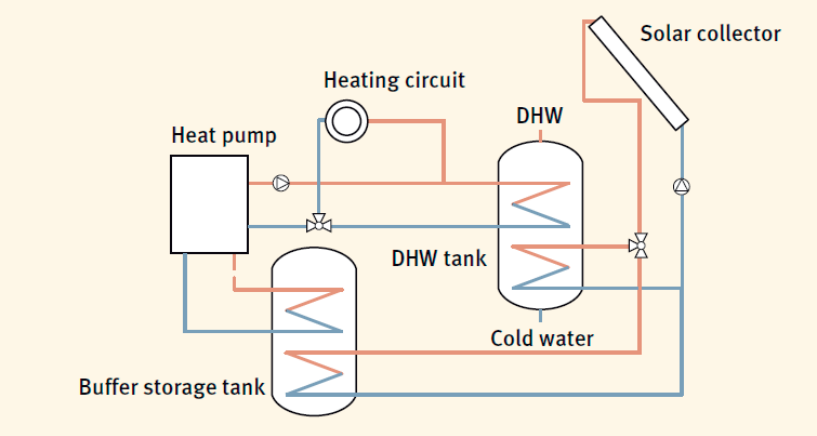

Figure 35. A solar thermal and heat pump system with indirect connection between the solar collector and heat pump. Figure from Braungardt, et al. [165] © Fraunhofer Institute for Solar Energy Systems ISE.

The control strategy and its implementation are key factors for the performance of the system. The control strategy determines how and when each energy source is exploited, which influences the performance of the system components as well as the energy demand of circulation pumps and other equipment.

In a separate system, the solar thermal output should have priority over the heat pump, since the efficiency of the solar thermal system can be very high. In integrated connection types, the control strategy is more complex, and depends on e.g. the level of irradiation, the types of components, and how they are dimensioned. So far, there has been no comprehensive analysis of the performance of the different concepts. [165]

Complex control systems can also lead to increased energy consumption of the system components. Studies by for example Kjellsson, et al. [166] has highlighted the importance of the control strategy in order to ensure good operation of the systems. In this study, the authors compared several versions of a small residential building with a solar thermal and ground source heat pump system. In their system, the solar thermal collectors could supply heating for four different purposes: producing DHW, directly for space heating, as input to the heat pump evaporator, or to regenerate the borehole. The study concluded that the electricity required to run the circulation pumps may easily exceed the energy savings if the solar thermal and bore hole system is allowed to run whenever possible. Careful planning and energy efficient components are therefore necessary.

The benefits of recharging the ground will also differ depending on e.g. the level of irradiation, the temperature, and the design of the ground source heat exchangers. In the study by Kjellsson, et al. [166] it was found that the effect of reduced energy withdrawal could be of importance in systems with boreholes that were thermally influencing each other. Alternatively, boreholes in new systems can be placed closer together. If the ground source system was originally working well, the best use of solar thermal energy was for DHW in the summer and recharging in winter.

The large benefit of the systems with separate connection for the solar thermal component and the heat pump is their relative simplicity [165]. According to one PV/T producer, the complexity of PV/T systems has been the main limiting factor for its wider spread since it requires a great deal from designers as well as installers [167]. The quickest development in the short term is therefore expected be in simpler systems, even though there is a great potential in well-designed systems with PV/T and ground source heat pumps.

A PV/T and ground source heat pump system is studied in the second case study in this thesis (the Living Lab). The ground source used in this study is a vertical closed loop system, buried at 1.5 m depth at the building site. The system is studied with separate as well as a direct integrated connection between the PV/T system and the heat pump. In addition, two different control strategies are analysed. The case building and its energy system are further described in Section 5.3.

Chapter 5: Energy performance of PV/T systems

5.1 Introduction

The energy performance of PV/T systems in Norwegian buildings has been evaluated through simulations of two case buildings: the ZEB residential concept (Section 5.2) and the Living Lab (Section 5.3). The case study of the ZEB residential concept is also described in Paper II. The case study of the Living Lab will be submitted for publication.

Both case buildings are residential, single family houses designed and developed by the ZEB Centre, and are relatively similar in size. The building models are based on previous research in the ZEB Centre, with some adaptation. While the ZEB residential concept is only a simulation model, simulated for Oslo climate, the Living Lab is an actual building on the campus of the Norwegian University of Science and Technology (NTNU) in Trondheim.

The energy performance of PV/T systems are simulated and compared to systems with separate PV modules and solar thermal collectors on the same building. The energy performance of each solar energy system is evaluated based on the actual energy output, but also based on the resulting energy balance of the building. The results for each case building are presented separately, but the chapter is concluded with a discussion and conclusions for both case studies in Section 5.4.

5.1.1 Energy performance simulations

The energy simulations are performed in the simulation program Polysun from Vela Solaris [14]. Polysun is a dynamic simulation tool for solar energy solutions including solar thermal, PV, and PV/T. The program can also be used to simulate various hydronic systems, such as heat pumps and district heating systems. In addition, the program includes an extensive database of commercial components, including PV/T, which has been used in the simulations. The model of the ZEB residential concept was based on a model created by Laurent Georges, which is described in detail in Appendix D of reference [72].

Not only the total energy demand, but also the energy demand *profiles* influence the energy performance. The thermal load profiles, especially the DHW profile, influence the performance of solar thermal systems, since the usefulness of the thermal output at each moment depends on the load and the status of the storage. If there is no load and the thermal storage has reached its maximum temperature, any further potential solar thermal output will be lost. The electricity profile is important if the grid interaction is to be analysed, or if the system includes battery storage.

At the time of writing, there was no measured data on energy demand available for either of the two case buildings. In the first case because the building only exists as a simulation model, and in the second case because the building had not been operational long enough. The input to the simulation program was therefore a combination of data from standards and earlier studies. The space heating demand for both buildings was simulated with the simplified building model in

Polysun, which uses the total annual energy demand and the outdoor temperature to create an annual profile for space heating.

In the ZEB residential concept, the DHW demand was simulated using the annual energy demand from Houlihan Wiberg, et al. [6], given in Table 5, and the "Single family residential" profile template from Polysun. No electricity demand profile was simulated in this case, but the annual value from Table 5 was used in the calculations of energy balance.

For the Living Lab, the DHW and electricity demand profiles were both simulated in the same way. The annual energy demand values from Finocchiaro, et al. [10], listed in Table 10, were combined with hourly user profiles from the preliminary standard prEN 3031:2015 [20].

5.1.2 Selection of solar modules

The objective of the two case studies was to compare the energy performance of a PV/T system to that of systems with separate PV modules and solar thermal collectors. The studies are furthermore focused on solar energy components that are available on the market today, that is, neither of the studies is an explicit evaluation of the future potential of PV/T modules. Since PV/T modules combine two energy sources into one module, it is not possible to find solar thermal, PV, and PV/T modules that are fully comparable in both electric and thermal characteristics. If a PV/T module has the same efficiency as a PV module, its thermal efficiency is typically lower than a solar thermal collector in the same market range, and vice versa. The simulation results for the two case buildings are not compared, but only the systems on the same case building.

The process of selecting modules for the systems was slightly different in the two cases. This is further described in Section 5.2.2.1 and Section 5.3.2.1. A recent analysis of the PV/T market in Germany by Adam, et al. [168] was used to identify available PV/T products, but also direct communication with companies, and information included in Polysun's database. In accordance with the limitations in the scope of this thesis (see Section 1.2.2), only flat plate PV/T modules with liquid heat transfer were considered.

5.1.3 Assessment methods

The energy performance of the systems were evaluated through different assessment methods. Firstly, the thermal and electric energy output of the systems were determined through simulation. Since the areas of the systems within each case study are slightly different, the results were also normalized per installed area and per heated floor area (A_{fl}).

Secondly, the net zero energy balance, which was described in detail in Section 2.2.2, is calculated for each case.

Thirdly, the load match and grid interaction indices are analysed. The calculation methods for these factors are described in Section 2.2.4.

5.2 Case study 1: ZEB residential concept

5.2.1 The case building

The residential concept model (Figure 36) was created by the ZEB Centre in 2012, together with a similar concept model for an office building. The objective was to develop simple, standardized models for two typical Norwegian buildings, which could be used for realistic calculations and simulations of e.g. energy performance, embodied emissions, and energy supply systems. The buildings are not real constructions, but exist only as models. The materials and methods are, however, selected to represent what is currently available in the building industry [6].

The focus in this thesis is only on the residential concept model, and not the office building. It is described in detail in a report from the ZEB Centre [75], as well as in a subsequent publication by Houlihan Wiberg, et al. [6]. The environmental impact of the building has furthermore been investigated in a master thesis from NTNU [169].

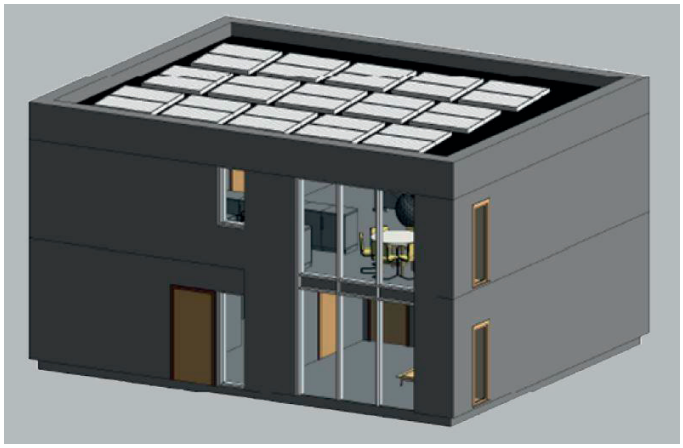

Figure 36. The residential concept model. Figure from [75].

The building model has a simple rectangular shape and two storeys. The footprint is approximately 8 m x 10 m, resulting in a total heated floor area of 160 m^2. The building is modelled with the climate for Oslo (59.9° N, 10.6°), which has an annual average temperature of 6.3°C and an annual solar irradiation is 1000 kWh/m^2 on the horizontal 1200 kWh/m^2 on an optimally inclined surface. The building is designed to fulfil the requirements of the Norwegian passive house standard [170][12].

5.2.1.1 Building energy system

The heating is provided by a 5 kW air-to-water heat pump and a solar collector system, which are both connected to a 600 l storage tank for space heating and DHW. A simplified sketch of the heating system is shown in Figure 37. The space heating is distributed by a low temperature

[12] The Norwegian passive house standard has been revised since the residential concept model was created, and the NS 3700:2013 is now available.

hydronic system with floor heating (inlet/return temperatures 30/25°C) and radiators (inlet/return temperatures 40/30°C). A tank-in-tank system is used for the tap water, with a store temperature of 55°C and a temperature at the tap of 45°C. The DHW tank is heated to 70°C once per week to avoid legionella growth. The HVAC system also includes mechanical ventilation with heat recovery. Heat recovery is also used on the grey water, i.e. the water from dishwasher, showers, and washing machine.

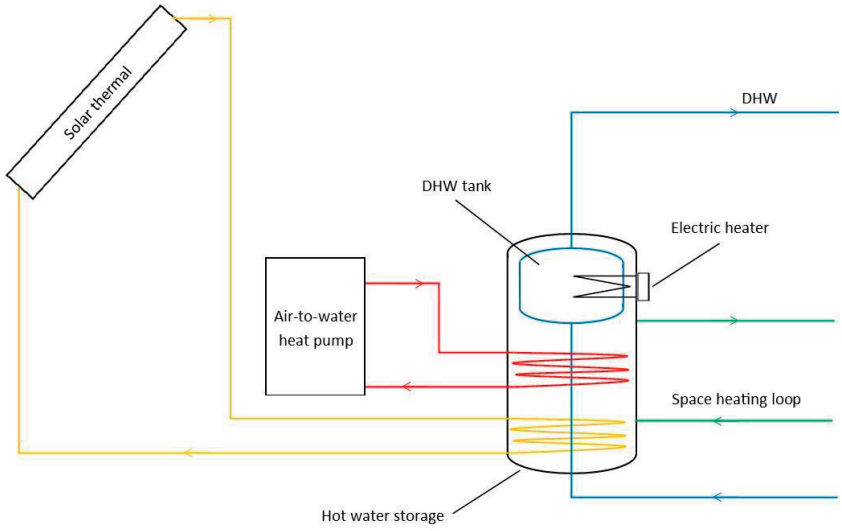

Figure 37. A simplified drawing of the heating system in the residential concept building.

5.2.1.2 Solar energy system in the original study

This section describes the configuration on of the solar energy system in the original study by Houlihan Wiberg, et al. [6]. This system is used as a reference and a starting point for the present case study, and will be referred to as the original system.

The original solar thermal installation on the building consists of 8.3 m^2 of vacuum tube solar collectors. The system is dimensioned to cover most of the heating demand during the summer months, when it is almost only due to the DHW demand, which is a common way to design systems in Northern Europe. Design of solar thermal systems is further discussed in Chapter 4.

The building has a roof mounted PV system which provides electricity. The building has a flat roof, which makes the design of the PV system a little more demanding with respect to self-shading. In Oslo, the optimal orientation for yearly yield is 40° and south facing. This relatively high tilt angle makes is necessary to have rather large distances between the rows in order to avoid self-shading.

On the case building, the modules are mounted south facing at 15° inclination, which is a lower tilt angle than the optimal. This means that the rows can be installed at a closer distance without shading. In addition, the gap between the rows are used to install modules facing the opposite

direction (north). Installations with lower tilt angles are more prone to snow pile-up, and a small gap between the rows are kept to enable snow to slide off. A total of 69 m^2 PV modules can be installed on the roof with this arrangement (49 m^2 south-facing and 20 m^2 north-facing) [75].

A further discussion on the design of PV systems on flat roofs is found in Section 4.1.1. The effect of different system designs for the installation on the ZEB residential building is also studied in Section 6.3.

5.2.1.3 Energy and emission balance

In the original study of the ZEB residential concept, the energy and emission balances of the building were analysed based on supplied energy and energy demand [6]. The objective was to reach a ZEB-OM balance (see Section 2.2.1), and the demand was therefore composed of the operational energy and the energy embodied in materials. Since heating is provided by solar thermal collectors and a heat pump, the only form of delivered energy is electricity.

The energy performance of the building was determined by simulations in SIMIEN [171] and are shown in Table 5. Thanks to the efficient heating system with solar thermal collectors and a heat pump, the amount of supplied electricity is a total of 6224 kWh per year, or 38.9 kWh/$m^2 A_{fl}$. This is the amount of electricity that has to be generated by the PV system in order to reach a ZEB-O balance weighted by energy. [6]

Table 5. Simulated energy demand of the residential concept model [6].

	Energy demand	
	kWh/year	*kWh/m^2 year*
Space heating	3349	20.9
Domestic hot water	3811	23.8
Electricity	4074	25.5
Total	11234	70.2

The roof-mounted PV system in the original study generated 71 kWh/$m^2 A_{fl}$, almost double that of the supplied electricity, which means that a ZEB-O level was easily reached. However, the authors of the original study concluded that the PV system had to generate a total of 94 kWh/$m^2 A_{fl}$ electricity in order to reach a ZEB-OM level weighted by emissions, i.e. to balance the operational as well as the embodied emissions. That is, only 75% of the electricity needed to reach the ZEB-OM level was generated. [6]

The original version of the residential concept model had solar thermal collectors mounted on the façade and high-efficiency PV modules installed on the roof. The two solar technologies were therefore not directly competing for the space on the building. In the energy performance analysis in this thesis, however, only the roof area has been used for solar thermal collectors, PV, and PV/T modules.

5.2.2 Analysis of alternative solar energy systems

5.2.2.1 Selection of modules

For this case study, an effort was made to use solar modules and collectors that represented the market average in terms of performance. One average solar thermal collector (ST_{avg}) and one average PV module (PV_{avg}) were selected, and a state-of-the art module was also included for each technology in order to cover a wider market range (ST_{high} and PV_{high}). The characteristics of the modules in the ZEB residential concept case study are shown in Table 6.

The PV/T market is still significantly smaller than the markets for both PV modules and solar thermal collectors, and it was difficult to find a market average in such a small range of products. Two types of flat plate PV/T modules were therefore used in an attempt to cover a range of market options. High-performing modules were chosen for both types: one uncovered and uninsulated with high electric efficiency (PV/Ta), and one covered and insulated with high thermal efficiency (PV/Tb). The difference between uncovered and covered modules is described in Section 3.1.2.1. It can be noted that the number of covered modules on the market is very small, and the simulation of the PV/Tb module is therefore based on a more limited amount of data.

Table 6. Characteristics of the solar collectors, PV modules and PV/T modules used in the simulations of the ZEB residential concept.

Module	Technology	Gross area	Electric efficiency at STC*	Rated electric power	Thermal zero-loss efficiency, η_0
		m2	*%*	*kWp*	*%*
ST_{avg}	Flat plate	2.00	-	-	80
ST_{high}	Flat plate	2.00	-	-	85
PV_{avg}	Poly-Si	1.65	15.8	260	-
PV_{high}	Mono-Si	1.64	20.3	333	-
PV/Ta	Mono-Si, uncovered, uninsulated	1.64	17.4	285	61.4
PV/Tb	Poly-Si, covered, insulated	2.26	12.0	240	71.5

**Standard test conditions, see Section 2.1.3.1.*

5.2.2.2 System design

Six different versions of the building were simulated, with six different solar energy systems using combinations of the modules described in the previous section. Only the roof area was used for the solar installations in the case study – not both roof and façade as in the original case described above. The reason for not replicating this design was to eliminate variable

parameters by keeping the area constant and all module types at the same orientation and tilt angle. This strategy avoids a PV/T installation with two different orientations.

The roof area is approximately 8 m x 10 m, and the modules are installed at a 45° tilt angle. This is close to optimal for PV modules, but solar thermal collectors would typically have been installed at a slightly higher tilt angle. An analysis of the resulting shading revealed that only two rows could fit on the roof at this tilt angle if unnecessary row-to-row shading were to be avoided. This is one row less than in the original study, where the modules were furthermore installed at a lower tilt angle and with dual orientations [6]. A more detailed description of how shading influences the system design is found in Chapter 4.

Since the size and dimensions of market-available modules are used in this study, the active area in each of the systems is not exactly the same. A generic spacing of 5 cm between modules is used. A schematic drawing of the installations is shown in Figure 38. As the output of PV modules is more dramatically influenced by shading than that of solar thermal collectors, the latter are placed in the back row. (Note that the back row in building C and C* includes only PV modules.)

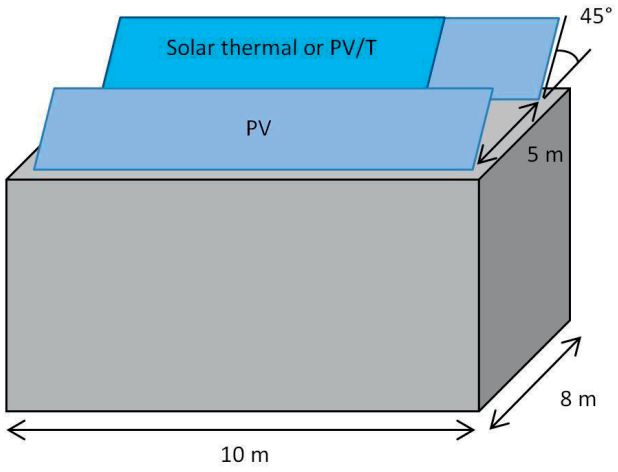

Figure 38. A schematic drawing of the solar energy system design on the residential concept building.

The system parameters are shown in Table 7. The dimensioning of the system for building A is based on the solar thermal system. In accordance with common design guidelines for Northern European regions, the solar thermal system is designed to cover most of the thermal energy demand during the summer months (here defined as May to August), when the heat demand is only that for DHW preparation. The area of solar collectors required to do this is slightly smaller with the high efficiency modules, which is why the collector area for building C* is smaller than for building C. The PV/T modules have lower thermal efficiency than the solar thermal collectors, and the required area is therefore larger for building B2.

Table 7. The main parameters of the simulated system variants.

System	Description	Installed area ST / PV/T / PV	Rated electric power	Tank volume
		m^2	kW_p	l
A	ST_{avg} and PV_{avg}	10 / 0 / 21	3.4	1300
A*	ST_{high} and PV_{high}	8 / 0 / 23	4.7	1300
B1	Only PV/Ta	0 / 30 / 0	5.1	1800
B2	PV/Tb and PV_{avg}	0 / 16 / 17	4.3	1000
C	Only PV_{avg}	0 / 0 / 30	4.7	300
C*	Only PV_{high}	0 / 0 / 30	6.0	300

Since covered and uncovered PV/T modules have different output profiles, two versions of building B are evaluated: B1 with uncovered PV/T modules and B2 with covered PV/T modules.

Due to the relatively low thermal output of the uncovered modules, it was not possible to reach high thermal solar fractions with this technology. Simulations of building B1 with different ratios between the PV/Ta and PV_{avg} module areas showed that the annual net energy, E_{net}, increased with increasing PV/T area, and uncovered PV/T modules were therefore used on the whole roof area, maximising E_{net}. It was also found that a tank size of around 60 l/m^2 collector was suitable for a larger PV/Ta system and a slightly higher tank volume to area ratio for smaller systems.

The same design strategy as for solar thermal (building A) was used for building B2. That is, the PV/T system was sized to meet most of the energy demand during summer, and the rest of the roof area was covered with PV modules. Simulations showed that a PV/T area of around 16 m^2 (7 modules) was required in order to reach the same thermal coverage as for building A.

In building C and C*, all available roof space was used for a PV installation. This building includes the same hydronic heating system as buildings A and B, but without the solar thermal contribution. The tank size was therefore decreased to only work as a buffer tank for the heat pump. The stand-by volume for the DHW was, however, kept the same as in the other systems.

5.2.3 Calculations

5.2.3.1 Energy output

As mentioned in Section 2.2.3.1, the primary energy value of the energy output from a solar energy system can be calculated based on the value of imported and exported energy. No profile for the electricity consumption is used in this case study and the interaction with the electricity grid is therefore not considered in detail.

A simplified calculation is used in this case study to evaluate the primary energy value of the solar energy output. The method is based on the value of avoided electricity use, but without considering grid interaction specifically. The electricity generated by the PV and PV/T modules is considered to replace 1 kWh of electricity from the grid and is therefore given the value 2.3 kWh_{PE} (primary energy) from Table 1. The thermal output from the solar energy systems is considered to replace 1 kWh of thermal output from the heat pump. The average coefficient of performance of the heat pump in this case study was 2.43, and 1 kWh thermal output from the heat pump thus requires 0.4 kWh electricity from the grid. 1 kWh solar thermal output is therefore given the value $(0.4 \cdot 2.3)\ kWh_{PE} = 0.9\ kWh_{PE}$.

5.2.3.2 Energy balance

The load/generation[13] balance is used in the ZEB residential concept case study, and grid interaction is therefore not considered in this case. The solar thermal load influences the electricity loads by increasing or reducing the load of the heat pump and to some extent the circulation pumps. It is equal to regarding the solar thermal system as an energy efficiency measure rather than an energy source. The balance is therefore calculated using only the electricity load and renewable electricity generation. This approach is similar to the one used by Dokka, et al. [75] in the original study of the building.

The load/generation net energy balance can then be calculated according to Equation (11) from Section 2.2.3.1, but adapted for the load/generation balance into Equation (21).

$$E_{net} = E_{gen,el} - E_{load,el} \qquad (21)$$

$E_{gen,el}$ generated electricity (kWh)
$E_{load,el}$ electricity load (kWh)

5.2.3.3 Load match index (solar fraction)

Calculation of a generalized load match index $f_{load,i}$ was shown by Equation (16) in Section 2.2.4. As mentioned, the load match index is also referred to as the solar fraction (SF) when only solar energy is considered. In the present case study, the solar fraction for thermal energy (SF_{th}), and electricity (SF_{el}) are calculated.

The solar thermal fraction is calculated according to Equation (22), where Q_{sol} is the thermal energy to the systems, Q_{aux} is the auxiliary energy to the system, and Q_{load} is the thermal load of the building.

[13] In Paper II, the calculated balance is erroneously referred to as the delivered/exported balance. It is in fact the balance between load and generation that is calculated.

$$SF_{th} = \frac{1}{N}\sum_{year} min\left[1, \frac{Q_{sol}(t)}{Q_{load}(t)}\right] = \frac{1}{N}\sum_{year} min\left[1, \frac{Q_{sol}(t)}{Q_{sol}(t) + Q_{aux}(t)}\right] \quad (22)$$

The thermal load in the solar fraction can be calculated in several ways, depending on how the system losses are allocated. With the calculation method in Equation (22), the losses are divided between the solar and auxiliary heat sources.

An electric solar fraction (SF_{el})[14] for the building, including also electric loads for the heat pump, is defined according to Equation (23) where E_{sol} is the electric solar output, and E_{load} is the total electricity load of the building.

$$SF_{el} = \frac{1}{N}\sum_{year} min\left[1, \frac{E_{sol}(t)}{E_{load}(t)}\right] \quad (23)$$

SF_{el} can here also be interpreted as the total solar fraction. The solar thermal output is included as an energy efficiency measure, according to the method described in the previous section.

The yearly (N = 1, t = 1 year) and monthly (N = 12, t = 1 month) solar fractions are calculated in the study. For thermal energy, the summer solar fraction between May and August is also calculated (N = 4, t = 1 month, the sum only over four months).

5.2.4 Results

5.2.4.1 Energy output

The thermal and electric output of the six different solar energy systems are shown in Figure 39 in unweighted kWh, that is, without weighting between thermal and electric energy. The thermal and electric energy demand of the building is shown for comparison.

[14] In Paper II the total solar fraction SF_{tot} is referred to as the ratio $E_{exported}/E_{delivered}$.

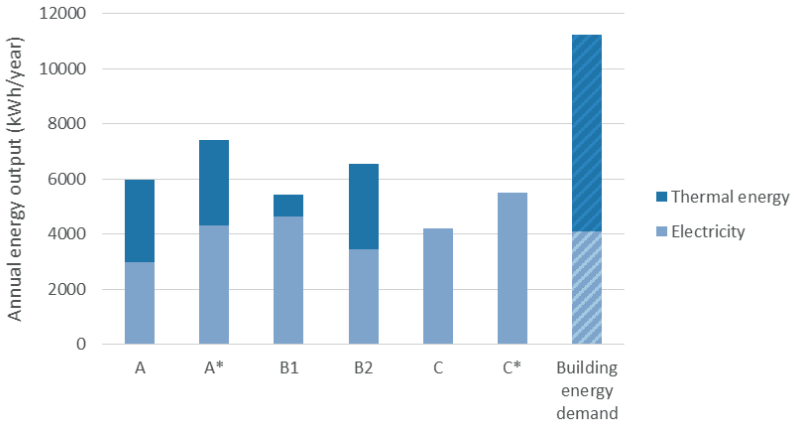

Figure 39. The thermal and electric energy output of the different systems on the ZEB residential concept (unweighted kWh). The systems are described in Table 7.

The installed areas of the systems are different, and the energy output normalized per installed area for each case is shown in Figure 40. Both the thermal and electric energy outputs are divided by the *total* installed area, i.e. the sum of all installed modules in each system.

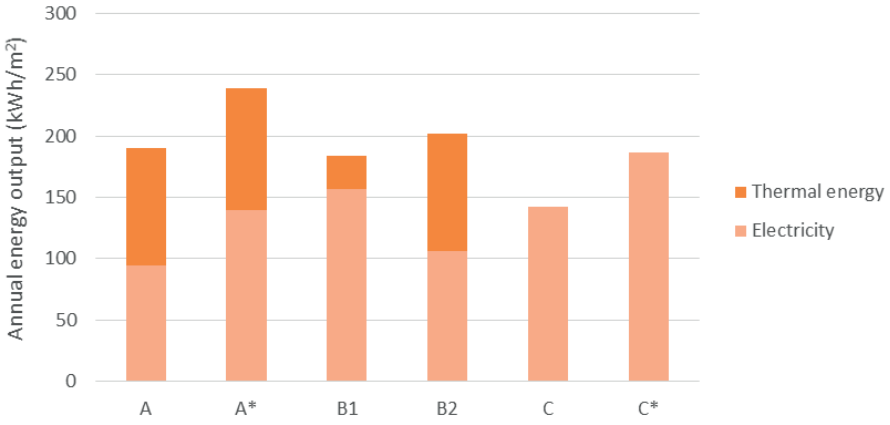

Figure 40. The thermal and electric energy output normalized by the total installed area of the different systems on the ZEB residential concept (unweighted kWh/m^2).

Since the installed areas are relatively similar, the differences between the systems in Figure 40 are similar to those in Figure 39. Both the systems with PV/T modules have lower thermal and electric output per area compared to the other systems.

The primary energy output is calculated with the simplified method described in Section 5.2.3.1. The total (thermal and electric) primary energy output per installed area is shown in Figure 41.

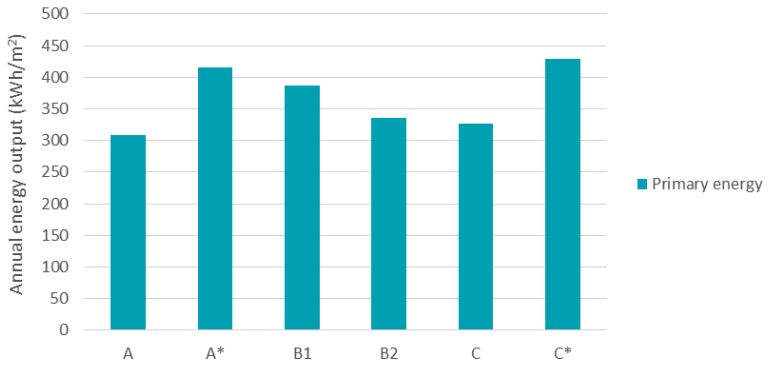

Figure 41. The total (thermal and electric) primary energy output per installed area of the different systems.

5.2.4.2 Energy balance

The net energy demand (E_{net}) calculated with the load/generation balance is shown in Table 8 for the different solar energy systems. The values are normalized by the heated floor area of the building (160 m^2). The net energy demand is shown for two of the ZEB ambition levels described in Section 2.2.1, namely the ZEB-O level (operation), and the ZEB-O÷EQ level (operation, not including electric equipment). The value E_{load} is only shown for the ZEB-O level (not ZEB-O÷EQ), that is, it also includes the loads for equipment. As discussed earlier, the thermal solar energy output is taken into account as a reduction in the load, which is why the systems with high solar thermal output (A, A* and B2) have the lowest values of E_{load}.

Table 8. The net energy demand calculated for the ZEB residential concept.

System	E_{gen}	E_{load}	E_{net} (ZEB-O)	E_{net} (ZEB-O÷EQ)
	kWh/m^2A_{fl}	kWh/m^2A_{fl}	kWh/m^2A_{fl}	kWh/m^2A_{fl}
A	18.6	42.4	-23.7	1.7
A*	27.0	42.2	-15.3	10.2
B1	29.0	46.6	-17.6	7.8
B2	21.4	42.1	-20.6	4.8
C	26.4	47.3	-21.0	4.5
C*	34.5	47.5	-13.0	12.4

The annual net energy, E_{net} (ZEB-O balance), is below zero for all systems, which means that none of them reaches a net zero energy balance at the ZEB-O level. The system that comes closest to reaching a balance is system C*, with only high-efficiency PV modules. The state-of-the-art system with separate solar thermal and PV (A*) is the second closest to reaching a balance, while the system with average PV and solar thermal (A) is furthest from a balance. Of

the two PV/T systems studied, the system with only uncovered PV modules (B1) is closest to a ZEB-O balance.

The thermal and electric solar fractions were calculated as described in Section 5.2.3.3, and the results are shown in Table 9. The solar fractions with yearly energy output ($N = 1$, $t = 1$ year) are referred to as $SF_{th,year}$ and $SF_{el,\ year}$, and the solar fractions calculated with monthly data ($N = 12$, $t = 1$ month) are referred to as $SF_{th,month}$ and $SF_{el,month}$. The value $SF_{th,month}$ (summer) is the monthly thermal fraction for the summer months ($N = 4$, $t = 1$ month, only May to August).

System C*, which was closest to a ZEB-O balance, reaches an electric solar fraction of 73% when yearly data is used in the calculation ($SF_{el,year}$), but 96% when the monthly data is used ($SF_{el,month}$). The solar thermal fraction of this system is, however, zero regardless of which time interval is used since no thermal collector is installed.

Table 9. The thermal and electric solar fractions of the systems on the ZEB residential concept using data for different time intervals.

System	**$SF_{th,year}$**	**$SF_{th,month}$**	**$SF_{th,month}$ (summer)**	**$SF_{el,year}$**	**$SF_{el,month}$**
	%	*%*	*%*	*%*	*%*
A	33	56	98	44	66
A*	33	57	99	64	96
B1	9	17	38	62	85
B2	34	58	99	51	77
C	0	0	0	56	74
C*	0	0	0	73	96

System A* with high-efficiency solar thermal and PV reaches lower value of $SF_{el,year}$ than system C*, 64%, in the yearly calculation, but the same value, 96%, using monthly calculation in $SF_{el,month}$. The solar thermal fractiom is 33% with the yearly data ($SF_{th,year}$), but 56% with monthly data ($SF_{th,month}$).

Of the two PV/T systems, the value of SF_{el} is highest for system B1 with the yearly as well as monthly calculation. The solar thermal fraction of system B1 is, however, lowest of all the systems with thermal components, only 9% if calculated with the total yearly output. The summer solar thermal fraction $SF_{th,month}$ (summer) is 38% for this system, compared to 98-99% for the three other systems (A, A* and B2). Due to the use of a heat pump for auxiliary energy, the systems with high electricity output score high in the calculation of SF_{el}. System A and B2 are the two systems with the lowest electricity output, and also the systems with the lowest values of $SF_{el,year}$. However, when the electric solar fraction is calculated with the monthly data, $SF_{el,month,}$, system B2 scores higher than system C (77% versus 74%), because of the high solar thermal fraction during the summer months.

5.3 Case study 2: Living Lab

5.3.1 The case building

The Living Lab (Figure 42) is one of the laboratories of the ZEB Centre. It was first designed as +Hytte, a concept developed by Finocchiaro and his architecture students [10]. The purpose of the laboratory is to study the interaction between people and technology, and how this influences e.g. the energy demand. For example, the building is equipped with different types of heating systems, motor-controlled shading systems and windows, as well as an extensive sensor system. As the name suggests, the Living Lab will be occupied by actual people who have volunteered to be part of the experiments. The building is described in more detail in reference [172]. The construction was finished in late 2015, and the first volunteers moved in shortly after.

Figure 42. The ZEB Living Lab, as seen from the south. (Photo: Clara Good)

The building is located on Campus Gløshaugen of the Norwegian University of Science and Technology (NTNU) in Trondheim. It is a one storey building with a total heated floor area of approximately 100 m^2. The two roof areas are south-facing with a 30° tilt angle (the optimal in Trondheim is around 40°).

The interior has an open and flexible floor plan which can be adapted for different living conditions. Close cooperation with industry has led to custom-made solutions, such as PCM panels integrated into the ceiling, and aerogel windows. A more detailed description of the building and the planned experiments can be found in Goia, et al. [173]. The following description of the technical systems are taken from this publication, if not otherwise specified.

5.3.1.1 Building energy system

The baseload heating in the Living Lab is provided by a brine-to-water heat pump with a horizontal ground collector as the heat source. The ground collector consists of 105 m^2 plastic piping which is buried at around 1.5 m depth on the north side of the building. As in the residential concept building, a storage tank is the centre of the HVAC system. The tank in the

Living Lab is a combined tank with a total volume of 400 l, composed of a 240 l DHW tank in the upper part, and a 160 l tank for space heating in the lower part. The water circuit from the heat pump is connected to the lower buffer tank in a "tank-in-the-flow" configuration. A simplified sketch of the system is shown in Figure 43.

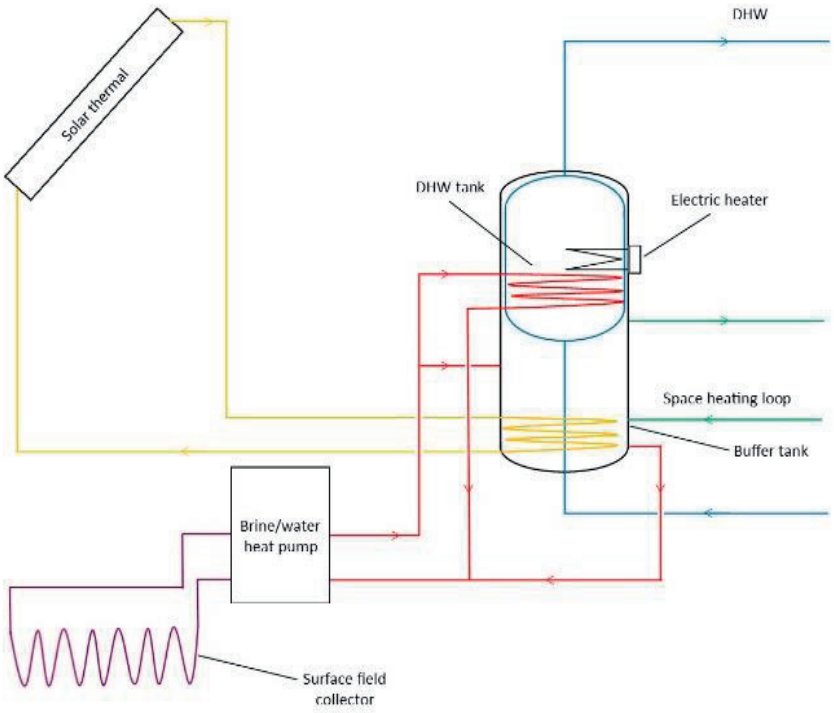

Figure 43. A simplified sketch of the heating system in Living Lab.

5.3.1.2 Solar energy system

Similar to the ZEB residential concept building, the Living Lab has both solar thermal collectors on the façade and a PV system on the roof. The 4.2 m^2 solar thermal collectors (Figure 44) are integrated in the façade next to the south-facing windows. The solar collectors are also connected to the buffer tank in the lower part of the combined tank (Figure 43).

The 79.2 m^2 roof-mounted PV system is visible in Figure 42. It consists of 48 PV modules, with polycrystalline silicon solar cells. The total installed power is 12.48 kW_p, and the PV system is connected to the electricity grid via two 3.2 kW inverters.

Strictly speaking, the modules are not fully integrated into the roof, but added to an already weather proof roof surface of tar roofing and an added plastic membrane. The PV modules can therefore not be said to be a part of the building envelope, which is the definition of building integration. These types of systems are sometimes referred to as in-roof systems (*indach* in German).

Figure 44. The façade-integrated solar thermal collectors on Living Lab. Photo: Clara Good.

Due to the shape of the roof on the Living Lab, the solar cell system on the back (northern) roof is subject to significant shading. In order to minimise the effects of shading, the modules are installed in two vertically oriented strings on each roof area. The modules are furthermore installed in landscape orientation, which helps to reduce the effect of shading (see Section 4.1.3). The system has at the time of writing not been in operation long enough to have given any statistical data on snow cover. Snow cover is not taken into account in the case study, but a 3% soiling throughout the year is assumed. The effects of shading and snow covering on solar energy systems, and strategies to minimise them, are discussed in more detail in Chapter 4.

5.3.1.3 Energy and emission balance

The energy demand for three versions of the building was simulated by Finocchiaro, et al. [10]. Table 10 shows the energy demand for the most energy efficient of the three versions, which is used as the basis for the present study. Even with this version, the Living Lab did not comply with the Norwegian passive house requirements, partly due to the large volume of the building compared to the floor area.

Table 10. The energy demand of the Living Lab [10][15].

	Energy demand	
	kWh/year	*kWh/m$^2A_{fl}$ year*
Space heating	2848	27.9
Domestic hot water	3040	29.8
Electricity	2349	23.0
Total	8237	80.8

Finocchiaro, et al. [10] found that the required delivered electricity to the building (based on the demand in Table 10) was 37.8 kWh/m^2 per year, distributed as 23.0 kWh/m^2 for direct electricity use, 13.8 kWh/m^2 for the heat pump and 0.96 kWh to run the solar thermal system. To balance this load with onsite generation, a PV system with a yearly output of around 3900 kWh would be required.

However, the ambition in the original study was for the building to reach a ZEB-OM balance weighted by emissions. The authors also calculated an emission balance based on emission factors for grid electricity, and an approximated value of the embodied emissions of 5.0 kg CO_{2eq}/m$^2A_{fl}$ per year over a 60 year lifetime. The embodied emissions were approximately equal to the emissions associated with the delivered electricity (the operational emissions). In order to reach a ZEB-OM balance based on emissions, the authors calculated that a PV output of around 7800 kWh[16] would be required

The analysis of the embodied emissions was later done in more detail by Inman and Houlihan Wiberg [12], who concluded that the embodied emissions are much higher. A study of the emission balance of the building with the different solar energy systems is the topic of Section 6.4 of this thesis.

5.3.2 Analysis of alternative solar energy systems

5.3.2.1 Selection of solar modules

In this case study, the PV/T modules were selected taking the actual installation of PV modules on the Living Lab into consideration. Market-available PV/T modules with similar electric efficiency and area were selected. The selected PV/T modules were of the uncovered type, and the thermal efficiency of the modules were therefore lower than that of the solar thermal collectors. The characteristics of the modules used in the Living Lab case study are shown in Table 11.

[15] The energy demand per area is the same as the one simulated by Finocchiaro et al., but the total energy demand is slightly lower due to a change in the heated floor area of the building. The required energy output of the PV system is here calculated with the new area.
[16] This value is calculated according to the equation used by Finocchiaro et al., but has been adjusted for the new and slightly smaller heated floor area.

Table 11. Characteristics of the solar collector, PV module, and PV/T module used in the simulation of ZEB Living Lab.

Module	Technology	Gross area	Electric efficiency at STC*	Rated electric power	Thermal zero-loss efficiency η_0
		m^2	%	kW_p	%
ST	Flat plate	2.09	-	-	81
PV	Poly-Si	1.65	15.8	260	-
PV/T	Mono-Si, uncovered	1.64	15.8	260	58

**See Section 2.1.3.1*

5.3.2.2 System design

The design of the PV/T system on Living Lab follows a similar strategy as in the case study of the ZEB residential concept. As in the first case study, it was decided to use only the roof area (and not the façade) for the PV/T installation, in order to avoid a PV/T system with dual orientations.

Neither the shading of the south roof on the north roof nor snow cover is taken into account in this study due to limitations of shading modelling in the simulation program. An annual soiling factor of 3% is used to account for e.g. dirt on the modules.

In addition to the different solar technologies, a secondary focus in the Living Lab case study was the connection between the solar energy system and the ground source heat pump. In the first four systems, the thermal solar components (collectors or PV/T modules) and the heat pump have separate connections to the tank, as shown in Figure 43, and work more or less independently of each other.

In Systems 5, 6, and 7, the thermal solar components and the heat pump have been integrated. The concept is shown in Figure 45. This type of system can have several modes of operation. In this simulation study, three different modes are used for the solar thermal components:

A) DHW preparation: The solar thermal output is used to heat the water in the combined DHW and space heating tank.
B) Heat pump assistance: The solar thermal output is used as input to the heat pump on the source side. The solar thermal flow is mixed with the ground source flow (if necessary) to provide an appropriate temperature for the heat pump.
C) Idle: The solar collector temperature is too low to provide heating to the tank or to assist the heat pump. Any necessary heating is provided by the heat pump.

Which of these modes that is used at any given moment is determined by a control system.

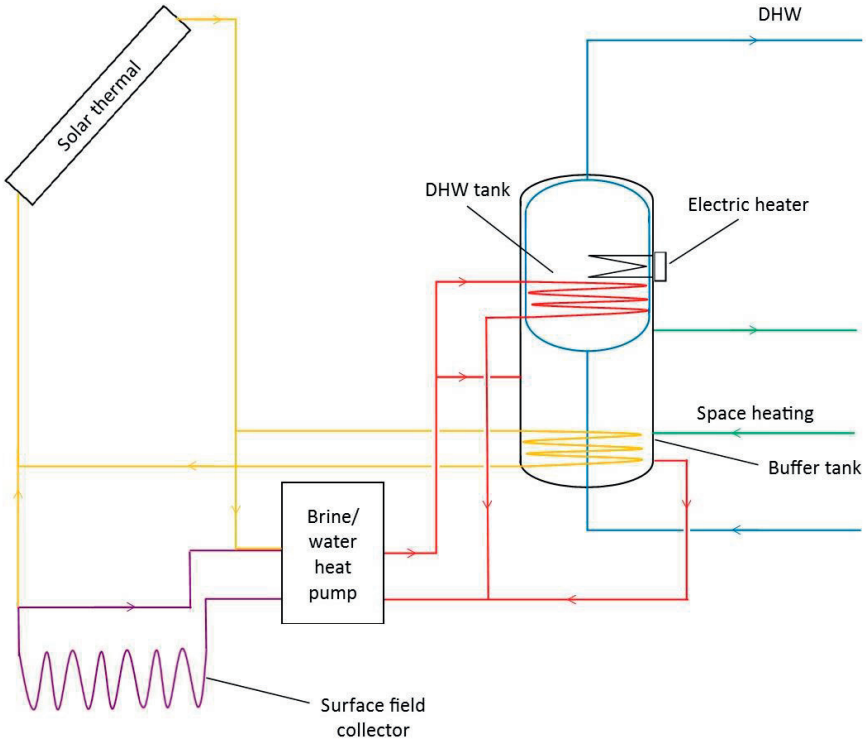

Figure 45. A simplified sketch of the system on Living Lab, with integrated solar thermal and heat pump connection.

Several different systems were analysed, and the main parameters are summarised in Table 12. All the systems have the same installed electric power (12.48 kW_p), except for System 3 and 5, which have a slightly smaller PV system (11.7 kW_p). All of the systems also have the same auxiliary heat source (3.5 kW heat pump and 105 m ground collector).

System 1 is the existing system on the Living Lab, with PV modules on the roof and solar thermal collectors in the façade. The solar collectors and the heat pump are separately connected to the storage tank. System 2 is similar to System 1, but without the façade mounted solar collectors. In System 3, the solar collectors are moved to the roof, and the PV module area is consequently reduced. The heat pump and solar collectors are connected to the tank separately, as in System 1 and System 2. System 4 is similar to System 2, but the PV modules have been replaced by PV/T modules.

The solar installation in System 5 is the same as in System 3 (solar collectors and PV on the roof), but the integrated solar thermal/heat pump connection is used. The control strategy is to always use Mode A when the temperature is high enough, i.e. when the temperature of the output from the solar thermal component is higher than the temperature at the input level in the tank (cut-in and cut-off temperature differentials are used). Mode B is used when the

temperature from the solar thermal component is too low for Mode A, but higher than the temperature of the output from the ground loop. In all other cases, Mode C is used.

Table 12. An overview of the system parameters for the different systems on the Living Lab. The tilt angle of the roof is 30°.

System	Solar technologies	Installed area	Heat pump/solar connection
1	PV + solar thermal	79.2 m2 PV (roof) + 4.2 m2 solar thermal (façade)	Separate
2	PV	79.2 m2 PV (roof)	N/A
3	PV + solar thermal	74.3 m2 PV (roof) + 4.2 m2 solar thermal (roof)	Separate
4	PV/T	78.7 m2 (roof)	Separate
5	PV + Solar thermal	74.3 m2 PV (roof) + 4.2 m2 solar thermal (roof)	Integrated, DHW priority, no seasonal control
6	PV/T	78.7 m2 (roof)	Integrated, DHW priority, no seasonal control
7	PV/T	78.7 m2 (roof)	Integrated, DHW preparation during summer (Apr-Sep), heat pump assistance during winter

System 6 and System 7 have the same solar installation as System 4 (PV/T on the whole roof) but an integrated connection between PV/T and heat pump. The control strategy in System 6 is the same as in System 5, namely temperature control with priority for Mode A (DHW preparation). In System 7, the mode of operation is seasonally controlled. Mode A is used during summer, whenever the temperature in the PV/T collector is high enough, and Mode B is used during winter. Several variations of the length of the summer season were simulated, but the one used in System 7 is April to September, since this system reached the highest value of E_{net}.

5.3.3 Calculations

5.3.3.1 Energy output

The energy output in primary energy is calculated in the same simplified way as for case study 1. Electricity from the solar energy systems is given the value of avoided electricity from the grid (2.3 kWh_{PE}). The average COP of the heat pump is in this case 3.89, which gives a thermal primary energy factor of 0.59.

5.3.3.2 Energy balance

The exported/delivered energy balance is calculated according to Equation (12) from Section 2.2.3.1, using the non-renewable primary energy factors from Table 1. Since the non-renewable primary energy factor for PV electricity delivered from onsite ($f_{Pgen,el(PV)}$) is zero, the equation can be simplified to Equation (24).

$$E_{net} = (E_{exp,el,tmp} \cdot f_{P,exp,el,tmp} + \mathrm{E}_{\mathrm{exp,el,grid}} \cdot f_{P,exp,el,grid}) - E_{del,el} \cdot f_{P;del;el} \qquad (24)$$

5.3.3.3 Load match and grid interaction

The load match and grid interaction calculations were described in Section 2.2.4. The thermal load match (solar fraction, SF_{th}) is calculated using yearly and monthly data. The grid interaction factor for electricity ($f_{grid,el}$) is calculated using monthly and hourly data.

5.3.4 Results

5.3.4.1 Energy output

The thermal and electric output of the systems are shown in Figure 46 as unweighted kWh, with the building energy demand as comparison. Comparing this figure to Figure 39, it can be noted that the installed system areas are significantly larger than the ones on the ZEB residential building, while the building itself is smaller and consequently has a lower energy demand. The electric system area is also significantly larger than the thermal system area for all systems (except those with PV/T).

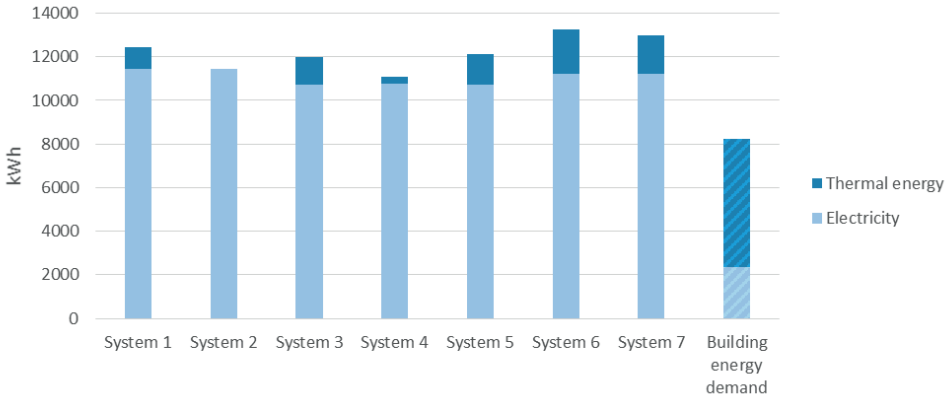

Figure 46. The thermal and electric energy output of the different solar energy systems on the Living Lab in unweighted kWh. The building energy demand is shown for comparison.

The installed areas are different also in this case study, and the energy output per installed area is shown in Figure 47. The energy output is divided by the total installed area, according to the same principle as in Figure 40. It should be noted that the solar collectors and PV modules in System 1, the original system, are installed with two different orientations (vertically on the façade and at 30° tilt on the roof), while in all the other cases, all modules are installed on the roof.

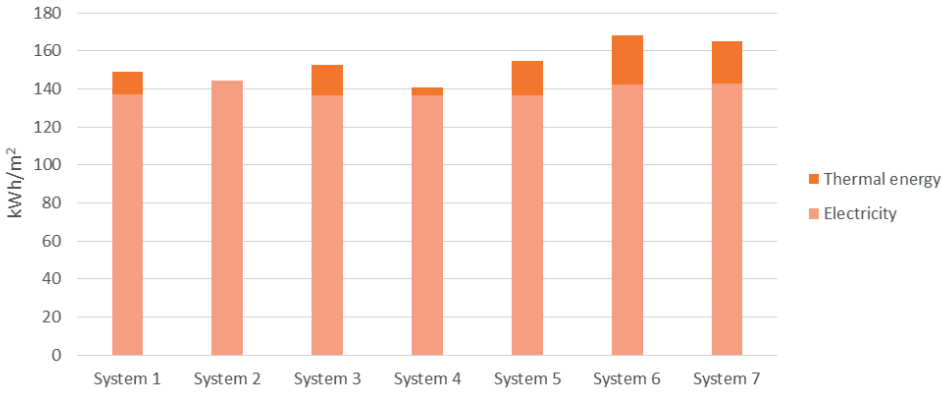

Figure 47. The energy output normalized by the total installed area for the different systems on the Living Lab in unweighted kWh.

The electricity output is more or less similar for all the systems, but slightly smaller for the PV/T systems. The output in kWh per total installed area is largest for the PV/T systems with an integrated heat pump connection (System 6 and System 7) and smallest for the solar thermal and PV/T system with separate heat pump connection (System 4). The solar collector and PV system with an integrated heat pump connection (System 5) has a slightly increased output compared to the system with separate connection (System 3).

The thermal output in kWh is largest for the PV/T modules on System 6 and System 7, but the output temperature is different from the systems with pure solar collectors. The output also depends on the type of connection to the heat pump. The temperature during operation of the thermal components of the systems are shown in Figure 48. The average temperature of the PV modules is also included in the graph.

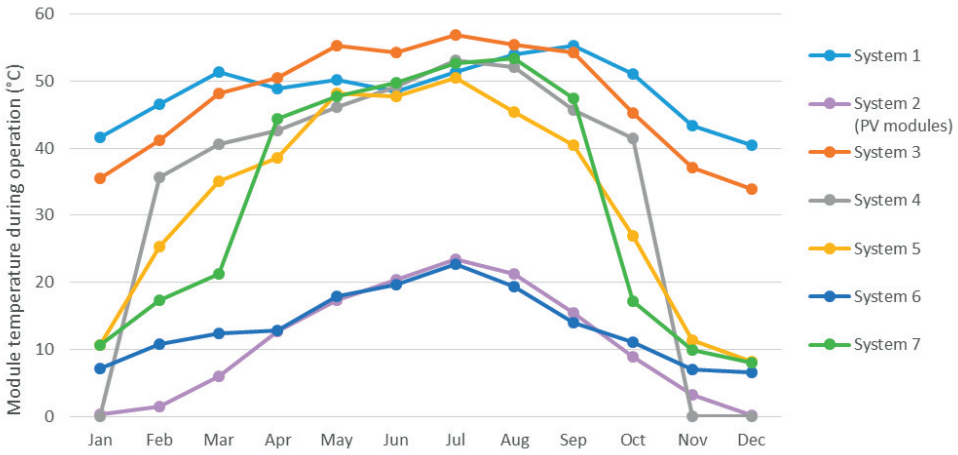

Figure 48. Solar collector or PV/T module temperature during operation for the system on the Living Lab. The average PV module temperature for System 2 is also included.

The module temperature during operation is significantly lower in System 6, where the PV/T collectors assist the heat pump, compared to all the other systems with thermal output. The PV/T modules in System 6, which assist the heat pump during summer, are also slightly cooler than the PV modules (shown for System 2 in the figure) during this period, which could suggest that using PV/T modules in this way could also improve the electricity output. The PV/T modules that operate in DHW mode during summer (System 4 and 7) reach higher temperatures than the PV modules. The same is true for all the PV/T systems during October to April. System 4, where the PV/T modules are separately connected to the storage tank, does not contribute at all during November to January (the values in Figure 48 are zero since the module is not in operation during this time).

The total primary output, as determined by the simplified calculation method described in Section 5.3.3.1, is shown in Figure 49 , normalized per heated floor area (A_{fl} = 102 m^2). The primary energy output is highest for the PV/T systems with the integrated heat pump connections (System 6 and System 7) and lowest for the PV/T system with separate heat pump connection (System 4). The primary energy output per installed area of System 2, with only PV, is higher than that of Systems 1, 3, and 5, with solar collectors and PV, because of the higher primary energy value of electricity.

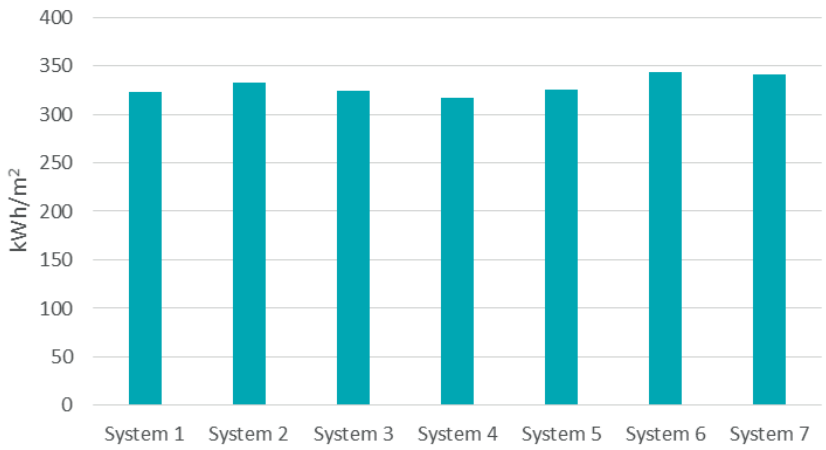

Figure 49. The total (thermal and electric) primary energy output per total installed area for the different systems on the Living Lab.

5.3.4.2 Energy balance

The net energy (E_{net}) is calculated according to the exported/delivered balance described by Equation (24), and the results are shown in Table 13. The values for temporary exported and later imported electricity ($E_{exp,el,tmp}$), surplus exported electricity ($E_{exp,el,grid}$), and delivered electricity ($E_{del,el}$) are also shown in the table, calculated using the factors from prEN15603 [74] shown in Table 1. The non-renewable primary energy factors from Table 1 are used. Since the non-renewable primary energy factor, and thereby the primary energy value, for solar energy delivered from onsite is zero, this item ($E_{gen,el}$) is not included in the table.

Table 13. The exported/delivered net energy balance for the systems on the Living Lab, calculated as primary energy per heated floor area A_{fl}.

System	$E_{exp,el,tmp}$	$E_{exp,el,grid}$	$E_{del,el}$	E_{net} (ZEB-O)
	kWh_{PE}	kWh_{PE}	kWh_{PE}	kWh_{PE}
1	50.0	116.7	57.5	109.2
2	51.2	114.3	58.8	106.6
3	50.1	106.3	57.6	98.8
4	51.0	104.6	58.7	97.0
5	51.1	105.1	58.8	97.5
6	53.2	108.3	61.1	100.3
7	53.4	110.0	61.5	102.0

In contrast to the first case study, all systems result in a positive net energy, that is, a ZEB-O balance is reached for all the cases. The highest value of E_{net} is reached by the original system (System 1), which also has the largest installed area. Of the other systems, which are all similar in area and orientation, the highest value is achieved for System 2, with only PV, followed by the two systems with PV/T and an integrated connection with the heat pump (System 6 and System 7). The system with PV/T and separate heat pump connections (System 4) has the lowest value of E_{net}.

5.3.4.3 Load match and grid interaction

The solar thermal fraction SF_{th} calculated with yearly and monthly data are shown in Table 14, as well as with the monthly data for the summer months only (May-August). The grid interaction index (f_{grid}) calculated with monthly and hourly data is shown in the same table. The total solar fraction SF_{tot} was 100% for all the systems, when calculated with yearly as well as with monthly data, since the solar energy systems cover the total energy demand in all the cases.

Table 14. The thermal solar fraction (SF_{th}) and grid interaction index (f_{grid}) of the different systems on the Living Lab, using data for different time intervals.

System	$SF_{th,year}$	$SF_{th,month}$	$SF_{th,month}$ (summer)	$f_{grid,month}$	$f_{grid,hour}$
	%	%	%	%	%
1	13.2	17.1	26.3	44.9	23.5
2	-	-	-	45.0	23.5
3	16.3	23.3	49.3	45.7	23.7
4	0.0	0.1	0.2	45.7	20.7
5	18.1	25.1	51.3	45.9	23.7
6	22.6	27.0	46.6	45.5	21.6
7	19.8	11.1	0.0	46.5	21.7

The thermal solar fraction calculated both with yearly and monthly data is highest for System 6, with PV/T modules and heat pump in integrated connection, with no seasonal control. The highest value during summer is for System 5, with PV and solar collectors on the roof in integrated connection with the heat pump, and System 3, with PV and solar thermal on the roof in separate connection with the heat pump.

The thermal solar fraction is lowest for the original system (System 1), where the solar collectors are mounted on the façade. However, the solar thermal output and thermal solar fraction during spring and autumn is slightly higher for the façade mounted collectors. Figure 50 presents a comparison of the thermal output and thermal solar fraction of System 1 and System 3, showing that the façade mounted collectors perform better during these so-called shoulder seasons.

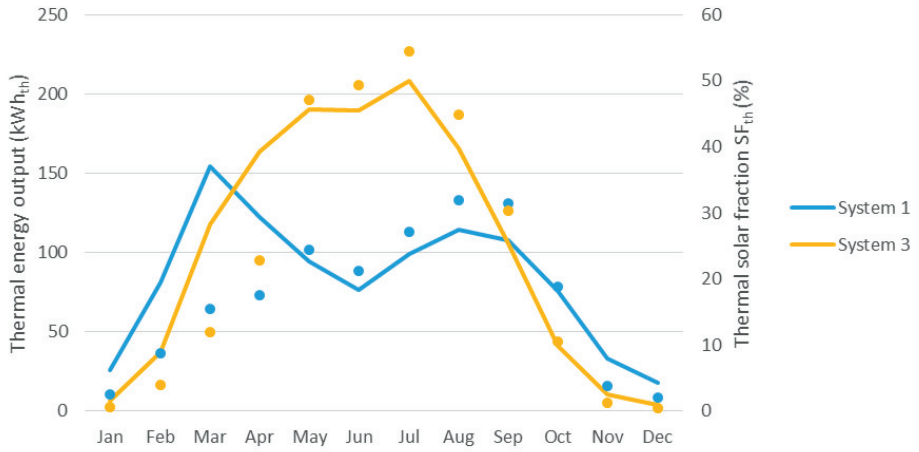

Figure 50. The solar thermal output (lines) and thermal solar fraction SF_{th} (dots) of System 1, with facade mounted collectors, and system 3, with roof mounted collectors.

As described in Section 2.2.4, the grid interaction index, f_{grid}, is a value of how much the grid transfer varies over the studied period. It does not show if the transfer is export or import of electricity. The grid interaction index is relatively similar for all the systems. The value of f_{grid} calculated with monthly data is highest for System 7, with PV/T and heat pump in integrated connection with different summer/winter operation. This might be a result of the lower solar thermal output during summer which means that more electricity is needed for the operation of the heat pump.

For f_{grid} calculated with hourly data, System 4 with separate PV/T and heat pump connection stands out as significantly lower than the rest of the systems. The values for the two other systems with PV/T (Systems 6 and 7) are also lower, which could simply be due to the slightly lower PV output of these systems.

5.3.4.4 Heat pump and ground source loop

The seasonal performance factor (*SPF*) of the heat pump is shown in Table 15. The table also shows the seasonal performance factor of the whole system (SPF_{sys}), which also includes energy use of circulation pumps and the electric heater in the tank. Both factors are calculated for the whole year.

Table 15. The seasonal performance factor of the heat pump, SPF, and of the total energy system, SPF_{sys} for the different systems on the Living Lab.

System	SPF	SPF_{sys}
	-	-
1	4.0	3.4
2	4.0	3.1
3	4.0	3.5
4	4.0	3.2
5	3.9	3.4
6	3.6	2.9
7	3.8	3.1

Even though the solar energy output is largest in Systems 6 and 7, these systems do not have the highest value of E_{net}, nor the highest SPF and SPF_{sys} values. Table 15 shows that the systems without an integrated connection between heat pump and solar energy components (Systems 1-4) have higher values of SPF and SPF_{sys}. The highest values are achieved by System 3, with PV and solar thermal collectors on the roof.

One of the reasons for using an integrated connection is to recharge the ground to prevent cooling of the ground over time. None of the analysed systems actively recharge the ground, but they allow the ground to recharge naturally by assisting the heat pump during parts of the year. To evaluate the effect of this, the systems were also simulated after 20 years of operation. The ground loop outflow temperatures after 1 year and after 20 years of operation are shown in Table 16, together with the annual energy withdrawal from the ground loop.

Table 16. Annual energy withdrawal from the ground together with the temperatures during year 1 and year 20 of operation for the systems on the Living Lab.

System	Energy from ground loop	Outflow temperature from ground loop, year 1	Outflow temperature from ground loop, year 20
	kWh	*°C*	*°C*
1	4937	5.50	5.30
2	5428	5.30	5.10
3	4796	5.50	5.30
4	5273	4.60	4.30
5	4454	5.50	5.30
6	3284	6.00	5.90
7	3693	5.90	5.80

The energy withdrawal from the ground is highest in the systems with the lowest solar thermal energy output (System 2 and 4), and lowest in the systems with the highest solar thermal output (Systems 6 and 7). The difference between the three systems with the lowest (System 6), highest (System 2), and middle (System 3) withdrawal is shown in Figure 51. System 6, where the PV/T modules assist the heat pump all year, has a consistently lower energy withdrawal than the other two systems. The energy withdrawal from the ground during the summer is significantly higher in System 2, with only PV modules, than in System 3, with PV and solar collectors, since the solar thermal collectors cover around half of the total thermal energy demand during this period.

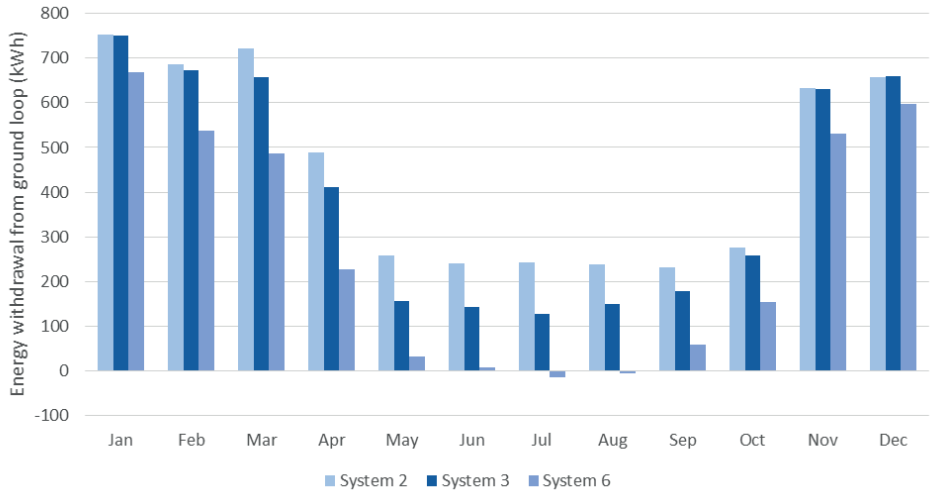

Figure 51. Energy withdrawal from the ground loop for three of the systems on the Living Lab.

The temperature in the ground is affected by the energy withdrawal over time. Table 16 shows the change in the annual average outflow temperature of the ground loop over time. The systems with lowest energy withdrawal have the smallest temperature changes. However, the largest change is around 0.3°C, which is almost negligible.

5.4 Discussion and conclusions

Two case studies of PV/T systems in residential buildings have been presented in this chapter in order to evaluate the energy performance of different solar energy systems.

The case studies share some similarities: both are single family residential buildings in Norway, both are designed according to energy efficiency principles, and both use solar energy systems in combination with a heat pump. In addition, the two cases are pilot buildings of the ZEB Centre.

The main difference between the buildings is that the first one, the ZEB residential concept, is only a model while the second one, the Living Lab, is a recently constructed building. The former is also significantly larger, but the latter has a larger volume compared to the floor area. The ZEB residential concept has a flat roof where solar modules are installed in rows, while the system in the Living Lab is semi-integrated into the sloped roof. The choice of heat pump is also different: the ZEB residential concept has an air-to-water heat pump and the Living Lab a ground source heat pump with a horizontal collector.

Both case buildings are studied using simulations of different solar energy solutions. The original solar energy system did in both cases include PV modules and solar thermal collectors in combination with a heat pump. Alternative energy systems were designed to study the effect

of the choice of solar energy technology on the energy output and performance of the energy system, as well as the overall energy balance of the building.

The solar energy system on the ZEB residential concept is significantly smaller than that on the Living Lab when compared to the heated floor area of each building. It also has a higher area ratio of thermal collectors compared to PV modules.

5.4.1 Weaknesses and uncertainties

A weakness in both case studies, which was also touched upon in Section 1.3.4, is the difficulty of performing a comparative analysis. The basis for comparison in both case studies has been the energy demand of the case building and the area available for the installation. Within these boundaries, the selection of "comparable" systems is still difficult due to the large number of possible variations.

A difficulty in comparing PV/T modules to PV and solar collectors is that the energy output of PV/T modules is in the form of two energy carriers – electricity and heat – compared to only one energy carrier from PV modules or solar thermal collectors. The question is therefore whether the technologies should be rated and compared based on their electric or thermal performance, or based on some other standard?

Two different approaches were taken in the case studies, each with its benefits and drawbacks. In the first case study, the modules were selected based on their performance relative to other modules in the same market. The problem with this solution is that the best PV module and the best solar thermal collector are much better than the best PV/T collector on the market in terms of efficiency. The development of PV/T technology has a long way to go to reach the same maturity and robustness as PV and solar thermal technology, and the performance of the state-of-the art PV/T modules can therefore be expected to increase in conjunction with an increase in the size of the market. In addition, it is also a relatively difficult basis for comparison, since none of the compared modules had the same rated efficiency.

This study only focused on currently available technology, for PV/T as well as for PV and solar thermal technologies. It is difficult to predict the future for PV/T technology, as it depends on both technological and market developments. Some future research areas have been discussed by Michael, et al. [112], including development of better adhesives, improved lamination methods, and the use of nanotechnology. Better certification and testing standards are also important for the PV/T market development [174].

In the second case study, the comparison was based on the electric efficiency of the PV modules. This mode of comparison proved to be more robust. The focus on electric efficiency also made sense, since unglazed PV/T modules were primarily used as a replacement for PV modules, and reaching a high solar thermal fraction was not the primary objective.

The general uncertainties and weaknesses related to energy simulations were discussed in Section 1.3.3. As in all simulation studies, the results may deviate significantly from the performance of a real system. Due to the lack of PV/T installations in Norway, and the fact that

no measurement data is available for any of the case buildings, there has been no effort to compare the simulated data to real measurement data. In addition, the thermal load of the building was calculated using a simplified method in Polysun based on annual values from previous publications. The impact of shading on the Living Lab systems was disregarded due to the limited possibilities to model shading in Polysun. It is possible that taking shading into account would have altered the results since it would have affected the thermal output of the PV/T modules more than the thermal output of the solar thermal collectors, as the former covers both the south roof area and the shaded north roof area. Solar thermal collectors were only installed on the unshaded south façade or south roof. Weather and irradiation data for northern latitudes is also, in general, an uncertainty. However, the objective of the case studies was to compare different energy systems for each case separately. The absolute values are therefore of less importance than the differences between the systems in the same case study.

5.4.2 Case study 1: ZEB residential concept

In the first case study, the energy output in unweighted kWh was largest for the two systems with solar thermal collectors (A and A*). In primary energy output, however, the output was higher for the two PV/T systems (B1 and B2) than for the systems with average PV modules and solar collectors (A and C), but it was highest for the systems with high-efficiency PV modules and solar collectors (A* and C*).

The net energy, E_{net}, calculated at the net ZEB-O ambition level, is negative for all the systems in case study 1. This means that none of them reaches a net ZEB-O energy balance. If the ambition level is lowered to ZEB-O÷EQ, all the systems reach a balance. The systems that are closest to reaching a net ZEB-O balance are systems A*, with high-efficiency PV and solar thermal collectors, and C*, with high-efficiency PV modules. The third closest system is the one with only uncovered PV/T modules (system B1). The system that is furthest from a balance is system A with average PV modules and solar collectors.

The annual SPF of the heat pump is a sensitivity factor in the analysis. The SPF is around 2.3 for the systems with a high solar thermal fraction (A, A*, and B2), and 2.5 for the other systems. The SPF is increased since the heat pump is also operational during the summer, when the outdoor temperatures are higher. The same heat pump was used in all the systems and was dimensioned for the winter load, when outdoor temperatures are lower.

The thermal solar fraction is similar for the three systems A, A*, and B2, with covered PV/T collectors, since the solar thermal fraction was the basis for the system design. The solar thermal fraction of system B1, with uncovered PV/T collectors, is low. The thermal output of this system is small and of low temperature, which means that an auxiliary energy source is necessary also during summer.

The electric solar fraction, which is also the total solar fraction since the auxiliary heat source is a heat pump, is highest for the systems with highest electricity output, namely systems C* and B1, and for system A*, with high solar thermal output and relatively high electricity output.

The two PV/T systems analyzed in the first case study were based on the design of system A, where the solar modules and the heat pump are connected in parallel, and the performance could no doubt be improved with further system adjustments. In particular, the uncovered PV/T system would work better if it was used for preheating, since the temperatures in the collectors are not high enough, even during summer, to provide heating of domestic hot water.

5.4.3 Case study 2: Living Lab

In the second case study, the energy output of a PV/T system was shown to be higher than a similarly sized system with PV and solar thermal collectors, or only PV modules, in unweighted energy as well as in primary energy. In the system with an integrated solar thermal and heat pump connection, the thermal energy output in kWh/m^2 total installed area was increased by up to 45% in the systems with PV/T modules compared to a the system with separate PV modules and solar collectors. The system with a separate PV/T system and heat pump connection had the lowest energy performance of all the simulated systems.

The electricity output was decreased by around 1% in the PV/T systems compared to a similarly sized PV system. This is contrary to the idea of improved electricity output in PV/T modules due to the increase of PV efficiency, but in line with findings presented in e.g. the PV/T Roadmap [119]. The average temperature of the PV modules in System 3 is lower than that of the PV/T modules. As shown in Figure 48, however, the PV/T modules that assist the heat pump during summer are cooled as a result. A different control system could probably have increased the cooling, resulting in higher electricity output. A system where PV/T modules were only connected to the source side of the heat pump, and not to the tank, would probably also have been more appropriate.

Due to among other factors the increased energy demand of circulation pumps the seasonal performance factor (SPF_{sys}) of the systems with PV/T modules was not higher than that of the systems with PV modules and solar thermal collectors. The system with the highest value of SPF_{sys} was in fact the one with only PV modules.

The net energy, E_{net}, was larger (i.e. there was a larger energy surplus over the year) for the systems with PV/T with an integrated connection to the heat pump than for the system with PV only. However, the value of E_{net} was largest for the system with PV modules and solar collectors side by side. All systems on the Living Lab resulted in a positive net ZEB-O balance by a large margin. As discussed in Section 4.2.5, the control system and its implementation are key factors to system performance. The system design in the Living Lab case study could no doubt be significantly improved to reach a better performance of the system.

The annual solar thermal fraction was largest for the PV/T systems with an integrated heat pump connection. The solar thermal fraction calculated with monthly data for the summer SF_{month} (summer), is, however, largest for the system with separate PV modules and solar thermal collectors. None of the systems reach very high solar thermal fractions; the solar thermal collector area would have to be increased to reach higher values. The solar fraction of the PV/T system with a separate connection to the heat pump (System 4) is next to zero,

showing that unglazed PV/T modules are not suitable for direct preparation of DHW in a Scandinavian climate.

The grid interaction index was relatively similar for all the systems when calculated with monthly data ($f_{grid,month}$). There was a larger difference when the calculation was performed with hourly data ($f_{grid,hour}$), and the grid interaction factor was then lowest for the three systems with PV/T modules. One possible reason is that these three systems have the highest energy use by circulation pumps, which could mean lower levels of electricity export to the grid. Further analyses of self-consumption of the generated energy could have provided more information on the actual dynamics.

The two systems with an integrated PV/T and heat pump connection (System 6 and 7) have the lowest values of energy withdrawal from the ground. The ground is therefore allowed to recharge naturally during summer. As a result, these two systems also have the lowest levels of ground cooling over a 20 year period. However, the ground cooling is in this case negligible for all systems. The case building studied here had a horizontal ground collector at a shallow depth (1.5 m). It is possible that the avoided ground cooling would be a larger benefit in the case of a vertical borehole ground collector.

5.4.4 Final remarks

The results of the two case studies give no clear responses to the question of whether it would be better to install a PV/T system than a system with separate PV modules and solar thermal collectors. The performance of the systems are to a large extent case-specific, and factors such as location, type of auxiliary heat source and other components, and modes of connection have a large influence on the results.

Results from the ZEB residential concept case study suggest that covered PV/T could give an increased output compared to solar thermal collectors. This analysis is, however, quite uncertain since the analysis is based on a small number of products. This is due to the fact that the number of collectors with this technology available on the market is very small. The small market for covered collectors could partly be due to the material challenges involved in producing these types of modules due to higher temperatures and more demanding thermal cycling compared to uncovered modules.

The system with uncovered PV/T modules holds up well in this comparison where electricity is favored, but the thermal output is small and of low temperature, which means that an auxiliary energy source is necessary also during summer. Integrating the solar thermal collector to the source side of the heat pump, such as in the second case study, might have improved the system efficiency.

The Living Lab case study indicates that there is be a benefit of integrating solar thermal or PV/T systems on the source side of a ground source heat pump, compared to using the components separately from each other. However, the potential benefit might just as easily disappear due to an increased electricity demand for e.g. circulation pumps. The control strategy and implementation are key factors which determine the performance of the system.

Based on experiences from review of earlier research as well as actual installed systems, the integrated solar thermal or PV/T and ground source heat pump system design appears to be beneficial for refurbishment of under-dimensioned ground source heat pump systems, or systems where the energy load has increased. The second case study showed that the use of a PV/T system to assist the ground source heat pump resulted in lower energy withdrawal from the ground. For new systems, the use of integrated system design means that the ground source collectors can be made smaller or installed closer together while still providing the same amount of heating to the building.

Chapter 6: Environmental impact of PV/T systems

6.1 Introduction

6.1.1 Scope of the analysis

This chapter deals with the emissions related to solar energy systems, in particular to PV/T systems. As mentioned earlier, solar energy systems, especially those including PV cells, can be responsible for a large share of the total embodied emissions of a building.

There has been quite extensive research related to the embodied emissions of PV systems, and to some extent solar thermal systems, but a rather limited amount of research on PV/T systems. This is especially true for commercial products. A review of previous research on the environmental impact of PV/T systems is given in Section 6.1.2 and Paper IV.

The first part of this chapter deals with the embodied emissions of PV/T modules. A life cycle assessment of a PV/T module which was performed based on data from two commercial producers of unglazed PV/T modules is presented in Section 6.1.3.7.

The second part of the chapter focuses on how the design of the system influences the embodied emissions, as well as the emission balance of the building. The first case building, the ZEB residential concept, is used for this study, which deals only with PV systems. The study is presented in Section 6.3 and Paper V.

The third part of the chapter is focused on how the choice of solar technology influences the embodied emissions and emission balance of a building. The emissions associated with PV/T modules and systems are compared to the emissions of separate PV and solar thermal systems. The second case building, the Living Lab, is used in this study, which is presented in Section 6.4. The inventory of the specific embodied emissions of the PV/T modules that were determined in Section 6.2 is used as an input.

6.1.2 Review of previous research

A detailed study of previously published research on the environmental impact of PV/T modules is given in Paper IV, and only a summary is presented here. In general, there are few available studies on the environmental impact of PV/T modules and systems.

All studies included the balance of system (BOS) in the calculations, but they differ in what is included in the BOS, and how often (if ever) the components are replaced. Not all of the studies follow the LCA methodology, as described by ISO [87], or use only parts of it. Two commonly used impact factors are the global warming potential at 100 years (GWP100), as defined by IPCC [9], and the cumulative energy demand (CED) or primary energy resources (PER). Some of the research groups have used the LCA software SimaPro [175] to perform their analyses.

A general conclusion is that the payback time in both energy and greenhouse gas emissions of the PV/T systems are much shorter than their expected lifetime, and that PV/T installations

therefore “make sense” environmentally. However, due to the unclear method and lack of sources in some of the publications, it is sometimes hard to evaluate the validity and the transferability of the results.

An overview of the results of the embodied energy and emission factors, energy payback time (EPBT), and greenhouse gas emission payback time (GPBT) found in the review is given in Table 17. Not all of the publications included values for embodied energy and emissions per m^2, but it has been calculated based on data given in the publication whenever possible (calculated values are shown in italic text in the table).

As shown in the table, most of the studies were focused on PV/T-air modules. The analysed systems are located in Asia, Australia, and Southern Europe. The irradiation (when given) is around 1200-1650 kWh per year. None of the studies analysed systems in areas with lower levels of irradiation or colder climates. The energy output of the systems, which is a very important parameter in the calculation of payback times, was sometimes approximated or calculated in a simplified way. Most of the analysed systems are at least partly custom-made, and no study describing the industrial manufacturing of PV/T modules were found.

The study presented in the following sections was made to try to address some of the issues that were missing from published studies, namely analysing commercial PV modules in a Northern European climate with lower levels of irradiation.

Table 17. Overview of environmental impact assessments of PV/T modules and systems. Text in italics indicates that the value is calculated based on data given in the publication.

Publication	**PV/T technology**	**PV efficiency**	**Location of system**	**Embodied energy**	**Embodied emissions**	**EPBT**	**GPBT**
		%		*kWh/m²*	*kg CO_{2eq}/m²*	*years*	*years*
Tripanagnostopoulos, et al. [36], 2005	PV/T-liquid, glazed and unglazed	*10.6-12.6%*	Patras, Greece	*1281 (glazed module)*	*396 (glazed module)*	0.8-4.1	0.8-2.2
Battisti and Corrado [38], 2005	PV/T-air	10.7%	Rome, Italy	*1442*	*451*	1.7-2.8	1.6-2.8
Tripanagnostopoulos, et al. [176], 2006	PV/T-air, glazed and unglazed	*10.6-12.6%*	Patras, Greece	*1074-1194*	*343-377*	1.0-1.9	1.3-2.2
Crawford, et al. [39], 2006	PV/T-air	Not mentioned	New, South Wales, Australia	*6570-8064 (c-Si) 4575-4738 (a-Si)*	-	6-14 (c-Si)	
Tiwari, et al. [37], 2007	PV/T-liquid	11%	New Dehli and Leh, India	*1380-2078*	-	4-9 (a-Si)	-
Chow and Ji [177], 2012	PV/T-liquid	13%	Hong Kong	*1303-1726*	*387-513*	11.4-14.33	
Kamthania and Tiwari [178], 2012	PV/T-air (9 different PV technologies)	5-17% (different technologies)	Srinagar, India	*603-1772*	-		-
Agrawal and Tiwari [179], 2013	PV/T-air	Not mentioned	New Dehli, India	*1235*	-	2.8-3.8	3.2-4

6.1.3 Method

6.1.3.1 Assessment of embodied emissions

The embodied emissions of the solar energy systems are determined using life cycle assessments (LCA). The LCA methodology was described in detail in Section 2.3. Details on the goal and scope, the life cycle inventory (LCI), and the impact assessment of each analysis is presented in each section.

The analyses presented in this thesis cannot be considered full LCAs, but only life cycle impact assessments (LCIA). The LCA standard is quite extensive and a full LCA has to include, among other things, a comprehensive reporting including an assessment of data quality, reference flows, and the categorisation models. In addition, an LCA that will be disclosed to the public should preferably undergo an external review. Furthermore, the analyses presented here focus only on one impact category, namely the global warming potential at 100 years (GWP100a), as described by the Intergovernmental Panel on Climate Change (IPCC) [9]. A full LCA should include analyses of a comprehensive set of impact factors.

6.1.3.2 Guidelines and methodologies

Any LCA is sensitive to assumptions, approximations, and generalizations made by the LCA practitioner. It is therefore difficult, or even impossible, to directly compare the results of different LCAs to each other. In order to conform as much as possible to other studies, two LCA guidelines have been used in the following analyses.

The first one is the Methodology Guidelines on Life-Cycle Assessment of Photovoltaic Electricity [79], which was published in the project IEA PVPS Task 12 – PV Environmental Health and Safety. This set of guidelines gives suggestions for e.g. the lifetime of PV modules and components. The suggested lifetime for mature PV technologies is 30 years, based on common commercial warranties of 25 years and the expectation that modules will last beyond their warranties. Since the PV/T modules that were analysed in this thesis also had a warranty of 25 years, their lifetime is assumed to be the same as for PV modules. Inverters and other electric components are assumed to have a lifetime of 15 years, and they therefore require one replacement during the lifetime of the PV system.

Solar thermal systems are not mentioned in the guidelines. According to [80], solar thermal systems can be assumed to have a lifetime of 20-25 years. Previous LCA studies of solar thermal systems assume a 25 year lifetime for the solar collectors, 15 years for pumps and other equipment, and a recommended replacement of the heat transfer fluid every 10 years [180]. In the analysis of different solar technologies in Section 6.4, the lifetime of the solar thermal system is assumed to be 30 years to simplify the comparative elements of the analysis. A sensitivity analysis is also performed with a lifetime of 20 years.

The other set of guidelines, which is presented in the upcoming publication "A Norwegian ZEB Definition Guideline" [73], describes the methodology used in the ZEB Centre. This report includes a complete methodology for the assessment of embodied emissions of materials,

calculation of the net zero emission balance, and reporting of results. The methodology described in the report has been followed as far as possible in this thesis.

The recommendation in the ZEB Centre guidelines is to assume that a new building has a lifetime of 60 years, which means that the solar energy systems will need to be replaced once. It also recommends to use the functional unit 1 m^2 heated floor area per year (1 $m^2 A_{fl}$/year) in the analysis of a whole building. The benefit of using this unit is that it is similar to the common form of reporting the energy performance of a building, namely in kWh per m^2 heated floor area per year. According to the guidelines, it is also recommended to report the total embodied emissions (kg CO_{2eq}) of the building. [73]

The system boundary can be defined according to the process stages given in EN 15978 [85]. The definition of the ZEB ambition levels according to these process stages was given in Figure 16.

6.1.3.3 Emission factor

The ZEB Centre guidelines also recommend to use the ZEB ultra-green grid factor, which was described in Section 2.2.3.2 [73]. The value of this factor is declining from the value of the current EU grid (0.361 kgCO_{2eq}/kWh) down to 0.032 kgCO_{2eq}/kWh in 2050. Average grid factors are used in studies presented here, and the averages are calculated over the number of years that are analysed in each case. The full lifetime of the building (60 years) is used in the study of the impact of system design (Section 6.3), which results in an average ZEB ultra-green grid factor of 0.132 kgCO_{2eq}/kWh. In the study of the impact of the choice of solar technology, the lifetime of the solar energy systems (30 years) is used, which results in an average ZEB grid factor of 0.238 kgCO_{2eq}/kWh. Symmetric emission factors ($f_{GHG,el,sym}$) are used in both analyses, meaning that electricity is given the same emission value regardless of whether it is imported from or exported to the grid.

The ZEB ultra-green scenario is quite optimistic regarding the development of the European electricity grid as well as the implementation of energy efficiency measures in Europe. In each of the studies, the current average EU factor (0.361 kgCO_{2eq}/kWh) is also used to provide an analysis with a more pessimistic, or conservative, outlook of the grid development. This grid factor is assumed to remain constant over time in the analyses.

The emission factor of the solar energy systems is calculated in the two case studies in Section 6.3 and Section 6.4. This factor, which is sometimes also referred to as the emission rate, is calculated by dividing the total embodied emissions of the systems by the energy output during their lifetime. The unit of the emission factor is kg CO_{2eq}/kWh and it is directly comparable to the grid emission factors.

6.1.3.4 Net avoided emissions

The net avoided emissions, GHG_{netPV} (kg CO_{2eq}), are defined in this study as the emission reduction (avoided emissions) that a PV system contributes to during its lifetime, when the embodied emissions of the PV system has been subtracted. It is therefore the net contribution to reduced emissions from the PV system.

The net avoided emissions are calculated according to Equation (25), where $GHG_{avoided,j}$ (kg CO_{2eq}/year) are the avoided emissions due to renewable energy generation during year j, $E_{embodiedPV}$ (kg CO_{2eq}) are the embodied emissions of the PV modules, and N_{PV} (years) is the expected lifetime of the modules.

$$GHG_{netPV} = \sum_{j}^{N_{PV}} GHG_{avoided,j} - GHG_{embodiedPV} \qquad (25)$$

6.1.3.5 Emission payback time and return on investment

The greenhouse gas payback time (GPBT) is the number of years of operation it takes the solar energy modules to generate enough renewable energy to offset the emissions caused by their production, by replacing non-renewable forms of energy [181]. The GPBT calculations in this thesis focus only on renewable electricity which replaces electricity from the grid.

GPBT is calculated as shown in equation (26), where $GHG_{embodiedPV}$ (kg CO_{2eq}) are the total embodied emissions of the technology and $GHG_{avoided,year}$ (kg CO_{2eq}/year) are the emissions that are avoided per year due to the replacement of grid electricity.

$$GPBT = \frac{GHG_{embodiedPV}}{GHG_{avoided,year}} \qquad (26)$$

The average value of avoided emissions over the 30 year lifetime of the modules is used here, which is a simplification. If the avoided emissions were instead calculated using e.g. the variable grid emission factor shown in Figure 15 the GPBT would be shorter, since the grid is associated with higher emissions during the first years. The method used here therefore leads to conservative values of GPBT.

The impact of different technologies and products can also be assessed using the greenhouse gas return on investment (GROI), first introduced by Reich-Weiser, et al. [181]. GROI is calculated as the lifetime of the technology divided by the GPBT. The GROI is a dimensionless number, analogous to the metrics economic return on investment (ROI) and energy return on investment (EROI). A GROI below 1 indicates that the technology does not bring about a net reduction in emissions. Neither GPBT nor GROI is a measure of the energy generated by the PV modules in absolute terms; a high GROI can either be the effect of low embodied emissions or a high energy output.

It should be noted that while the factors E_{net} refers to a particular building, the GBPT and GROI only concern the PV modules and are therefore independent of the building energy demand.

6.1.3.6 Zero emission balance

The annual net emissions (GHG_{net}) are calculated according to Equation (15) from Section 2.2.3.3. Since symmetrical grid emission factors are used it can be simplified to Equation (27). The net emissions are calculated as an annual value, and the embodied emissions ($GHG_{embodied}$) are therefore also annualized based on the expected lifetime of the system or the building in question.

$$GHG_{net} = (E_{exp,el} - E_{del,el}) f_{GHG,sym,el} - GHG_{embodied} \quad (27)$$

$E_{exp,el}$	exported electricity (kWh)
$E_{del,el}$	delivered electricity (kWh)
$f_{GHG,sym,el}$	GHG factor for electricity (symmetric) (kg CO_{2eq}/kWh)
$GHG_{embodied}$	annualized embodied emissions (kg CO_{2eq})

Equation (27) shows the net emissions calculated using the delivered/exported balance, which is used in the study of the Living Lab presented in Section 6.4. In the case study of the ZEB residential concept, presented in Section 6.3, the net emissions are instead calculated using the load/generation balance. Equation (27) is used also in this case, with $E_{exp,el}$ replaced by $E_{gen,el}$ and $E_{del,el}$ replaced by $E_{load,el}$.

6.1.3.7 Sensitivity analysis

Life cycle assessments and environmental impact assessments are inherently connected to high levels of uncertainty. The use of generic, statistical, or average data is the source of uncertainty, as well as the use of different practices and methods. A typical LCA includes several links between materials and processes, which means that uncertainties also propagate through the chain of analysis. There is also uncertainty related to the impact assessment methods, and it increases further if endpoint indicators are used.

The data on materials and processes in Ecoinvent includes uncertainty distributions, which indicate a range of possible values. The standard is lognormal uncertainty distribution, which occur when values with normal distribution are multiplied. [91]

SimaPro uses Monte Carlo simulations to perform sensitivity analyses, based on the uncertainty distributions of the impact of materials and processes. A model in SimaPro is typically made up of a large number of materials and processes. A Monte Carlo analysis uses randomised values within the uncertainty distribution of each material or process to calculate a range of statistically probable results for the final model. [91]

Monte Carlo simulations with SimaPro are used in the comparison of the environmental impact of different solar energy technologies in Section 6.2.

6.2 Embodied emissions of PV/T modules

In the review of previous research, no analyses of commercially or industrially produced PV/T modules were found. On the other hand, the available information on the environmental impact of PV modules and solar thermal collectors was to a large extent based on industrially produced modules. It was therefore important to also evaluate the environmental impact of commercially produced PV/T modules in order to enable a fair comparison of the solar technologies.

Detailed production data for any product is hard to come by, and it is especially so for products on a small and relatively new market such as that of PV/T modules. The analysis presented here is based on information from two European producers of unglazed flat plate PV/Tmodules [182, 183]. The provided information was mainly quantities of materials used in the module, their

country of production, and to some extent descriptions of the production processes and energy demand.

6.2.1 Description of the modules

The information from neither of the two producers was complete, and it was combined to model a generic commercially produced PV/T module. The generic module is therefore not a perfect representation of either of the two products, but is considered to be a more representative model of a modern, commercial PV/T module. The information from producer A was given as material quantities, and in some cases the country of production, of the major components in the module. The information from producer B was more detailed about the origin of the components, but less so about the quantities of materials. Information on energy use in the production was also given by producer B. Information on specific producers or countries of production was not used for the generic PV/T module, which is assumed to be manufactured in an unspecified European country.

Both the PV/T modules are made in Europe, but the production processes are a little different. PV/T module A has a heat exchanger that is laminated to the module during the original lamination process of the PV cells, to form one integrated laminate. The heat exchanger is produced by two stainless steel sheets that are stamped and welded together, which means that the water can flow across most of the module's backside. The module has a thin aluminium frame (0.6 kg per module). Producer A manufactures exclusively PV/T modules.

The absorber in PV/T module B is attached to the PV laminate by a plastic frame. The attachment process includes heat treatment, which according to the producer is a relatively energy intensive and expensive process. In the second generation of their PV/T modules, producer B has abandoned this technology in favour of aluminium frames. PV/T module B has no aluminium frame. As in PV/T module A, the heat exchanger is made of thin stainless steel, but with channels or groves from the top to the bottom of the module. Producer B makes PV modules, as well as PV/T modules. Information about energy demand during production was also received from producer B, which showed that the production of their PV/T modules demanded 2-3 times more energy during production than a comparable PV module.

6.2.2 Life cycle assessment

6.2.2.1 Goal and scope definition

The goal of this assessment is to calculate the embodied emissions of a generic, commercial PV/T module. The analysis is performed cradle-to-gate, that is, only process stages A1-3 are included (see Figure 16). A flow chart of the included processes is shown in Figure 52.

The functional unit is 1 m^2 of produced PV/T module. This unit is chosen to enable easy comparison to other solar technologies. The calculation does not include any other components than the module, nor does it include energy generated by the module. These factors will be taken into account in the assessment of the complete system (Section 6.4).

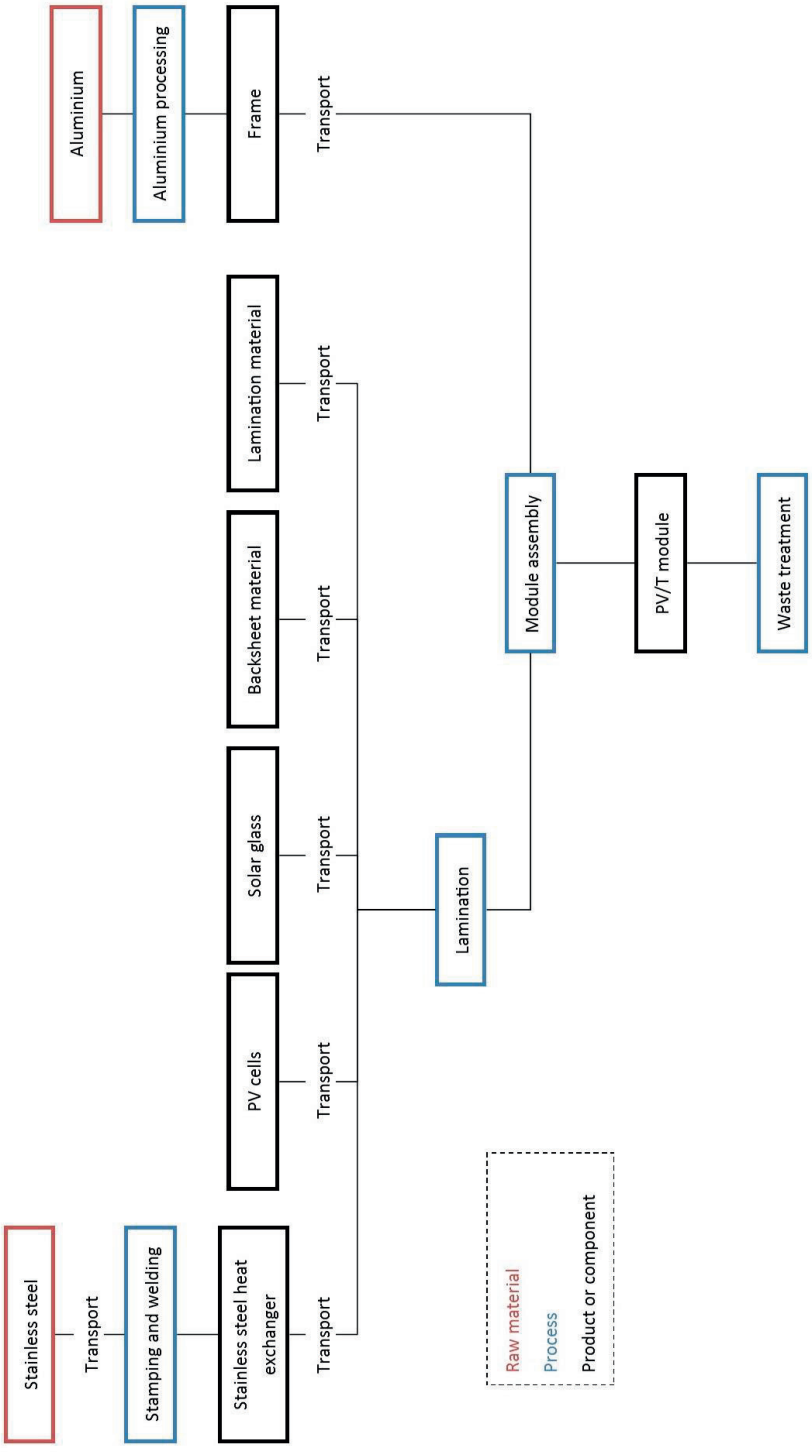

Figure 52. The flow chart describing the processes included in the assessment of the PV/T modules.

6.2.2.2 Life cycle inventory

The life cycle inventory is based on a combination of generic data from Ecoinvent[17] and data from the two PV/T producers mentioned above. Since an uncovered PV/T module (which is analysed in this case) bears most similarity to a PV module, the process model of a PV module from Ecoinvent is used as a starting point. Modifications are made according to the information provided by the PV/T producers.

Both PV/T modules use monocrystalline silicon solar cells, and the process model "Si-mono PV panel (RER)[18]" from Ecoinvent 3.1 is therefore used. This process model uses global market data for the materials, but the production is modelled with European energy mix. Global market processes in Ecoinvent represents and average based on the composition of the global market It also includes a generalized value for transportation.

The inventory for PV modules in Ecoinvent has not been specifically updated between versions 2 and 3 of the database, although some of the included processes have changed. This means that some of the data is relatively old, parts of it from as far back as 2001. The PV industry has undergone a substantial development during this time and the data may not be representative of modern PV modules. The PV module from Ecoinvent was updated in this study in order to mitigate this, and also to enable fair comparison with the PV/T module which is based on current practices. The following changes were made to the Ecoinvent model:

- The PV cell thickness was changed from 270-300 μm to 200 μm. This is more in line with current standards, and is also similar to information from the PV/T module producers [45].
- The glass was changed from 4 mm to 3.2 mm, based on the PV module currently used in the Living Lab [184].
- The amount of material for the aluminium frame was reduced from 2.63 to 0.36 kg per 1 m^2 module. This is similar to the aluminium frame used in PV/T module A.

The most important materials in the two PV/T modules (to the left, in grey) and the generic PV/T module (based on the information from these two) is shown in Table 18. Information on the updated PV module is shown in the same table. The complete inventory of the generic PV/T module is shown in Table A.1 in Appendix A. The complete inventory for the updated PV module is shown in Table A.3 in Appendix A.

[17] The default allocation version of all Ecoinvent processes are used unless otherwise specified.
[18] Some terminology from Ecoinvent is used in this chapter. Global market processes are denoted "(GLO), market for", while country-specific production processes are denoted "([country code]), production". RoW stands for "Rest of World", RER means Europe without Switzerland, and FR stands for France.

Table 18. Inventory of the most important materials in PV/T module A and B (left, in grey), the generic PV/T module, and the updated PV module from Ecoinvent 3.1.

	PV/T module A (laminated)	**PV/T module B (glued)**	**PV/T module (generic, based on PV/T A and B)**	**PV module (updated from Ecoinvent 3.1)**
PV cells	Mono-Si cells 60 pc Thickness: 200 µm Origin: France	Mono-Si cells 48 pc Thickness: 200 µm Origin: Germany	Mono-Si cells 60 p 200µm thickness Origin: Global*	Mono-Si cells 60 pc Thickness: 200 µm Origin: Global*
Glass cover	Solar glass Thickness: 2 mm Origin: Belgium	Solar glass Thickness: 3.2 mm Origin: Germany	Solar glass Thickness: 3.2 mm Origin: Global*	Solar glass Thickness: 3.2 mm Origin: Global*
Lamination material	EVA Thickness: 0.6 mm Origin: Japan	EVA Thickness: 0.46 mm Origin: N/A	EVA Thickness: 0.5 mm Origin: Global*	EVA Thickness: N/A Origin: Global*
Backsheet	Polyvinylflouride film (3 layer) Thickness: 0.42 mm Origin: Austria	Polyvinylflouride film (3 layers) Thickness: N/A Origin: Germany	Polyvinylflouride film Thickness: 0.42 mm Origin: Global*	Polyvinylflouride film 0.37 mm thickness Origin: Global*
Frame	Aluminium 0.36 kg/ m^2 module Origin: Turkey	Plastic Amount not known Origin not known	Aluminium 0.36 kg/m^2 module Origin: Global*	Aluminium 2.63 kg/m2 module Origin: Global*
Heat exchanger	Stainless steel Thickness: 1.2 mm Origin: France Comment: Laminated in the same process as the PV laminate	Stainless steel Thickness: N/A Origin: N/A Comment: Glued to the module via a plastic framing.	Stainless steel Thickness: 1.2 mm Origin: Global* Comment: Laminated in the same process as the PV laminate	Not included
Backside insulation	Polystyrene Thickness: 2.9 mm Origin: N/A	Not included	Polystyrene Thickness: 2.9 mm Origin: Global*	Not included

**The origin of each component is an average based on the composition of the global market (global process in Ecoinvent). The manufacturing of the module is assumed to take place in Europe.*

6.2.2.3 Impact assessment

This analysis uses a single issue assessment method, i.e. only one impact category is analysed. The analysed impact category is global warming potential at 100 years (GWP100a), as described by the Intergovernmental Panel on Climate Change (IPCC) [9]. The global warming potential is measured in carbon dioxide equivalents (CO_{2eq}) per functional unit.

6.2.3 Results

The embodied emissions per m^2 (kg CO_{2eq}/m^2) of the generic PV/T module and the updated mono-Si PV module from Ecoinvent are shown in Figure 53. The cut-off in the figure is set to 1%, which means that materials and processes that contribute to less than 1% are shown together in the category "Other". The total amount of embodied emissions of the PV/T module is 250 kg CO_{2eq}/m^2 (or 245 kg CO_{2eq}/m^2 without backside insulation) compared to 188 kg CO_{2eq}/m^2 for the PV module. In other words, the embodied emissions of the PV/T module is 30-33% higher than those of the PV module. These values also includes the heat

transfer fluid in the PV/T module. If this is subtracted, the embodied emissions of the generic PV/T module are 243 kg/CO_{2eq}/m^2, 29% higher than the updated mono-Si PV module. The value without heat transfer fluid will be used for the rest of the calculations in this section and in Section 6.4.

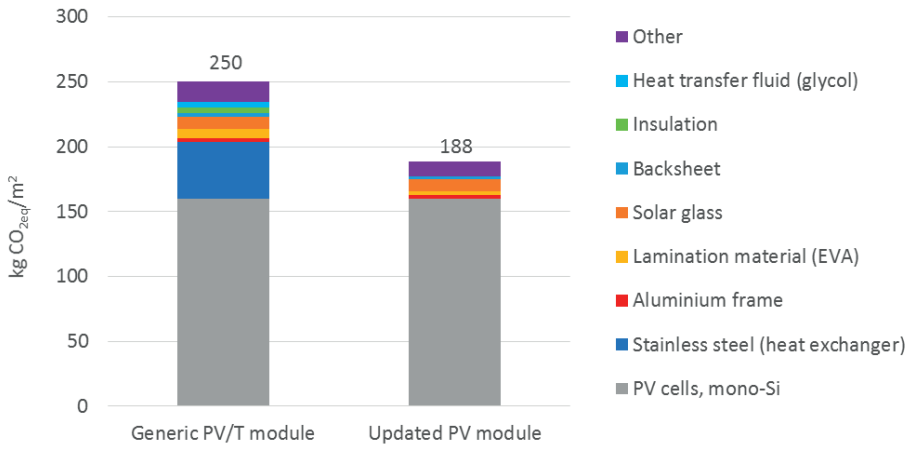

Figure 53. The embodied emissions of the generic PV/T module and the updated mono-Si PV module from Ecoinvent.

The largest contributor to the embodied emissions is in both cases the PV cells, which account for 84.9% of the emissions of the PV module and 65.9% of the emissions of the PV/T module. As shown in Figure 53, the main difference between the two module types is the stainless steel for the heat exchanger, which accounts for 18.0% of the total embodied emissions.

6.2.4 Discussion

6.2.4.1 Uncertainties

Calculations of embodied emissions are associated with significant uncertainties. Average factors are used for some materials, and assumptions and generalizations are made for unknowns. In the analysis presented here, it is clear that the results are very sensitive to variations in a few of the materials and processes included.

A simple sensitivity analysis was performed for the most influential factor in the case of the PV/T module, which was the manufacturing of the stainless steel heat exchanger. Since no information on the heat exchanger was available for PV/T module B, the one in the generic PV/T module is based on information given by producer A.

The heat exchanger is modelled here by a given amount of material and the energy related to processing of that material. The material process "Steel, chromium steel 18/8, hot rolled (RER), production" in Ecoinvent was used, where "RER" refers to Europe without Switzerland. According to producer A, the heat exchanger is welded and stamped together. The process "Welding, arc, steel (RER), processing" was used in the original version of the generic PV/T

module to estimate this. However, no details were available from the producer and an average process, "Metal working, average for chromium steel product manufacturing (GLO), market for", was therefore also used as a comparison. This process step had a large influence on the final results.

If average metal working is used instead of welding, the embodied emissions of the generic PV/T module is increased to 267 kg CO_{2eq}/m^2 and the steel heat exchanger accounts for 24.9% of the total embodied emissions. The original generic PV/T module (with welding) is shown together with the version with average metal working in Figure 54. The stainless steel absorber has been divided into a material and a processing part in the graph to show the large influence of the latter.

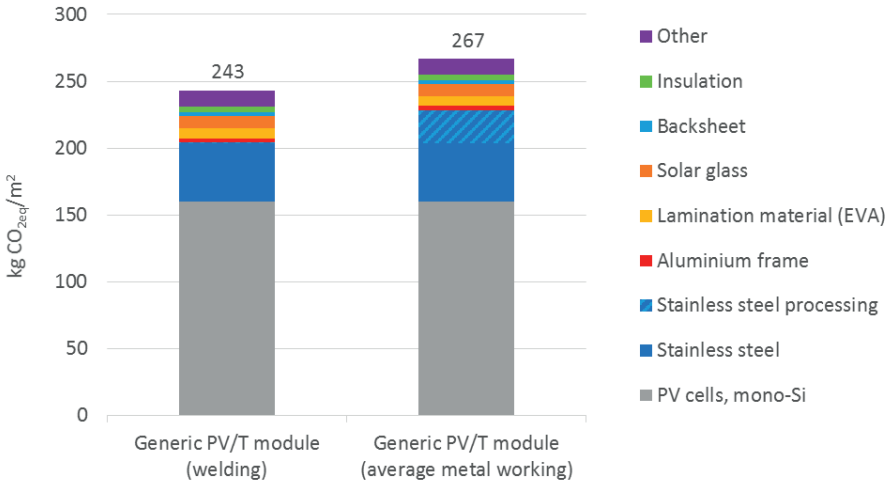

Figure 54. The embodied emissions of the generic PV/T module with welding (left) and average metal working (right).

The generic PV/T module was modelled using market processes in Ecoinvent, which means that the values represent average market values and that a generic transport assumption is included in each material process. The production is also generalised for a region, such as Europe, rather than a country or specific producer, and average energy mixes are used.

The difference between a PV/T module with generalized values and market processes, and a similar PV/T module with country-specific processes and transport distances was analysed to evaluate how much the use of specific data influences the resulting embodied emissions. PV/T module A was used in the comparison since no country-specific information was used in the modelling of the generic PV/T module. The PV/T module A was modelled in two versions: one with generalised market data and one with country specific data. The global warming potential of the generic PV/T module and the two versions of PV/T module A are shown in Figure 55. The inventory for the PV/T module A with country-specific data is shown in Table A.2 in Appendix A.

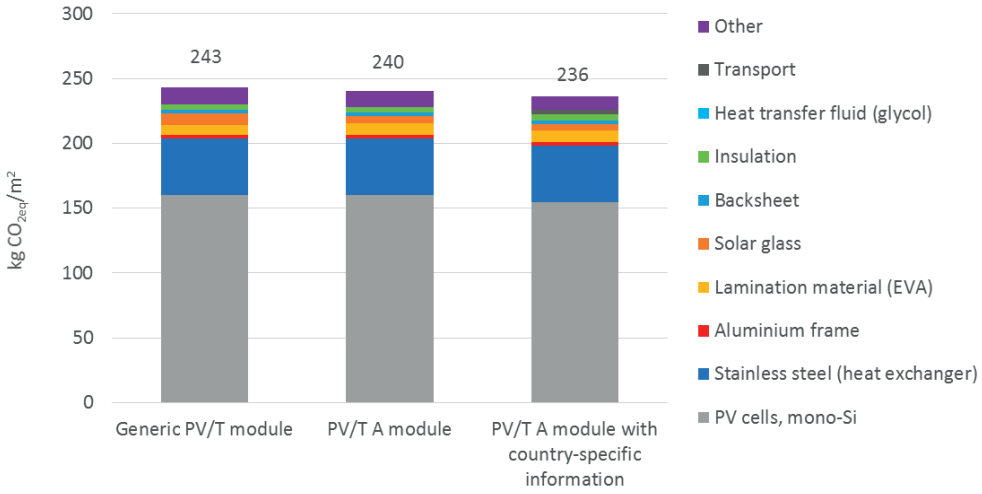

Figure 55. Embodied emissions of PV/T modules with generic and specific data on country of production and transport.

As Figure 55 shows, there is a slight positive impact (lower emissions) of using country-specific information for production. The version of PV/T A module without country-specific data has lower embodied emissions than the generic PV/T module. The embodied emissions are further decreased if the country-specific version of PV/T A is used. A conclusion to be drawn from this is that the generic PV/T module is a conservative assessment of a commercial PV/T module.

Another uncertainty in the modelling of the PV/T module was the use of energy for manufacturing. The values in the original PV module from Ecoinvent was used to model the generic PV/T module. The impact of changes to this value has not been specifically analysed here since the impact was relatively small to start with. In the PV module, the use of energy in the module assembly accounted for only 1.0-1.5% of the total embodied emissions, and in the generic PV/T module it accounted for 1.0-1.1%. As mentioned, the energy demand in module production was stated by producer B to be 2-3 times higher for the PV/T module than the PV module. However, this figure was for the first version of their module, which had a plastic frame. The process of producing this frame, which was done during module assembly, was responsible for a large share of the process energy, and the producer has now changed to using an aluminium frame. The figure on energy demand from producer B was therefore considered not to be applicable in for the generic PV/T module.

An uncertainty analysis was also performed for the different module types, using Monte Carlo simulation as described in Section 6.1.3.7. The result of these simulations are a range of probable values for each module type. The results for the confidence interval 95% is shown in Figure 56.

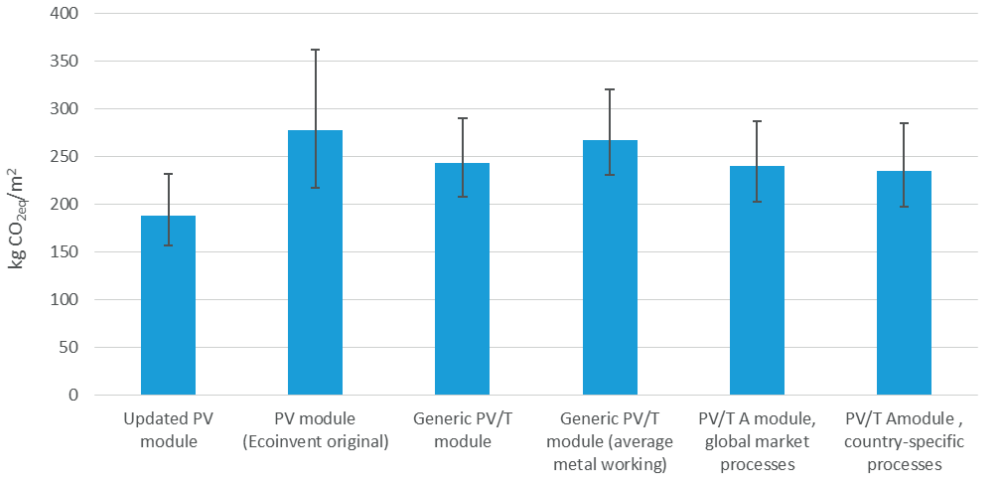

Figure 56. Results of the uncertainty analysis for the PV and PV/T modules. The confidence interval is 95%.

As the figure shows, the range of values is relatively large. The range of values in the 95% confidence interval for the original Ecoinvent PV module is 217-362 kg CO_{2eq}/m^2. The range of values for different modules are also overlapping. For example, the range of values for the updated PV module is between 157 kg CO_{2eq}/m^2 and 232 kg CO_{2eq}/m^2, and for the generic PV/T module between 208 kg CO_{2eq}/m^2 and 291 kg CO_{2eq}/m^2.

To evaluate the difference between the modules with overlapping ranges, a similar analysis was also performed for the *difference* between the PV and PV/T modules. The results for some of the modules are shown in Table 19, also with a confidence interval of 95%. As the table shows, the differences in embodied emissions are between the PV and PV/T modules can be regarded as certain.

Table 19. The result of uncertainty analyses of the difference between module types. The confidence interval is 95%.

A	B	Instances where A ≥ B
PV module (Ecoinvent original)	Updated PV module	100%
Generic PV/T module	Updated PV module	100%
PV/T module A, country-specific processes	Updated PV module	99.4%

6.2.4.2 Update of PV module

As mentioned in Section 6.2.2.2, the technological development in the PV industry has been substantial in the last decades, and the efficiencies of PV modules have increased. As Frischknecht, et al. [185] point out, the publicly available data on PV module production does not always mirror the current situation. As an example, a typical crystalline solar cell is now

significantly thinner than a decade ago, and the process chain for silicon for the solar industry has become more efficient [186]. For crystalline silicon modules, there is a 30-40 % decrease in greenhouse gas emissions reported from 2006-2009, and a corresponding decrease of 30% for CdTe thin film [185]. In addition, the production of PV modules has to a large extent moved from Europe to Asia in the last decade. The influence of the country of production on the embodied emissions of PV modules has been studied by Yue, et al. [187], who found that crystalline silicon PV modules produced in China had a 28-48 % higher primary energy demand compared to modules produced in Europe.

The update of the PV module in Ecoinvent which was performed for this analysis focused on the reduction in the use of materials. Since silicon and aluminium are materials that are energy demanding to produce, the updates that were made to the original PV module in Ecoinvent had a large impact on the total embodied emissions. A comparison of the embodied emissions of the original and updated module is shown in Figure 57. The emissions of the original Ecoinvent process was 277 kg CO_{2eq}/m^2, and the embodied emissions was thus reduced by 31.9% in the updated version.

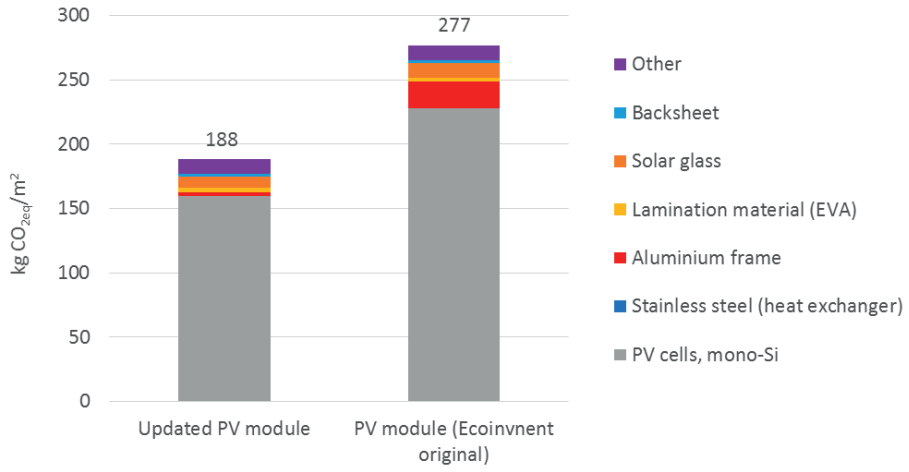

Figure 57. The embodied emissions of the original and updated version of the mono-Si PV module in Ecoinvent.

As shown in Figure 57, the reduction in the thickness of the PV cells had a very significant impact on the total embodied emissions. The aluminium frame also had quite a large impact in the original Ecoinvent process, making up around 7.5% of the embodied emissions, compared to 1.5% in the updated module. The update of the module was made in a quite simple manner, where the amount of materials was simply reduced according to the details given in Section 6.2.2.2. Emissions values on the energy needed for manufacturing or the handling of process waste were not updated.

6.2.4.3 Comparison to previous research

The values of embodied emissions of PV/T modules calculated here are low compared to the values found in previous research (Section 6.1.2), which were in the range

343-451 kg CO_{2eq}/m^2. If only PV/T-liquid modules are included, the values in literature were in the range of 387-513 kg CO_{2eq}/m^2. However, most of the studies had only calculated the embodied energy, and few had calculated the embodied emissions. There is thus very little grounds for a comparison. In addition, it is not possible to directly compare values from different LCA or environmental impact assessments, since any such analysis will include a number of assumptions and generalisations.

What can be said, however, is that the present analysis is based on relatively updated values on e.g. solar cell thickness and the amount of aluminium used in the frame. It may therefore be reasonable to assume that the values found in previous literature are high compared to the commercially manufactured PV/T modules presented.

6.3 Embodied emissions and solar energy system design

The embodied emissions of a solar energy system can be likened to a loan that needs to be paid back by the generation of renewable energy from the system. Once a system is installed, it is not possible to influence the amount of embodied emissions (other than for replacements, maintenance, and demolition). It is therefore important that the "borrowed" emissions are invested wisely, so that the net emission benefit is as high as possible. That is, that the energy performance of the system is as good as possible.

As was discussed in Chapter 4, the design of a solar energy system has a significant influence on its performance. The study presented in this section was performed in order to determine how the design of a solar energy system, in this case a PV system, influences the emission balance of a building. Different design concepts for flat roofs are analysed. The ZEB residential concept was used as a case, and the study is described in Paper V.

6.3.1 The case building: embodied and operational emissions

The case building, the ZEB residential concept, was described in detail and the net *energy* balance analysed in Section 5.2. The focus of this study is on the *emission* balance of the same building.

The embodied emissions of the building were analysed by Houlihan Wiberg, et al. [6], who found that the embodied emission of materials accounted for 5.0 kg $CO_{2eq}/m^2 A_{fl}$ over the 60 year lifetime of the building. A breakdown of the embodied emissions of materials are shown in Figure 58. The embodied emissions of the PV system are calculated in the present study and are therefore not included in the figure.

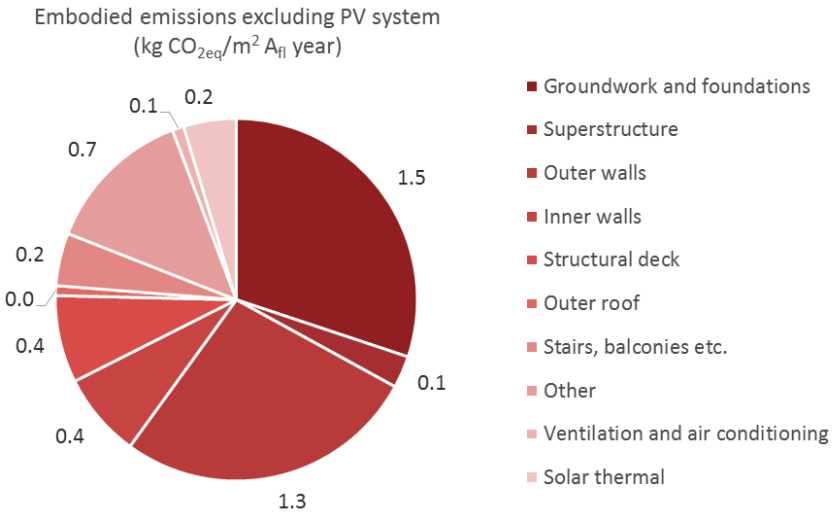

Figure 58. The embodied emissions of materials in the case building, excluding the PV system (kg CO_{2eq}/m^2A_{fl}, year). Data from Houlihan Wiberg, et al. [6].

The operational emissions based on data from the same publication are shown in Figure 59, calculated with the ZEB grid emission factor. The operational emissions account for 5.1 kg CO_{2eq}/m^2A_{fl} if calculated with the ZEB grid emission factor. That is, they were more or less equal to the embodied emissions. The operational emissions accounted for 13.9 kg CO_{2eq}/m^2A_{fl} if the current EU grid factor was used in the calculations.

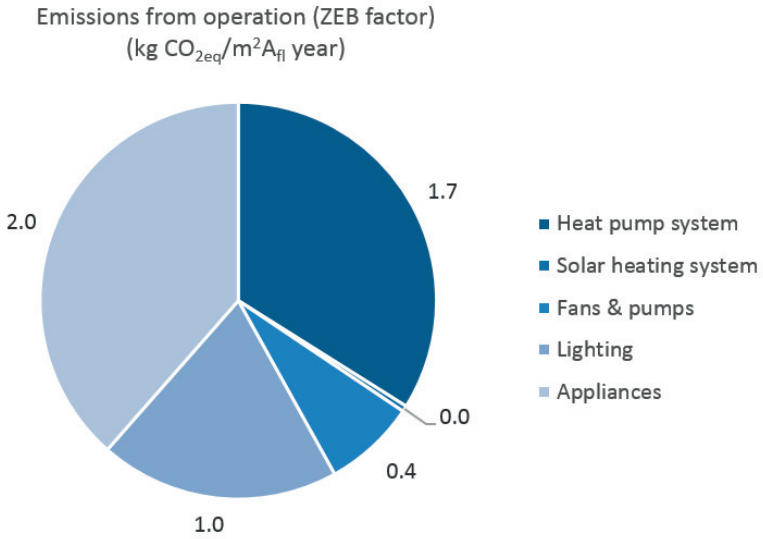

Figure 59. The operational emissions of the case building, using the ZEB ultra-green grid factor. Data from Houlihan Wiberg, et al. [6].

6.3.2 Method

6.3.2.1 System design

The case building has a flat roof of 8 m x 10 m, oriented with the long sides south and north. As discussed in Section 4.1, there are two general strategies for PV installations on flat roofs: either the modules are installed at an optimal tilt angle with enough distance between the rows to avoid shading, or they are installed at a lower tilt angle but closer together.

Four different system designs were compared in this study. They are described in Table 20 and shown schematically in Figure 60. More details on the designs are given in Paper V.

Table 20. The design options for the PV systems on the roof of the ZEB residential concept.

Design	Azimuth of modules	Tilt angle of modules	Description	Module area*
		°		m^2
A	South	40	Optimal tilt angle and orientation for Oslo. This high tilt requires large row spacing to avoid mutual shading. High energy output for each module, but a low number of modules can fit on the roof.	30.4
B	South	15	Lower tilt angle to reduce the required spacing. Lower yield per module but more modules can fit on the roof.	40.5
C	South/North	15	A development of design B, where north-facing modules are added in the space between the south-facing modules. More modules can fit on the roof but the north-facing modules will have a lower output.	70.9
D	East/West	15	The same low tilt angle as in C, but modules oriented east/west. The advantages of low self-shading are the same as in C, but output is shifted towards autumn and spring.	59.1

**The total PV area of each system is not exactly equal for the different PV technologies, since dimensions of commercial modules are used. The area of the mono-Si version of each design is given here.*

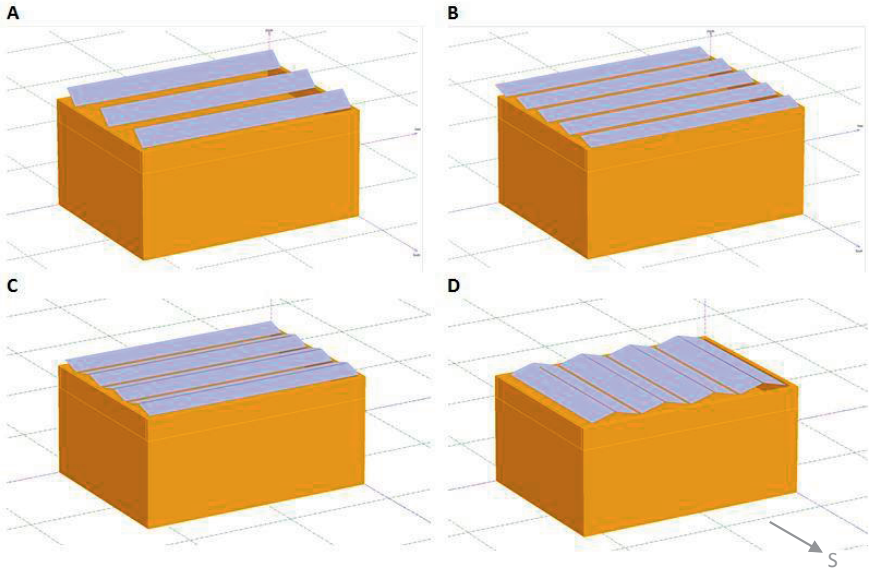

Figure 60. Schematic drawing of the four system designs on the ZEB residential concept. Figures from PVsyst [21].

6.3.2.2 Simulation

The energy output of the PV systems was calculated using the simulation software PVsyst v5.73 [21] together with Meteonorm meteorological data for Oslo [188]. The annual irradiation on a horizontal surface in Oslo is around 1000 kWh/m^2.

In addition to the different designs, the study also included four different types of PV modules: monocrystalline silicon (mono-Si), polycrystalline silicon (poly-Si), cadmium indium selenide (CIS) thin film modules, and finally high-efficiency mono-Si. Thin film modules have significantly lower embodied emissions than crystalline silicon modules, but on the other hand they also have significantly lower efficiencies.

The objective of using different module types was to evaluate whether low embodied emissions or high efficiency of the modules would be most important in order for the building to reach a zero emission balance. The simulations were based on data on commercially available modules. The selected modules were chosen to represent the average in performance of each PV technology, using efficiency values from 2012 [189].

6.3.2.3 Embodied emissions of PV modules

Emissions data was extracted from the Ecoinvent database v.3.1 [190]. For comparison, the high-efficiency mono-Si module from SunPower that was used in the original study by Houlihan Wiberg, et al. [6] was also analysed. The emission data for this module is taken from a life cycle assessment presented by Fthenakis, et al. [191].

Table 21. Characteristics of the three PV modules used in the simulations: the module dimensions are taken from producer data sheets and the emissions data (except high-efficiency mono-Si) from Ecoinvent database [190, 191].

PV technology	Module area	Rated power	Efficiency at STC	Embodied emissions per m^2 of module
	m^2	W_p	%	$kg\ CO_{2eq}/m^2$
Mono-Si	1.69	255	15.1	278
Poly-Si	1.65	250	14.7	213
CIS thin film	1.23	145	11.9	134
Mono-Si (high-efficiency)	1.63	333	20.4	281

The expected lifetime of the modules is set to 30 years, with a linear annual performance degradation of 0.7 %, in line with the value suggested for mature technologies in the Methodology Guidelines on Life-Cycle Assessment of Photovoltaic Electricity, developed by Fthenakis, et al. [79]. Since the production warranty for the CIS modules is the same as for the silicon modules, the same degradation factor has been used even though it can be argued that the technology is less mature.

The study includes only modules, and not the other necessary components referred to as BOS (balance-of-system). A further discussion on the impact of BOS on embodied emissions is included in the case study in Section 6.4 and in Paper VI.

6.3.2.4 Replacement of PV modules

Since the lifetime of the PV modules is assumed to be 30 years – half of the expected building lifetime – the PV systems need to be replaced once. It is of course difficult to predict the energy performance and embodied emissions of modules produced 30 years into the future. A simplified future scenario was introduced in Paper V, where the replacement modules are assumed to have 25.2% efficiency and embodied emissions of 100 kg CO_{2eq}/m^2. The background of this scenario is described in more detail in the paper.

6.3.3 Results

6.3.3.1 Electricity output

The annual simulated energy yield of the systems are shown in Figure 61. The figure shows the results for the first 30 years, i.e. without module replacements[19]. The annual electricity demand of the building is shown in the same figure (far right).

[19] Figure 6. in Paper V shows the values for the full 60 year lifetime, but it has mistakenly been labelled as only showing the first 30 years.

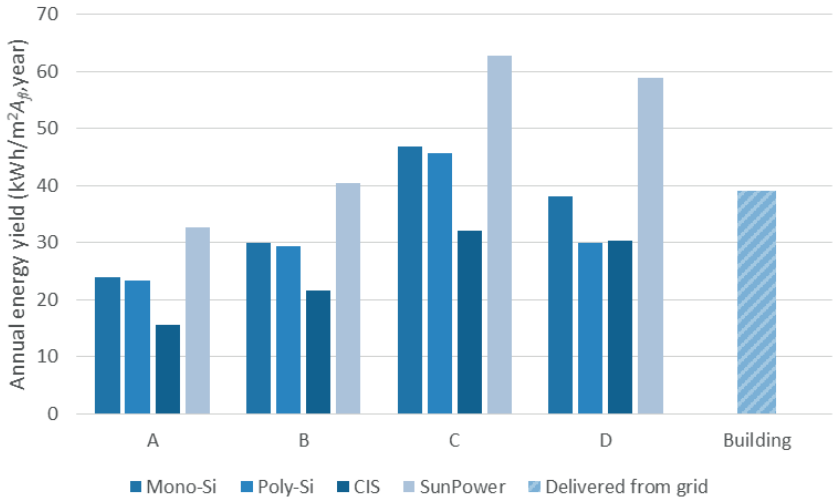

Figure 61. The annual simulated electricity yield of the different PV systems, shown per m^2 heated floor area.

The mono-Si modules (both high-efficiency and average) have the highest yield for all design options. Design C has the highest energy yield for all module types, which is a direct reflection of the size of the systems (see Table 2 in Paper V for detailed information on the systems). The mono-Si and poly-Si modules in design C and the high-efficiency mono-Si modules in design D generated more electricity than the annual electricity need of the building.

The influence of orientation and tilt angle is shown in Figure 62, using the values from the mono-Si systems as an example (the trend is the same for all technologies). The figure shows the annual specific energy output of the modules, measured in kWh/kW_p. The modules which are installed at 40° tilt and south facing (optimal orientation for the location) have around 40% higher yield than the modules installed at 15° tilt and north facing.

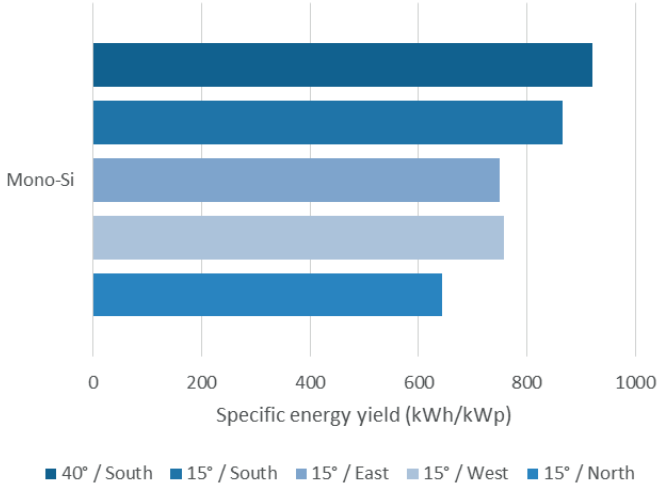

Figure 62. Specific yield (kWh/kW$_p$) of modules installed at different orientations. The systems with mono-Si modules are used as an example.

6.3.3.2 Embodied and net avoided emissions

The embodied emissions of each system were calculated based on the values from Table 21 and the details on each system design (shown in Table 2 in Paper V), and are shown in Figure 63. The embodied emissions are shown per m^2 heated floor area per year. The embodied emissions of future modules which are used for replacement after 30 years are also shown in the same graph.

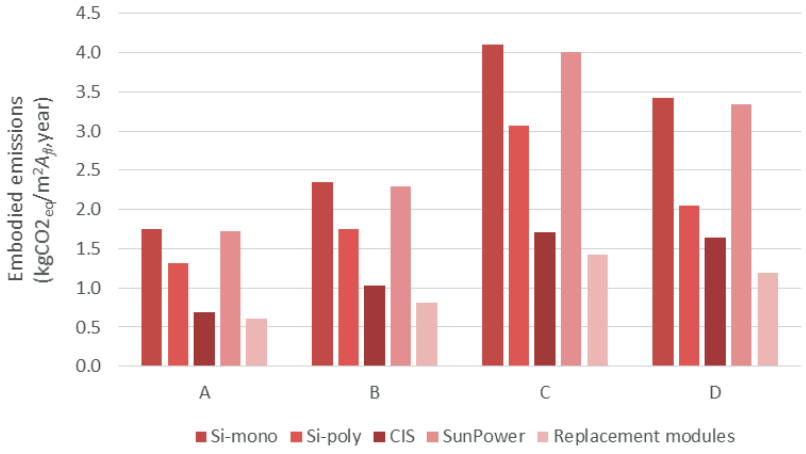

Figure 63. The embodied emissions of the different PV systems shown for the functional unit 1 m^2 heated floor area per year (1 m^{2}A$_{fl}$/year).

The net avoided emissions are the emissions that are avoided as a result of the generated PV electricity, after the embodied emissions of the modules themselves are subtracted. It is calculated according to Equation (25). The net emissions of the PV systems for the whole

building lifetime (60 years) are shown in Figure 64, calculated using the ZEB grid factor and the current EU grid factor. The average value of the original modules and the future replacement modules are used to calculate the annualized embodied emissions of the PV systems over the total 60 year lifetime of the building.

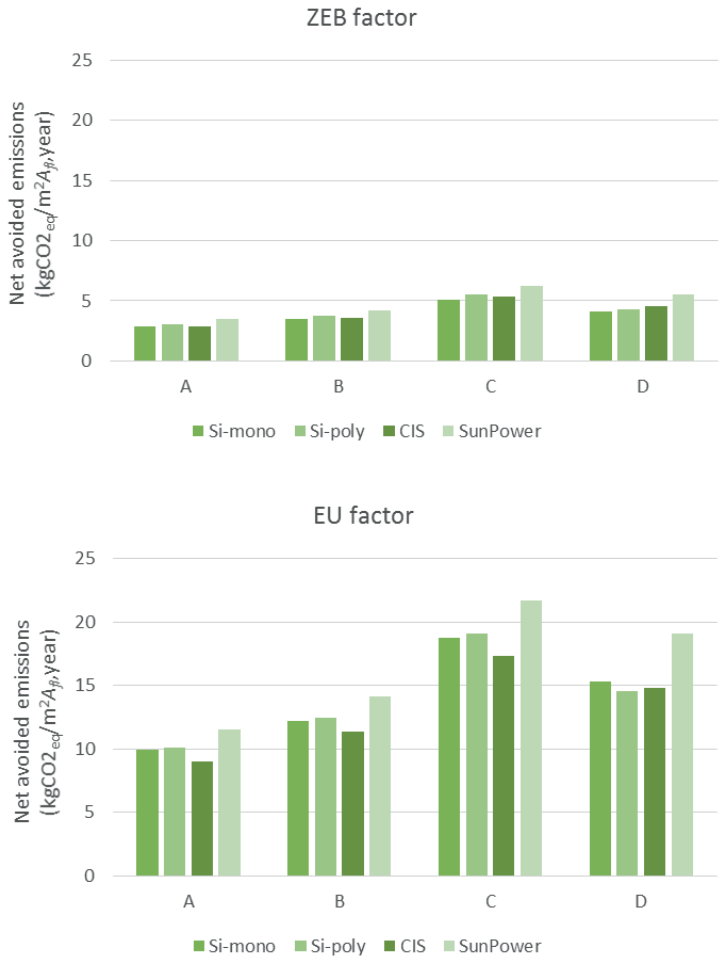

Figure 64. The net avoided emissions of the systems, calculated with the ZEB ultra-green grid factor (top) and the EU factor (bottom).

As Figure 64 shows, a high energy output is more important than low embodied emissions in order to reach high values of net avoided emissions. The PV modules in system A accounted for 11% (CIS), 16% (Si-poly) and 19% (Si-mono, both types) of the total embodied emissions of the building, while the modules in system C accounted for 24%, 31%, and 35% respectively. That is, the system that led to the largest net avoided emissions accounted for about a third of the embodied emissions of the building.

6.3.3.3 Emissions payback time and emission factor

The greenhouse gas payback time (GPBT) for all systems are well below the lifetime of the modules. In the ZEB ultra-green grid scenario, the GPBT of the systems range from 10 years (CIS, design A) to 20.4 years (Si-mono, design D). The larger systems (C and D) have longer GPBT than the smaller systems (A and B). The GPBT in the current EU grid is significantly shorter; the GPBT of the systems range from 3.7 years (CIS, design A) to 7.5 years (Si-mono, design C). The future modules have GPBT of 3.7-4.5 years in the ZEB ultra-green grid and 1.3-1.7 years in the current EU grid.

The emission factor[20] of the electricity generated by the solar energy systems, measured in kg CO_{2eq}/kWh, is calculated based on embodied emissions and energy yield of the systems. This number is directly comparable to the electricity grid emission factor. The resulting emissions factor of the systems are 0.045-0.055 kg CO_{2eq}/kWh for the mono-Si modules, 0.036-0.044 kg CO_{2eq}/kWh for the poly-Si modules, 0.030-0.037 kg CO_{2eq}/kWh for the CIS modules and 0.034-0.042 kg CO_{2eq}/kWh for the mono-Si high-efficiency modules.

This means that the emission factors for all systems are well below that of both the two grid emission factors (ZEB and EU) which were used in the calculations. The CIS thin film systems generally have the lowest emission factors and the mono-Si systems the highest.

6.3.3.4 Zero emission balance

The net emissions (GHG_{net}) of the building were calculated for all the different combinations of PV technology and system design, and are shown in Table 22. The calculation is performed using Equation (27) adapted for the load/generation balance, as described in Section 6.1.3.6.

Table 22. The net emissions, GHG_{net}, of the ZEB residential concept with the different PV systems. The load/generation balance at the ZEB-OM ambition level is calculated.

	GHG_{net} (ZEB grid factor)				**GHG_{net} (EU grid factor)**			
Design	**Mono-Si**	**Poly-Si**	**CIS**	**Mono-Si high-eff.**	**Mono-Si**	**Poly-Si**	**CIS**	**Mono-Si high-eff.**
	kg CO_{2eq}/m^2 A_{fl}, year				*kg CO_{2eq}/m^2 A_{fl}, year*			
A	-7.1	-6.9	-7.1	-6.5	-8.9	-8.7	-9.8	-7.3
B	-6.5	-6.3	-6.4	-5.8	-6.6	-6.4	-7.5	-4.7
C	-4.9	-4.4	-4.6	-3.8	0.0	0.3	-1.5	2.9
D	-5.8	-5.7	-5.5	-4.4	-3.5	-4.3	-4.0	0.3

As shown in Table 22, only four systems reach a balance when the current EU grid factor is used: the mono-Si, poly-Si and mono-Si high-efficiency modules in design C, as well as the

[20] The emission factor is referred to as "emission rate" in Paper V.

mono-Si high-efficiency modules in design D. None of the systems reach a net zero emission balance if the ZEB ultra-green grid factor is used.

6.3.4 Discussion

The results from this analysis show that while the CIS thin film modules have the lowest amount of embodied emissions, the shortest greenhouse gas payback times (GPBT), and the lowest emission factors of generated electricity, these systems are also the ones that have the lowest net avoided emissions over the system lifetime, i.e. the lowest absolute contribution to reduced emissions. The building with CIS systems are also farthest from reaching a net zero emission balance.

The optimally oriented PV modules in design A had the highest performance in terms of kWh/kW_p for all the module types, as well as the lowest emission rate and GPBT. Nevertheless, design C, with the largest number of modules, resulted in the highest net avoided emissions. As a total system, design C has the highest total yield for both types of Si-mono modules. However, the benefit of increasing the systems' size by mounting modules with north-facing orientation, as is done in design C, can be questioned. The yield of the north-facing modules in this system was only around 70% of the optimally inclined ones and the GPBT of these modules were up to 23.9 years for the Si-mono technology with the ZEB ultra-green grid mix. Considering that the modules have an expected lifetime of 30 years, this can be regarded as an inefficient use of the "invested" embodied emissions.

About half of the PV system combinations reach the ZEB-O level, but only the largest installations reach the ZEB-OM ambition level, showing that this is very demanding to achieve. The importance of reaching a zero emission balance for a single building can be questioned. As this analysis has shown, a relatively large PV installation is required for a single building to reach a net zero emission balance, and this can lead to periods of large export and import to the electricity grid. Recently, much of the research focus on zero emission concepts has shifted towards zero emission neighbourhoods, where buildings with different energy demand profiles can result in more balanced energy profiles on a neighbourhood scale.

A longer discussion of the results is provided in Paper V.

6.4 Embodied emissions and choice of solar technology

The study presented in this section is based on the second case building, the Living Lab, and solar energy systems that were described in Section 5.3. The case building was described in detail in Section 5.3.1 and the simulated energy demand of the building given in Table 10. While the first case study focused on the *energy* balance, the objective of the study presented here is to analyse the embodied *emissions* of systems with different solar technologies, as well as how the choice of solar technology affects the emission balance of the whole building. This study will be submitted for publication at a later date.

6.4.1 Solar energy systems

Three systems out of the seven studied in Section 5.3 will be studied here, each representing a different combination of technologies: System 2 (PV and heat pump), System 5 (PV and solar

thermal, integrated with heat pump), and System 7 (PV/T, integrated with heat pump). See Table 12 for more details on the systems. The exported and delivered energy to the building is different depending on which of the solar energy systems that is used, and the operational emissions are therefore calculated for each system separately.

PV modules with polycrystalline silicon (poly-Si) solar cells he PV installation on the actual building, but monocrystalline silicon (mono-Si) solar cells are assumed for the calculations in this section. The reasoning behind this simplification is that the use of poly-Si PV modules would have given the PV modules an unfair advantage in terms of embodied emissions, since the embodied emissions of poly-Si PV modules are lower. The PV modules on the Living Lab have the same electrical efficiency as the studied PV/T modules, and it is therefore assumed that the same silicon technology is used.

In addition to the modules themselves, a solar energy system requires several additional components. For PV systems, these are commonly referred to as BOS (balance of system). In this study, the concept BOS has been extended to also include the components necessary for a solar *thermal* system, and a distinction is made between electric BOS and hydronic BOS.

The electric BOS included in this study is the inverter and cables. The PV system on the actual building also includes a number of sensors for e.g. solar irradiation, weather data, and energy performance, but these are not included in the analysis since they are not necessary for the functionality of a normal residential solar energy system.

The hydronic BOS includes the piping, pumps, and valves. In addition to the BOS, the auxiliary energy components are also included in the analysis. This includes the storage tank, the heat pump, and the ground source collector. The boundary of the analysis is set to the tank, and components for heat distribution in the building are not included. Some of what is here regarded as auxiliary energy components, such as the storage tank, could have been regarded as part of the hydronic BOS. However, since System 2 also includes these components but no solar thermal systems, and thereby no hydronic BOS, it was considered more transparent to include these in the inventory of the auxiliary energy system.

The inventories of the systems are presented in Section 6.4.3.2, and an overview of the included components is shown in Figure 66.

6.4.2 Embodied emissions of the building

The values for embodied and operational emissions used in this study builds on previously published work performed by researchers in the ZEB Centre, in particular the work of Inman and Houlihan Wiberg [12, 169]. The embodied emissions of the building are only included to enable calculation of the building's emission balance and to put the embodied emission of the solar energy systems into a context. They will not be analysed in detail.

In her master thesis and subsequent research report, Marianne Inman performed a complete life cycle assessment of the Living Lab [12, 169]. A summary of the results from the entire building extracted from the report (life cycle steps A1-A3, A4-A5 and B4) is shown in Figure 65. The embodied emissions are shown as a total value for the building and normalized per unit of

heated floor area per year of the building's 60 year lifetime (kg $CO_{2eq}/m^2 A_{fl}$, year) as recommended by the ZEB Centre [73].

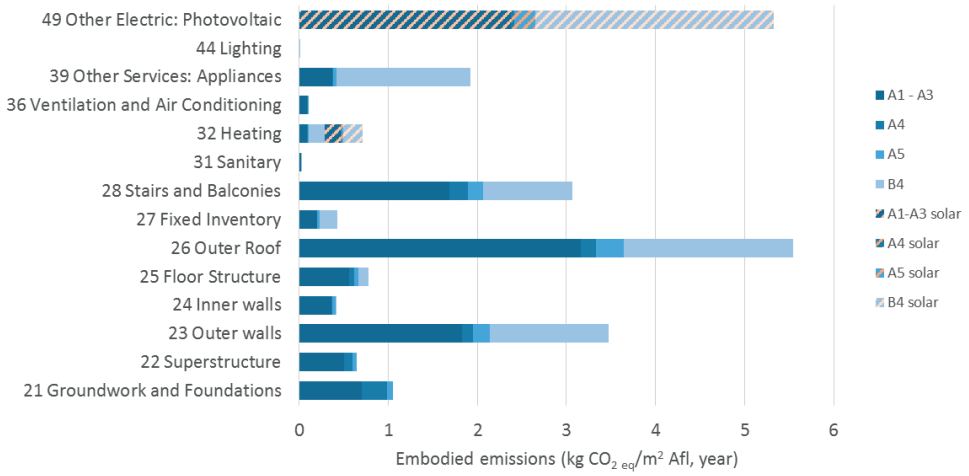

Figure 65. The embodied emissions of the building as calculated by Inman and Houlihan Wiberg [12]. The embodied emissions of the PV and solar thermal components in the original study, but not used in the present study, are marked by dashed columns in the figure.

The results from the original study by Inman and Houlihan Wiberg [12] have been used as a reference for the embodied emissions for the building components, except for the electric and thermal energy supply systems. These have been recalculated for both the original solar energy system and the alternative systems, although some data from the original study is used also in the present analysis.

The energy supply systems accounted for around 25% of the total embodied emissions in the original study. The embodied emissions data for the PV and solar thermal components from the original study are marked in Figure 65. The embodied emission values for the building with and without the original solar energy systems area shown in Table 23.

Table 23. Embodied emissions of the Living Lab, calculated based on the values presented by Inman and Houlihan Wiberg [12].

	Embodied emissions	
	Total	**Normalized**
	kg CO_{2eq}	*kg CO_{2eq}/m^2,year*
Building	143 788	23.5
Building without PV modules and solar collectors	109 996	18.0
Building without energy supply system including BOS	107 266	17.5

The BOS referred to in Table 23 includes both electric and hydronic BOS. The energy supply system includes all components related to energy supply: PV modules, solar thermal collectors, inverter, cabling, and sensors, piping, tank, heat pump, and ground collector pipes.

It can be noted that the value of embodied emissions of the building without the solar energy system (17.5 kg $CO_{2eq}/m^2 A_{fl}$) is significantly higher than the same value for the ZEB residential concept (5.0 kg $CO_{2eq}/m^2 A_{fl}$), which was discussed in Section 6.3.1. The very high value in the Living Lab can be caused by its large envelope are compared to the floor area, for example due to the shape of the roof (see Figure 42) well as the fact that more construction and technical material details have been included in the inventory. However, the large difference also shows that there is an inherent uncertainty in the calculation method, and that LCA performed by different practitioners cannot be directly compared.

6.4.3 Life cycle assessments of solar energy systems

6.4.3.1 Goal and scope definition

The goal of the LCA presented in this section is twofold. Firstly, the goal is to calculate the total embodied emissions of the three different solar energy systems, and the emissions per kWh of energy output of each system. Secondly, the goal is to determine which of the solar energy systems, if any, will enable the building to reach a net zero emission balance at the ZEB-OM level.

Since the first part of the analysis is focused on solar energy systems, it is useful to evaluate emissions based on the energy output of the solar energy systems per installed area. The functional unit for the analysis of the solar energy systems is therefore 1 kWh primary energy output during the system lifetime of 30 years (1 kWh_{PE}). In this way, the environmental impact from the solar energy systems can be directly compared to electricity from the grid.

An approximation of a future PV system was used in the analysis of PV systems in Section 6.3 in order to analyse the building over its 60 year lifetime. Since most installations using modern PV/T modules are quite recent, there is not much experience of how the systems perform over time, including the rate of degradation, failure modes etc. Any approximation of a system that would replace the current PV/T system 30 years on was therefore considered to add more

uncertainty than value to the analysis. The solution was to calculate the emission balance of the building over 30 years, that is, half the lifetime of the building. The functional unit used in the analysis of the whole building is therefore 1 m^2 heated floor area of the case building per year over 30 years, compared to 60 years in the analysis in Section 6.3. The embodied emissions of materials from Inman and Houlihan Wiberg [12] are used as annualized values.

The ambition level of the Living Lab is ZEB-OM, which means that operation and materials are included in the calculation. These are life cycle phases A1-A3, A4, B4 and B6 (see Table 18). A flow chart of the analysed solar energy systems is shown in Figure 66 (note that the rest of the embodied emissions of the building are not included in this figure).

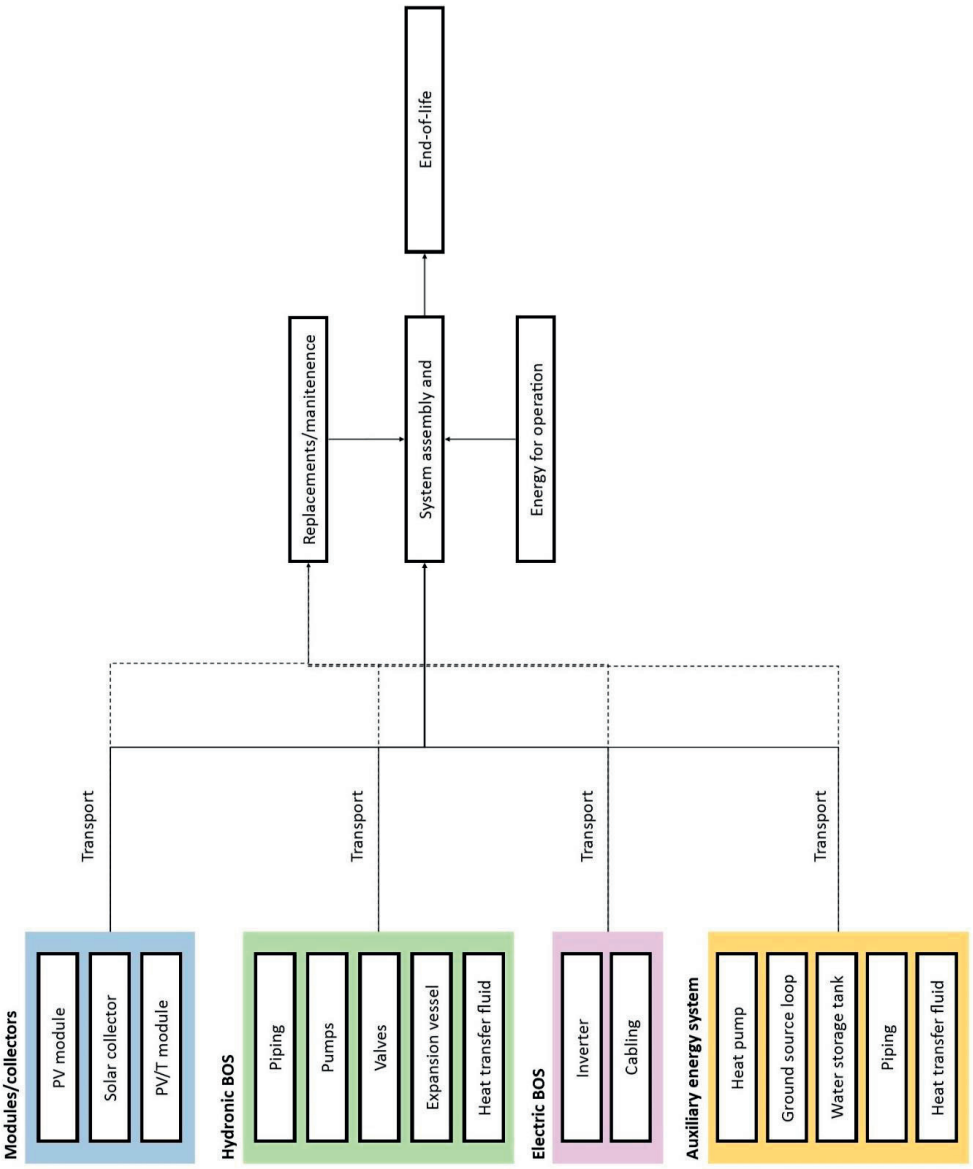

Figure 66. Flow chart of the analysed solar energy systems.

6.4.3.2 Life cycle inventory

Generic Ecoinvent processes are used for components other than the solar modules, but some of the processes have been slightly modified to better represent the system in question. All modifications are described below. Global market processes in Ecoinvent are used, which means that the production represents the average of the global production and an average transport distance.

6.4.3.2.1 Solar energy technologies

The life cycle inventories of the PV and PV/T modules were given in Section 6.1.3.7. The Ecoinvent process "Flat plate solar collector, Cu absorber (RoW), production[21]" is used to model the solar thermal collector. The technological developments have not been as large in the solar collector industry as in the PV industry. Even though the data in this process model is also relatively old, it is therefore considered to be comparable to the data on the two other solar technologies in its present form. An inventory of the most important materials in the solar thermal collector is given in Table 24, and a full inventory is given in Table A.4 in Appendix A.

Table 24. Inventory of the most important components in the solar thermal collector process model in Simapro 3.1.

Component	Amount	Unit	Ecoinvent process
Aluminium	3.9	kg	Aluminium, wrought alloy (GLO), market for
Stainless steel	4.1	kg	Steel, chromium steel 18/8, hot rolled (GLO), market for
Copper absorber	2.8	kg	Copper (GLO), market for
Sheet rolling, copper	2.8	kg	Sheet rolling, copper (GLO), market for
Selective coating, absorber	1.0	m^2	Selective coat, copper sheet, black chrome (GLO), market for
Solar glass	9.1	kg	Solar glass, low-iron (GLO), market for
Anti-reflective coating, glass	1.0	m^2	Anti-reflex-coating, etching, solar glass (GLO), market for
Glycol (heat transfer fluid)	1.0	kg	Propylene glycol, liquid (GLO), market for
Packaging	3.7	kg	Corrugated board box (GLO), market for
Insulation (Rock wool)	2.4	kg	Rock wool, packed (GLO), market for
Rubber	0.7	kg	Synthetic rubber (GLO), market for

6.4.3.2.2 Electric BOS

The inventory of the electric BOS is given in Table 25, and in more detail in Table A.5 in Appendix A. It is to a large extent based on information given in the publications by Inman and

[21] As in the previous sections, the default allocation version of all processes are used unless otherwise specified.

Houlihan Wiberg [12, 169] with some modifications. These values, in turn, are based on information from the installer.

The inverters are the most important components in the electronic BOS. The system on the Living Lab uses two 3.2 kW inverters, with a combined weight of 52 kg. The 2.5 kW inverter model in Ecoinvent is used in the analysis, scaled to the same weight as the 3.2 kW inverter. The same inverters are assumed for all three systems, even though the installed power is slightly smaller for System 5.

The cables and connectors are approximated by a generic model in Ecoinvent. The value in Table 25 is used for Systems 2 and 7, where PV or PV/T modules cover the whole roof. System 5 has a smaller number of modules than the other two (45 instead of 48), and the cable length has therefore been scaled down to 164 m.

Table 25. Inventory of the electric BOS. The inverter will be replaced once during the lifetime of the solar energy systems.

Component	Amount	Unit	Ecoinvent process	Lifetime
Inverters	52.0	kg	Inverter, 2.5kW (GLO), market for *(Scaled by weight.)*	15 years
Power cables	175	m	Cable, three-conductor cable (GLO), market for	30 years
Connectors	0.16	kg	Electric connector, wire clamp (GLO), market for	30 years

6.4.3.2.3 Hydronic BOS and auxiliary energy sources

The thermal configurations of the three systems are quite different from each other, and the hydronic BOS therefore needs to be modelled for System 5 and System 7 separately. The main difference between the systems is the piping. The required length of piping has been approximated based on the examples given by Stucki and Jungbluth [180].

Copper piping was assumed for all the three systems, and as in the examples in Stucki and Jungbluth [180] it was assumed to be composed of copper, insulation and a plastic coating. The quantities of materials used were calculated based on the diameter and length of the piping in each system. The heat transfer fluid is also based on the piping length, and assumed to be replaced twice (every ten years).

The inventory of the hydronic BOS for System 5 is shown in Table 26 and in more detail in Table A.6 in Appendix A. The solar thermal system with a 5 m^2 collector area from [180] is used as a basis for System 5, which has a collector area 4.18 m^2. The same pipe diameter was used (12 mm). The piping length was scaled down to the collector area, resulting in a length of 27 m.

Table 26. Inventory of the hydronic BOS of System 5 (PV and solar thermal).

Component	Amount	Unit	Ecoinvent process	Lifetime
Piping	5.7	kg	Copper (GLO), market for	30 years
Piping insulation	3.4	kg	Tube insulation, elastomere (GLO), market for	30 years
Piping coating	0.4	kg	Packaging film, low density polyethylene (GLO), market for	30 years
Expansion vessel	1	pc	Expansion vessel, 25l (GLO), market for	30 years
Circulation pumps	2	pc	Pump, 40W (GLO), market for	15 years
Glycol (heat transfer fluid, 35%)	0.8	kg	Propylene glycol, liquid (GLO), market for	10 years
Water (heat transfer fluid, 65%)	1.9	kg	Water, deionised, from tap water, at user (GLO), market for	10 years

The inventory of the hydronic BOS for System 7 is shown in Table 27 and in more detail in Table A.7 in Appendix A. The solar thermal system with 81 m^2 from [180] was used as a basis for the model of System 7, which has 79.2 m^2 of PV/T modules. The same pipe diameter (25 mm) was used. The piping length was scaled to the current PV/T area, giving a length of 138 m.

Table 27. Inventory of the hydronic BOS of System 7 (PV/T only).

Component	Amount	Unit	Ecoinvent process	Lifetime
Piping	124.2	kg	Copper (GLO), market for	30 years
Piping insulation	56.5	kg	Tube insulation, elastomere (GLO), market for	30 years
Piping coating	3.8	kg	Packaging film, low density polyethylene (GLO), market for	30 years
Expansion vessel	1	pc	Expansion vessel, 25l (GLO), market for	30 years
Circulation pumps	2	pc	Pump, 40W (GLO), market for	15 years
Glycol (heat transfer fluid, 35%)	36.2	kg	Propylene glycol, liquid (GLO), market for	10 years
Water (heat transfer fluid, 65%)	64.5	kg	Water, deionised, from tap water, at user (GLO), market for	10 years

System 2 does not include any solar thermal components and therefore no hydronic BOS. Piping is only required between the heat pump and the storage tank. This was approximated to 4 m, and the same piping as in System 5 was used. To make the the three systems comparable, 4 m of the piping in System 5 and System 7 was therefore counted in the inventory for auxiliary energy sources.

The inventory of the auxiliary energy system is shown in Table 28 and is the same for all three systems. A detailed version is shown in Table A.9 in Appendix A.

Table 28. Inventory of the auxiliary energy system, which is the same for all three systems.

Component	Amount	Unit	Ecoinvent process	Lifetime
Storage tank	400	l	Hot water tank, 600l (GLO), market for *(Scaled by extrapolation factor from Stucki and Jungbluth [180].)*	30 years
Heat pump, 3.5 kW	3.5	kW	Heat pump, brine-water, 10kW (GLO) market for *(25% of the impact scaled by power rating.)*	15 years
Horizontal ground collector	1	pc	See Table A. 8 in Appendix A for details	30 years
Piping	1.0	kg	Copper (GLO), market for	30 years
Piping insulation	0.6	kg	Tube insulation, elastomere (GLO), market for	30 years
Piping coating	0.1	kg	Packaging film, low density polyethylene (GLO), market for	30 years
Circulation pump	1	pc	Pump, 40W (GLO), market for	15 years
Glycol (heat transfer fluid, 35%)	0.2	kg	Propylene glycol, liquid (GLO), market for	10 years
Water (heat transfer fluid, 65%)	0.4	kg	Water, deionised, from tap water, at user (GLO), market for	10 years

The process "Hot water tank, 600l (GLO), market for" from Ecoinvent is used and scaled down to 400 l using the extrapolation factors for the calculation of different storage sizes from Stucki and Jungbluth [180].

The smallest available heat pump model in Ecoinvent is 10 kW (Heat pump, brine-water, 10kW (GLO), market for). No information on the weight of the heat pump was available. As a very rough approximation, it was assumed that 25% the impact of the heat pump would depend on its rated power, and the remaining 75% is associated with components that are similar regardless of rated power. 25% of the impact of the heat pump was therefore scaled down from 10 kW to a 3.2 kW heat pump (which was used in the Living Lab), giving a scaling factor of 0.83.

No model for a ground source collector was available in Ecoinvent. The collector was therefore modelled as a combination of 105 m plastic piping and the work required for burying the piping in the ground. The work was approximated by the Ecoinvent process "Excavation, hydraulic digger (RER), processing" and scaled by the ground volume required for the collector. The heat transfer fluid for the circuit is included with two replacements during the 30 year period. A detailed inventory for the horizontal ground collector is found in Table A.8 in Appendix A.

6.4.3.3 Impact assessment

Like the previous studies in this chapter, this assessment uses only the impact category global warming potential at 100 years (GWP100a), as described by the Intergovernmental Panel on Climate Change (IPCC) [9].

6.4.4 Results

6.4.4.1 Embodied emissions

The total embodied emissions of the three solar energy systems and auxiliary energy system are presented in Table 29. System 7, with PV/T modules, has the highest embodied emissions; 26% higher than System 3 and 28% higher than System 5. This is mainly due to the higher embodied emissions of the PV/T modules, but also to some extent to the higher emissions of the hydronic BOS. System 5 has the lowest embodied emissions, which is due to the lower area of PV cells in this system.

Table 29. The total embodied emissions of the three solar energy systems.

	System 2 (PV only)	**System 5 (PV and ST)**	**System 7 (PV/T only)**
	kg CO_{2eq}	*kg CO_{2eq}*	*kg CO_{2eq}*
PV modules	14921	13988	0
Solar collectors	0	552	0
PV/T modules	0	0	19113
Electric BOS	1951	1902	1951
Hydronic BOS	0	119	1515
Auxiliary energy	4963	4963	4963
Total	21835	21524	27542

The annualized emission values for the solar energy systems, normalized by the functional unit for the building analysis are shown in Figure 67. The BOS makes up a substantial part, 12-15%, of the embodied emissions of the solar energy systems. The electric BOS is by far the main contributor, and the emissions originate approximately 60% from the inverter and 40% from the cables.

The impact of the hydronic BOS is significantly larger for System 7, with PV/T, than for the other two systems. However, it is still lower than the impact of the electric BOS. The components of the auxiliary energy system (e.g. heat pump and ground collector) account for 18-29% of the total embodied emissions of the energy supply system.

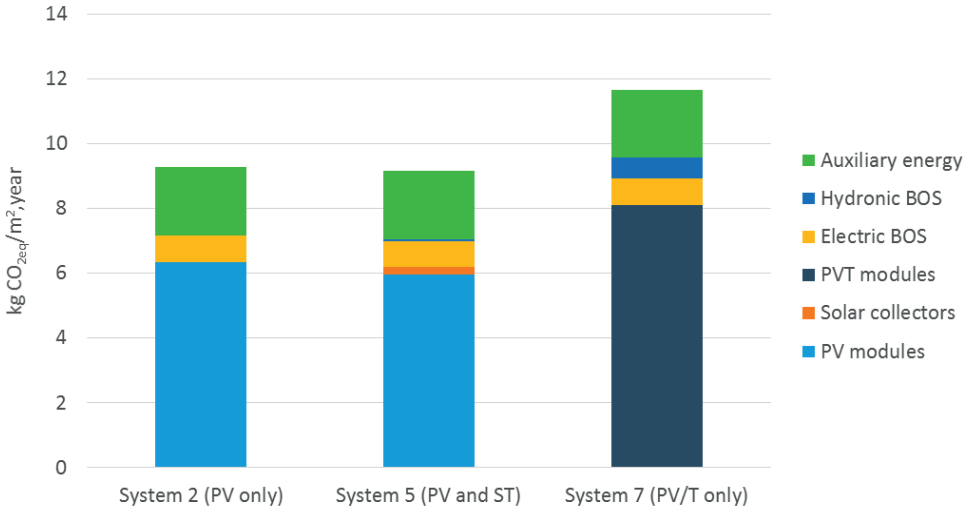

Figure 67. Embodied emissions of the different energy supply systems. The figure shows annualized values normalized by the functional unit (1 m^2A_{fl}/year)

6.4.4.2 Emission factor

The embodied emissions of the solar energy systems were normalized by the first functional unit, 1 kWh_{PE}, using the energy output values from Section 5.3. In this calculation, the total value of embodied emissions of the solar energy systems (modules, collectors, and BOS, but not the auxiliary energy system), was divided by the total primary energy output during the system's lifetime. This results in an emission factor (sometimes also referred to as emission rate) for the energy from each system, with the unit kg CO_{2eq}/kWh. This emission factor can be directly compared to the grid emission factor.

Since this calculation spans over 30 years, the degradation of the PV modules are taken into account. The value from the LCA guidelines for PV [79] is used, which is 0.7% reduction in efficiency per year. The PV/T modules are assumed to have the same degradation in electricity output as the PV modules. The thermal output of solar collectors and PV/T modules is here assumed to be constant over the 30 years. The annualized electric, thermal, and primary energy output per m^2 installed area of each of the solar energy systems is shown in Table 30. The primary energy is calculated using the same method as in Section 5.3.3.1.

Table 30. Annual energy output per installed area per year during 30 years, including degradation of the electric performance of the modules.

System	Electricity	Thermal energy	Primary energy
	kWh_{el}/m^2	kWh_{th}/m^2	kWh_{PE}/m^2
3 (PV only)	131	0	301
5 (ST and PV)	124	18	295
7 (PV/T only)	129	22	310

The emission factors for solar energy from each of the three systems are shown in Table 31. The ZEB grid emission factor over 30 years is 0.238 kg CO_{2eq}/kWh and the current EU emission factor is 0.361 CO_{2eq}/kWh. The emission factor of all three solar energy systems is thus significantly lower, which means that energy from the system is a source of less greenhouse gas emissions per delivered kWh than electricity from the grid. The emission factors of the solar energy systems are, however, slightly higher than the grid emission factor from the Norwegian grid, which is around 0.041 kg CO_{2eq}/kWh.

Table 31. Emission factors of the three solar energy systems over 30 years. Electric and hydronic BOS, but not auxiliary energy sources, are included in the right column.

System	Modules only	Modules and BOS
	kg CO_{2eq}/kWh	*kg CO_{2eq}/kWh*
System 2 (PV only)	0.048	0.054
System 5 (ST and PV)	0.048	0.055
System 7 (PV/T only)	0.060	0.071

6.4.4.3 Emissions payback time and return on investment

The greenhouse gas emissions payback time (GPBT) is shown in Table 32, calculated according to Equation (26). The GPBT is between 6.1-9.2 years using the ZEB factor and 4.0-5.9 years using the EU grid factor. The shortest payback time is found for the System 2 (PV only) with the ZEB grid factor (4.0 years for modules only or 4.5 years for modules and BOS). The longest payback time is found for the System 7 (PV/T only) with the ZEB grid factor (7.6 years for modules and 9.2 years for modules and BOS).

Table 32. The greenhouse gas emissions payback time (GPBT) calculated using the ZEB grid factor and the EU grid factor.

	GPBT (ZEB grid factor)		GPBT (EU grid factor)	
System	**Modules only**	**Modules and BOS**	**Modules only**	**Modules and BOS**
	years	*years*	*years*	*years*
System 2	6.1	6.8	4.0	4.5
System 5	6.1	6.7	4.0	4.6
System 7	7.6	9.2	5.0	5.9

The GPBT found in previous research on PV/T systems ranged from 0.8 years to 4 years (see Section 6.1.2), that is, slightly shorter than the values found for the PV/T system using the EU grid factor, and significantly shorter than the values found using the ZEB grid factor. The GPBT is directly related to the energy output of the system, and thereby to the level of irradiation at the location. Since all of the previous studies were made in locations with higher irradiation levels than Trondheim, it is not surprising that the values found in this study are lower. Compared to the expected lifetime of the solar energy systems, however, the GPBT values found in this study are low.

The greenhouse gas return on investment (GROI) is shown in Table 33, calculated as described in Section 6.1.3.5. The GROI shows how many times the system can pay back the embodied emissions that went into its production. A value above 1.0 means that the system pays back its embodied emissions and so to speak "makes sense" to install. All the GROI values of the systems are well above 1.0.

Table 33. The greenhouse gas emissions return on investment (GROI) calculated using the ZEB grid factor and the EU grid factor.

	GROI (ZEB grid factor)		GROI (EU grid factor)	
System	**Modules only**	**Modules and BOS**	**Modules only**	**Modules and BOS**
	-	-	-	-
System 2	5.0	4.4	7.5	6.6
System 5	4.9	4.5	7.5	6.6
System 7	4.0	3.3	6.0	5.1

The GPBT and the GROI shows essentially the same information, but in two different ways. While the GPBT shows how soon an installation will pay back its "invested" greenhouse gas emissions, the GROI shows how much total "profit" the investment will give during the lifetime of the installation.

6.4.4.4 Emission balance of the building

The embodied emissions of the solar energy systems were shown in Table 29 and the total embodied emissions of the building were shown in Table 23. Based on these values, the calculated embodied emissions of the building with the three solar energy systems are shown in Table 34 as recommended by the ZEB guidelines [73].

Table 34. The total embodied emissions of the building and the solar energy systems.

Building and system	**Embodied emissions**		
	kg CO_{2eq}	*kg CO_{2eq}/year*	*kg CO_{2eq}/m^2A_{fl}, year*
Building with System 2	75468	2516	24.7
Building with System 5	75157	2505	24.6
Building with system 7	81175	2706	26.5

The solar energy systems (modules, collectors and BOS) accounted for 22% (System 2 and (System 5) and 28% (System 7) of the total embodied emissions of the building. For System 2 and System 5, this was slightly lower than the 25% found in the original study by Inman and Houlihan Wiberg [12], but the systems are also slightly smaller than the original one. It was nonetheless in line with what has been found in earlier studies in the ZEB Centre.

The net emissions of the building with the three solar energy systems were calculated according to Equation (27). The results are shown in Table 35 using the ZEB grid factor ($f_{GHG,el,sym}$ = 0.238 kg CO_{2eq}/kWh) and in Table 36 using the EU grid factor ($f_{GHG,el,sym}$ = 0.361 kg CO_{2eq}/kWh). Also shown are the emissions related to exported electricity ($GHG_{exp,el} = E_{exp,el} \cdot f_{GHG,el,sym}$), the emissions associated with delivered electricity ($GHG_{del,el} = E_{exp,del} \cdot f_{GHG,el,sym}$), and the total embodied emissions ($GHG_{embodied}$).

Table 35. The net emission calculation (ZEB-OM ambition level) for the building with the three solar energy systems using the ZEB grid factor (0.238 kg CO_{2eq}/kWh).

System	$GHG_{exp,el}$	$GHG_{del,el}$	$GHG_{embodied}$	GHG_{net}
	kg CO_{2eq}/m^2A_{fl},year	*kg CO_{2eq}/m^2A_{fl},year*	*kg CO_{2eq}/m^2A_{fl},year*	*kg CO_{2eq}/m^2A_{fl},year*
System 2	20.9	5.5	24.7	-9.3
System 5	19.7	5.4	24.6	-10.3
System 7	19.6	5.5	26.5	-12.5

Table 36. The net emission calculation (ZEB-OM ambition level) for the building with the three solar energy systems using the EU grid factor (0.361 kg CO_{2eq}/kWh).

System	$GHG_{exp,el}$	$GHG_{del,el}$	$GHG_{embodied}$	GHG_{net}
	kg CO_{2eq}/m^2A_{fl},year	*kg CO_{2eq}/m^2A_{fl},year*	*kg CO_{2eq}/m^2A_{fl},year*	*kg CO_{2eq}/m^2A_{fl},year*
System 2	31.7	8.4	24.7	-1.3
System 5	29.9	8.2	24.6	-2.9
System 7	29.7	8.3	26.5	-5.2

As the two tables show, all values of GHG_{net} are negative, which means that none of the systems reaches a net zero emission balance at the ZEB-OM ambition level, regardless of the grid emission factor used. The system that is closest to reaching a balance is System 2, which includes only PV modules. The system with PV/T modules is farthest from a balance.

6.4.5 Discussion

6.4.5.1 Uncertainties

The solar energy systems contribute to a significant fraction of the embodied emissions of the building, and the largest share of those emissions are due to the PV and PV/T modules. Uncertainties regarding the amount of embodied emissions in these modules will therefore have a significant impact on the end result. A further discussion of the uncertainties in the analysis of the PV/T and PV modules was provided in Section 6.2.4.1 and will not be repeated here.

Another source of uncertainty in the analysis of the solar energy systems is the length of the piping in the hydronic BOS. Since no specific information on the piping was available, examples from previous research were used in the case study [180]. The thermal solar components in System 5 covers only 4.18 m^2, while all of the 78.25 m^2 solar installation is part of the thermal installation in System 7. The piping length therefore has to be increased to some degree in System 7. However, as Figure 68 shows, some PV/T systems do not require much piping between the modules and the large amount of piping in the hydronic BOS of System 7 (138 m) might therefore be exaggerated.

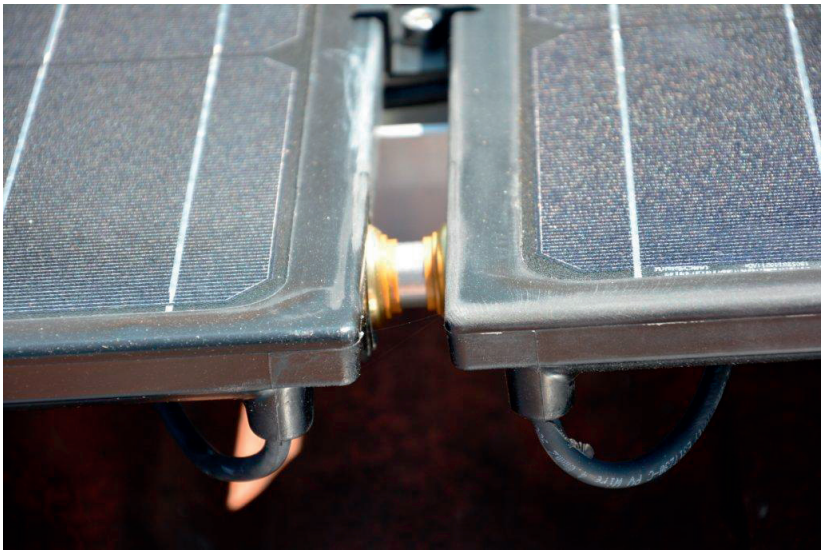

Figure 68. Piping connection between two PV/T modules from Wiosun. Photo: Johan Ahlgren, Energiförbättring Väst AB.

A simple sensitivity analysis of System 7 was performed to determine how much the piping length influenced the overall results. The emissions of System 7 were calculated again but this time with the hydronic BOS of System 5, which includes only 27 m of piping.

The results of the original and new version of System 7 are shown in Table 37. The reduction of embodied emissions due to the reduced pipe length results in a reduction in both the emission factor and the GPBT. However, the values for System 7 are still higher than the values for System 2 and System 5. Furthermore, the building with System 7 and reduced pipe length did not reach a net ZEB-OM balance using either of the two grid emission factors.

Table 37. Embodied emissions, emission factor, and GPBT of the original and new version of System 7. The modules and BOS are included in the embodied emissions.

	Embodied emissions	**Emission factor**	**GPBT (ZEB grid)**	**GPBT (EU grid)**
	kg CO_{2eq}/m^2A_{fl},year	*kg CO_{2eq}/kWh_{PE}*	*years*	*years*
System 7 (138 m piping)	7.4	0.071	9.2	5.9
System 7 (27 m piping)	6.9	0.067	8.6	5.5

As mentioned in Section 6.4.1, the emissions data for mono-Si PV modules are used in the calculations even though the actually installed modules are of poly-Si type. The embodied emissions of the Ecoinvent model of a poly-Si PV module (Photovoltaic panel, multi-Si wafer (RER), production) are 212 $kgCO_{2eq}/m^2$. If it is updated according to the same criteria as the mono-Si PV module (see Section 6.2.2.2, the embodied emissions are reduced to 142 kg CO_{2eq}/m^2. Using the Ecoinvent data for a poly-Si module instead of a mono-Si module

would have reduced the embodied emissions of System 2 (solar modules and BOS) with around 21% and of system 5 with around 16%. This would have resulted in lower emission factors and GPBT, and higher GROI for both these systems. The results for System 2 with mono-Si and poly-Si modules is shown in Table 38. System. 2 is very close (-0.1 kg $CO_{2eq}/m^2 A_{fl}$, year) to reaching a zero emission balance if calculated with the current EU grid factor.

Table 38. Embodied emissions, emission factor, and GPBT of System 2 with mono-Si and poly-Si PV modules. The modules and BOS are included in the embodied emissions.

	Embodied emissions	**Emission factor**	**GPBT (ZEB grid)**	**GPBT (EU grid)**
	kg $CO_{2eq}/m^2 A_{fl}$,year	*kg CO_{2eq}/kWh_{PE}*	*years*	*years*
System 2 (mono-Si PV)	5.5	0.054	6.8	4.5
System 2 (poly-Si PV)	4.3	0.043	5.4	3.5

Another source of uncertainty is the lifetime of the solar thermal system. As mentioned in Section 6.1.3.1, the lifetime of a solar thermal system is commonly assumed to be 20-25 years, but was here assumed to be 30 years. To evaluate how much this assumption influenced the results, a simple sensitivity analysis was performed where the lifetime of the solar thermal system was reduced to 20 years. The building lifetime is 60 years, which means that the system would be replaced twice. However, as this study only covers 30 years, the solar thermal system has been accounted for one and a half times. The results comparing System 5 with 30 year lifetime and 20 year lifetime is shown in Table 39. Only the lifetime of the solar collectors is changed. As Table 39 shows, the impact of the reduced lifetime of the solar thermal collectors is very modest.

Table 39. Embodied emissions, emission factor, and GPBT of System 5 with 30 and 20 year system lifetime. The modules and BOS are included in the embodied emissions.

	Embodied emissions	**Emission factor**	**GPBT (ZEB grid)**	**GPBT (EU grid)**
	kg $CO_{2eq}/m^2 A_{fl}$,year	*kg CO_{2eq}/kWh_{PE}*	*years*	*years*
System 5 (30 year lifetime)	5.4	0.055	6.7	4.6
System 5 (20 year lifetime)	5.5	0.056	6.8	4.6

The inverter was the BOS component with the single largest impact on the embodied emissions. Since the same inverter was used in all three solar energy systems it does not influence the comparison between the systems, and no sensitivity analysis was therefore performed for this component.

6.4.5.2 Embodied emissions and emission factors

The analysis of the emission balance of the building includes both the solar energy systems and the rest of the building. The fact that the analyses are performed by different researchers using slightly different methods suggests that they might not be fully comparable. In the building

analysis, Inman and Houlihan Wiberg divided the emissions into life cycle phases (see Figure 65) and calculated specific transport distances depending on country of production. Furthermore, the full 60 year lifetime of the building was used in the analysis by Inman and Houlihan Wiberg, while only the 30 year lifetime of the solar energy systems were used in the analysis presented in this thesis.

The calculation of the embodied emissions of the solar energy systems which was performed in this thesis made use of global market processes in Ecoinvent, which means that the results are less specific for the actual case. As shown in the example of PV/T module A (see Figure 55), this can have an impact on the embodied emissions. The use of more specific data in the calculation of the solar energy systems might have changed their share of the total embodied emissions of the building slightly. However, as the main objective of this analysis was to compare different solar energy technologies to each other, it was seen as acceptable to include less detail on components that are common for all three systems.

In studies of embodied energy or embodied emissions, the influence of the BOS on the emissions of solar energy systems is sometimes assumed to be negligible. The results presented here show that the environmental impact of the BOS is not negligible, but accounts for up to 15% of the emissions. This issue is studied in more detail in Paper VI, where the original system on the Living Lab is compared to solar energy systems on two of the ZEB Centre's other pilot buildings. This publication also shows that it is very important to consider embodied emissions in the choice of mounting structure for building integrated or building added solar energy systems.

The choice of grid emission factor is another influential parameter. Since one "pessimistic" (the current EU grid) and one "optimistic" (the ZEB ultra-green scenario) grid emission factor was used in the calculation, the results can be regarded as a range of possible results. In any case, the emission factor for all of the studied solar energy systems was significantly lower than both grid emission factors, which shows that the solar energy systems contribute to reduced emissions over their lifetime in both the optimistic and the pessimistic development scenarios for the emissions of the European electricity grid.

6.5 Conclusions

Chapter 6 has been focusing on the embodied emissions of solar energy systems in general and PV/T modules in particular.

Section 6.1.2 presented a review of previous research on the environmental impact of PV/T modules. The review showed that there was a lack of research on commercially produced modules. To add to this research, a model of a generic PV/T module was constructed based on information from two PV/T producers in combination with a model for a PV module from the Ecoinvent database. The embodied emissions of this PV/T module was analysed using methods from life cycle assessments (LCA).

The major difference in the inventory of a PV module and a PV/T module is the heat exchanger, which is only included in the latter. The analysis showed that the embodied emissions of a PV/T

module was around 30% higher than that of the PV module. This was mostly due to the material in the heat exchanger. Both the two commercial PV/T modules that were used as references in the analysis had similar heat exchangers made of stainless steel sheets. Other PV/T modules on the market use other technologies, for example piping similar to solar thermal collectors. This type of heat exchanger was, however, not analysed here.

The study in Section 6.1.3.7 also included an update of the PV module in the Ecoinvent database to more current values on the amount of materials used for the solar cells, glazing, and aluminium frame. One finding from the study was that the impact of the aluminium frame in the modern modules was relatively small, only around 1.5% of the emissions, compared to around 7.5% in the original module. The solar cells still accounted for the major share of embodied emissions in the updated module.

The model of one specific PV/T module with country specific data on production and transport distances resulted in a slightly lower value of embodied emissions. This result shows that the model of the generic PV/T module was relatively conservative, at least for modules produced in Europe.

Another knowledge gap found in the review of previous research in 6.1.2 was that none of the studies were performed in areas with lower irradiation and a colder climate. The location of the installation has a large impact on the energy and emissions payback time of the system, and the results of studies in more sunny climates are therefore not directly transferable to Scandinavia. Installations in locations with higher irradiation levels will in most cases have a higher energy output and thereby shorter emissions payback time.

As discussed in Chapter 4, the design of solar energy systems also impact their energy performance to a great extent, and the design needs to be adapted to the location. The objective of the study presented in Section 6.3 was therefore to study how the design of a solar energy system on a building influences the emission balance of the building. The ZEB residential concept model was used as the case building for this study, which focused only on PV systems.

The results showed that the net avoided emissions of the solar energy systems depended more on the amount of generated electricity than the on embodied emissions. While the amount of embodied emissions of the thin film modules was much lower than that of the crystalline silicon modules, the low efficiency of the thin film modules resulted in a lower total contribution to emissions reduction over the system lifetime in this case.

The study also showed that even though modules mounted at an optimal orientation perform significantly better in terms of delivered kWh per installed kW_P, these systems did not contribute to the largest reduction in emissions over the system lifetime, or enabled the building to reach a net zero emission balance. The only version of the building that reached a zero emission balance had north/south facing modules or east/west facing high efficiency mono-Si modules. This was the case even though the GPBT of the north facing modules was up to 23.9 years. Based on the results of the study, it can be questioned whether it is of importance to reach a zero emission balance at any cost, or whether the embodied emissions could have been "invested" better.

The study presented in Section 6.4 focused on how the choice of solar energy technology influences the embodied emissions, the emission factor of the generated energy, and the emission balance of the building. In the results presented here, no improvement in the environmental performance was found from the use of PV/T modules instead of solar thermal and PV modules separately, or instead of only PV modules. The model of the generic PV/T module is, however, based on a very small number of sources, and many assumptions are used in the life cycle impact assessment. It is highly possible that a more detailed model of the PV/T module, perhaps including measured values on energy demand from the production, could result in a lower value of embodied emissions. As discussed previously, it is impossible to make any generalizable conclusions based only on this small number of case studies.

The results from both Section 6.3 and Section 6.4 show that it is quite difficult for a building to reach a net zero emission balance at the ZEB-OM ambition level. The building in the second case study, the Living Lab, came closer to reaching a balance than the building in the first case study, the ZEB residential concept. The solar energy systems on the Living Lab were, however, much larger than those on the ZEB residential concept, which also had a larger heated floor area. The system that was closest to reaching a balance was the PV system on the Living Lab (System 2).

The roof on the Living Lab where the solar energy systems are installed is close to optimally inclined, and it is therefore difficult to increase the energy performance of the system to any significant degree.[22] The energy demand of the case building is low (close to passive house level). It can therefore be concluded that a significant reduction in the embodied emissions would be necessary in order to reach a net ZEB-OM balance.

The solar energy systems were found to account for 22-28% of the embodied emissions in the two case studies. The major part of the embodied emissions of PV and PV/T systems are associated with the use of high-purity silicon for crystalline silicon solar cells. Reductions in the embodied emissions of PV and PV/T modules are possible with further improvements in production technology. The use of other solar cell materials, such as thin films, could also be a method of reducing the embodied emissions. However, as the first case study showed, further efficiency improvements are needed for these technologies to really compete with crystalline silicon technology, even though the embodied emissions are lower.

The studies showed that all three types of solar technologies studied resulted in lower emission factors than the emission factors for electricity from the European grid. The payback times were also found to be significantly lower than the lifetimes of the systems. This shows that even though the amount of embodied emissions of the systems are relatively high, they still contribute to reduced emissions over their lifetime.

The embodied emissions of solar modules, or indeed any other product, would also be lowered by using more renewable energy in the manufacturing process. So, while solar energy systems

[22] It should be noted that shading was not included in the Living Lab case study (see Section 5.3.2.2).

with solar cells are associated with high amounts of embodied emissions they also contribute to greening the power system, thereby reducing the embodied emissions of products manufactured in the future.

Chapter 7: Conclusions

The objective of this thesis was to answer the research question: *What is the potential of PV/T systems to minimize the life cycle greenhouse gas emissions of a residential building?* The research question was divided into three sub-questions:

a) How should PV/T technology be used in buildings to achieve high energy output and good load coverage?
b) How does the energy performance of PV/T systems compare to that of separate PV and solar thermal systems?
c) How does the environmental impact of PV/T systems compare to that of separate PV and solar thermal systems?

These questions were addressed through case studies, which have been presented in this thesis. The findings from the studies are summarized with regard to each of the three sub-questions in the following sections. There are of course many connections between the sub-questions, and the division into sections is not completely strict. The main research question is addressed in Section7.4.

7.1 Sub-question a

How should PV/T technology be used in buildings to achieve high energy output and good load coverage?

This question was primarily addressed in Chapter 4, where the design of solar energy systems in general and PV/T systems in particular was discussed. The information in Chapter 4 was based mainly on guidelines and published literature on the design of PV systems and solar thermal systems, but also on the review of PV/T installations on buildings which was presented in Chapter 3 and Paper I.

Since PV/T is a hybrid technology, the design of a well-functioning PV/T system should consider aspects of both PV system design and solar thermal system design. These design aspects can sometimes be conflicting. For example, grid connected PV systems do not necessarily have to be limited in size since surplus energy can be injected to the grid, while an over-dimensioned solar thermal system will experience overheating, lower efficiency, and possibly even damage to components. On the other hand, the energy output of PV modules is more affected by shading than that of solar thermal collectors.

Some general guidelines can be given based on design principles for PV and solar thermal systems: The orientation of the modules should be adapted to the intended use of the energy output. Higher tilt angles result in a flatter energy output profile over the year and slightly increases the yield during the shoulder seasons, while lower tilt angles will favour energy generation during summer. Over-dimensioning should be avoided if covered PV/T modules are used, due to the risk of overheating. Shading should be avoided as far as possible. If shading is unavoidable, the orientation of the modules can be adapted to minimise the impact, or micro-

inverters or power optimisers can be used. The impact of snow, and how it can be removed if necessary, also needs to be considered. If possible, measurements or observations should be performed on the site prior to the installation to assess the impact. High tilt angles are recommended to avoid snow accumulation, and also the use of frameless modules.

Whether it is the PV system or solar thermal system design aspects that will be of more importance in the design of a PV/T system depends on the type of PV/T modules that are used and the intended use of the energy.

The review of PV/T systems in buildings revealed that the PV/T modules in what is probably one of the largest systems to date, the installation in Suurstoffi in Switzerland (Figure 25), were installed almost horizontally on flat roofs. In this case, the electricity output was the priority, and the heat exchangers in the PV/T modules were used for cooling the PV cells during summer rather than providing water at as high temperature as possible. The collected heat was then used to thermally charge boreholes in the ground.

In other examples of PV/T systems, such as the off-grid system on the Arpont Shelter in France (Figure 23), the PV/T system was designed according the load of the building. In this case, the load was largest during the morning and evening, and the PV/T system was therefore mounted on the façade with orientation ranging from east to west to catch the morning and evening sun.

In general, the thermal output of PV/T systems are of lower temperature than that of similar installations of solar thermal collectors. The difference is smaller for covered PV/T modules than for uncovered PV/T modules. The latter type was found to be the most commonly available on the market today and has also been the main focus of this thesis. Because of the relatively low temperature of the thermal output, PV/T modules perform best when they are integrated into an energy system where low temperature heat is useful.

Covered PV/T modules can to some extent be seen as an alternative to solar thermal collectors, but a larger installed area is necessary to get the same thermal energy output. In the first case study (Section 5.2 and Paper II) a thermal solar fraction of close to 100% during the summer was achieved with 8-10 m^2 solar collectors compared to 16 m^2 covered PV/T modules.

Due to their lower thermal efficiency, uncovered PV/T modules cannot be used in the same way as solar thermal collectors and should be regarded more as an alternative to PV modules. With uncovered PV/T modules, it was only possible to reach a thermal solar fraction during summer of around 40% in the first case study, even with a system covering the whole available area (30 m^2). This system was, however, able to cover the full electricity load of the building.

In the second case study (Section 5.3), the uncovered PV/T modules were found to be unsuitable for direct heating of domestic hot water, but useful for space heating, or preheating for domestic hot water or a heat pump. The system with 78.7 m^2 uncovered PV/T modules in this study reached a similar thermal solar fraction as a solar thermal collector system of 4.2 m^2, around 50%. The PV/T system did, however, also generate around three times the annual electricity load.

The combination of PV/T modules and heat pumps of different types was frequently found both in literature and in installed systems. In smaller residential systems, PV/T modules were generally found to be combined with air-source heat pumps into energy systems that could provide domestic hot water and space heating. In larger systems, it was common to combine the PV/T modules with ground source heat pumps. However, it was also found that the energy demand for operation of circulation pumps and other equipment could easily be larger than the increase in energy output from the use of PV/T modules.

Different integration options between PV/T modules and heat pumps were discussed in Chapter 4 and studied in the case studies in Chapter 5, and the use of PV/T modules as pre-heaters for heat pumps was found to be particularly interesting. The second case study (Section 5.3) showed that the use of PV/T for pre-heating of a ground source heat pump could increase the primary energy output of the modules. The conclusions from the study of PV/T modules in combination with heat pumps is further discussed in the next section.

To summarise, the following points should be considered for the use of PV/T modules in building energy systems in Scandinavia:

- The design of PV/T systems needs to consider design aspects for both PV systems and solar thermal systems. Which of these aspects that are more important depends on the type of PV/T modules used as well as the intended use of the energy output.
- Covered PV/T modules can be used in a similar way to solar thermal collectors, but a larger area is required due to the lower thermal efficiency.
- Uncovered PV/T modules should be integrated into an energy system where low temperature heating is useful. Uncovered PV/T modules are not useful for direct preparation of domestic hot water, but for space heating or for preheating in combination with heat pumps.
- Combining PV/T modules with heat pumps was found to be a promising solution, both in the review of previous research and in the case studies presented here. The use of PV/T modules on the source side of ground source heat pumps resulted in an increase in energy output from the PV/T modules.

7.2 Sub-question b

How does the energy performance of PV/T systems compare to that of separate PV and solar thermal systems?

The energy performance of PV/T systems was the focus of Chapter 5. Case studies of two Norwegian residential buildings were performed, and the theoretical performance of PV/T modules was compared to that of separate PV modules and solar thermal collectors through simulations. The analysis boundary was in both cases the area of the roof where the solar energy systems were installed.

Any comparison of different solar technologies is related to several methodological choices, for example on what grounds the modules should be compared, how the output of different energy carriers should be weighted, and how the energy is going to be used. The results that were

presented in Chapter 5 must therefore be regarded with reference to the methodological choices made in each case.

In previous research as well as in this thesis, electricity output as well as the thermal energy output of a PV/T module was found to be lower than the output of a comparable PV module or a solar collector, respectively. However, as shown in both the first case study in Section 5.2 and Paper II, and the second case study in Section 5.3, the total combined output of electricity and thermal energy of a PV/T module in a well-designed system was higher per unit area. The increase was up to 18% in the first case study and around 6% in the second case study.

The original idea of the PV/T concept was to increase the electricity output of PV modules by cooling them, and at the same time making use of the waste heat. None of the simulations in this thesis found a decreased temperature of PV/T modules compared to PV modules. This was also the general conclusion found in the PV/T roadmap from 2006 [119]. However, measurements from some installed systems show that the electricity output can be higher in the PV/T modules compared to PV modules. Measurements from the Suurstoffi installation mentioned above found that the energy output from PV/T modules was higher than that of PV modules by around 10% over the year, and up to 20% in the summer [134]. This could indicate that the benefit of cooling is higher in warmer climates, where modules are oriented to favour summer yield, or where the ground is available as a free source for cooling.

The results from the first case study (Section 5.2 and Paper II), where the solar energy system is combined with an air-to-water heat pump, suggests that covered PV/T modules could give an increased output compared to solar thermal collectors. The output temperature of covered PV/T modules is relatively high, and this type of modules can therefore contribute to both DHW preparation and space heating in a building. However, the analysis of covered PV/T modules presented in this thesis is uncertain since it is based on a very limited set of data sources. The system with uncovered PV/T modules had a higher energy output than side-by-side installations of PV modules and solar thermal collectors of average efficiency, but a lower energy output than a side-by-side installation using state-of-the art PV modules and solar thermal collectors. Due to the use of modules with different efficiencies, it was difficult to draw any general conclusions from the first case study.

PV and PV/T modules with similar electric efficiency were used in the second case study (Section 5.3). In this study, PV/T modules and a ground source heat pump were simulated with two different system designs: a separate connection type, where they operate mostly independently of each other, and an integrated connection type, where PV/T modules can also contribute to the source side of the heat pump. In primary energy per installed area, the PV/T system where the modules were connected to the source side of the heat pump had the highest primary energy output of all the studied systems, while the system where the PV/T modules were connected directly to the storage tank had the lowest output. The integrated connection to the heat pump increased the primary energy output of the PV/T system by 7-8%. The same number of PV/T modules was used in both cases.

In terms of net energy demand of the building, the systems where the PV/T modules were integrated on the source side of the heat pump resulted in higher net energy surplus over the

year compared to the systems with side-by-side PV modules and solar thermal collectors on the same area. On the other hand, the system with only PV modules resulted in the highest net energy surplus of all the systems. The results from this case study highlight the importance of system design for optimal performance of PV/T systems: uncovered PV/T modules need to be used in low temperature applications, such as assisting a heat pump, due to the low temperature of their thermal output.

The results from the second case study also show the influence of the control system. Two control strategies were tested for the PV/T and heat pump system with integrated connection: temperature control and seasonal control. In the first system, the mode of operation of the PV/T and heat pump system was controlled by the fluid temperatures, so that the PV/T modules contributed firstly to DHW preparation when the module temperature was high enough, and secondly to assist the heat pump. In the system with seasonal control, the PV/T modules were used for DHW preparation during summer and heat pump assistance during winter.

The results showed that the temperature-controlled system had the highest primary energy output, while the seasonally controlled system resulted in the highest net energy surplus. In other words, the temperature-controlled system resulted in the highest energy output from the solar thermal system, but the system with seasonal control reached the best performance if the whole building was considered in the analysis. The primary reason was that the increase in energy demand of circulation pumps was larger than the increase in energy output in the system with temperature control compared to the seasonally controlled system. The energy consumption of circulation pumps in the PV/T systems with integrated heat pump connection was also up to 27% higher than in a system with a separate connection of the PV/T modules and the heat pump. An implication of this is that there is a large potential in developing the control system to reach a good compromise between PV/T performance and the energy use of the system.

The main conclusions from the studies of energy performance are:

- PV/T modules were found to have lower electricity as well as thermal energy output than a comparable PV module or a solar thermal collector, but a higher total energy output per unit area.
- None of the simulations in this thesis showed a cooling effect on the PV cells in the PV/T modules. Increased electricity output from cooling of the PV cells is probably of less importance in a Scandinavian climate compared to warmer climates, and not in itself sufficient to warrant the use of PV/T modules.
- The first case study, of a building with a solar energy and air-source heat pump system, suggests that covered PV/T modules could give an increased output compared to solar thermal collectors, and that uncovered PV/T modules may be beneficial compared to side-by-side installations of PV modules and solar collectors. However, the results are inconclusive due to the method used for comparing different module types.
- The results from the second case study show that, given the same available roof area, a system with uncovered PV/T modules and a ground source heat pump in an integrated connection resulted in a slightly higher energy surplus for the building than a system with separate PV modules and solar thermal collectors, but a lower energy surplus than

that of a system with only PV modules. The same PV/T system, but without integration on the heat pump source side resulted in lower primary energy output than all the other systems.

- Integrating PV/T modules on the source side of the heat pump resulted in a lower energy withdrawal from the ground. The length of the ground collector could therefore have been decreased, with lower cost and material use as a result.
- Due to the lower energy withdrawal, this resulted in less cooling of the ground over time. However, the impact of this was negligible in the case study of the Living Lab, but may be of importance in other situations, such as refurbishment of under-dimensioned ground source heat pump systems.
- The control strategies used in systems with an integrated connection between PV/T modules and ground source heat pumps are of great importance for the overall performance of the systems. The use of energy for circulation pumps can be larger than the energy saving from integrating PV/T in the system if it is not properly designed.

Finally, it should be pointed out that the results of the two case studies give no clear responses to the question of whether it would be better to install a PV/T system than separate PV and solar collector systems. The performance of the systems are to a large extent case-specific, and factors such as location, type of auxiliary heat source and other components, and mode of connection have a large influence on the results. In addition, the results of the analyses are affected by the methodological choices in the analyses. One conclusion is, however, that it is easier to design and construct a well-functioning system of separate PV modules and solar thermal collectors, than a system with PV/T modules.

7.3 Sub-question c

How does the environmental impact of PV/T systems compare to that of separate PV and solar thermal systems?

The environmental impact of solar energy systems was the focus of Chapter 6. The analyses in this chapter looked at the embodied emissions of different solar technologies and different system designs. A review of published research on the environmental impact of PV/T modules revealed that there were no studies performed on industrially produced modules or in regions with irradiation levels similar to those in Scandinavia.

To address the gap in earlier research, a generic uncovered PV/T module was modelled based on data from two European PV/T producers (Section 6.1.3.7). An updated version of a PV module from the Ecoinvent database was used as a starting point. The embodied emissions of the PV/T module were determined by using methods from life cycle assessments (LCA). A single issue assessment of the impact factor Global Warming Potential at 100 years (GWP100a) [9] was used.

It was found that the PV/T module had around 30% higher embodied emissions than a comparable PV module, and that the difference was mainly due to the stainless steel heat

exchanger. The results were thus very dependent on the impact of one single component about which there was not much information available, and they need to be used with care. The main source of embodied emission for both the PV and PV/T modules was the crystalline silicon solar cells. Furthermore, an analysis performed with more detailed information of production countries and transport distances instead of global data resulted in a lower value of embodied emissions from the PV/T module, indicating that the first results are on the conservative side.

A case study was used to evaluate the influence of system design on the net emissions of a building (Section 6.3). If was found that a high module efficiency was more important than low embodied emissions in order to achieve a high total emissions reduction. It was therefore not the system with the shortest greenhouse gas payback time (GPBT) that resulted in the largest total reduction in emission during its lifetime, but the system with the highest total energy output. The highest energy output was furthermore a result of the system size rather than the performance of the modules. It was therefore not the systems with the best performance in terms of kWh output per installed kW_p that reached the highest total emissions reduction, but the systems with the largest total module area.

A second case study evaluated how the choice of solar energy technology affected the net emissions of the building (Section 6.4). The building with a PV/T system had the highest embodied emissions due to the higher embodied emissions of the PV/T modules compared to the other two technologies. As the case study on energy performance in Section 5.3 showed, the primary energy output was highest for the PV/T system. However, the output was not high enough to make up for the higher embodied emissions. None of the three studied systems in this case study enabled the building to reach a net zero emission balance. The building with only PV modules came closest, and the building with PV/T modules was farthest from a balance.

The GPBT of the modules and systems were determined in both case studies. The GPBT depends on the design of the installation and on the value of the generated electricity, which in this case was related to the choice of electricity grid factor. All GPBTs were lower than the expected lifetime of the modules, which means that the solar installations would result in a net reduction in greenhouse gas emissions over their lifetime. However, the GPBT of PV/T modules were slightly longer than that of PV modules and solar thermal collectors.

As the case studies presented in this thesis have shown, the choice of grid emission factor has a large impact on the results. Two different factors have been used to a represent a range of plausible scenarios: the current EU grid mix (0.361 kg CO_{2eq}/kWh) and average grid mix from the ultra-green scenario for the European energy system which was developed in the ZEB Centre (0.132 kg CO_{2eq}/kWh during 60 years or 0.238 kg CO_{2eq}/kWh during 30 years). The positive impact of using renewable energy systems is much higher with a higher grid impact factor. In a grid with higher associated emissions, every kWh provided by solar energy off-sets more greenhouse gas emissions than a kWh in a grid with lower associated emissions. In a grid with a high emission factor, it would therefore be considered more “acceptable” to install a solar energy system with high embodied emissions.

Another result from both case studies was that it is very demanding to reach a zero emission balance at the ZEB-OM ambition level (including operation and materials, see Section 2.2.1). Only four out of the 19 systems studied reached a balance. All of these systems included modules with non-optimal orientations, even north facing modules. The GPBT time of the north facing modules was up to 23.9 years, which must be regarded as a poor "investment" of embodied emissions considering an assumed system lifetime of 30 years. The ultimate goal of reaching a net ZEB-OM balance can therefore be questioned: is it necessary to reach zero emissions if it means that the embodied emissions of the building are unnecessarily high? A smaller solar energy system could have nearly reached a zero emission balance, but with less environmental impact in the production phase. Another point is that *all* buildings perhaps do not have to reach a zero emission balance; some buildings have high energy demand and little available space, while others have low energy demand but large available areas. It might therefore be more useful to look at zero emission balance from a neighbourhood perspective, something which is getting more and more focus in the research community.

The main conclusions from the studies of environmental impact are:

- The studied generic PV/T module was found to have 30% higher embodied emissions than a modern PV module. The difference in embodied emissions was due in most part to the use of a stainless steel heat exchanger in the PV/T module. The embodied emissions of the PV/T module were, however, lower than values found in published literature.
- The modules with the lowest greenhouse gas payback times did not result in the largest total reduction in emissions. High efficiency was found to be more important than low embodied emissions in order to achieve this.
- No benefit of PV/T modules was found in the analysed case study compared to solar thermal collector and/or PV modules in terms of their contribution to reduced greenhouse gas emissions. This result from a single study can, however, not be generalised for other cases.
- The choice of grid emission factor had a significant impact on the results. The emission factors for energy from all the solar energy systems, regardless of technology, were well below the emission factor of the European grid, also in the optimistic ZEB ultra-green scenario for the European energy system. This means that 1 kWh of energy from the solar energy systems is the source of less emissions than 1 kWh of energy from the grid. The emission factors of the solar energy systems were, however, slightly higher than those for the current Norwegian electricity grid.
- The solar energy systems accounted for 22-35% of the total embodied emissions of the studied buildings. This result was in line with earlier findings in the ZEB Centre.
- The embodied emissions of BOS (balance of system) were found not to be negligible, as they account for up to 15% of the embodied emissions of the solar energy system.

7.4 Main research question

What is the potential of PV/T systems to minimize the life cycle greenhouse gas emissions a residential building?

In the presented studies, the potential of PV/T systems to fulfil the energy demand of a zero emission residential building is not significantly larger or significantly smaller than that of other solar energy technologies.

No clear benefit of cooling the PV cells was found in the simulations; the electricity output of the PV/T modules was actually lower than that of a PV module with similar efficiency. Based on results from installed systems, the impact of cooling the modules is probably of greater importance in warmer climates and in systems where the focus is on high electricity yield during summer.

The thermal output of PV/T modules is in general useful only in an energy systems where low temperature heat is valuable, and the system design is therefore of great importance to achieve good performance of PV/T modules. The combination of PV/T modules and ground source heat pumps showed potential to increase the efficiency of a building's energy system compared to other solar energy technologies, especially when PV/T modules were installed on the source side of the heat pump. However, the studies also showed that it is a complex task to design such as system, and the energy demand required to operate it can be higher than the gains, if not properly designed.

In terms of emissions, no benefit of PV/T modules were found in the case studies. The PV/T module had around 30% higher emissions than a comparable PV module, but the increase in energy output from the PV/T module was not high enough to allow for this. The lowest emission factor for the generated energy was found to be for the system with only PV modules.

The cost of PV/T modules was not investigated in this thesis. However, it can be expected that the cost of a PV/T installation will be higher than that of an installation with only PV modules. The cost of PV modules have plummeted over the last decades, along with the increase in the market and development of more efficient production methods. In addition, a PV/T system requires hydronic components which are not necessary in a PV system. The cost difference between a system with only PV/T modules and a system with PV modules and solar thermal collectors is more uncertain.

Even though all of the studied solar energy systems were the source of a high share of the embodied emissions of a building, they also contributed to a large reduction in greenhouse gas emissions over their lifetime. The generated energy from the systems was associated with significantly lower emissions than the alternative energy source, which in this case was the European electricity grid. That is, solar energy installations, PV/T systems included, contribute to reduced emissions also in a Scandinavian climate.

It was in general found to be quite difficult to reach a net zero emission balance for a building, at least when the embodied emissions of materials were included. A large solar energy installation was necessary to reach a balance, which sometimes resulted in non-optimal system

designs. Nearly zero emission buildings, or zero emission neighbourhoods, might be a more feasible goal for new buildings.

Finally, it should be taken into account that integration of renewable energy sources into the energy system will contribute to a reduction of the environmental impact of grid electricity. This reduces the embodied emissions of future products, for example solar energy modules, which are produced using energy from this grid.

7.5 Suggestions for further research

The use of PV/T systems in zero emission buildings have been studied from several perspectives in this thesis. However, it has only been possible to cover a small fraction of the potential applications within the limited scope of a Ph.D. project. Several limitations were put on the work from the start, which also limits the transferability of the results: the focus has been only on single-family residential buildings in Scandinavia, and only uncovered flat plate PV/T modules with liquid heat transfer has been analysed.

The results from the thesis, as well as from installed systems, suggests that the combination of PV/T systems and ground source heat pumps could be of interest. However, in this case there is great potential for development of the system design and the control strategy in order to reach better energy performance. Only single family buildings were studied here, but larger benefits could possibly be found for this type of system in multi-family houses or non-residential buildings, which may be a better application for PV/T systems, and where the issues of limited available roof area is of greater importance.

Only a limited study of the life cycle environmental impact of PV/T modules was presented in this thesis. More work is necessary to provide a more detailed and more reliable model of a commercially produced PV/T module. A closer cooperation with a PV/T producer could make it possible to create a more detailed model of the production chain, and to also include a more detailed assessment of the energy consumption during production.

The case studies in this thesis are based solely on simulations. There are so far few PV/T installations in Scandinavia and none in Norway, and there has been limited possibilities to find measurement data to validate the simulation results. It would therefore be of great interest to study actual installations in Scandinavia, and to be able to perform measurements over time.

The load match and grid interaction was only briefly studied in this thesis, and deserve more focus. It would also be of interest to investigate how energy storage could be used to increase the self-consumption and load match, as well as improving the economic benefit of the solar energy systems. The economics of PV/T systems compared to other alternatives should also be analysed in general.

Other possible areas for future research include different combinations of PV/T modules and heat pumps, a further study of covered PV/T modules or other PV/T technologies in addition to uncovered flat plate PV/T, and performance measurements of different PV/T installations in

Scandinavian climate. Aspects related to the technical building integration would also be of interest, such as methods for physical integration and architectural integration.

References

[1] International Energy Agency, Transition to Sustainable Buildings - Strategies and Opportunities to 2050, Directorate of Sustainable Energy Policy and Technology (SPT), Paris, France, 2013.

[2] IPCC, Core Writing Team, Climate Change 2014: Synthesis Report. Contribution of Working Groups I, II and III to the Fifth Assessment Report of the Intergovernmental Panel on Climate Change, IPCC, Geneva, Switzerland, 2013.

[3] European Parliament, Directive 2010/31/EU of the European Parliament and of the Council of 19 May 2010 on the energy performance of buildings, Directive 2010/31/EU, Brussels, 2010.

[4] Forskrift om tekniske krav til byggverk (Byggteknisk forskrift), Kommunal- og moderniseringsdepartementet/Ministry of Local Government and Modernisation FOR-2010-03-26-489, Lovdata, http://lovdata.no/dokument/SF/forskrift/2010-03-26-489, 2015.

[5] Arnstad-utvalget, Energieffektivisering av bygg. En ambisiøs og realistisk plan mot 2040 Kommunal- og moderniseringsdepartementet/Ministry of Local Government and Modernisation, 2010.

[6] A. Houlihan Wiberg, L. Georges, T.H. Dokka, M. Haase, B. Time, A.G. Lien, S. Maltha, A net zero emission concept analysis of a single-family house., Energy and Buildings, 74 (2014) 101-110.

[7] C. Good, T. Kristjansdottír, A. Houlihan Wiberg, L. Georges, A.G. Hestnes, Influence of PV technology and system design on the emission balance of a net zero emission building concept, Solar Energy, 130 (2016) 89-100.

[8] T.F. Kristjansdottir, C.S. Good, M.R. Inman, R.D. Schlanbusch, I. Andresen, Embodied greenhouse gas emissions from PV systems in Norwegian residential Zero Emission Pilot Buildings, Solar Energy, 133 (2016) 155-171.

[9] IPCC, Climate Change 2013: The Physical Science Basis. Contribution of Working Group I to the Fifth Assessment Report of the Intergovernmental Panel on Climate Change Cambridge University Press, Cambridge, United Kingdom and New York, NY, USA, 2013.

[10] L. Finocchiaro, T.H. Dokka, A. Gustavsen, +HYTTE. A versatile construction system for zero emission buildings, in: ZEMCH International Conference, Glasgow, UK, 2012.

[11] L. Georges, M. Haase, A. Houlihan Wiberg, T.F. Kristjansdottir, B. Risholt, Life cycle emissions analysis of two nZEB concepts, Building Research & Information, 43 (2015) 82-93.

[12] M.R. Inman, A. Houlihan Wiberg, Life Cycle GHG Emissions of Material Use in the Living Laboratory, Sintef Buildings and Infrastructure & Norwegian University of Science and Technology (NTNU), Oslo, Report 24-2015, 2015.

[13] Statistics Norway, Construction, housing and property, Statistics Norway,, Online, 2016.

[14] Vela Solaris AG, Polysun Simulation Software, Institut für Solartechnik SPF, Rapperswil, 2012.

[15] S.A. Klein, W.A. Beckman, J.W. Mitchell, J.A. Duffie, N.A. Duffie, T.L. Freeman, J.C. Mitchell, J.E. Braun, B.L. Evans, J.P. Kummer, R.E. Urban, A. Fiksel, J.W. Thornton, N.J. Blair, P.M. Williams, D.E. Bradley, T.P. McDowell, M. Kummert, D.A. Arias, M.J. Duffy, TRNSYS 17 - a TRaNsient SYstem Simulation program - Documentation, Solar Energy Laboratory, University of Wisconsin-Madison, 2012.

[16] H.G. Beyer, J. Bethke, A. Drews, D. Heinemann, E. Lorenz, G. Heilscher, S. Bofinger, Identification of a general model for the MPP performance of PV-modules for the application in a procedure for the performance check of grid connected systems, in: 19th European Photovoltaic Solar Energy Conference & Exhibition, Paris, France, 2004.

[17] Vela Solaris AG, Polysun Simulation Software User Manual, 2014.

[18] EN ISO 9806:2013 - Solar Energy - Solar thermal collectors - Test methods European Committee for Standardization (CEN), Brussels, Belgium, 2013.

[19] Polysun customer support, personal communication with C. Good, E-mail correspondence 2015.

[20] prNS 3031 - Calculation of energy performance of buildings - Method and data (revision for hearing), Standard Norge, Lysaker, 2015.

[21] PVsyst SA, PV-syst 5.73, Photovoltaic System Software A. Mermoud (Ed.), University of Geneva, 2011.

[22] J.A. Duffie, W.A. Beckman, Solar Engineering of Thermal Processes, Wiley, Hoboken, 2013.

[23] PVsyst SA, PVsyst Contextual Help University of Geneva, 2011.

[24] Ø. Byrkjedal, A.L. Løvholm, S. Liléo, Resource mapping of solar energy - An overview of available data in Norway, Kjeller Vindteknikk, Report KVT/OB/2013/R046, 2013.

[25] J. Remund, S.C. Müller, Solar radiation and uncertainty information of meteonorm 7, in: EU PVSEC (Eurpean PV Solar Energy Conference and Exhibition), Hamburg, Germany, 2011.

[26] V. Delisle, M. Kummert, A novel approach to compare building-integrated photovoltaics/thermal air collectors to side-by-side PV modules and solar thermal collectors, Solar Energy, 100 (2014) 50-65.

[27] T. Fujisawa, T. Tani, Annual exergy evaluation on photovoltaic-thermal hybrid collector, Solar Energy Materials and Solar Cells, 47 (1997) 135-148.

[28] M. Rommel, D. Zenhäusern, A. Baggenstos, O. Türk, S. Brunold, Application of Unglazed PVT Collectors for Domestic Hot Water Pre-heating in a Development and Testing System, Energy Procedia, 48 (2014) 638-644.

[29] O.B. Kazanci, M. Skrupskelis, P. Sevela, G.K. Pavlov, B.W. Olesen, Sustainable heating, cooling and ventilation of a plus-energy house via photovoltaic/thermal panels, Energy and Buildings, 83 (2014) 122-129.

[30] K. Vats, G.N. Tiwari, Energy and exergy analysis of a building integrated semitransparent photovoltaic thermal (BISPVT) system, Applied Energy, 96 (2012) 409-416.

[31] A. Girard, E.J. Gago, T. Muneer, G. Caceres, Higher ground source heat pump COP in a residential building through the use of solar thermal collectors, Renewable Energy, 80 (2015) 26-39.

[32] E. Bertram, J. Glembin, G. Rockendorf, Unglazed PVT collectors as additional heat source in heat pump systems with borehole heat exchanger, Energy Procedia, 30 (2012) 414-423.

[33] M. Bakker, H.A. Zondag, M.J. Elswijk, K.J. Strootman, M.J.M. Jong, Performance and costs of a roof-sized PV/thermal array combined with a ground coupled heat pump, Solar Energy, 78 (2005) 331-339.

[34] M. Canelli, E. Entchev, M. Sasso, L. Yang, M. Ghorab, Dynamic simulations of hybrid energy systems in load sharing application, Applied Thermal Engineering, 78 (2015) 315-325.

[35] E. Entchev, L. Yang, M. Ghorab, E.J. Lee, Performance analysis of a hybrid renewable microgeneration system in load sharing applications, Applied Thermal Engineering, 71 (2014) 697-704.

[36] Y. Tripanagnostopoulos, M. Souliotis, R. Battisti, A. Corrado, Energy, cost and LCA results of PV and hybrid PV/T solar systems, Progress in Photovoltaics: Research and Applications, 13 (2005) 235-250.

[37] A. Tiwari, V. Raman, G.N. Tiwari, Embodied energy analysis of hybrid photovoltaic thermal (PV/T) water collector, International Journal of Ambient Energy, 28 (2007) 181-188.

[38] R. Battisti, A. Corrado, Evaluation of technical improvements of photovoltaic systems through life cycle assessment methodology, Energy, 30 (2005) 952-967.

[39] R.H. Crawford, G.J. Treloar, R.J. Fuller, M. Bazilian, Life-cycle energy analysis of building integrated photovoltaic systems (BiPVs) with heat recovery unit, Renewable and Sustainable Energy Reviews, 10 (2006) 559-575.

[40] PRé Consultant, Simapro 8.0 Amersfoort, The Netherlands, 2015.

[41] Swiss Centre for Life Cycle Inventories, Ecoinvent database v 3.1, 2014.

[42] O. Edenhofer, Renewable energy sources and climate change mitigation: special report of the Intergovernmental Panel on Climate Change, Cambridge University Press, New York, 2012.

[43] R. Perez, M. Perez, Update 2015 - A fundamental look at the energy reserves of the planet, SHCP Solar Update, 62 (2015).

[44] Fornybar.no - Solenergi, NVE, Enova, Research Council of Norway and Innovasjon Norge, Online (access date 2016.02.29), http://www.fornybar.no/solenergi, 2016.

[45] Fraunhofer Institute for Solar Energy Systems (ISE), Photovoltaics report, 2016.

[46] K. Voss, J. Weinold, L. Vandaele, P. Lund, M.K. Tyholt, M. Santamouris, G. Mihalakakou, J.O. Lewis, W. Wangusi, S. Burton, SOLGAIN - The Contribution of Passive Solar Energy Utilization to Cover the Space Heating Demand of the European Residential Building Stock, in: 3rd ISES Europe Solar Congress, Eurosun, Copenhagen, Denmark, 2000.

[47] PVCDROM, Arizona State University Online (access date 2013.0128).

[48] R.A. Messenger, J. Ventre, Photovoltaic Systems Engineering, Third Edition, 3rd ed. ed., CRC Press, Hoboken, 2010.

[49] Solar Photovoltaic Technology, EPIA - European Photovoltaic Industry Association, Online (access date 2014.04.28), http://www.epia.org/about-us/about-photovoltaics/solar-photovoltaic-technology/, 2014.

[50] J. Nelson, The physics of solar cells, Imperial College Press, London, 2003.

[51] SMA Solar Technology AG, Performance ratio - Quailty factor for the PV plant, Report Technical Information Perfratio-UEN100810.

[52] M.C. Munari Probst, C. Roecker, Architectural integration and design of solar thermal systems, EPFL Press, Oxford, 2011.

[53] B. Thorud, S.H. Nordahl, L. Bugge, M.L. Authen, P. Bernhard, Solstrøm i Norge, KanEnergi & Multiconsult, 2011.

[54] I. Andresen, Planlegging av solvarmeanlegg for lavenergiboliger og passivhus. En introduksjon, Sintef Byggforsk, 2009.

[55] The German Solar Energy Society, Planning and installing solar thermal systems: a guide for installers, architects and engineers, James & James, London, 2005.

[56] L. Andrén, T. Persson, G. Lennermo, Handbok för kombinerade sol och biovärmesystem, 2012

[57] K. Farkas, Architectural Integration of Photovoltaics - Formal and Symbolic Aesthetics of Photovoltaics, Thesis for the degree Philosophiae Doctor, Norwegian University of Science and Technology (NTNU), Doctoral theses at NTNU, 2013:78, ISBN 978-82-471-4255-4 (printed ver.), ISBN 978-82-471-4256-1 (electronic ver.), Trondheim, 2012.

[58] B. Petter Jelle, C. Breivik, H. Drolsum Røkenes, Building integrated photovoltaic products: A state-of-the-art review and future research opportunities, Solar Energy Materials and Solar Cells, 100 (2012) 69-96.

[59] Solar District Heating - Supplying Renewable Zero-Emission Heat, www.solar-district-heating.eu.

[60] Solfangeranlegget, Online (access date 2016.03.03), http://akershusenergi.no/no/energi-varme/varmesentraler/akershus-energipark/solfangeranlegget, 2016.

[61] S. Merlet, B. Thorud, Solenergi i Norge: Status og fremtidsutsikter, in: A. Bjartnes (Ed.) Hva betyr solenergirevolusjonen?, Norsk Klimastiftelse/Norwegian Climate Foundation, 2015.

[62] European Commission, Electricity prices for domestic consumers - bi-annual data (from 2007 onwards), Eurostat, Online, 2016.

[63] Ø. Holm, National Survey Report of PV Power Applications in Norway 2014, Forskningsrådet, 2015.

[64] J. Lindahl, National Survey Report of PV Power Applications in Sweden 2014, Swedish Energy Agency, Uppsala University, 2015.

[65] Enovatillskudded - Programkriterier el-produksjon Online (access date 2016.04.03), http://www.enova.no/finansiering/privat/enovatilskuddet-/programkriterier-enovatilskuddet/programkriterier-el-produksjon-/963/2004/, 2015.

[66] Statistikk, Online (access date 2016.03), http://solenergi.no/statistikk/, 2016.

[67] International Energy Agency Solar Heating and Cooling Programme, Country Report - Norway - Status of Solar Heating/Cooling and Solar Buildings - 2014 Online, 2014.

[68] Enovatillskudded - Programkriterier solfanger Online (access date 2016.04.03), http://www.enova.no/finansiering/privat/enovatilskuddet-/programkriterier-enovatilskuddet/programkriterier-solfanger-/963/2001/, 2015.

[69] A.J. Marszal, P. Heiselberg, J.S. Bourrelle, E. Musall, K. Voss, I. Sartori, A. Napolitano, Zero Energy Building – A review of definitions and calculation methodologies, Energy and Buildings, 43 (2011) 971-979.

[70] The National Institute of Building Sciences, A Common Definition for Zero Energy Buildings, U.S.D.o. Energy, U.S. Department of Energy, 2015.

[71] I. Sartori, A. Napolitano, K. Voss, Net zero energy buildings: A consistent definition framework, Energy and Buildings, 48 (2012) 220-232.

[72] T.H. Dokka, I. Sartori, M. Tyholt, K. Lien, K. Byskov Lindberg, A Norwegian Zero Emission Building Definition, in: Passivhus Norden 2013, Gothenburg, Sweden, 2013.

[73] S.M. Fufa, R. Dahl Schlanbusch, I. Andresen, M.R. Inman, A Norwegian ZEB Definition Guideline (upcoming publication), SINTEF Building and Infrastructure Norwegian University of Science and Technology (NTNU), 2016.

[74] prEN 15603:2013 - Energy performance of buildings - Overall energy use and definition of energy ratings, European Committee for Standardization (CEN), Brussels, Belgium, 2013.

[75] T.H. Dokka, A.H. Wiberg, L. Georges, S. Mellegård, B. Time, M. Haase, M. Maltha, A.G. Lien, A zero emission concept analysis of a single family house, The Research Centre on Zero Emission Buildings, Oslo, 2013.

[76] European Committee for Standardization (CEN), Energy Performance of buildings — Module M1-x — Accompanying Technical Report on draft Overarching standard EPBD (prEN 15603), Nederlands Normalisatie-instituut, Delft, The Netherlands, Report ICS: 91.140.99, 2013.

[77] Estimated CO2 emission factors for public electricity production in EU-27, 2008, Online (access date 2016.03.14), http://www.eea.europa.eu/data-and-maps/figures/estimated-co2-emission-factors-for, 2008.

[78] I. Andresen, K. Lien, T. Berker, I. Sartori, O. Wolfgang, B. Risholt, Life time compensation of greenhouse gas emissions in Zero Emission Buildings (ZEB) – Revisiting the conversion factor for electricity (upcoming publication), SINTEF Building and Infrastructure & Norwegian University of Science and Technology (NTNU), 2016.

[79] V. Fthenakis, R. Frischknecht, M. Raugei, H.C. Kim, E. Alsema, M. Held, M. de Wild-Scholten, Methodology Guidelines on Life-Cycle Assessment of Photovoltaic Electricity, 2 ed., 2011.

[80] F.A. Peuser, K.H. Remmers, M. Schnauss, Solar Thermal Systems: Successful Planning and Construction, Beuth, 2011.

[81] I. Graabak, B.H. Bakken, N. Feilberg, Zero emission building and conversion factors between electricity consumption and emissions of greenhouse gases in a long term perspective Environmental and Climate Technologies, 13 (2014) 12-19.

[82] European Commission, Energy Roadmap 2050, Publications Office of the European Union, Report COM(2011) 885, 2012.

[83] ECF, Roadmap 2050: a practical guide to a prosperous, low-carbon Europe, European Climate Foundation, 2010.

[84] T. Lützkendorf, M. Balouktsi, Evaluation of Embodied Energy and CO2eq for Building Construction - Discussion report v 1.6, International Energy Agency Energy Conservation in Buildings and Community Systems Programme (IEA EBC) Annex 57: Evaluation of Embodied Energy and CO2eq for Building Construction, Karlsruhe Institute of Technology - KIT, 2016.

[85] EN 15978: Sustainability of construction works. Assessment of environmental performance of buildings. Calculation method, 2011.

[86] J. Salom, A.J. Marszal, J. Widén, J. Candanedo, K.B. Lindberg, Analysis of load match and grid interaction indicators in net zero energy buildings with simulated and monitored data, Applied Energy, 136 (2014) 119-131.

[87] Environmental management - Life cycle assessment - Principles and framework, 2006.

[88] H. Baumann, A.-M. Tillman, The hitch hiker's guide to LCA : an orientation in life cycle assessment methodology and application, Studentlitteratur, Lund, 2004.

[89] Environmental management - Life cycle assessment - Requirements and guidelines, 2006.

[90] J.B. Guinée, Handbook on life cycle assessment : operational guide to the ISO standards, Kluwer, Dordrecht, 2002.

[91] M. Goedkoop, M. Oele, J. Leijting, T. Ponsioen, E. Meijer, Introduction to LCA with SimaPro, 5.2 ed., PRé, 2016.

[92] Understanding Global Warming Potentials, Online (access date 2016.03.05), https://www3.epa.gov/climatechange/ghgemissions/gwps.html, 2016.

[93] J.C. Bare, P. Hofstetter, D.W. Pennington, H.A.U. De Haes, Midpoints versus endpoints: the sacrifices and benefits, The International Journal of Life Cycle Assessment, 5 (2000) 319-326.

[94] D.D. Hsu, P. O'Donoughue, V. Fthenakis, G.A. Heath, H.C. Kim, P. Sawyer, J.K. Choi, D.E. Turney, Life Cycle Greenhouse Gas Emissions of Crystalline Silicon Photovoltaic Electricity Generation: Systematic Review and Harmonization, Journal of Industrial Ecology, 16 (2012) S122-S135.

[95] R.U. Ayres, Life cycle analysis: A critique, Resources, Conservation and Recycling, 14 (1995) 199-223.

[96] G. Finnveden, M.Z. Hauschild, T. Ekvall, J. Guinée, R. Heijungs, S. Hellweg, A. Koehler, D. Pennington, S. Suh, Recent developments in Life Cycle Assessment, Journal of Environmental Management, 91 (2009) 1-21.

[97] T.T. Chow, G.N. Tiwari, C. Menezo, Hybrid solar: A review on photovoltaic and thermal power integration, International Journal of Photoenergy, 2012 (2012).

[98] X. Zhang, X. Zhao, S. Smith, J. Xu, X. Yu, Review of R&D progress and practical application of the solar photovoltaic/thermal (PV/T) technologies, Renewable and Sustainable Energy Reviews, 16 (2012) 599-617.

[99] V.V. Tyagi, S.C. Kaushik, S.K. Tyagi, Advancement in solar photovoltaic/thermal (PV/T) hybrid collector technology, Renewable and Sustainable Energy Reviews, 16 (2012) 1383-1398.

[100] M. Wolf, Performance analyses of combined heating and photovoltaic power systems for residences, Energy Conversion, 16 (1976) 79-90.

[101] E.C. Kern, Jr., M.C. Russell, Combined photovoltaic and thermal hybrid collector systems, in: 13th Photovoltaic Specialists Conference, Institute of Electrical and Electronics Engineers, Inc, Washington, D.C., 1978, pp. p. 1153-1157.

[102] M.J. O'Leary, L.D. Clements, Thermal-electric performance analysis for actively cooled, concentrating photovoltaic systems, Solar Energy, 25 (1980) 401-406.

[103] K. Sopian, K.S. Yigit, H.T. Liu, S. Kakaç, T.N. Veziroglu, Performance analysis of photovoltaic thermal air heaters, Energy Conversion and Management, 37 (1996) 1657-1670.

[104] B. Sandnes, J. Rekstad, A photovoltaic/thermal (PV/T) collector with a polymer absorber plate. Experimental study and analytical model, Solar Energy, 72 (2002) 63-73.

[105] H.A. Zondag, D.W. De Vries, W.G.J. Van Helden, R.J.C. Van Zolingen, A.A. Van Steenhoven, The thermal and electrical yield of a PV-thermal collector, Solar Energy, 72 (2002) 113-128.

[106] M. Collins, A review of PV, solar thermal, and PV/thermal collector models in TRNSYS, Report A technical report of Subtask B, 2009.

[107] M. Stegmann, E. Bertram, G. Rockendorf, S. Janβen, Model of an unglazed photovoltaic thermal collector based on standard test procedures, in: ISES World Congress, ISES - International Solar Energy Society, Kassel, Germany, 2011.

[108] Y. Tripanagnostopoulos, T. Nousia, M. Souliotis, P. Yianoulis, Hybrid photovoltaic/thermal solar systems, Solar Energy, 72 (2002) 217-234.

[109] T.T. Chow, W. He, J. Ji, An experimental study of façade-integrated photovoltaic/water-heating system, Applied Thermal Engineering, 27 (2007) 37-45.

[110] C.D. Corbin, Z.J. Zhai, Experimental and numerical investigation on thermal and electrical performance of a building integrated photovoltaic-thermal collector system, Energy and Buildings, 42 (2010) 76-82.

[111] P. Dupeyrat, C. Ménézo, S. Fortuin, Study of the thermal and electrical performances of PVT solar hot water system, Energy and Buildings, 68, Part C (2014) 751-755.

[112] J.J. Michael, I. S, R. Goic, Flat plate solar photovoltaic–thermal (PV/T) systems: A reference guide, Renewable and Sustainable Energy Reviews, 51 (2015) 62-88.

[113] H.A. Zondag, D.W. de Vries, W.G.J. van Helden, R.J.C. van Zolingen, A.A. van Steenhoven, The yield of different combined PV-thermal collector designs, Solar Energy, 74 (2003) 253-269.

[114] S. Fortuin, M. Hermann, G. Stryi-Hipp, P. Nitz, W. Platzer, Hybrid PV-thermal Collector Development: Concepts, Experiences, Results and Research Needs, Energy Procedia, 48 (2014) 37-47.

[115] M.D. Bazilian, F. Leenders, B.G.C. Van Der Ree, D. Prasad, Photovoltaic cogeneration in the built environment, Solar Energy, 71 (2001) 57-70.

[116] L. Mei, D. Infield, U. Eicker, V. Fux, Thermal modelling of a building with an integrated ventilated PV façade, Energy and Buildings, 35 (2003) 605-617.

[117] A.K. Athienitis, J. Bambara, B. O'Neill, J. Faille, A prototype photovoltaic/thermal system integrated with transpired collector, Solar Energy, 85 (2011) 139-153.

[118] The IEA SHC Task 35 - 'PV / Thermal Solar Systems', Online (access date 2012.11.20), http://www.iea-shc.org/task35/.

[119] P. Affolter, W. Eisenmann, H. Fechner , M. Rommel , A. Schaap, H. Sörensen, Y. Tripanagnostopoulos, PVT Roadmap - A European guide for the development and market introduction of PV-Thermal technology, 2006.

[120] F. Ille, M. Adam, R. Radosavljevic, H.P. Wirth, Market and simulation analysis of PVT applications for the determination of new PVT test procedures, in: E. Frank, P. Papillon (Eds.) Eurosun 2014, ISES, Aix-les-Bains, France, 2014.

[121] PV/Thermal; Solar Power Wall - Electricity + Heating, Online (access date 2016.03.17), http://solarwall.com/en/products/pvthermal.php, 2016.

[122] O.Z. Sharaf, M.F. Orhan, Concentrated photovoltaic thermal (CPVT) solar collector systems: Part II – Implemented systems, performance assessment, and future directions, Renewable and Sustainable Energy Reviews, 50 (2015) 1566-1633.

[123] Zenith Solar, Z20 Product Description, Online, 2016.

[124] Absolicon Solar Collector AB, Online (access date 2016.03.17), http://www.absolicon.com/, 2016.

[125] The MCT panel, Online (access date 2016.03.19), http://chromasun.com/MCT.html, 2013.

[126] C. Williams, of Naked Energy, personal communication with C. Good, 2016.

[127] T.N. Anderson, M. Duke, G.L. Morrison, J.K. Carson, Performance of a building integrated photovoltaic/thermal (BIPVT) solar collector, Solar Energy, 83 (2009) 445-455.

[128] H. Davidsson, B. Perers, B. Karlsson, System analysis of a multifunctional PV/T hybrid solar window, Solar Energy, 86 (2012) 903-910.

[129] H. Davidsson, B. Perers, B. Karlsson, Performance of a multifunctional PV/T hybrid solar window, Solar Energy, 84 (2010) 365-372.

[130] J.S. Coventry, K. Lovegrove, Development of an approach to compare the 'value' of electrical and thermal output from a domestic PV/thermal system, Solar Energy, 75 (2003) 63-72.

[131] Solar Keymark Network, Specific CEN Keymark Scheme Rules for Solar Thermal Product version 21.00, CEN Certification, 2013.

[132] 2-in-1 solar, Online (access date 2016.03.20), https://dualsun.fr/en/product/2-in-1-solar/.

[133] Wiosun PV-Therm (product datasheet), Online, http://www.solarzentrum-wiosun.com/products/pv-therm/principle-infos, 2014.

[134] Meyer Burger Group, Building Integrated Photovoltaic PV and thermal hybrid systems (product presentation), 2014.

[135] Volther hybrid collectors (producer datasheet), Online, http://www.solimpeks.com/pv-t-hybrid-solar-collectors/, 2014.

[136] Hybrid - The intelligent combination of solar thermal energy and photovoltaics (product datasheet), Online, http://energysystems.meyerburger.com/en/products/hybrid/, 2014.

[137] PA-ID GmbH, 2Power - Power and Warmth - One module (product brochure), Online, 2012.

[138] IEA SHC Task 35, Overview of PV/T products and projects, 2008.

[139] Conserval Engineering Inc., AIM associates, 2004.

[140] Solimpeks Energy Corp, Case studies of Volther hybrid collector.

[141] Case Studies Hybrid PV-Thermal, Online (access date 2016.03.19), http://solimpeks.com.au/downloads/Solimpeks%20Case%20Studies;%20Hybrid%20PV-Thermal.pdf.

[142] A. Morgan, Can Solar PV-T protect the UK from energy black-out?, Greener Business, Excel Publishing, Online, 2014.

[143] Domestic Renewable Heat Incentive, Ofgem Online (access date 2014.05.10), https://www.ofgem.gov.uk/environmental-programmes/domestic-renewable-heat-incentive, 2014.

[144] DualSun, Suivi de performances des installations DualSun, 2014.

[145] An off grid solar installation at the Arpont Chalet, Online (access date 2016.03.18), https://dualsun.fr/en/2014/12/off-grid-solar-installation-arpont-chalet/, 2014.

[146] T. Kinert, personal communication with C. Good, (Email and phone.), 2016.

[147] PV-Therm references, Online (access date 2016.03.18), http://www.solarzentrum-wiosun.com/products/references/pv-therm, 2016.

[148] J. Ahlgren, Solhybridteknik - i kombination med värmepumpar som är kopplade mot ett borrhåls- eller markvärmelager., Energiförbättring Väst AB, Mölnlycke, Sweden, Report Report 2014:03, 2014.

[149] M. Rommel, Technical feasibility of the PV-T concept, SPF - Institut für Solartechnik, Eurosun 2014 Workshop PVT, 2014.

[150] Meyer Burger Group, Arealüberbauung Suurstoffi Rotkreuz: Wirtschaftlich, CO2-neutral, ganzheitlich, Nachhaltig Bauen, 2014, pp. 34.

[151] H. Leibundgut, The Sol2ergie concept, Presentation at FutureBuilt breakfast seminar, 2013.

[152] Energie/Concept énergétique, Online (access date 06.10.2014), http://wohnenimoberfeld.ch/web/rubriken/energie, 2014.

[153] M. Valle, Her installeres Norges første hybrid mellom solcelle og solfangere, Teknisk Ukeblad, Teknisk Ukeblad Media AS, Online, 2015.

[154] Absolicon, Local Hospital Härnösand, 2010.

[155] New Solar Technology Deployed at the UA Tech Park's Solar Zone Gains Momentum, Tech Parks Arizona, https://techparks.arizona.edu/new-solar-technology-deployed-ua-tech-park's-solar-zone-gains-momentum, 2013.

[156] Photovoltaic Geographical Information System (PVGIS), European Commission, Joint Research Centre, Online (access date 2013.01.31).

[157] The German Solar Energy Society, Planning and installing photovoltaic systems: a guide for installers, architects and engineers, Earthscan, London, 2013.

[158] B.A. Fladen, E. Sandnes, Endringer i kontrollforskriften vedrørende plusskundeordningen - Oppsummering av høringsuttalelser og endelig forskriftstekst, Norges Energi- og Vassdragsdirektorat (NVE)/The Norwegian Water Resources and Energy Directorate, Report 47-2016, 2016.

[159] Projekteringsverktyg - Moduler och cellteknologi, Energiforsk, Online (access date 2016.03.30), http://www.solelprogrammet.se/Projekteringsverktyg/Moduler/.

[160] The IEA SHC Task 44 - 'Solar and Heat Pump Systems', Online (access date 2016.03.31), http://task44.iea-shc.org/.

[161] K. Ochsner, Geothermal Heat Pumps - A Guide for Planning & Installing, Earthscan London, UK, 2008.

[162] CIBSE, Ground Source Heat Pumps - CIBSE TM51: 2013, CIBSE.

[163] Energimyndigheten/Swedish Energy Agency, Luftluftvärmepumpar 2009-2013 Online, 2014.

[164] Energimyndigheten/Swedish Energy Agency, Bergvärmepumpar Online, 2014.

[165] S. Braungardt, D. Günther, M. Miara, J.W. Wapler, W. Weßing, Electrically driven heat pumps - Latest results from research and field tests, FIZ Karlsruhe GmbH · Leibniz Institute Eggenstein-Leopoldshafen, Germany, Report 1/2013, 2013.

[166] E. Kjellsson, G. Hellström, B. Perers, Optimization of systems with the combination of ground-source heat pump and solar collectors in dwellings, Energy, 35 (2010) 2667-2673.

[167] D. Browne, personal communication with C. Good, E-mail, 2016.

[168] M. Adam, H.P. Wirth, R. Radosavljevic, PVT-Marketsubersikt, 2014.

[169] M.R. Inman, The Living Lab Pilot Project: A Life Cycle Assessment, Thesis for the degree Master of Science, Norwegian University of Science and Technology (NTNU), Trondheim, 2015.

[170] NS 3700 - Criteria for passive houses and low energy houses - Residential buildings, Standard Norge, Lysaker, 2010.

[171] Programbyggene ANS, SIMIEN, SIMulation of Indoor climate and ENergy use (Version 5.0.14), 2012.

[172] L. Finocchiaro, F. Goia, S. Grynning, A. Gustavsen, The ZEB Living Lab: a multi-purpose experimental facility, in: Gent Expert Meeting, Ghent University, Belgium, 2014.

[173] F. Goia, L. Finocchiaro, A. Gustavsen, The ZEB Living Laboratory at the Norwegian University of Science and Technology: a zero emission house for engineering and social science experiments, in: 7th Passivhus Norden Copenhagen, 2015.

[174] K. Kramer, H. Helmers, The interaction of standards and innovation: Hybrid photovoltaic–thermal collectors, Solar Energy, 98, Part C (2013) 434-439.

[175] PRé Consultant, Simapro 7.3 Amersfoort, The Netherlands, 2013.

[176] Y. Tripanagnostopoulos, M. Souliotis, R. Battisti, A. Corrado, Performance, cost and life-cycle assessment study of hybrid PVT/AIR solar systems, Progress in Photovoltaics: Research and Applications, 14 (2006) 65-76.

[177] T.T. Chow, J. Ji, Environmental life-cycle analysis of hybrid solar photovoltaic/thermal systems for use in Hong Kong, International Journal of Photoenergy, 2012 (2012).

[178] D. Kamthania, G.N. Tiwari, Energy metrics analysis of semi-transparent hybrid PVT double pass facade considering various silicon and non-silicon based PV module Hyphen is accepted, Solar Energy, 100 (2014) 124-140.

[179] S. Agrawal, G.N. Tiwari, Exergoeconomic analysis of glazed hybrid photovoltaic thermal module air collector, Solar Energy, 86 (2012) 2826-2838.

[180] M. Stucki, N. Jungbluth, Update of the Life Cycle Inventories of Solar Collectors, ESU-services Ltd., Uster, Switzerland, 2012.

[181] C. Reich-Weiser, D. Dornfeld, S. Horne, Greenhouse Gas Return on Investment: A New Metric for Energy Technology, UC Berkeley: Laboratory for Manufacturing and Sustainability, 2008.

[182] PV/T producer A, personal communication with C. Good, (Information on material quanitites and country of production for PVT module A), 2015.

[183] PV/T producer B, personal communication with C. Good, (Information on material quanitites, production methods and energy demand of PVT module B), 2015.

[184] REC Peak Energy Series, 2014.

[185] R. Frischknecht, R. Itten, P. Sinha, M. de Wild-Sholten, J. Zhang, V. Fthenakis, H.C. Kim, M. Raguei, M. Stucki, Life Cycle Inventories and Life Cycle Assessment of Photovoltaic Systems, 2 ed., Report T12-04:2015, 2015.

[186] J. Peng, L. Lu, H. Yang, Review on life cycle assessment of energy payback and greenhouse gas emission of solar photovoltaic systems, Renewable and Sustainable Energy Reviews, 19 (2013) 255-274.

[187] D. Yue, F. You, S.B. Darling, Domestic and overseas manufacturing scenarios of silicon-based photovoltaics: Life cycle energy and environmental comparative analysis, Solar Energy, 105 (2014) 669-678.

[188] Meteotest, Meteonorm Database, 2009.

[189] M.J. de Wild-Scholten, Energy payback time and carbon footprint of commercial photovoltaic systems, Solar Energy Materials and Solar Cells, 119 (2013) 296-305.

[190] Swiss Centre for Life Cycle Inventories, Ecoinvent database v 2.2, 2013.

[191] V. Fthenakis, R. Betita, M. Shields, R. Vinje, J. Blunden, Life cycle analysis of high-performance monocrystalline silicon photovoltaic systems: energy payback times and net energy production, in: 27th European Photovoltaic Solar Energy Conference and Exhibition, Frankfurt, germany, 2012.

Appendix A: Life cycle inventories

Note: All values are default allocation unit from Ecoinvent 3.1, extracted using Simapro 8, unless otherwise specified.

Table A.1. Inventory and global warming potential for the generic PV/T module with global market processes. Values are shown for 1 m^2 module. The different electricity, heat, and waste treatment values have been summarized in one value each.

Component	Amount	Unit	Ecoinvent process	Global warming potential
				kg CO_{2eq}/m^2
Aluminium frame	0.4	kg	Aluminium alloy, AlMg3 (GLO), market for	2.86
Backsheet, polyvinylflouride	0.1	kg	Polyvinylfluoride, film (GLO), market for	2.78
Backsheet, polyethylene terephthalate	0.4	kg	Polyethylene terephthalate, granulate, amorphous (GLO), market for	1.26
Wire drawing	0.1	kg	Wire drawing, copper (GLO), market for	0.08
Tempering of glass	8.1	kg	Tempering, flat glass (GLO), market for	1.43
Etylacetat (auxiliary material)	1.6E-03	kg	Vinyl acetate (GLO), market for	0.00
Packaging	1.1	kg	Corrugated board box (GLO), market for corrugated board box	1.24
Lubricating oil	1.6E-03	kg	Lubricating oil (GLO), market for	0.00
Copper for wires	0.1	kg	Copper (GLO), market for	0.62
Brazing solder	8.8E-03	kg	Brazing solder, cadmium free (GLO), market for	0.05
Solar glass	8.1	kg	Solar glass, low-iron (GLO), market for	8.90
Cleaning fluid	1.3E-02	kg	Acetone, liquid (GLO), market for	0.03
Photovoltaic cells, mono-Si	0.7	m2	Photovoltaic cell, single-Si wafer (GLO), market for	160.02
Silicone	0.1	kg	Silicone product (GLO), market for	0.40
Soldering flux	8.1E-03	kg	1-propanol (GLO), market for	0.04
Nickel for wire plating	1.6E-04	kg	Nickel, 99.5% (GLO), market for	0.00
Factory	4.0E-06	p	Photovoltaic panel factory (GLO), market for	0.86
Junction box (plastic)	0.2	kg	Glass fibre reinforced plastic, polyamide, injection moulded (GLO), market for	1.71

(Table A.1 continued)

Methanol (auxiliary material)	2.2E-03	kg	Methanol (GLO), market for	0.00
Lamination material (EVA)	2.5	kg	Ethylvinylacetate, foil (GLO), market for	7.39
Water	21.3	kg	Processes for different countries	0.01
Heat exchanger (stainless steel)	9.2	kg	Steel, chromium steel 18/8, hot rolled (GLO), market for	43.65
Insulation (polystyrene)	1.1	kg	Polystyrene foam slab (GLO), market for	4.48
Piping (stainless steel)	0.1	kg	Chromium steel pipe (GLO), market for	0.45
Welding of heat exchanger	5.3	m	Welding, arc, steel (RER)| processing | Alloc Def, U	0.90
Electricity	4.7	kWh	Processes for different countries	2.44
Heat	4.9	MJ	Processes for different countries	0.34
Waste treatment	-	-	Processes for different materials	0.85
Total				243
Heat transfer fluid (water)	4.7	kg	Water, completely softened, from decarbonised water, at user (GLO), market for	0.00
Heat transfer fluid (glycol)	4.9	kg	Propylene glycol, liquid (GLO), market for	4.63
Waste treatment	-	-	Processes for different materials	3.34
Total (with heat transfer fluid)				250

Table A.2. Inventory and global warming potential for the PV/T A module with country specific information. Values are shown for 1 m^2 module. The different electricity, heat, and waste treatment values have been summarized in one value each.

Component	Amount	Unit	Ecoinvent process	Global warming potential
				kg CO_{2eq}/m^2
Aluminium frame	0.4	kg	Aluminium alloy, AlMg3 (RER), production	2.39
Backsheet, polyvinylflouride	0.1	kg	Polyvinylfluoride, film (GLO), market for	2.78
Backsheet, polyethylene terephthalate	0.4	kg	Polyethylene terephthalate, granulate, amorphous (RER), production	1.20
Wire drawing	0.1	kg	Wire drawing, copper (GLO), market for	0.08
Tempering of glass	5.0	kg	Tempering, flat glass (RER), processing	1.04
Etylacetat (auxiliary material)	1.6E-03	kg	Vinyl acetate (GLO), market for	0.00
Packaging	1.1	kg	Corrugated board box (GLO), market for	1.24
Lubricating oil	1.6E-03	kg	Lubricating oil (GLO), market for	0.00
Copper for wires	0.1	kg	Copper (GLO), market for	0.62
Brazing solder	8.8E-03	kg	Brazing solder, cadmium free (GLO), market for	0.05
Solar glass	5.0	kg	Solar glass, low-iron (RER), production	5.18
Cleaning fluid	1.3E-02	kg	Acetone, liquid (GLO), market for	0.03
Photovoltaic cells, mono-Si	0.7	m2	Photovoltaic cell, single-Si wafer (RER), production	154.77
Silicone	1.2E-01	kg	Silicone product (GLO), market for	0.40
Soldering flux	8.1E-03	kg	1-propanol (GLO), market for	0.04
Nickel for wire plating	1.6E-04	kg	Nickel, 99.5% (GLO), market for	0.00
Factory	4.0E-06	p	Photovoltaic panel factory (GLO), market for	0.86
Junction box (plastic)	0.2	kg	Glass fibre reinforced plastic, polyamide, injection moulded (GLO), market for	1.71
Methanol (auxiliary material)	2.2E-03	kg	Methanol (GLO), market for	0.00

(Table A.2 continued)

Lamination material (EVA)	3.0	kg	Ethylvinylacetate, foil (GLO), market for	8.87
Water	21.3	kg	Processes for different countries	0.01
Heat exchanger (stainless steel)	9.2	kg	Steel, chromium steel 18/8, hot rolled (RER)| production | Alloc Def, U	43.65
Insulation (polystyrene)	1.1	kg	Polystyrene foam slab (GLO), market for	4.48
Piping (stainless steel)	0.1	kg	Chromium steel pipe (GLO), market for	0.45
Welding of heat exchanger	5.3	m	Welding, arc, steel (RER), processing	0.92
Transport	131.7	tkm	Processes for different transport modes	3.87
Electricity	4.7	kWh	Electricity, medium voltage (FR), market for	0.52
Heat	4.9	MJ	Heat, district or industrial, natural gas (Europe without Switzerland)| market for heat, district or industrial, natural gas	0.34
Waste treatment	-	-	Processes for different materials	0.85
Total				236
Heat transfer fluid (water)	4.7	kg	Water, completely softened, from decarbonised water, at user (GLO), market for	0.00
Heat transfer fluid (glycol)	4.9	kg	Propylene glycol, liquid (GLO), market for	4.63
Waste treatment	-	-	Processes for different materials	3.34
Total (with heat transfer fluid)				243

Table A.3. Inventory and global warming potential for updated PV module (updated from Ecoinvent process "Photovoltaic panel, single-Si wafer (RER), production"). Values are shown for 1 m^2 module. The different electricity, heat, and waste treatment values have been summarized in one value each.

Component	Amount	Unit	Ecoinvent process	Global warming potential
				kg CO_{2eq}/m^2
Aluminium frame	0.4	kg	Aluminium alloy, AlMg3 (GLO), market for	2.86
Backsheet, polyvinylflouride	0.1	kg	Polyvinylfluoride, film (GLO), market for	2.45
Backsheet, polyethylene terephthalate	0.4	kg	Polyethylene terephthalate, granulate, amorphous (GLO), market for	1.11
Wire drawing	0.1	kg	Wire drawing, copper (GLO), market for	0.08
Tempering of glass	5.6	kg	Tempering, flat glass (GLO), market for	1.43
Etylacetat (auxiliary material)	1.6E-03	kg	Vinyl acetate (GLO), market for	0.00
Packaging	1.1	kg	Corrugated board box (GLO)| market for corrugated board box | Alloc Def, U	1.24
Lubricating oil	1.6E-03	kg	Lubricating oil (GLO), market for	0.00
Copper for wires	0.1	kg	Copper (GLO), market for	0.62
Brazing solder	8.8E-03	kg	Brazing solder, cadmium free (GLO), market for	0.05
Solar glass	5.6	kg	Solar glass, low-iron (GLO), market for	8.90
Cleaning fluid	1.3E-02	kg	Acetone, liquid (GLO), market for	0.03
Photovoltaic cells, mono-Si	0.7	m2	Photovoltaic cell, single-Si wafer (GLO), market for	160.02
Silicone	1.2E-01	kg	Silicone product (GLO), market for	0.40
Soldering flux	8.1E-03	kg	1-propanol (GLO), market for	0.04
Nickel for wire plating	1.6E-04	kg	Nickel, 99.5% (GLO), market for	0.00
Factory	4.0E-06	p	Photovoltaic panel factory (GLO), market for	0.86
Junction box (plastic)	0.2	kg	Glass fibre reinforced plastic, polyamide, injection moulded (GLO), market for	1.71
Methanol (auxiliary material)	2.2E-03	kg	Methanol (GLO), market for	0.00

(Table A.3 continued)

Lamination material (EVA)	1.0	kg	Ethylvinylacetate, foil (GLO), market for	2.95
Water	21.3	kg	Processes for different countries	0.01
Electricity	4.7	kWh	Processes for different countries	2.44
Heat	4.9	MJ	Processes for different countries	0.34
Waste treatment	-	-	Processes for different materials	0.85
Total				188

Table A.4. Inventory and global warming potential for the solar thermal collector model "Flat plate solar collector, Cu absorber [RoW], production" in Ecoinvent. Values are shown for 1 m^2 module. The different electricity and waste treatment values have been summarized in one value each.

Component	**Amount**	**Unit**	**Ecoinvent process**	**Global warming potential**
				kg CO_{2eq}/m^2
Silicone	0.1	kg	Silicone product (GLO), market for	0.19
Water	1.4	kg	Water, completely softened, from decarbonised water, at user (GLO), market for	0.00
Propylene glycol	1.0	kg	Propylene glycol, liquid (GLO), market for	4.63
Brazing solder	0.0	kg	Brazing solder, cadmium free (GLO), market for	0.02
Sheet rolling, copper	2.8	kg	Sheet rolling, copper (GLO), market for	1.46
Packaging	3.7	kg	Corrugated board box (GLO), market for corrugated board box	4.17
Rubber	0.7	kg	Synthetic rubber (GLO), market for	2.25
Solar collector factory	0.0	p	Solar collector factory (GLO), market for	0.32
Insulation	2.4	kg	Rock wool, packed (GLO), market for	3.60
Anti-reflex coating	1.0	m2	Anti-reflex-coating, etching, solar glass (GLO), market for	1.71
Copper	2.8	kg	Copper (GLO), market for	15.41
Aluminium	3.9	kg	Aluminium, wrought alloy (GLO), market for	60.99
Stainless steel	4.1	kg	Steel, chromium steel 18/8, hot rolled (GLO), market for	19.55
Selective coating	1.0	m2	Selective coat, copper sheet, black chrome (GLO), market for	2.58
Solar glass	9.1	kg	Solar glass, low-iron (GLO), market for	10.07
Solder	0.1	kg	Soft solder, Sn97Cu3 (GLO), market for	1.19
Tap water	9.4	kg	Processes for different countries	0.01
Electricity, medium voltage	1.2	kWh	Processes for different countries	0.89
Waste treatment	-	-	Processes for different materials	3.01
Total				132

Table A.5. Inventory and global warming potential for the electric BOS. Values are shown for one unit of BOS, i.e. the components required for one system on Living Lab. The electric BOS for the longer cable length is shown.

Component	**Amount**	**Unit**	**Lifetime**	**Total amount**	**Unit**	**Ecoinvent process**	**Global warming potential (total)**
			years				*kg CO_{2eq}*
Inverter, 2 pcs	52	kg	15	104	kg	Inverter, 2.5kW (GLO) *The weight of the 2.5 kW inverter in the original Ecoinvent process is 18 kg. It has been scaled by weight which results in 2.81 pcs of inverter per 15 years.*	1163.85
Power cables	175	m	30	175	m	Cable, three-conductor cable (GLO)	785.59
Connectors	0.16	kg	30	0.16	kg	Electric connector, wire clamp (GLO)	2.02
Total							1951

Table A.6. Inventory and embodied emissions for the hydronic BOS for System 5 (solar thermal collectors and PV modules). Values are shown for one unit of BOS, i.e. the components required for one system on Living Lab.

Component	**Amount**	**Unit**	**Lifetime**	**Total amount**	**Unit**	**Ecoinvent process**	**Global warming potential (total)**
			years				*kg CO_{2eq}*
Piping	5.7	kg	30	5.7	kg	Copper (GLO), market for	31.23
Piping insulation	3.4	kg	30	3.4	kg	Tube insulation, elastomere (GLO), market for	16.80
Piping coating	0.4	kg	30	0.4	kg	Packaging film, low density polyethylene (GLO), market for	1.10
Expansion vessel	1	Pc	30	2	pc	Expansion vessel, 25l (GLO), market for	23.49
Circulation pump	2	pc	15	4	pc	Pump, 40W (GLO), market for	34.62
Glycol (heat transfer fluid, 35%)	0.8	kg	10	2.5	kg	Propylene glycol, liquid (GLO), market for	11.64
Water (heat transfer fluid, 65%)	1.9	kg	10	5.8	kg	Water, deionised, from tap water, at user (GLO), market for	0.01
Total							119

Table A.7. Inventory and embodied emissions for the hydronic BOS for System 7 (PV/T modules). Values are shown for one unit of BOS, i.e. the components required for one system on Living Lab.

Component	**Amount**	**Unit**	**Lifetime**	**Total amount**	**Unit**	**Ecoinvent process**	**Global warming potential (total)**
			years				*kg CO_{2eq}*
Piping	124.2	kg	30	124.2	kg	Copper (GLO), market for	673.82
Piping insulation	5 6.5	kg	30	56.5	kg	Tube insulation, elastomere (GLO), market for	273.86
Piping coating	3.8	kg	30	3.8	kg	Packaging film, low density polyethylene (GLO), market for	11.07
Expansion vessel	1	Pc	30	2	pc	Expansion vessel, 25l (GLO), market for	23.49
Circulation pump	2	pc	15	4	pc	Pump, 40W (GLO), market for	34.62
Glycol (heat transfer fluid, 35%)	36.2	kg	10	36.2	kg	Propylene glycol, liquid (GLO), market for	497.46
Water (heat transfer fluid, 65%)	64.5	kg	10	64.5	kg	Water, deionised, from tap water, at user (GLO), market for	0.30
Total							1515

Table A.8. Inventory and embodied emissions for the horizontal ground collector. Values are shown for one unit of horizontal collector, i.e. the components required for one system on Living Lab.

Component	**Amount**	**Unit**	**Lifetime**	**Total amount**	**Unit**	**Ecoinvent process**	**Global warming potential (total)**
			years				*kg CO_{2eq}*
Piping	56.0	kg	30	56.0	kg	Polyethylene, high density, granulate (GLO), market for	115.09
Insulation (inlet/outlet)	1.1	kg	30	1.1	kg	Tube insulation, elastomere (GLO), market for	5.39
Glycol (heat transfer fluid, 35%)	75.8	kg	10	227.3	kg	Propylene glycol, liquid (GLO)| market for	1041.34
Water (heat transfer fluid, 65%)	134.0	kg	10	402.0	kg	Water, deionised, from tap water, at user (GLO) market for	0.63
Digging	157.5	m3	-	157.5	m3	Excavation, hydraulic digger (RER), processing	86.65
Total							1249

Table A.9. Inventory and embodied emissions for the auxiliary energy system. Values are shown for one unit of auxiliary energy system, i.e. the components required for one system on Living Lab.

Component	**Amount**	**Unit**	**Lifetime**	**Total amount**	**Unit**	**Ecoinvent process**	**Global warming potential (total)**
			years				*kg CO_{2eq}*
Storage tank, 400 l	0.96	pc	30	0.96	pc	Hot water tank, 600l (GLO), market for *Scaled by extrapolation factor (0.96 for 600l to 400l) from Stucki and Jungbluth [180].*	779.25
Heat pump, 3.2 kW	0.83	pc	15	1.66	pc	Heat pump, brine-water, 10 kW (GLO) market for *25% of the impact of the heat pump is scaled from 10 kW to 3.5 kW, resulting in a scaling factor of 1 pc 3.5 kW heat pump = 0.83 pc 10 kW heat pump.*	2905.62
Horizontal ground collector	1	pc	30	1	pc	*See Table A.8 for details.*	1249.10
Piping	1.0	kg	30	1.0	kg	Copper (GLO), market for	5.49
Piping insulation	0.6	kg	30	0.6	kg	Tube insulation, elastomere (GLO), market for	2.95
Piping coating	0.1	kg	30	0.1	kg	Packaging film, low density polyethylene (GLO), market for	0.19
Circulation pump	1	pc	15	2	pc	Pump, 40W (GLO), market for	17.31
Glycol (heat transfer fluid, 35%)	0.2	kg	10	0.642	kg	Propylene glycol, liquid (GLO), market for	2.94
Water (heat transfer fluid, 65%)	0.4	kg	10	1.134	kg	Water, deionised, from tap water, at user (GLO), market for	0.00
Total							4963

Appendix B: Papers

Paper I

Good, C., Chen, J., Dai, Y., & Hestnes, A. G. (2015). *Hybrid Photovoltaic-thermal Systems in Buildings – A Review.* Energy Procedia, 70(0), 683-690. doi:http://dx.doi.org/10.1016/j.egypro.2015.02.176.

Presented at SHC Conference 2014 in Beijing.

Paper II

Good, C., Andresen, I., & Hestnes, A. G. (2015*). Solar energy for net zero energy buildings – A comparison between solar thermal, PV and photovoltaic–thermal (PV/T) systems.* Solar Energy, 122, 986-996. doi:http://dx.doi.org/10.1016/j.solener.2015.10.013

Previously presented at CISBAT 2015, Lausanne, Switzerland, with the same title.

Paper III

Good, C. (2013). *Influence of system lifetime on environmental impact assessments of photovoltaic systems in buildings.* Presented at the Young Researcher Forum at CESB13, Prague.

Paper IV

Good, C. (2016*). Environmental impact assessments of hybrid photovoltaic–thermal (PV/T) systems – A review*. Renewable and Sustainable Energy Reviews, 55, 234-239. doi:http://dx.doi.org/10.1016/j.rser.2015.10.156

Paper V

Good, C., Kristjansdottir, T. F., Houlihan Wiberg, A., Georges, L., & Hestnes, A. G. (2015). *Influence of PV technology and system design on the emission balance of a net zero emission building concept.* Solar Energy, 130, 89-100. doi:http://dx.doi.org/10.1016/j.solener.2016.01.038.

Previously presented at Eurosun 2014, Aix-les-Bains, France, with the title "A comparative study of different PV installations for a Norwegian net zero emission building concept".

Paper VI

Kristjansdottir, T.F., Good, C., Inman, M.R., Dahl Schlanbusch, R., Andresen, I (2016). *Embodied greenhouse gas emissions from PV systems in Norwegian residential Zero Emission Pilot Buildings.* Solar Energy, 133, 155-171. doi:http://dx.doi.org/10.1016/j.solener.2016.03.06

Paper I

Good, C., Chen, J., Dai, Y., & Hestnes, A. G. (2015). *Hybrid Photovoltaic-thermal Systems in Buildings – A Review.* Energy Procedia, 70(0), 683-690.
doi:http://dx.doi.org/10.1016/j.egypro.2015.02.176.

Presented at SHC Conference 2014 in Beijing.

Available online at www.sciencedirect.com

ScienceDirect

Energy Procedia 70 (2015) 683 – 690

Energy Procedia

International Conference on Solar Heating and Cooling for Buildings and Industry, SHC 2014

Hybrid photovoltaic-thermal systems in buildings – a review

Clara Good[a*], Jinfeng Chen[b], Yanjun Dai[b], Anne Grete Hestnes[a]

[a]*Norwegian University of Science and Technology (NTNU), Alfred Getz vei 3, 7491 Trondheim, Norway*
[b]*Shanghai Jiaotong University (SJTU), 800 Dongchuan road,200240,Shanghai,China*

Abstract

This paper presents a review of projects where hybrid photovoltaic-thermal (PV/T) systems are used in buildings. PV/T systems convert solar radiation to electricity and heat simultaneously, in one module. The output of both electricity and heat suggests that the technology can be suited for use in buildings, especially when the available area for installation is limited. The market and research activities related to PV/T technology has increased in recent years. This article adds to existing reviews on PV/T technology by focusing on the building perspective. Different strategies for the use of PV/T in buildings are discussed, and examples of building projects are presented. An attempt is also made to assess to suitability of different PV/T technologies for use in buildings. Finally, the regional variations in market and applications are discussed.

Peer-review by the scientific conference committee of SHC 2014 under responsibility of PSE AG

*Keywords:*photovoltaic-thermal, PV/T, buildings, integration

1. Introduction

Hybrid photovoltaic-thermal (PV/T) modules generate heat and electricity simultaneously in one module. The basic idea of the concept is to utilize more of the solar radiation by also harvesting the waste heat that is generated in photovoltaic (PV) modules. Since PV cells generally become less efficient with increasing cell temperature, the heat removal has a double benefit: the waste heat is utilized and the modules are cooled.

* Corresponding author. Tel.: +47 73595090; fax: +47 73595083.
E-mail address: clara.good@ntnu.no

Peer-review by the scientific conference committee of SHC 2014 under responsibility of PSE AG
doi:10.1016/j.egypro.2015.02.176

The technology is not new; the first studies were published in the mid-1970s, and several different concepts and ideas have been studied during the past decades. A number of reviews have been published on the topic of PV/T technology in the last couple of years, for example by Zhang et al.[1], Tyagi et al. [2] and Chow et al. [3]. The focus of these reviews spans from laboratory work on new concepts to examples of applications. There are also a number of publications describing pilot installations of PV/T systems for different applications in many parts of the world, including buildings. This paper adds to the existing literature by focusing on the use of PV/T in buildings. Although there are a large number of laboratory and experimental installations of PV/T systems worldwide, the focus of this paper is largely on commercial systems. Different technologies and strategies that are used in buildings are discussed, and examples of building projects are presented. An attempt has also been made to assess the suitability of the different technologies for use in buildings by the use of specific indicators.

On a global scale, the building sector accounts for a third of the total energy demand. Increasing the use of renewable energy sources in buildings is therefore of great importance in the effort to reduce global greenhouse gas emissions. Since buildings require electricity as well as energy for heating and cooling, PV/T systems are a potentially attractive solution for buildings. Other claimed benefits of PV/T systems are that they require less space than separate solar thermal and PV systems, and can provide a more uniform architectural appearance.

2. Method

A number of different sources are used to collect the information presented in this paper. The paper is based on a review of relevant scientific publications and projects, as well as communication with PV/T system manufacturers and installers.

The list of projects and producers that was gathered in IEA SHC Task 35 – PV/Thermal solar systems have been used as a starting point [4]. This international project, which was active during the years 2005-2010, had partners from Canada, Denmark, Sweden, Italy and the Netherlands. Manufacturers, universities, and research institutes from Germany, Greece, Hong Kong, Italy, South Korea, Thailand, and Spain several other nations are also reported to have participated.

Other sources of information are publications in peer-reviewed journals and conference proceedings, as well as company information, case studies and personal communication. The review presented here is not intended to be a complete list of PV/T projects, but rather to provide an overview of the market development and some examples of the different cases.

A thorough evaluation of collector performance is beyond the scope of this publication, but the performance of PV/T technologies have been assessed on more general terms according to their suitability for use in buildings. The assessment was made using four indicators, described below. The evaluation is based on findings from the literature review, and information from producers and installers.

- Building integration potential. This indicator describes an estimation of how well the technology can be integrated into buildings. The focus is on the functional integration and not the aesthetic integration. Indicator values are *high* (the technology is well suited for building integration), *medium* (integration is possible, but the integration options are limited), *low* (not suitable for integration).
- Electricity output. This indicator describes if the electricity output *increased*, *similar* or *decreased* compared to a normal PV module without utilization of thermal energy.
- Thermal output. This indicator describes if the thermal output is most promising for *direct* use, such as heating of domestic hot water, or if it needs to be used *indirectly*, such as input to a heat pump.
- Available products. The number of available products. Indicator values are *low* (below 10 products), *medium* (10-40 products) and, *high* (above 40 products). Note that these indictor values cannot be directly compared to the number of available products for pure solar collectors or PV modules, where the market is much larger.

3. Results

3.1. PV/T collector technologies

There are several types of PV/T collectors, and the concepts are so different that is makes little sense to discuss 'PV/T systems' without further specification. Other reviews have also found that a more precise language needed to be defined in order to characterize the different systems [5]. In general, a distinction can be made between PV/T collectors with liquid heat transfer medium (PV/T-liquid), PV/T collectors with air as the heat transfer medium (PV/T-air) and concentrating PV/T collectors. In addition, the collectors can be made using PV technologies such as crystalline of thin film PV, and different solar thermal technologies such as flat plate collectors, evacuated tube collectors or heat pipes.

For flat plate PV/T modules (with either liquid or air as heat transfer medium), a distinction is made between covered and uncovered collectors (sometimes called glazed and unglazed). The nomenclature is in this case somewhat confusing, since both types are actually covered by a protective glass sheet like the one used for PV modules. The covered or glazed PV/T collectors have an additional transparent cover at a distance from the absorber surface for thermal insulation.

The basic idea of PV/T collectors is to utilize the waste heat from solar cells, but there is also a dilemma: the solar cell output is highest when the modules are cool, while the temperature should be high to maximize the thermal output. A high temperature may also damage the materials in the PV module, leading to e.g. delamination.

The thermal output of flat plate PV/T-liquid collectors is lower than that of pure solar thermal collectors, especially for the unglazed PV/T collectors where the heat loss to the surroundings is high. The design and integration of PV/T into the rest of the building energy system is therefore of high importance in order to reach good efficiencies. So far, covered PV/T collectors are relatively rare in the market [5].

In PV/T-air systems, air is used as the heat transfer medium. The heated air can be used in directly in the ventilation system, or it can be connected to a heat pump. In a ventilated PV system, such as a façade, both the electricity and the waste heat can be utilized, but specific PV/T components are not always needed. PV/T-air systems can also be ducted, so that the heated air can be transported from the modules to the ventilation system.

A few examples of evacuated tube PV/T collectors were also found. In addition, a small number of "add-on collectors" are also available on the market. These are can be added to the backside of a normal PV-module to turn it into a PV/T module. There are also a few other concepts under development, such as PV/T windows, PV/T roof tiles and PV/T ventilation units. The PV/T solar assisted heat pump (SAHP) can also be considered a concept of its own.

3.2. PV/T in buildings

Based on the findings in the literature review, four general types of installations can be identified: ventilated PV installations and air-based PV/T, small scale PV/T-liquid systems, large-scale PV/T-liquid systems with ground source heat pumps, and industrial and non-residential buildings with concentrating PV/T installations. In addition, a division can be made between projects with building integrated PV/T systems and projects where PV/T collectors are added onto building roofs. The ventilated PV/T projects are generally building integrated, at least to a certain degree. Ducted PV/T-air systems are both found integrated and added onto roofs. PV/T-liquid installations were found in both categories, but the concentrating PV/T installations are not suitable for building integration.

3.2.1. PV/T-air and ventilated PV systems

In their review of recent PV/T developments, Chow et al. [3] reports that, at least in published research, building integration of air-based PV/T systems are more popular than that of water-based systems. The overview of projects that were published by Task 35 in 2007 lists around 20 projects where PV/T products were developed as a part of the energy system [4]. Air-based PV/T systems were the most common type in these projects, and only two of the PV/T systems (one of which was a concentrating PV/T) used a liquid heat transfer medium.

One reason for the relative abundance of air-based projects may be that it is a quite simple step up from installing a PV system. An air gap is usually provided behind PV installations to ensure proper ventilation and cooling of the modules. Making active use of this heated air in such a ventilated PV system turns it into a PV/T

system. One early example of this type is the Mataró Library in Spain, which has a 20 kWp ventilated PV façade with solar air collectors for preheating of the ventilation air [6].

The Canadian company Conserval Engineering specializes in transpired solar collectors, a type of solar air collector. The company has also developed a PV/T air system (SolarWall PVT), and has made several large scale installations around the world with both façade integrated systems and roof mounted systems with air ducts. The PV/T concept was developed at Concordia University, Montreal, and demonstration system (Fig. 1, left) was installed at the university in 2007 [7]. The gross area is close to 300 m^2 and has is rated at 24.5 kW electric and 75 kW thermal power. The installation provides heating to the ventilation system, and the system performance is monitored by the university.

An example of the ducted type of installation is the system at the Beijing Olympic village [8]. The 50 m^2 system, shown in Fig. 1 (right), is rated at 10 kW electric and 20 kW of thermal power, and was built to showcase renewable energy during the Beijing Olympics. The heat from the PV modules is ducted to the ventilation system of the building. The panels on the upper edge of the roof in Fig. 1 are building integrated transpired solar thermal collectors (without PV) from the same company.

Fig. 1. The SolarWall PV/T facade at Concordia University, Montreal (left), and the SolarWall PV/T installation on the Olympic village in Beijing (right). SolarWall® PV/T system, photos courtesy of Conserval Engineering.

3.2.2. Small and medium scale PV/T-liquid systems

While having the advantage of being simpler, air based systems are generally found to be less efficient than liquid based ones, and recent projects incorporate liquid-based PV/T systems to a greater extent. Since the Task 35 overview from 2007, there has been a large increase in the number of PV/T projects. There also appears to have been a shift in the type of installations, from mostly ventilated or PV/T-air systems to now also including a high share of projects with PV/T-liquid collectors. However, the markets still appear to be quite country-specific and are sometimes dominated by one manufacturer or installer.

The use of PV/T-liquid collectors makes it possible to integrate the PV/T system into hydronic heating systems in buildings, which can be adapted to low temperature heat sources. The collectors can be connected to a storage tank and combined with other heat sources, such as different typed of heat pumps or biomass boilers. The systems can be used for space heating, domestic hot water (DHW) preparation or both. Examples of these types of systems are found in several countries.

In the U.K., the number of PV/T installations has increased rapidly in the past decade. The company Newform Energy claims to have hundreds of installations across the country, from small systems up to complex multi-source energy installations [9]. Based on the available case studies, most of the systems are grid-connected in the range 2-10 kWp and a majority is installed on residential buildings. Both covered and uncovered PV/T collectors are used, sometimes also together in the same system.

In France, the PV/T startup DualSun has around 30 monitored installations throughout the country. Most are in the range of 6 to 12 modules (1.5-2 kWp), but there are also larger installations. The smaller residential systems typically include both flat plate PV/T collectors and regular PV modules. A system of 6 modules and a 300 l storage tank, shown in Fig. 2 (left), is reported to cover around 65% of the hot water demands for a single family building in Marseille in southern France [10].

Several of the small and medium scale installations that were found use heat pumps for auxiliary heating as a part of the energy supply system. Fang et al. [11], also reports that PV/T hot water systems and PV/T heat pumps are the most commonly studied systems in China. On type of system that is studied is the PV/T solar assisted heat pump (SAHP), where the PV/T module is integrated in the heat pump and used directly as evaporator. According to REN21 [12], there are 130 hybrid solar thermal-heat pump systems available from 80 producers, although it is not clear how many (if any) of these incorporate PV/T collectors.

Fig. 2. A roof integrated PV/T system in Marseille, southern France (left, photo courtesy of DualSun), and the Absolicon PV/T installation to the local hospital in Härnösand (right, photo courtesy of Absolicon).

3.2.3. Large scale PV/T-liquid systems with ground source heat pumps

Ground source heat pumps and borehole thermal storage is also used in combination with PV/T systems. In such systems the low temperature thermal output can be used either directly in the heating circuit or, when heating is not needed, to regenerate the ground. Three examples of such systems were installed in the Gothenburg region of Sweden, where the heating from PV/T collectors is used to improve the performance of under-sized bore holes [13]. The largest of the installation is Jättens Gömme, where 400 m^2 of unglazed PV/T collectors from German producer Wiosun, 272 kW collected heat pump power, and 28 bore holes provide heating and hot water to 90 apartments.

The housing complex Bern Oberfeld in Switzerland is still under construction, but it will, when it is finished, include around 1000 m^2 hybrid PV/T collectors which are expected to generate 190 MWh of electricity per year. The thermal energy will be pumped into boreholes to thermally regenerate the ground, from which energy is extracted by a heat pump system. The project is designed according to the requirements of the Swiss MINERGIE-P-ECO code for energy efficient buildings .

3.2.4. Concentrating PV/T

Concentrating PV/T collectors of parabolic trough type provide water of a higher temperature than most flat plate collectors, making them interesting for industrial and other non-residential projects. While these types of collectors are not suitable for building integration, they have been used in building added rooftop installations in several larger projects, such as hospitals and schools. The technology is proven to work in both hot and cold climates. An example from Sweden is shown in Fig. 2 (right), where Swedish manufacturer Absolicon's concentrating PV/T collectors are installed on a local hospital in Härnösand. The installation provides electricity, heating and solar cooling to the operation theatre and the dental clinic [14].

An example from a hotter climate is the Cogenra installation on a building at the University of Arizona Tech Park, which delivers 191 kW thermal and 36 kW electric power to the building [15].The project was funded partly through a local incentive program.

3.2.5. PV/T in buildings

The assessment of the suitability of the different technologies for use in buildings was performed using the indicators presented in Section 2. The assessment was based findings from the literature review, and information from producers and installers. The results are presented in Table 1.

It should be noted that while the number of ventilated PV is low, this type of systems can also be achieved with regular PV products. Judging from previous projects, these systems do also tend to be custom made to a larger extent. This flexibility is also the reason that this category is given a *high* value for the building integration potential.

Table 1. Result of the evaluation of the suitability for use in buildings of different PV/T technologies based on four indicators.

Indicator/Technology	**Ventilated PV**	**Air-based PV/T**	**PV/T liquid (covered)**	**PV/T liquid (uncovered)**	**Concentrating PV/T**
Building integration potential	*High*	*Medium*	*Medium*	*Medium*	*Low*
Electricity output	*Increased*	*Increased*	*Decreased*	*Increased*	*N/A*
Thermal output	*Indirect*	*Direct/indirect*	*Direct/indirect*	*Indirect*	*Direct*
Available products	*Low*	*Low*	*Low*	*Medium*	*Low*

Covered PV/T-liquid collectors may be used directly in in DHW systems, in a similar way to solar thermal systems, but can also be used in combination with heat pumps or other heat sources. Several authors conclude that uncovered flat plate PV/T collectors are a promising technology when used in combination with heat pumps (i.e. indirect use) [3, 5], also in combination with bore holes [13, 16]. The choice of technology is of course also dependent on the location and climate of the project. As for example Ille et al. [5] point out, the electricity output is directly dependent on the solar radiation, while the thermal output is to a larger degree influenced on the systems design.

Architectural integration potential of solar technologies has been extensively studied in for instance IEA SHC Task 41, which defines it as the combination of functional and formal (aesthetic) integration potential [17]. The aesthetic integration of the PV/T technologies has not explicitly been investigated in the study presented here. Farkas [18] describes the architectural potential of photovoltaics as depending on the possibility of structural integration, the formal flexibility (the availability of different shapes, colors etc.), the product system (availability of components available for mounting etc.) and the availability of dummies (fake modules used for creating a uniform appearance). The PV/T market is still relatively small, but if it continues to increase more products dedicated for building integration might enter the market, including modules of different colors and shapes as well as dummies.

3.3. The PV/T market

The market for PV/T systems is still very small compared to the markets for pure photovoltaic or solar thermal systems, but an increase in the number of commercially available products can be identified in the last decade. The increased interest in PV/T is probably, at least to a certain extent, driven by the increasing interest in energy efficient buildings worldwide. Stricter energy requirements for buildings, such as the European Commission's goal that all new buildings shall be 'nearly zero energy buildings' by 2020 [19], puts pressure on building industry to find solutions for on-site renewable energy generation.

A market survey published in Task 35 in 2007 found ten producers of commercial PV/T products, and six that had gone out of the market [4]. In addition, the study found 25 concepts that were under development. A recent study in the project PVT-Norm in Germany found 41 producers of PV/T collectors, showing a significant increase in commercially available products [5]. The large majority of these, around 80%, were uncovered PV/T collectors. Even though the PV and solar thermal markets are both dominated by Chinese companies, most of the PV/T producers found in the study were European.

Task 35 also published a study in which architects, engineers, building owners and solar dealers in Canada, Germany, Denmark, Sweden, Italy and Spain were interviewed [11]. One conclusion from the survey was that the markets were very country-specific, and depended to a large degree on the composition of the existing PV and solar thermal markets. The PV/T market maturity was found to depend mainly on to what degree PV was a part of the previous market.

The type of PV/T systems that was dominating the market was also found to be country-specific. In Canada, the aforementioned Conserval Engineering who produces transpired solar collectors and PV/T-air systems was found to be dominating the market with their SolarWall. Sweden has traditionally had a stable market for liquid-based solar thermal collectors, and air-based PV/T systems were regarded with skepticism by the Swedish interviewees, even though the climate in Sweden and Canada is relatively similar. (However, the number of PV/T systems installed in Sweden to this date is very small.)

China is by far the largest solar thermal market in the world with 86% of the market and 64% of the total installed capacity [12]. Most of the solar thermal systems in China are evacuated tube collectors for water heating, while glazed flat plate collectors dominate in the rest of the world. PV/T-air systems is not at the focus of research and development in China, but more interest is put in PV/T systems for water heating and with direct connection to heat pumps. According to Fang et al [11], it is expected that PV/T hot water systems will become one of the main solar systems in buildings in China.

3.4. Market drivers and barriers

Favorable government policies and economic incentives are probably the largest drivers for all types of solar installations. However, since a PV/T system delivers both electricity and heat, there may be confusion related to how it should be classified. Different approaches are seen in different countries. In the U.K., PV/T systems owners are eligible to receive feed-in tariffs from the export of electricity, but they are not eligible for economic support through the Renewable Heat Incentive (RHI) [20]. In Norway as another example, PV/T systems can receive funding as solar collectors, but no incentives are available for PV modules.

As mentioned above, there is also a lack in adequate terminology to describe PV/T systems, which can also influence the incentives. Ille et. al [5] mentions that the word ‘uncovered’ previously made this type PV/T collectors not eligible for funding within the German market incentive program for solar collectors, which excludes uncovered swimming pool collectors. However, the description in the program was then updated to ‘panels without transparent cover on the front panel’, which means that uncovered PV/T collectors should now be eligible.

The relation between standards and innovation, and the effect on market development, has been analyzed by Kramer and Helmers [21]. They find that the lack of standards and certifications is a strong barrier to market development. It leads to a lack of technical information on the products, restrictions in government incentives and an uncertainty among consumers. The recent developments in certifications specifically for PV/T products, such as the Solar Keymark [22], can therefore be expected to have a positive influence on the market.

4. Discussion

The PV/T market is still very small and it shows in different countries a strong dependence on individual companies. The respondents in the Task 35 market survey pointed to economic benefits and the possibility of building integration as the two most important factors. In the PV/T installations found in this review, however, PV/T systems are rarely or never reported to be cheaper than alternative installations. The choice of PV/T seems to be driven by other factors. The economic benefit of PV/T systems today depends to a large degree on the availability of subsidies, or funding of pilot projects.

5. Conclusion

In the past decade, PV/T installations have gone from largely project-specific developments to relatively standardized systems. The market is still very small compared to the PV and solar thermal markets, but a number of commercial products are now available. Different types of systems have gained ground in different countries based

on the composition of the earlier markets for PV and solar thermal, but also depending on the success of individual companies. The available economic subsidy schemes may also have contributed to shape the markets in the different countries.

There seems to have been a shift from PV/T-air systems to a larger share of PV/T-liquid systems, including PV/T systems with heat pumps. A few large scale projects with seasonal storage in bore holes were also found. The thermal energy output of PV/T collectors are generally of low temperature, and several authors emphasize the importance of the complete system design, e.g. the connection to heat pumps, thermal storage solutions and other HVAC equipment, in order to make good use of this energy.

Recent developments in certification and testing has also led to more standardization, which may encourage more installers to choose PV/T systems in favor of pure PV or solar thermal systems.

6. Acknowledgements

This publication was created as part of the Joint Research Centre in Sustainable Energy between Shanghai Jiao Tong University and the Norwegian University of Science and Technology (JRC SJTU-NTNU). The Joint Research Centre is funded by the Research Council Norway, project number 221 657.

References

[1] X. Zhang, X. Zhao, S. Smith, J. Xu, X. Yu, Review of R&D progress and practical application of the solar photovoltaic/thermal (PV/T) technologies, Renewable and Sustainable Energy Reviews, 16 (2012) 599-617.
[2] V.V. Tyagi, S.C. Kaushik, S.K. Tyagi, Advancement in solar photovoltaic/thermal (PV/T) hybrid collector technology, Renewable and Sustainable Energy Reviews, 16 (2012) 1383-1398.
[3] T.T. Chow, G.N. Tiwari, C. Menezo, Hybrid solar: A review on photovoltaic and thermal power integration, International Journal of Photoenergy, 2012 (2012).
[4] IEA SHC Task 35, Overview of PV/T products and projects, 2008.
[5] F. Ille, M. Adam, R. Radosavljevic, H.P. Wirth, Market and simulation analysis of PVT applications for the determination of new PVT test procedures, Eurosun 2014 *In Reveiw*, ISES, Aix-les-Bains, France, 2014.
[6] L. Mei, D. Infield, U. Eicker, V. Fux, Thermal modelling of a building with an integrated ventilated PV façade, Energy and Buildings, 35 (2003) 605-617.
[7] A.K. Athienitis, J. Bambara, B. O'Neill, J. Faille, A prototype photovoltaic/thermal system integrated with transpired collector, Solar Energy, 85 (2011) 139-153.
[8] Conserval Engineering Inc., 2008 Beijing Olympic Village Case Study, SolarWall case studies, 2008.
[9] Newform Energy, http://www.newformenergy.com/ [Online] 05.10 2014
[10] DualSun, Suivi de performances des installations DualSun, 2014.
[11] X. Fang, D. Li, Solar photovoltaic and thermal technology and applications in China, Renewable and Sustainable Energy Reviews, 23 (2013) 330-340.
[12] J.L. Sawin, F. Sverrisson, (Lead authors), Renewables 2014 Global Status Report, REN21 (Ed.), REN21 Secretariat, , Paris, France, 2014.
[13] J. Ahlgren, SOLHYBRIDTEKNIK - i kombination med VÄRMEPUMPAR som är kopplade mot ett borrhåls- eller markvärme- lager., Energiförbättring i Väst, Mölnlycke, Sweden, 2014.
[14] Absolicon, Local Hospital Härnösand, Absolicon reference installations, 2010.
[15] New Solar Technology Deployed at the UA Tech Park's Solar Zone Gains Momentum, Tech Parks Arizona, https://techparks.arizona.edu/new-solar-technology-deployed-ua-tech-park's-solar-zone-gains-momentum, 2013.
[16] M. Rommel, Technical feasibility of the PV-T concept, SPF - Institut für Solartechnik, Eurosun 2014 Workshop PVT, 2014.
[17] K. Farkas, F. Frontini, L. Maturi, M.C. Munari Probst, C. Roecker, A. Scognamiglio, I. Zanetti, T.41.A.2: Solar Energy Systems in Architecture - Integration Criteria and Guidelines, M.C. Munari Probst, C. Roecker (Eds.) IEA SHC Task 41 publications, 2013.
[18] K. Farkas, Architectural Integration of Photovoltaics - Formal and Symbolic Aesthetics of Photovoltaics, Faculty of Architecture and Fine Art, Department of Architectural Design, History and Technology, Norwegian University of Science and Technology (NTNU), Trondheim, 2012.
[19] Directive 2010/31/EU of the European Parliament and of the Council of 19 May 2010 on the energy performance of buildings, Directive 2010/31/EU, Brussels, 2010.
[20] Ofgem, Domestic Renewable Heat Incentive, https://www.ofgem.gov.uk/environmental-programmes/domestic-renewable-heat-incentive [Online] 05 10 2014
[21] K. Kramer, H. Helmers, The interaction of standards and innovation: Hybrid photovoltaic–thermal collectors, Solar Energy, 98, Part C (2013) 434-439.
[22] Solar Keymark Network, Specific CEN Keymark Scheme Rules for Solar Thermal Product version 21.00, J.E. Nielsen (Ed.), CEN Certification, 2013.

Paper II

Good, C., Andresen, I., & Hestnes, A. G. (2015*). Solar energy for net zero energy buildings – A comparison between solar thermal, PV and photovoltaic–thermal (PV/T) systems.* Solar Energy, 122, 986-996. doi:http://dx.doi.org/10.1016/j.solener.2015.10.013

Previously presented at CISBAT 2015, Lausanne, Switzerland, with the same title.

Available online at www.sciencedirect.com

ScienceDirect

Solar Energy 122 (2015) 986–996

SOLAR ENERGY

www.elsevier.com/locate/solener

Solar energy for net zero energy buildings – A comparison between solar thermal, PV and photovoltaic–thermal (PV/T) systems

Clara Good *, Inger Andresen, Anne Grete Hestnes

Department of Architectural Design, History and Technology, Norwegian University of Science and Technology (NTNU), Alfred Getz vei 3, 7491 Trondheim, Norway

Received 10 June 2015; received in revised form 2 October 2015; accepted 5 October 2015

Communicated by: Associate Editor Brian Norton

Abstract

In a net zero energy building (nZEB), the energy demand from the operation of the building is met by renewable energy generated on site. Buildings require energy both in the form of heat and electricity, and solar energy utilization is important in order to reach a net zero energy balance. In projects with ambitious energy targets or limited available areas for local energy generation, solar thermal and photovoltaic (PV) installations will eventually compete for space on roofs and facades. Hybrid photovoltaic–thermal (PV/T) modules, in which heat and electricity is generated simultaneously, are therefore an interesting technology for building applications, which can potentially lead to a higher total efficiency and lower use of space. This paper describes a comparative simulation study of different solar energy solutions for a Norwegian residential building concept aiming for a net zero energy balance. Separate PV and solar thermal systems are compared to PV/T systems, and the resulting energy balances analyzed. The results show that the building with only high-efficiency PV modules comes closest to reaching a zero energy balance, but that the results depend greatly on the nZEB definition, the boundary conditions and the design of the building's energy system.

Keywords: Net zero energy building; PV/T; PV; Solar thermal

1. Introduction

Buildings account for around a third of the global energy use and a similar share of the greenhouse gas emissions (International Energy Agency, 2013). Making buildings more energy efficient and sustainable is therefore important in order to reduce global energy demand as well as emissions. In a net zero energy building (nZEB), the amount of energy required to operate the building is generated by renewable energy sources on or near the building (Marszal et al., 2011). During a specified period of time, typically a year, the building reaches a net zero energy balance. In its recast of the Energy Performance of Buildings Directive (EPBD), the European Union has directed its member states to ensure that by 2020, all new buildings shall be *nearly* zero energy buildings (European Parliament, 2010).

Abbreviations: nZEB, net zero energy building; EPBD, Energy Performance of Buildings Directive; ZEB Centre, The Research Centre for Zero Emission Buildings (www.zeb.no); DHW, domestic hot water; HVAC, heating, ventilation and air conditioning; STC, standard test conditions; kW_p, kilowatt peak; SPF, seasonal performance factor.

* Corresponding author.

http://dx.doi.org/10.1016/j.solener.2015.10.013
0038-092X/

Nomenclature

Q_{sol}	thermal energy from solar energy system (kW h)	E_{net}	the difference between energy imported to and exported from the building (kW h)
Q_{aux}	thermal energy from auxiliary heat source (kW h)	β	tilt angle of modules (°)
E_{sol}	electricity from solar energy system (kW h)	γ	sun height above horizon (°)
SF_{th}	thermal solar fraction (–)	T_m	mean collector temperature (K)
SF_{el}	electricity-specific solar fraction (–)	T_a	ambient temperature (K)
$E_{delivered}$	delivered (imported) energy to the building (kW h)	ΔT	difference between mean collector temperature, T_m, and ambient temperature, T_a (K)
$E_{exported}$	exported energy from the building (kW h)	η	thermal efficiency (–)
		η_0	thermal zero-loss efficiency (–)

Active solar energy utilization is one of the main strategies used to provide on-site renewable energy to buildings, which is necessary to reach a zero energy balance. Buildings require energy both in the form of heat and electricity during operation, which can be provided by solar thermal collectors and photovoltaic (PV) modules. In projects with ambitious energy targets or limited available area for installations, solar thermal collectors and PV modules may be competing for the available space on the buildings' roofs and facades. In a hybrid photovoltaic–thermal (PV/T) module, electricity and heat is generated simultaneously. This can lead to a high total efficiency per module and possibly to a reduced use of space compared to separate systems. PV/T is therefore an interesting technology for buildings.

This paper describes a comparative simulation study of solar thermal, PV and PV/T systems, applied to the case of a Norwegian low energy residential building. The goal is to achieve a zero energy balance over a year. The energy yield of the different systems are analyzed and compared, and the building energy balance is calculated.

1.1. Hybrid photovoltaic–thermal (PV/T) modules

PV/T technology has so far not had a commercial breakthrough comparable to that of PV or solar thermal, but interest in the technology is increasing, especially in connection to low or zero energy buildings (Chow et al., 2012). The market for PV/T has increased in the past decade, and a number of solar energy manufacturers now also produce PV/T modules. Some manufacturers even specialize in PV/T technology. A number of different PV/T technologies are available. They can be classified for example based on the type of heat transfer medium (air or liquid), the configuration of the glazing, and the PV technology used (see for example Chow et al., 2012; Tyagi et al., 2012).

PV modules convert only around 10–20% of the radiation to electricity, while the rest is reflected or dissipated as heat in the module. The basic idea behind the PV/T technology is to utilize more of the incoming solar radiation by also harvesting the waste heat from PV modules. Since PV cell efficiency typically decreases with increased cell temperature, removing the waste heat can also lead to an increased electricity output. An additional benefit of PV/T modules for building use is that architectural uniformity can be achieved between the thermal and electric installations.

A number of PV/T technologies are available, but this study focuses only on flat plate PV/T modules with liquid heat transfer medium. For this type, a basic distinction can be made between covered and uncovered modules (sometimes called glazed and unglazed) (Aste et al., 2014). The difference is illustrated in Fig. 1. Simply put, an uncovered PV/T module is a PV module with cooling. It produces an equal or larger amount of electricity than a regular PV module, and in addition some low-temperature heat. Both types of modules generally include some type of cover for structural stability, but covered PV/T modules have an additional, suspended glazing to prevent heat loss through convection. A covered PV/T module is similar to a solar thermal collector with added PV cells, and has a higher thermal output than an uncovered PV/T module. Adam et al. (2014) performed a market survey of PV/T products available in Germany. This has been used to find products for this study. A large majority of the available products were found to be uncovered collectors (30 out of 41 producers).

1.2. Zero energy buildings

There are several different definitions of a net zero energy building (nZEB). In general, an nZEB can be defined as a building that reaches a net zero energy balance over a specified time period, typically a year. The EU targets set out in the EPBD describes a *nearly* zero energy building as a building with a very high energy performance where "the nearly zero or very low amount of energy required should be covered to a very significant extent by energy from renewable sources, including energy from renewable sources produced on-site or nearby" (European Parliament, 2010).

In addition, the zero energy balance can be calculated in different ways, depending among other things on the system boundary and weighting factors for the different

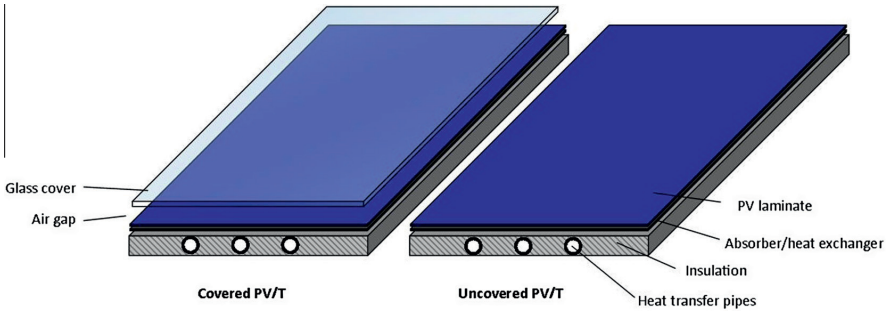

Fig. 1. A schematic drawing of a covered (left) and uncovered (right) flat plat PV/T module. Note that the PV laminate also usually includes a cover for structural stability.

energy sources that are used (Marszal et al., 2011). The balance may include the energy used for heating ventilation and air conditioning (HVAC), lighting, and use of electrical equipment. In more ambitious definitions, the balance may also include the energy used in the production of materials, as well as the construction and subsequent dismantling of the building itself. The amount of energy that should be generated on site to reach the zero energy balance therefore depends on the nZEB definition. A proposal for a consistent nZEB definition was presented by Sartori et al. (2012). The system boundary used in the case presented here is the building itself, and the annual energy import/export balance is used. That is, the balance is calculated between energy delivered, or imported, to the building ($E_{delivered}$) and the energy exported from the building ($E_{exported}$). The solar energy installations on the roof are considered to be inside the system boundary. Based on Sartori et al. (2012), the energy balance is then calculated according to Eq. (1). The balance in this case is calculated with total annual values. A net zero energy balance is reached if E_{net} (kW h) is zero.

$$E_{net} = |E_{exported}| - |E_{delivered}| \quad (1)$$

To reach a net zero energy balance, the first priority should be to decrease the need for delivered energy, and then to meet the remaining demand with on-site renewable energy sources (Sartori et al., 2010). The delivered energy could include electricity, biomass, district heating, or other energy carriers. The exported energy is in general only electricity, but it could in some cases also include heat, for example to a district heating network. Weighting factors are used to compare energy from different sources in the same equation. According to EN 15503 (EN 15603, 2008), the weighing factors can be primary energy, carbon dioxide emissions, or factors determined at national level. A policy rating, imposed to penalise or favor some energy carriers, is also mentioned as a possibility. The factors for delivered and exported energy of the same energy carrier can be different or equal (symmetric weighting).

The Research Centre on Zero Emission Buildings (the ZEB Centre, www.zeb.no) in Trondheim, Norway, has defined four different ambition levels for net zero *emission* buildings. This can be transferred also to net zero *energy* buildings. The ambition levels, as well as a complete definition framework, is further described in Dokka et al. (2013). In the case presented here, the ambition is to reach nZEB-O, which means that the energy need for operation of the building is considered in the energy balance calculation. The energy demand of equipment, such as computers and lighting, is included, but standardized values are used. Energy demand for materials, construction and demolition is excluded.

1.3. Solar fraction

In addition to E_{net}, it is interesting to know the solar fraction, i.e. how much of the heat and electricity that is met by solar energy. The thermal solar fraction (SF_{th}) is calculated according Eq. (2), where Q_{sol} (kW h) is the thermal energy from the solar energy system, and Q_{aux} (kW h) is the thermal energy from the auxiliary energy source. The solar fraction can be calculated in slightly different ways, depending on how the system losses are allocated. The calculation used here divides the losses between the solar and auxiliary systems.

$$SF_{th} = \frac{Q_{sol}}{Q_{sol} + Q_{aux}} \quad (2)$$

The thermal solar fraction is commonly used in solar thermal calculations, but here we have also chosen to define a corresponding electricity-specific solar fraction (SF_{el}), calculated according to equation (3), where E_{sol} (kW h) is the electricity from the solar energy system, E_{need} (kW h) is the electricity-specific energy demand of the building.

$$SF_{el} = \frac{E_{sol}}{E_{need}} \quad (3)$$

Since the building model used in this study has a heat pump as auxiliary energy source, the total electricity demand also includes electricity for heating. This has not been included in $E_{need,}$ which encompasses only

electricity-specific energy use, i.e. energy need that cannot be covered by another energy source than electricity, such as use of electric equipment or lighting. The total electric solar fraction, including electricity for heating, is the ratio $E_{exported}/E_{delivered}$ shown in Table 4.

2. Background

2.1. ZEB residential concept model

The building model (Fig. 2) used in the simulations is based on a concept building model developed at the ZEB Centre. It was created in order to have a simple and realistic building as the basis for various building performance studies. The concept model is designed based on current state-of-the-art in building technology, and is designed to fulfil the requirements of the Norwegian passive house standard (NS 3700, 2010). The material use, embodied energy and emissions, design of a HVAC system, technical details and energy performance is well documented and is presented in Houlihan Wiberg et al. (2014). The model is therefore well suited to be used as a basis for the solar energy system analysis.

The building model is a two-storey residential building with 160 m^2 heated floor area. It is located in Oslo in Southern Norway (59.9 °N, 10.6°), which has an annual average temperature of 6.3 °C. The annual energy demand of the building is shown in Table 1, as determined by Houlihan Wiberg et al. (2014). The energy demand for domestic hot water (DHW) and electricity is specified in accordance with standard values from the Norwegian standard NS 3031 (NS 3031, 2011), as are the internal heat gains from people and equipment.

The monthly space heating need (kW h/m^2) is shown in Fig. 3, together with the solar irradiation for Oslo on a surface oriented for maximum annual solar irradiation (45° tilt and south-facing) and a vertical surface, such as a facade. The largest fraction of the solar radiation is available in the summer when there is no space heating need. However, there is still a heating demand during spring and autumn, which coincides with a significant part of the irradiation.

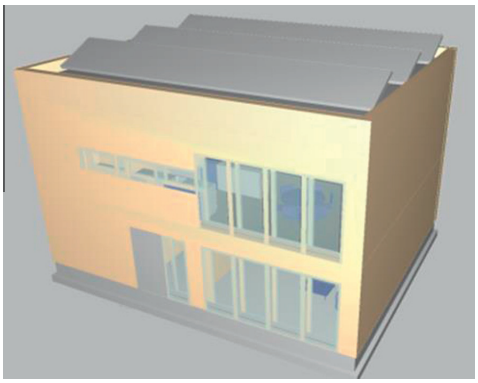

Fig. 2. The ZEB concept model of a single family residential building, from Houlihan Wiberg et al. (2014). The three rectangles on the roof indicate the location of the PV system (note that only two rows are used in this analysis).

Table 1
The energy demand of the ZEB concept building.

Energy demand	kW h/year	kW h/m^2 year
Space heating	3349	20.9
Domestic hot water	3811	23.8
Electricity	4074	25.5
Total	11234	70.2

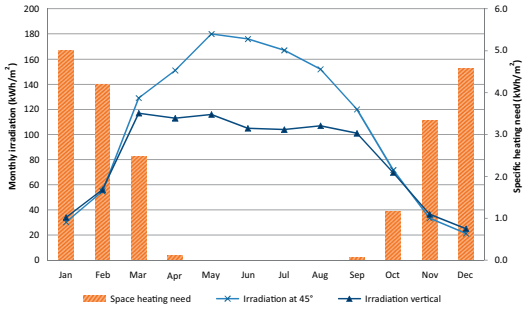

Fig. 3. Monthly irradiation on an optimally inclined surface (45° tilt) and a vertical surface is shown on the left axis, together with the specific heating need of the building (kW h/m^2 heated floor area) on the right axis, as determined by Houlihan Wiberg et al. (2014). Irradiation data from PVGIS (Institute for Energy – Renewable Energy Unit).

2.2. Building energy system

The building has an HVAC system with mechanical ventilation and heat recovery, which is thoroughly described in Houlihan Wiberg et al. (2014). A schematic drawing of the thermal part of the building energy system is shown in Fig. 4. The heating is distributed by a low-temperature hydronic system with floor heating (inlet/return temperature 30/25 °C) and radiators (inlet/return temperature 40/30 °C). The central part of the heating system is a well-insulated water storage tank, which stores energy and buffers between heat sources and loads at different temperatures. A tank-in-tank system is used for the tap water. With a store temperature of 55 °C and a temperature at the tap of 45 °C, the stand-by volume that needs to be available at all times is estimated to around 100 l. This volume is kept the same in all the simulated systems.

The solar thermal system with glycol/water mix as heat transfer medium is connected to the tank by an internal heat exchanger. The space heating loops are directly connected to the tank. The control strategy prioritizes the heating from the solar energy systems. When necessary, auxiliary thermal energy is provided by an air to water heat pump (7 kW). The heat pump delivers a temperature of up

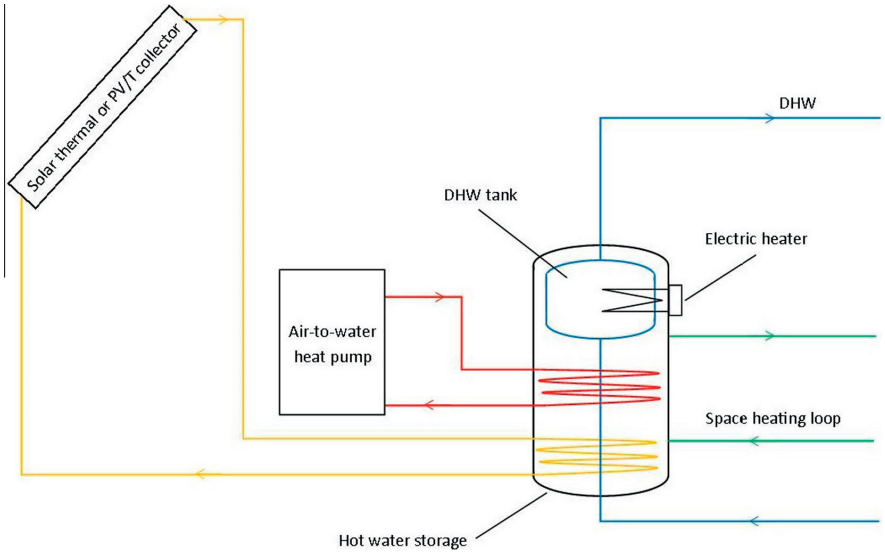

Fig. 4. A schematic drawing of the thermal part of the building energy system (not including PV system).

to 55 °C, depending on the outdoor temperature, which is sufficient for the hot tap water preparation. An electric heater in the upper part of the tank is used to prevent legionella growth. The system is described in detail in Dokka et al. (2013). The PV systems (not shown in the figure) and the electric part of the PV/T systems are grid-connected, using standard DC/AC inverters. No module level power optimizers or batteries are used in the system.

3. Method

3.1. Comparative study

Three versions of the building model (A, B and C) are simulated to study the performance of different solar energy systems for zero energy buildings. Building A has a system with a combination of solar thermal collectors and PV modules and represents the original design of the building model. Building B has a system of PV/T and PV modules, and building C has only PV modules installed. The hydronic heating system is the same in all versions of the building, except for the dimensions of the tank and piping.

The simulations are performed in the program Polysun, which is a dynamic simulation tool for solar energy solutions including solar thermal, PV and PV/T, as well as for various hydronic systems, such as heat pumps and district heating system (Vela Solaris, 2012). Meteonorm weather data is used in the simulation (Meteotest, 2009). The modelling of the systems for this study was based on a combination of in-program models and data from manufacturers. The energy output, thermal and electric solar fraction, and energy balance are calculated for each of the systems.

3.2. Objective and boundary conditions

Thermal energy and electricity have different uses in buildings and thereby different value. The objective and boundary conditions will therefore have a significant impact on the results and the conclusions that can be drawn. A review of methodologies to evaluate PV/T systems in comparison with PV and solar thermal collectors were outlined by Delisle and Kummert (2014). They found that a number of methodologies were used by different authors, such as combined energy or exergy efficiency, combined primary energy saving efficiency, equivalent area or economic factors. In this study we have chosen to use the available area as the boundary condition, but the comparison is based on the calculated import/export energy balance.

The objective is to investigate which of the three building alternatives comes closest to achieving a net zero energy balance. The ambition level is ZEB-O according to the guidelines developed by the ZEB Centre, which were outlined in the Section 1.2 and are further described in Dokka et al. (2013). Since the auxiliary heating in this case is provided by a heat pump, electricity is the only form of delivered energy to the building. The exported energy is likewise only electricity from the PV or PV/T systems. As there is only one energy carrier being imported and exported, and the purpose is to compare the buildings against each other, no weighting factors are used.

It is assumed that there are no restrictions on the electricity exchange with the grid, and electricity generated by the solar energy systems is therefore in this analysis

considered useful at all times. In reality, electricity will be valued differently at different times. Using as much as possible of the self-generated electricity directly in the building can therefore be desirable, but this will not be further considered here. The thermal energy from the solar collectors is only useful if it can be used or stored. Once the storage tank has reached its upper temperature limit, additional thermal output cannot be used.

Only the roof area (8 m × 10 m) is considered to be available for the solar installations. Installing solar energy systems on flat roofs, especially in northern regions, requires that row-to-row shading is considered, but it is assumed here that there are no surrounding buildings or structures shading the installations. The required distance d (m) between rows can be calculated according to Eq. (4), where b (m) is the module height, β (°) is the tilt angle of the modules, and γ (°) the sun angle, which is the angle between the sun and the horizon. (The German Solar Energy Society, 2013).

$$d = b \cdot \frac{\sin(180^\circ - \beta - \gamma)}{\sin(\gamma)} \quad (4)$$

The optimal orientation in Oslo is around 45° tilt and south-facing. The lowest sun angle in Oslo is around 7° (beginning of January, note that the sun angle refers to the sun height at noon), meaning that the modules would have to be spaced around 10 m to avoid shading completely. Since the roof is only 8 m wide, this means that only one row would fit on the roof. As 2–8% of the solar radiation is received during the winter months, it was assumed that some shading could be tolerated in order to fit two rows on the roof. Accounting for the length of the modules themselves, the longest spacing possible is 7 m, which means that the modules are unshaded from the beginning of February. A schematic drawing of the installations is shown in Fig. 5. The shading analysis is performed internally in the simulation program. The row-to-row shading is accounted for in a somewhat simplified manner using a composite horizon line.

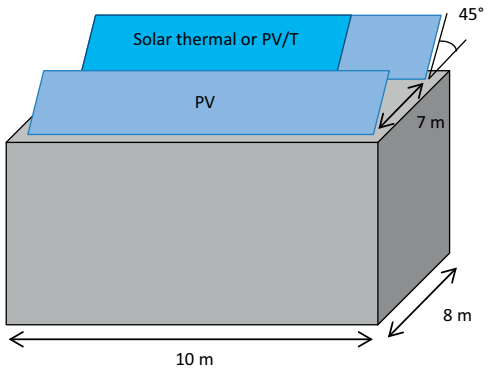

Fig. 5. A schematic drawing (not to scale) of the solar installations on the roof. The back row includes solar thermal in building A, PV/T in building B, and only PV in building C.

Since geometric dimensions from market-available modules are used in this study, the active area in each of the different systems is not exactly the same. A generic spacing of 5 cm between modules is used. As the output of PV modules is more dramatically influenced by shading than that of solar thermal collectors, the latter are placed in the back row. Note that the back row in building C and C* includes only PV modules.

The tilt angle of 45° is close to optimal for PV modules, but solar thermal collectors are typically installed at a somewhat steeper angle or even vertically on the facade. This slightly increases the yield at times when heating is needed, i.e. spring and autumn when the sun is low. Since the modules analyzed here include PV, solar thermal and combinations of the two, all modules are installed at the same tilt angle to simplify the comparison.

The modules could also have been mounted at a lower tilt angle and with less spacing, which would increase the installed power on the roof but reduce the specific yield (kW h/kW$_p$). If the tilt angle was reduced to around 10°, another row of modules could have been installed with the same level of shading. The consequences of different installation designs are studied in more detail in Good et al. (2014). Other installations options, such as facades and different tilt angles, will be included in further studies.

3.3. Selection of solar modules

An overview of characteristics of the selected modules is given in Table 2. The solar thermal collectors and PV modules used in the simulation are selected to represent average (STavg and PVavg) to high-end (SThigh and PVhigh) products available on the market, in terms of performance.

The market for PV/T modules is still relatively small compared to that of solar thermal and PV. There is also still a lack of regulations regarding testing and certification of PV/T modules, but since 2013 it is possible to certify modules according to Solar Keymark (2013). According to the certification guidelines, the thermal zero-loss efficiency (η_0) should be measured with the PV cells working at their maximum power point. In addition, since the performance of a PV/T module depends both on the thermal and electric characteristics, it is difficult to find a module that represents a market average. In an attempt to account for these differences, two different PV/T modules were used in the simulations: an uncovered PV/T module with good electric performance (PV/Ta), and a covered PV/T module with good thermal performance (PV/Tb). Both of these modules are selected from the upper market range.

Table 2
Characteristics of the solar thermal (ST), PV and PV/T modules used in the simulations.

Module	Technology	Gross area (m^2)	Electric efficiency at STC (%)	Rated electric power (kW_p)	Thermal zero-loss efficiency η_0 (%)
STavg	Flat plate	2.00	–	–	80
SThigh	Flat plate	2.00	–	–	85
PVavg	Poly-Si	1.65	15.8	260	–
PVhigh	Mono-Si	1.64	20.3	333	–
PV/Ta	Mono-Si, uncovered, uninsulated	1.64	17.4	285	61.4
PV/Tb	Poly-Si, covered, insulated	2.26	12.0	240	71.5

3.4. Solar energy system design

The main parameters and system dimensions used in the simulations of buildings A, B and C are shown in Table 3. The building versions with high efficiency solar thermal collectors and PV modules are denoted A* and C*.

The dimensioning of the system for building A is based on the solar thermal system. In accordance with common design guidelines for Northern European regions, the solar thermal system is designed to most of the thermal energy demand during the summer months (here defined as May to August), when the heat demand is only that for DHW preparation. The area of solar collectors required to do this is slightly smaller with the high efficiency modules, which is why the collector area for building C* is smaller than for building C.

Since covered and uncovered PV/T modules have different output profiles, two versions of building B are evaluated: B1 with uncovered PV/T modules and B2 with covered PV/T modules.

Simulations of B1 with different ratio between the PV/Ta and PVavg module areas showed that E_{net} increased with increasing PV/T area. For building B1, uncovered PV/T modules were therefore used on the whole roof area, minimizing E_{net}. Since the thermal output of the uncovered modules is relatively low, it was not possible to reach high thermal solar fractions with this technology. It was also found that a tank size of around 60 l/m^2 collector was suitable for a larger PV/Ta system and a slightly higher tank volume to area ratio for smaller systems.

For building B2, the same design strategy as for solar thermal (building A) was used, i.e. that the PV/T system was sized to meet most of the energy demand during summer, and the rest of the roof area was covered with PV modules. Simulations showed that it requires a PV/T area of around 16 m^2 (7 modules) in order to reach the same thermal coverage as for building A. The rest of the available area was used for PV modules.

In building C, all available roof space has been used for a PV installation. This building includes the same hydronic heating system as buildings A and B, but without the solar thermal contribution. The tank size was decreased to only work as a buffer for the heat pump. The stand-by volume for the DHW was kept the same as in the other systems.

4. Results

The buildings A, B and C were simulated according to the conditions described in the previous sections. The annual thermal and electricity output of the systems are shown in Fig. 6, measured in kilowatt-hours. No weighing factors between thermal energy and electricity are taken into account in this figure. The systems with the highest thermal energy output (A, B2 and A*) are also the systems with the highest total output with this way of evaluation.

The thermal and electric solar fractions are shown in Table 4, together with the import/export energy balance calculations. None of the systems reach a net zero energy balance ($E_{net} > 0$). A higher number means a higher coverage by on-site energy (a building with $E_{net} = 0$ would have 100% coverage). The ratio $E_{exported}/E_{delivered}$ in the third column in Table 4 shows the percentage of the delivered energy that can be covered by exported energy, i.e. how close the building is to reaching a zero energy balance. As mentioned in Section 1.3, this can in this case also be interpreted as the total electric solar fraction.

The system that is closest to reaching a balance is system C*, with only state-of-the-art PV modules and no thermal collectors. This system meets 73% of the delivered electricity with exported solar electricity. The state-of-the-art

Table 3
The main parameters of the simulated system variants.

System	Description	Installed area ST/PVT/PV (m^2)	Rated electric power (kW_p)	Tank volume (l)
A	STavg and PVavg	10/0/21	3.4	1300
A*	SThigh and PVhigh	8/0/23	4.7	1300
B1	Only PV/Ta	0/30/0	5.1	1800
B2	PV/Tb and PVavg	0/16/17	4.3	1000
C	Only PVavg	0/0/30	4.7	300
C*	Only PVhigh	0/0/30	6.0	300

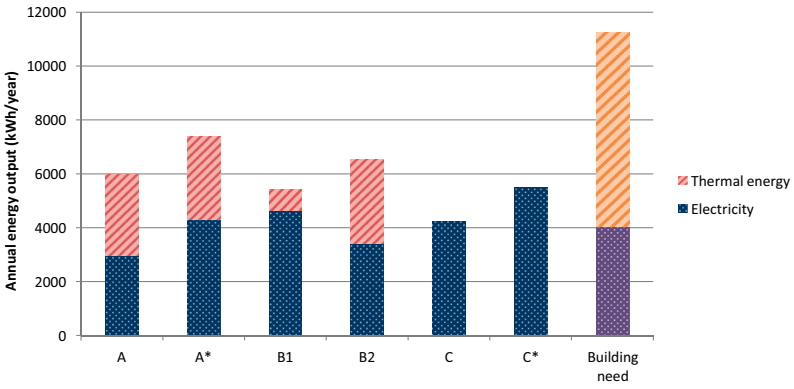

Fig. 6. The annual thermal and electric output of the different systems. The rightmost column shows the simulated net thermal and electric energy need of the building. No weighting between thermal energy and electricity is taken into account in this figure.

Table 4
The thermal and electric solar fractions, the ratio between exported and delivered energy, the ratio $E_{exported}/E_{delivered}$, and the net delivered energy E_{net} is shown.

System	SF_{th} (%)	SF_{el} (%)	$E_{exported}/E_{delivered}$ (%)	E_{net} (kW h)
A	33	73	44	−3796
A*	33	105	64	−2446
B1	9	113	62	−2822
B2	34	84	51	−3300
C	0	103	56	−3353
C*	0	134	73	−2086

system with solar thermal and PV (A*) has the highest solar fraction, and is the second closest to reach a balance, with 64% of the delivered energy met by on-site electricity. Of the systems with PV/T studied, the uncovered PV/T system in B1 is the closest to a balance, with 62% of the delivered electricity met by solar generated electricity. Due to the use of a heat pump for auxiliary energy, the systems with high electricity output are favored in this calculation.

System C* has the highest coverage of on-site energy generation, even though it has the highest value of $E_{delivered}$, while building A* has the lowest value. The difference between these two buildings is shown in Fig. 7. According to the nZEB definition is used here, building C* is closer to reaching a zero energy balance since the value of E_{net} for this building is smaller.

The values for E_{net} for the two building versions with PV/T modules, B1 and B2, are relatively similar, but the output profiles are different. The monthly average collector temperatures during operation of the solar thermal collectors and PV/T modules are presented in Fig. 8. As expected, the state-of-the-art solar thermal collectors (SThigh) generally have the highest temperature. The uncovered PV/Ta modules have the lowest temperature, and reach only an average operational temperature of 40 °C during the summer months. During November to February, the temperature reached by the PV/Ta modules cannot be used by the system, compared to November–January for the three other module types.

5. Discussion

5.1. Solar energy and the nZEB definition

The results presented here do not give an unambiguous answer to the question of which solar energy system is the best choice for this type of building. Many factors influence the answer, for example how the energy balance is calculated, what the boundary conditions are, and if the goal

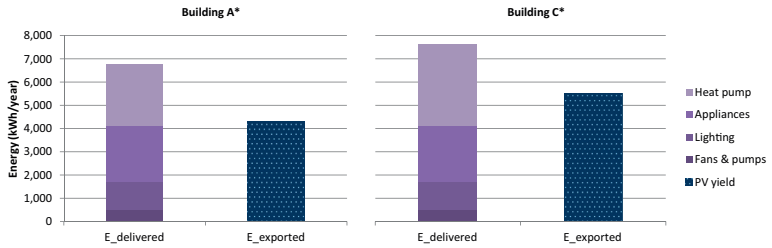

Fig. 7. The energy balance of building A* and building C*. Even though the amount of energy delivered to building A* is lower than that to building C*, the latter is closer to reaching a zero energy balance.

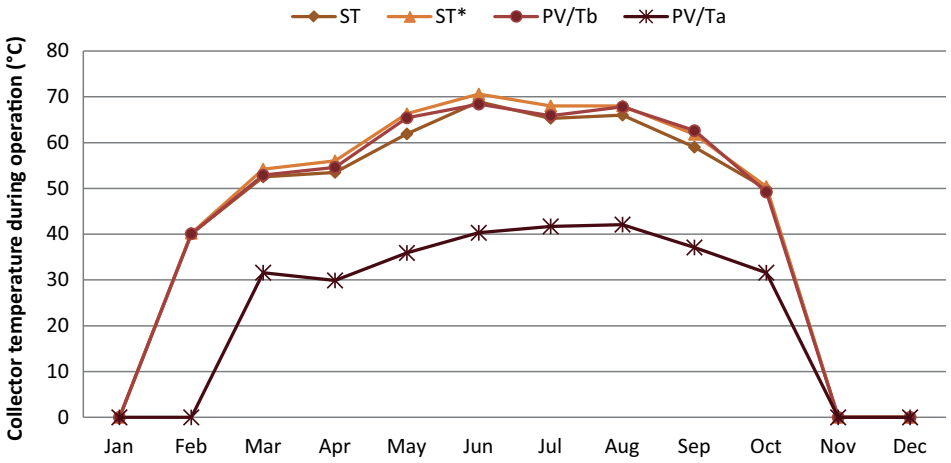

Fig. 8. The monthly average collector temperature during operation in the solar thermal collectors (A and A*) and PV/T modules (B1 and B2) during the year, given as monthly averages.

is to reach the lowest possible energy use or a lowest value of delivered energy, primary energy, greenhouse gas emissions, or other metric.

To reach a zero energy balance, the imported energy should be balanced by the export of locally generated renewable energy. Normally, the only form of energy export that takes place in an nZEB building is that of electricity to the grid (although e.g. thermal export to a district heating network could be possible as well). This means that an electricity source needs to be included in any building where the aim is a net zero energy balance. In this case, the choice of auxiliary heat source is also an important factor, since e.g. the use of a heat pump means that only electricity is imported and exported. This favors systems with a high electricity output in the net energy balance calculations.

It is not uncomplicated to design systems with different technologies in a way that makes a reasonable comparison possible. The systems for building A, A* and B2 were dimensioned to get full solar thermal coverage during the summer. All systems could instead have been dimensioned to maximize E_{net}. However, the result of such an optimization is that the thermal part of the system (solar collectors or covered PV/T) should be as small as possible, that is, a system of only PV modules. The exception is the system with uncovered PV/T modules, where the thermal output is an addition that is not at the sacrifice of the electric output. The results from this study appear to support the idea that it is more efficient to use PV in combination with heat pumps for residential buildings, than it is to use solar thermal collectors. If the ambition is only to reach a net zero energy balance, the best choice would according to the results presented here be a high efficiency PV system (building C*), even though the thermal solar fraction is zero. However, the building that is second closest to reaching the nZEB criterion is the one with a combination of a state-of-the-art PV system and solar thermal collectors (building A*), which has the highest solar thermal fraction.

5.2. Energy performance of PV/T systems

The building with only uncovered PV/T modules (building B1) is the third closest to reaching a net zero energy balance. The thermal solar fraction for this building is only 9%, and the output from the PV/T modules during the summer only reaches moderate temperatures. This means that auxiliary heating is necessary for this building also during the summer, which is not the case for the systems with solar thermal collectors

The two PV/T systems analyzed here were based on the system design of building A, where the solar modules and the heat pump are connected in parallel, and the performance could no doubt be improved with further system adjustments. The seasonal performance factor (SPF) of the heat pump is a sensitivity factor in the analysis. The SPF of the heat pump is around 2.3 for the systems with high solar thermal fraction (A, A* and B2), and 2.5 for the other systems. The SPF is increased since the heat pump is also operational during the summer, when the outdoor temperatures are higher. The same heat pump was used in all the systems and was dimensioned for the winter load, when outdoor temperatures are colder. In particular, the uncovered PV/T system would work better if it was used for preheating, since the temperatures in the collectors are not high enough, even during summer, to provide heating of domestic hot water. In addition to the parallel connection used here, Ille et al. (2014) analyzed systems with PV/T modules and heat pumps in both series and parallel connection. Their studies also included a system with the option of feeding a borehole heat exchanger. With these configurations, the temperature at which the collector loop starts could be lowered and the operation times of

the PV/T modules extended. In such a system it may be possible to utilize the very low temperature output during winter to preheat the input to the heat pump. More research is needed to analyze the usefulness of these systems for Northern European conditions.

As Fig. 8 shows, there is a large difference in the temperature of the thermal output from the uncovered and the covered PV/T modules. The thermal energy output of the covered PV/T system, as applied in building B2, is similar to that of the solar thermal collectors, although a larger area of PV/T modules are required to reach this temperature. Even though the whole available area was used for the installation of uncovered PV/T modules in building B1, temperatures high enough for direct use for DHW preparation were seldom reached The average operational temperature during summer was 40 °C, compared to around 66 °C for the other module types. Comparing the energy yield and net energy demand of building A and building B2 (Fig. 6 and Table 4), there seems to be a benefit from replacing solar thermal collectors with covered PV/T modules.

5.3. The PV/T market

This study is based on solar products that are available on the market. The market for PV/T modules is still small, which means that the analysis is probably in favor of the PV and solar thermal technologies, whose markets are larger and more mature. Even though modules from the upper end of the market in terms of efficiency were used here, they are still far behind the efficiencies found in the PV and solar thermal markets. For example, the state-of-the-art PV modules had an efficiency of over 20%, while the highest electrical conversion efficiency found in a PV/T module was 17.4%. There is also some uncertainty with respect to the performance data of these modules since it is only recently that standards for testing and certification of PV/T modules have been developed. The analysis of the covered PV/T collector is especially uncertain, since there are very few market-available products of this type.

The thermal efficiencies are likewise lower for PV/T modules on the market than for solar thermal collectors, also for the covered ones. The heat loss is also larger from the PV/T modules compared to pure solar thermal collectors. While thermal insulation gives a higher output temperature and thermal output, it reduces the efficiency of the PV cells and also introduces higher demands on the materials used in the modules.

This study is only focused on currently available technology, for PV/T as well as PV and solar thermal. It is difficult to predict the future for PV/T technology, as it depends on both technological and market developments. Some future research areas have been discussed by Michael et al. (2015), including development of better adhesives, improved lamination methods and the use of nanotechnology. Better certification and testing standards are also important for the PV/T market development (Kramer and Helmers, 2013).

5.4. Limitations and further work

The work presented here is based on simulations of one residential passive house with hydronic heating and heat pump, located in a Northern European climate. The results are therefore limited in their validity, and cannot be directly translated to other cases. They can, however, be used to show some general differences between the technologies and to highlight questions for further analysis.

The zero energy balance calculation used here does not include the full life cycle of the building, but is only focuses on energy use during operation. Furthermore, we have used the term 'nZEB' here to mean a zero *energy* building. Future work will also focus on zero *emission* buildings, and will include analyses of the energy and emissions embodied in the building during the construction phase, as well as replacements and deconstruction

Some aspects in the comparison of the solar technologies are left out of the analysis. The zero energy balance is here calculated on an annual basis. A more detailed analysis should take the monthly, daily or even hourly load match into account, which may change the fractions of delivered and exported energy. Such an analysis could also include measures to increase self-consumption of energy.

Another important factor is of course cost, which is likewise not considered here. The cost of PV modules has plummeted during the last few years and the market is expanding, while PV/T is still an emerging technology and the market is relatively small. Exchanging PV modules for PV/T modules also means that a hydronic system is necessary, which may increase the system complexity. Architectural integration is not covered in this paper, but there are clearly benefits of the uniform appearance that can be achieved with PV/T compared to separate installations of PV and PV/T.

6. Conclusions

Three alternative solar energy systems for a single family building were studied through energy performance simulations. The studied systems were a combination of solar thermal and PV (building A), uncovered PV/T or a combination of covered PV/T and PV (building B), and a system with only PV (building C). The systems are based on commercially available modules and standardized templates.

The objective of the comparative study was to evaluate whether the building with the different installations would reach a net zero energy balance. The goal was to balance the energy demand for operation, according to ambition level ZEB-O, as determined by Dokka et al. (2013). The auxiliary energy in the system was provided by an air-to-water heat pump, which meant that the import/export energy balance could be calculated only in terms of electricity.

The results show that the system that gets closest to reaching net zero energy balance according to this definition was the system with only high-efficiency PV modules (building C*), even though the solar thermal fraction in this case was zero. The second closest was the system with high-performance solar thermal collectors and PV modules (building A*), which had the highest solar thermal fraction. However, the interpretation of the results depends greatly on the criteria used in the nZEB definition, what boundary conditions are used, and the choice of a heat pump as auxiliary energy source.

The results suggest that covered PV/T could give an increased output compared to solar thermal collectors. The number of collectors with this technology available on the market is, however, very small, which could partly be due to the material challenges involved in producing these types of modules. The system with uncovered PV/T modules holds up well in this comparison where electricity is favored, but the thermal output is small and of low temperature, which means that an auxiliary energy source is necessary also during summer.

Acknowledgements

This publication was created as part of the Joint Research Centre in Sustainable Energy between Shanghai Jiao Tong University and the Norwegian University of Science and Technology (JRC SJTU-NTNU). The Joint Research Centre is funded by the Research Council of Norway, project number 221 657.

This work is based on the results and research of the Norwegian Research Centre for Zero Emission Buildings (www.zeb.no). The authors gratefully acknowledge the support from the Research Council of Norway and several partners through the ZEB Centre.

The authors would like to thank Laurent Georges at the Department of Energy and Process Technology at NTNU for assistance with developing the Polysun model.

References

Adam, M., Wirth, H.P., Radosavljevic, R., 2014. Verbundprojekt: Standardisierung und Normung von multifunktionalen PVT Solarkollektoren (PVT-Norm). Teilvorhaben: PVT-Systemanwendungen und Simulationen, Düsseldorf.

Aste, N., del Pero, C., Leonforte, F., 2014. Water flat plate PV–thermal collectors: a review. Sol. Energy 102, 98–115.

Chow, T.T., Tiwari, G.N., Menezo, C., 2012. Hybrid solar: a review on photovoltaic and thermal power integration. Int. J. Photoenergy 2012.

Delisle, V., Kummert, M., 2014. A novel approach to compare building-integrated photovoltaics/thermal air collectors to side-by-side PV modules and solar thermal collectors. Sol. Energy 100, 50–65.

Dokka, T.H., Sartori, I., Tyholt, M., Lien, K., Byskov Lindberg, K., 2013. A Norwegian Zero Emission Building Definition. In: Passivhus Norden 2013, Gothenburg, Sweden, 2013.

Dokka, T.H., Wiberg, A.H., Georges, L., Mellegård, S., Time, B., Haase, M., Maltha, M., Lien, A.G., 2013. A zero emission concept analysis of a single family house. The Research Centre on Zero Emission Buildings, Oslo.

EN 15603:2008 – Energy performance of buildings – Overall energy use and definition of energy ratings, European Committee for Standardization (CEN), Brussels, Belgium, 2008.

European Parliament, Directive 2010/31/EU of the European Parliament and of the Council of 19 May 2010 on the energy performance of buildings, Directive 2010/31/EU, Brussels, 2010.

Good, C., Houlihan Wiberg, A., Kristjansdottir, T.F., Georges, L., Hestnes, A.G., 2014. A comparative study of different PV installations for a Norwegian net zero emission building concept. In: Frank, E., Papillon, P. (Eds.), Eurosun 2014. ISES, Aix-les-Bains, France.

Houlihan Wiberg, A., Georges, L., Dokka, T.H., Haase, M., Time, B., Lien, A.G., Maltha, S., 2014. A net zero emission concept analysis of a single-family house. Energy Build. 74, 101–110.

Ille, F., Adam, M., Radosavljevic, R., Wirth, H.P., 2014. Market and simulation analysis of PVT applications for the determination of new PVT test procedures. In: Frank, E., Papillon, P. (Eds.), Eurosun 2014. ISES, Aix-les-Bains, France.

Institute for Energy – Renewable Energy Unit, Photovoltaic Geographical Information System (PVGIS), European Commission, Joint Research Centre.

International Energy Agency, Transition to Sustainable Buildings – Strategies and Opportunities to 2050, Directorate of Sustainable Energy Policy and Technology (SPT), Paris, France, 2013.

Kramer, K., Helmers, H., 2013. The interaction of standards and innovation: hybrid photovoltaic–thermal collectors. Sol. Energy 98 (Part C), 434–439.

Marszal, A.J., Heiselberg, P., Bourrelle, J.S., Musall, E., Voss, K., Sartori, I., Napolitano, A., 2011. Zero energy building – a review of definitions and calculation methodologies. Energy Build. 43, 971–979.

Meteotest, Meteonorm Database, 2009.

Michael, J.J., Iniyan, S., Goic, R., 2015. Flat plate solar photovoltaic–thermal (PV/T) systems: a reference guide. Renew. Sustain. Energy Rev. 51, 62–88.

NS 3031 – Calculation of energy performance of buildings – Method and data, Standard Norge, Lysaker, 2011.

NS 3700 – Criteria for passive houses and low energy houses – Residential buildings, Standard Norge, Lysaker, 2010.

Sartori, I., Graabak, I., Dokka, T.H. Proposal of a Norwegian ZEB definition: Storylines and Criteria. In: Renewable Energy Conference, Trondheim, 2010.

Sartori, I., Napolitano, A., Voss, K., 2012. Net zero energy buildings: a consistent definition framework. Energy Build. 48, 220–232.

Solar Keymark Network, Specific CEN Keymark Scheme Rules for Solar Thermal Product version 21.00, CEN Certification, 2013.

The German Solar Energy Society, Planning and installing photovoltaic systems: a guide for installers, architects and engineers, Earthscan, London, 2013.

Tyagi, V.V., Kaushik, S.C., Tyagi, S.K., 2012. Advancement in solar photovoltaic/thermal (PV/T) hybrid collector technology. Renew. Sustain. Energy Rev. 16, 1383–1398.

Vela Solaris, A.G., 2012. Polysun Simulation Software. Institut für Solartechnik SPF, Rapperswil.

Paper III

Good, C. (2013). *Influence of system lifetime on environmental impact assessments of photovoltaic systems in buildings.* Presented at the Young Researcher Forum at CESB13, Prague.

INFLUENCE OF SYSTEM LIFETIME ON ENVIRONMENTAL IMPACT ASSESSMENTS OF PHOTOVOLTAIC SYSTEMS IN BUILDINGS

Clara Good
NTNU Norwegian University of Science and Technology, Norway, clara.good@ntnu.no

Summary

Increased energy efficiency in buildings is important in order to reduce the global greenhouse gas emissions, and a number of solutions are being developed worldwide. Zero emission buildings (ZEB) are very energy efficient buildings that can cover their small energy needs by local generation of renewable energy. In a full ZEB, the local production should not only cover the emissions associated with the operational energy of the building, but also the emissions embodied in the building during its production.

Solar energy is often the most suitable option for on-site energy generation, technically and architecturally. However, a photovoltaic (PV) solar energy system can contribute significantly to the embodied energy of a building, due to the energy-intensive PV manufacturing process and the anticipated replacement of the system during the building lifetime.

A realistic lifetime estimation for PV systems is important both in the assessment of embodied energy and economic feasibility of PV installations. The aim of this paper is to investigate which factors are used in lifetime assessments of PV systems and how the lifetime influences the embodied energy of a building.

It is found that a lifetime of 30 years is recommended by international guidelines, but that both longer and shorter lifetimes are used as estimates in calculations. Field tests of PV modules, though uncertain, also show evidence of both longer and shorter lifetimes. In addition, the definition of failure of PV systems is to some degree subjective.

Keywords: photovoltaic systems, lifetime, degradation, environmental impact, embodied emissions, zero emission buildings

1 Introduction

The global community needs to drastically reduce its greenhouse gas emissions in order avoid catastrophic climate change. Fossil fuels need to be replaced by renewable energy sources, but a large part of the reductions will also need to be achieved through increased energy efficiency. Buildings represent 40 % of the primary energy use in most countries and are a significant source of greenhouse gas emissions. However, making buildings energy efficient is also one of the most cost-effective ways of reducing the emissions.

Zero emission buildings (ZEB) are very energy-efficient buildings that offset the emissions associated with their small energy needs by renewable energy generation on-site or nearby, thereby reaching a zero emission balance. A full ZEB should not only account for the emissions associated with building operation, but also the emissions related to the construction of the building – the embodied emissions. This also includes the emissions embodied in the energy producing system.

Solar energy is often the most suitable option for on-site generation, technically and architecturally. The increased interest in solar energy, both building integrated installations and power plants, have rightly prompted questions of their environmental impact.

This paper is focused on the environmental impact of photovoltaic (PV) cells for electricity generation. The production of PV cells is energy intensive, and high-energy materials like steel and aluminum are often used in the installations. Recent publications on ZEBs have reported high embodied emissions of PV systems, some as much as half of the embodied emission of the building [1]. Since photovoltaics provides less than 1 % of the global energy today, the total environmental impact is small, but if solar energy is going to be a major energy source in the future, the environmental impact needs to be studied.

Life cycle assessments (LCA) and other estimations of environmental impact are important tools, but the results must not be used without knowledge of the underlying assumptions. The lifetime of a PV system is one factor that has a large impact on the final result. The building lifetime is commonly assumed to be 50-100 years, and materials and components that have a shorter lifetime, such as PV installations, need to be accounted for accordingly.

2 Background

2.1 Photovoltaics systems

Solar energy systems can be used to provide energy, using solar thermal collectors, and electricity, using photovoltaic cells (also called PV cells or simply solar cells). PV cells are the focus of this paper.

There are a number of PV technologies, but crystalline silicon solar cells currently account for about 80 % of the market [2]. The cells are either made from monocrystalline silicon (m-Si cells) or polycrystalline silicon (p-Si cells). The efficiencies have increased continuously, and commercial cells today typically have efficiencies around 12-14 % for p-Si and 14-20 % for m-Si. M-Si cells have a slightly higher efficiency but are on the other hand more expensive to produce.

Silicon solar cell technology for terrestrial applications was developed in the 1950s, and the technology is robust and well proven [3]. The base of the silicon solar cell is a thin wafer of silicon (typically around 200 µm thick). The backside is covered in metal and thin metal lines are added on top of the cell as electrical contacts. The cells are connected by metal strips that are soldered to the cells, into modules of various sizes.

The production of the raw material and the wafer is very energy intensive. The production of m-Si wafers includes one extra step compared to p-Si wafers, and therefore requires even more energy. However, the production processes are continuously getting more efficient. For example, it is estimated that reducing the wafer thickness to 100 µm could reduce the energy required in production by 50 % [4].

A typical silicon solar module is a laminate of a polymer back sheet, the solar cells encapsulated on the front and back by a polymer encapsulant, and a tempered glass frontside. The whole laminate is most often inserted into a metal frame. Typical materials today are a back sheet of Tedlar (polyvinyl flouride, PVF), an encapsulant of ethylene vinyl acetate (EVA) and an aluminum frame.

In other 20 % of the market is composed of a diverse group of technologies called thin film cells. This includes amorphous silicon cells (s-Si), cadmium telluride cells (CdTe) and cadmium indium gallium diselenide cells (CIGS). They typically have lower efficiencies than the crystalline cells, commercial values are around 10-13 %, but are less expensive to produce

[2]. Some of them can also be made flexible, which may be an advantage in building integration.

Thin film cells are a few μm thick and produced on a substrate of glass, metal or plastic, which provides rigidity. In contrast to silicon solar modules, thin film modules are not limited by the size and shape of a silicon wafer, which gives more freedom in shape and size of the modules.

A PV system includes not only the modules but also components such as cabling, mounting structure, inverters (for grid-connected systems) or batteries (for standalone systems). These components are referred to as balance-of-system, or BOS. The design of the BOS is important for the overall performance of the system.

2.2 Environmental impact assessments

There are several ways to assess the environmental impact of a product, with varying degrees of complexity. The cumulative energy demand (CED) is the total energy used in the manufacture of a product. CED should be expressed in terms of primary energy [4]. It is sometimes also referred to as the embodied energy of a product. A corresponding factor is the embodied emissions, which quantifies the greenhouse gas emissions associated with the embodied energy.

The energy payback time (EPBT) is a commonly used factor for energy producing systems. Simply put, it is the CED divided by the annual energy yield of the system, i.e. the number of years it takes for the system to "pay back" its embodied energy [4]. For PV systems, the energy yield depends on the geographic location, cell technology and design of the specific system.

Life cycle assessment (LCA) is a method to account for several environmental aspects and impacts during the complete lifetime of a product or service [5]. LCA is a broad evaluation method that takes into account not only the amount of energy or emissions, but also quantifies their effect on climate change, ecosystems and human health. Consequently, LCA is a complex assessment method and the final result depends greatly on the quality of the data used. The whole lifecycle should be included in the analysis, e.g. material extraction, production and recycling. The data can be measured, calculated, estimated or gathered from relevant databases such as Ecoinvent. The data is gathered in a life cycle inventory (LCI) and interpreted based on the scope and goal of the LCA.

To calculate the environmental impact of a PV system (or any other energy source), the generated energy must also be taken into account. This means that the total impact of the system depends not only on the emissions generated during its lifetime, but also on the emissions avoided by its lifetime energy generation. Accordingly, the expected lifetime of the system, and thereby its total yield, has a strong influence on the results. A useful unit is the specific emissions, which is the emissions required to generate one unit of electricity, expressed as e.g. g CO_2 emissions per kWh.

3 Method

This paper is a review of published results related to lifetime and degradation of PV systems, and how this influences their environmental impact. Particular interest has been given to PV systems integrated into or installed on buildings.

First, guidelines and recommendations of how to assess the environmental impact PV system were reviewed. Secondly, published results from field tests of PV system were studied, to elucidate how and why PV systems fail. Lastly, the influence of PV system lifetime on environmental impact assessments is studied.

4 Results

4.1 Recommendations for life cycle assessment of PV systems

For a PV system, the lifetime environmental impact depends on three major factors: the specific energy yield of the system, the environmental impacts of its production and its lifetime [4]. The specific energy yield is a factor of the efficiency of the modules, the geographic location and other local factors such as shading and orientation. The environmental impacts of the production depend on the type of module, the efficiency of the process, but also on which energy source is used during the production. The lifetime of the system has a large impact on the result, since this determines the total energy production of the system.

The International Energy Agency Photovoltaic Power Systems Programme (IEA-PVPS) has produced guidelines for life cycle assessments of PV modules [6]. The guidelines were created to provide guidance in the areas where the ISO standards give some freedom and thereby giving "consistency, balance and quality" to LCA calculations involving PV modules, and are said to represent a consensus among PV experts in the United States, Europe and Asia.

The guidelines recommend using a lifetime of 30 years for mature module technologies, based on the typical warranties and "the expectation that modules last beyond their warranties". They also recommend using a linear degradation rate of 0.7 % per year, which means that the modules would reach 80 % of their nominal power after 30 years. Cabling and structural components are assumed to have the same lifetime as the modules. The guidelines recommend using a lifetime of 15 years for small scale inverters, while 30 years with 10 % replacement of parts can be used for larger inverters.

4.2 Estimating PV module lifetime

PV module lifetime is often assumed to be 20-30 years for silicon solar cells and 20-25 years for thin film technologies, while higher and lower values can also be found in literature [1, 4, 7, 8]. There is, however, little specific data to support these assumptions. They values are generally based on a combination of warranties, accelerated testing, field tests and estimations. The reliability and lifetime of a PV system is also influenced by the quality and design of the BOS.

4.2.1 Warranties

A PV module today typically comes with a power warranty that guaranties 90 % of the initial nominal power after 10-12 years, and 80 % of the power after 20-25 years of operation. This is a drastic increase from the 5 year warranties in that were typical before the 1990s [9, 10]. The producer's definition of the initial power may, however, allow for both manufacturing tolerance and measurement tolerance, which means that it can be significantly lower than the stated nominal power [10].

PV modules are often considered to be the most reliable part of a PV system. In general, PV modules do not experience one catastrophic failure resulting in system break-down, but rather a slow, steady degradation in performance. There are few returns of PV modules but most results are, however, the result of such a catastrophic failure. A reason for this is that it is very difficult to monitor the performance of individual modules in a PV system, and underperforming modules may therefore go unnoticed [10].

4.2.2 Accelerated testing

In order to assure high reliability and quality of PV modules, the International Electrotechnical Commission (IEC) has introduced a set of standards for accelerated tests, so-called type approval tests, leading to module certification. Most modules on the market today are certified. The standard (IEC 61215 [11] for crystalline silicon modules, IEC 61646 [12] for thin film modules and IEC 62108 [13] for concentrator modules), describe the so-called "design qualification and type approval". This series of test attempts to simulate long-term outdoor exposure, including for example hot-spot endurance, thermal cycling and humidity-freeze tests. To pass the qualification test, the modules must meet the criteria for maximum power degradation, electrical safety and level of visual defects.

The type approval test is a way for the producers to verify that their modules meet a minimum standard. However, the test does not guarantee that the module survives 25 years of outdoor operation, nor does it provide a definite value of module lifetime [9]. A general view seems to be that the tests are only useful to detect early product failure [14]. In fact, about a third of the modules fail the type approval tests [15]. Several authors point out the need for better adaptation of the accelerated tests to reveal failures that actually occur in the field.

4.2.3 Field tests

So far, the only way to reveal actual failure modes for PV module is field testing. A number of field tests a performed worldwide since the 1970s but as they were not performed according to one certain method, it may be difficult to compare the results [16]. The degradation of PV systems may also depend on other components than the modules.

Another reported problem with field testing is the time scale. It is not possible to test a module for 25 years before it is introduced in the market. In addition, the modules that have been in operation for 25 years today are not representative for current module production, and test results cannot be used directly.

The degradation rate of 0.7 % (which leads to 80 % of initial module power after 30 years) that is stated in the IEA guidelines refers to results from field tests published by Skoczek et al. [9]. They studied the performance of 204 crystalline silicon modules after an average of 21 years of field exposure at the Joint Research Center in Ispra, Italy. The average degradation rate was found to be 0.8 % per year, or 0.67 % of the modules that failed completely were excluded. However, a difference was found between modules that had been connected to a battery charger and those in open circuit conditions, where the latter category performed significantly better.

A comprehensive review of PV module field testing during the last 40 years was recently published by Jordan and Kurtz at the U.S. National Renewable Energy Laboratory (NREL) [17]. The paper gathers data from nearly 2000 degradation measurement on modules and systems worldwide. Several module technologies were studied. The review concludes that the average degradation of the modules was 0.8 % per year with a median value of 0.5 %. The average degradation for thin film modules was larger than for crystalline silicon modules, but the difference had narrowed since year 2000.

The degradation rates presented in the review vary significantly. However, 78 % of the modules in the study showed a degradation rate of less than 1 %. Some studies presented measured rates down to 0.17 % [18]. If this rate was assumed to continue, it would mean that the modules reached 80 % of their initial power after 130 years. (Such a performance is, however, very unlikely.)

Jordan and Kurtz [17] also points out that the modules in the field tests may not represent a statistically valid selection. Modules with high degradation rates are unlikely to be left in the field and reported on as often as those with low degradation rates. In fact, the

authors found that the reported annual degradation rates were lower the longer the field exposure. In addition, some of the field studies rely on a small number of tests.

4.2.4 Common degradation issues

Disregarding the differences in degradation rates, the field studies have identified a number of commonly occuring degradation mechanisms. Regularly occurring issues were discoloration, delamination or bubbles in the encapsulant; back sheet cracks; soiling/ingrained dirt in the glass; hot spots; corrosion in the metal interconnects between the cells and in the connection to the junction boxes; and glass breakage. [9, 15, 16]

Quintana et al. [16] identified five categories of degradation: packaging material degradation, adhesional degradation, interconnect degradation, degradation from moisture intrusion and finally degradation of the semiconductor device. Roughly 90 % of the failures in the field are reported to be caused by damages to cell interconnects, circuitry and packaging, and not to the solar cells themselves [19]. Ferrera and Philipp [15] found the polymers in the modules to be the weakest point.

While degradation of the semiconductor material may be a factor, it is not a primary cause of performance loss. The exception is a phenomenon called 'light-induced degradation', which causes a decrease in output of 1-3 % during the first few hours of light exposure [16]. In accordance with this, field studies have also reported a higher performance loss during the first year [9].

The local climate and environment has an effect on the degradation of PV modules. Outdoor weathering of PV modules is the result of environmental stresses such as temperature fluctuations, precipitation, humidity, wind, sand, pollution etc. High temperature is well known to decrease the efficiencies (especially for silicon modules) of PV modules during operation, but can also contribute to module degradation.

While sunlight is essential to energy production, it is also damaging to modules. High temperature is both a stress and an acceleration factor. It can speed up other reactions, such as crack formation. In addition to temperature stresses, the UV radiation can cause degradation both on the inside and outside of the modules [15].

Very high temperatures that occur it hot-spots are reported to have burned holes through the back sheet and cracked the glass. Hot-spots in modules can occur in faulty modules, but also as a result of local shadowing of parts of modules. This highlights the importance of a well-designed system.

Water in the form of rain or humidity can enter into modules with damaged packaging and lead to delamination and corrosion. Hail and sand can damage the glass through abrasion. Wind and snow subjects the modules to mechanical loads [15].

4.3 PV systems in buildings

Due to the relative novelty of the concept of building integrated PV (BIPV), there are not many examples of 25 year old systems available. Overheating is possibly a larger problem for building integrates systems than free-standing systems, which may cause modules to degrade faster. On the other hand, façade integrated systems in cold climates have reported low degradation rates, possibly related to reduced snow load [17].

However, the evaluation of lifetime and the assessment of different failures types may not be the same for BIPV systems as for free-standing or roof mounted systems. For a highly visible façade integrated system, visual degradation may for example be considered a problem, even if the energy production was still satisfactory. On the other hand, a lower energy production could be tolerated if the modules showed no visible signs of degradation [16].

Replacement of PV systems in buildings may also be more complicated than the replacement of free-standing systems. In some cases, the owner may choose to not replace the system at all. In the example of the BIPV wall on the Solaire Building in New York City [7], the architect and designer stated that the PV system it was not likely to be replaced, even if they were no longer functioning, unless the owners wanted an esthetic change. In this case, the PV system was estimated to have the same structural lifetime as the building itself, even though the period of energy production was shorter.

4.4 Influence of lifetime on environmental impact

Since the PV system generates energy during its lifetime, the specific emissions, i.e. emissions per generated energy unit, is a useful factor for assessment of environmental impact. The PV module lifetime thus has a large influence, since it determines the total energy generation of the system. Simply put, for a particular PV system, the environmental impact of the produced energy is directly proportional to the inverse of the lifetime [4].

Results from a simplified calculation of the influence of lifetime on the specific emissions of PV are shown in **Fig. 1**. The PV system is a freestanding, optimally oriented system with crystalline silicon modules. The specific emissions are calculated for lifetimes of 20 to 50 years for three locations in Europe with different annual irradiation: Trondheim (1000 kWh/m^2), Prague (1200 kWh/m^2) and Rome (1700 kWh/m^2). The specific emissions are expressed relative to the reference case (100 % in the figure) which is a system in Trondheim with a 30 year lifetime. Irradiation and yield data is gathered from PVGIS [20]. An annual degradation rate of 0.7 % is assumed for all systems.

If the base case system in Trondheim was instead expected to generate energy for 40 years, the specific emissions are reduced to 78 %. On the other hand, if 20 years is used, the specific emissions are 45 % higher.

The energy that a PV system generates over its lifetime is of course also dependent on the level of irradiation at the site. The specific emissions for a PV system in Rome are lower than in Trondheim due to the higher level of irradiation. As **Fig. 1** shows, the specific emissions for a PV system with a lifetime of 20 years in Rome are approximately the same as for a system with a lifetime of 35 years in Trondheim. It should be note that this is a simplified calculation which is only meant to roughly illustrate the influence of lifetime and location on specific emissions.

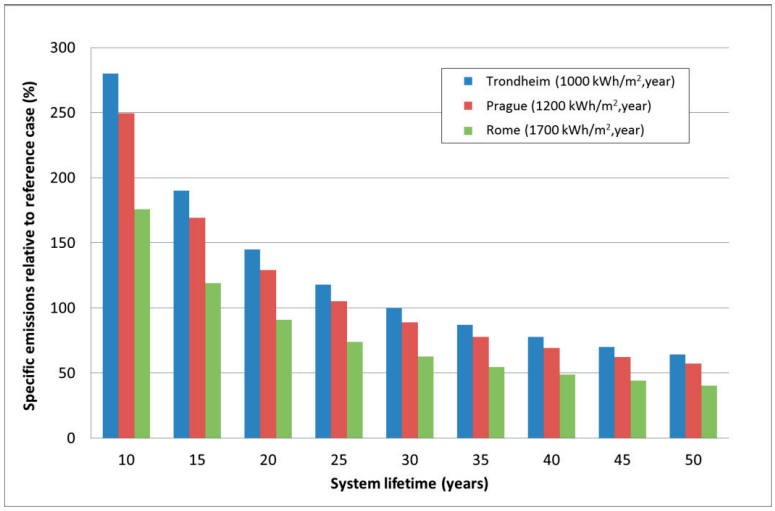

Fig. 1 The change in specific emissions depending on lifetime of a PV system in three European locations with different annual irradiation. The reference case is a system in Trondheim with a lifetime of 30 years. Annual degradation of 0.7 % is assumed for all systems.

5 Discussion

The design of the PV system is important for its long term performance. Local shading may lead to hot-spots, which can cause severe damage to the modules. In areas with large snow loads, the angle of the modules should be adjusted to let snow slide off easily. Overheating is damaging to PV systems both in the short and long term. It is therefore important to ensure proper ventilation around the modules, especially in building integrated systems.

There is no consensus on the failure definition for solar systems. As the field studies show, most modules do not experience a catastrophic point of failure, but rather a steady degradation. A power reduction to 80 % of the initial power is often considered as the failure point. As Jordan and Kurtz [17] point out, a high-efficiency module with 50 % degradation may still perform better than a less efficient module at its initial power. Ultimately, the failure definition is subjective and may be different from case to case. If the energy generation still is satisfactory to the owner, it cannot be said to have reach its failure point. BIPV systems may even be considered to have two lifetimes: one as an energy generating unit and one as a structural building component.

LCAs involve complex calculations as well as a number of assumptions and estimations. A common estimation of building lifetime is 60 years, and it is difficult to predict what replacements and improvements that will be made in the future. If the recommended PV system lifetime of 30 years is used in the calculations, how should the replacement system be estimated? Should an increased efficiency and lifetime of the modules be expected for the new system, and how should the embodied emissions be estimated? These choices have a large impact on the resulting LCA.

6 Conclusions

Published literature on life cycle assessments of PV systems has been reviewed. Recent calculations of LCA of buildings reveal that PV systems account for a large fraction of the embodied emissions.

The three major factors that influence the environmental impact of PV systems is the specific yield, the impacts of production and the lifetime. LCA results always include a number of estimations and assumptions. For PV systems, these assumptions include the expected lifetime and degradation rate, projected efficiencies of future modules and BOS.

The IEA recommends using a lifetime of 30 years for PV modules in in LCA calculations, based on module warranties, published field studies and some assumptions. PV module producers typically guarantee that the modules produce 80 % of the initial energy after 25 years. PV modules are certified according to standardized accelerated testing. These tests confirm that the modules satisfy minimum quality standards, but do not guarantee a lifetime of 25 years. Actual module lifetimes depend on the system design, the geographic conditions and how the system is operated.

Knowledge on how PV modules degrade may also help system designers to design durable systems. In addition, since the general failure of PV systems is a gradual degradation, the definition of failure is to some degree subjective and depends on what the system owner is willing to tolerate. More results from field tests are necessary to provide reliable information on PV module lifetimes. In addition, field degradation data can make it possible design accelerated tests that better reproduce the actual failures that occur in the field.

7 Acknowledgements

The author would like to thank Aoife Houlihan Wiberg at NTNU for valuable discussion during the work with this paper.

References

[1] HAASE, M. & GRUNER, M. F*rom Passive House to Zero Emission Building from an Emission-Accounting Perspective,* in Passivhus Norden 2012, L. Postmyr, Editor 2012, Akademika forlag Trondheim, Norway.

[2] EDENHOFER, O. *Renewable energy sources and climate change mitigation: special report of the Intergovernmental Panel on Climate Change2012*, New York: Cambridge University Press. XII, 1076 s. : ill.

[3] GREEN, M.A. *Silicon photovoltaic modules: A brief history of the first 50 years.* Progress in Photovoltaics: Research and Applications, 2005. 13(5): p. 447-455.

[4] LUTHER, J. & BUBENZER, A. *Photovoltaics guidebook for decision-makers: technological status and potential role in energy economy2003,* Berlin: Springer. XXX, 266 s. : ill.

[5] ISO, *Environmental management -- Life cycle assessment -- Principles and framework*, in ISO 14040:20062006. p. 20.

[6] FTHENAKIS, V., FRISCHKNECHT, R., RAUGEI, M., KIM, H. C., ALSEMA, E., HELD, M. & WILD-SCHOLTEN, M. D. *Methodology Guidelines on Life-Cycle Assessment of Photovoltaic Electricity*, 2011.

[7] PEREZ, M. J. R., FTHENAKIS, V., KIM, H. C. & PEREIRA, A. O. *Façade-integrated photovoltaics: A life cycle and performance assessment case study.* Progress in Photovoltaics: Research and Applications, 2012. 20(8): p. 975-990.

[8] PENG, J., LU, L. & YANG, H. *Review on life cycle assessment of energy payback and greenhouse gas emission of solar photovoltaic systems*. Renewable and Sustainable Energy Reviews, 2013. 19: p. 255-274.

[9] SKOCZEK, A., SAMPLE, T. & DUNLOP, E. D. *Resluts of Performance Measurements of Field-aged Crystalline Silicon Photovoltaic Modules.* Progress in Photovoltaics: Research and Applications, 2009. 2009(17): p. 227-240.

[10] VÁZQUEZ, M. & REY-STOLLE, I. *Photovoltaic module reliability model based on field degradation studies*. Progress in Photovoltaics: Research and Applications, 2008. 16(5): p. 419-433.

[11] IEC, *IEC 61215: Crystalline silicon terrestrial photovoltaic (PV) modules – Design qualification and type approval,* 2005.

[12] IEC, *IEC 61646: Thin-film terrestrial photovoltaic (PV) modules - Design qualification and type approval,* 2008.

[13] IEC, *IEC 62108: Concentrator photovoltaic (CPV) modules and assemblies - Design qualification and type approval*, 2008.

[14] HERRMANN, W. & BOGDANSKI, N. *Outdoor weathering of PV modules - Effects of various climates and comparison with accelerated laboratory testing.* 2011. Seattle, WA.

[15] FERRARA, C. & PHILIPP, D. *Why do PV modules fail?* 2012. Singapore.

[16] QUINTANA, M. A., KING, D. L., MCMAHON, T. J. & OSTERWALD, C. R. *Commonly observed degradation in field-aged photovoltaic modules*. in Photovoltaic Specialists Conference, 2002. Conference Record of the Twenty-Ninth IEEE. 2002.

[17] JORDAN, D. C. & KURTZ, S. R. *Photovoltaic Degradation Rates - An Analytcal Review.* To be published in Progress in Photovoltaics: Research and Applications, 2012.

[18] HEDSTRÖM, J. & PALMBLAD, L. *Performance of old PV modules - Measurement of 25 years old crystalline silicone modules,* in Elforsk Report2006.

[19] MCMAHON, T. J. *Solar cell/module degradation and failure diagnostics.* in Reliability Physics Symposium, 2008. IRPS 2008. IEEE International. 2008.

[20] INSTITUTE FOR ENERGY, R. E. U. *Photovoltaic Geographical Information System (PVGIS)* [Online]. European Commission, Joint Research Centre. [Accessed 31 January 2013].

Paper IV

Good, C. (2016*). Environmental impact assessments of hybrid photovoltaic–thermal (PV/T) systems – A review*. Renewable and Sustainable Energy Reviews, 55, 234-239. doi:http://dx.doi.org/10.1016/j.rser.2015.10.156

Renewable and Sustainable Energy Reviews 55 (2016) 234–239

Contents lists available at ScienceDirect

Renewable and Sustainable Energy Reviews

journal homepage: www.elsevier.com/locate/rser

Environmental impact assessments of hybrid photovoltaic–thermal (PV/T) systems – A review

Clara Good

Department of Architectural Design, History and Technology, Norwegian University of Science and Technology (NTNU), Alfred Getz vei 3, 7491 Trondheim, Norway

ARTICLE INFO

Article history:
Received 26 August 2015
Received in revised form
28 October 2015
Accepted 30 October 2015

Keywords:
Photovoltaic–thermal
PV/T
Environmental impact assessment
Life cycle assessment
LCA

ABSTRACT

In a hybrid photovoltaic–thermal (PV/T or PVT) module, electricity and thermal energy are generated simultaneously in the same module. By combining a PV module and a solar thermal collector, more of the solar radiation can be harvested, and the total efficiency of the module is increased. The combination of two technologies in one module also has the potential to reduce the use of materials and the required space. In order to assess and quantify these possibilities, several research groups have presented life cycle assessments (LCA) of different PV/T concepts and installations. This paper presents a review of the published results, and aims to find a common ground. In general, the payback time for both energy and greenhouse gas emissions of the PV/T systems are much shorter than their expected lifetime. However, due to the use of different methods and unclear data sources, it is difficult to make any wide-ranging conclusions about the environmental impact of PV/T modules.

Contents

1. Introduction

In a hybrid photovoltaic–thermal (PV/T or PVT) module, electricity and thermal energy is generated simultaneously in the same module. The basic idea of the concept is to utilise more of the solar radiation by also harvesting the waste heat that is generated in photovoltaic (PV) modules. Since PV cells generally become less efficient with increasing cell temperature, the heat removal has a

Abbreviations: PV, photovoltaic; PV/T, photovoltaic–thermal; LCA, life cycle assessments; LCI, life cycle inventory; GWP, global warming potential; CED, cumulative energy demand; IPCC, Intergovernmental Panel on Climate Change; BOS, balance of system (auxiliary components for PV systems)

E-mail address: clara.good@ntnu.no

http://dx.doi.org/10.1016/j.rser.2015.10.156
1364-0321/

double benefit: the waste heat is utilised and the modules are cooled.

The technology is not new; the first studies were published in the mid-1970s, and several different concepts and ideas have been studied during the past decades. A number of reviews have been published on the topic of PV/T technology in the last couple of years, for example by Zhang et al. [1], Tyagi et al. [2] and Chow et al. [3]. The focus of these reviews spans from laboratory work on new concepts to examples of applications. There are also a number of publications describing pilot installations of PV/T systems for different applications in many parts of the world, including buildings.

The combination of two technologies in one module also has the potential to reduce the use of materials, the time of installation, and the required space. In order to assess and quantify this possibility, several research groups have presented environmental impact assessments of PV/T modules and systems, for example using lifecycle assessments (LCA). LCA is a method used to evaluate the environmental impact of a product or service over its entire life cycle.

This paper presents a review of publications concerning LCA of PV/T technology, and aims to find a common ground in the assessments. It is found that most of the publications focused on custom-made modules and systems, which is not surprising due to the small size of the PV/T market. Most of the studies also focused on payback times for energy and greenhouse gas emissions.

The paper starts with a description of the methodology in Section 2. The results of the review are presented in Section 3, followed by a discussion in Section 4 and a summary of the conclusions in Section 5.

2. Method

This section starts with a description of the method used for performing the review (Section 2.1), followed by an introduction life cycle assessments (LCA), which is one of the more common methods for evaluation of environmental performance (Section 2.2). A selected number of assessment metrics for energy systems are described in Section 2.3.

2.1. Review method

This paper is based on information found in scientific publications from peer reviewed journals and conferences. Direct information from companies has also been used. Some of the figures presented in the results section are converted from or calculated based on data in the reviewed publications, in order to make it easier to compare the results against each other.

2.2. Life cycle assessments (LCA)

LCA is a methodology for assessment of the environmental impact of a product or service over its whole life cycle. Depending on the scope of the assessment, this may include all processes from the extraction of raw materials to recycling or disposal. An international standard for the performance of an LCA is described in [4], and should be divided into the four following steps:

1. Goal and scope definition.
2. Life cycle inventory (LCI).
3. Life cycle impact assessment (LCIA).
4. Interpretation.

The goal and scope is an important step, where the objective, choice of functional unit, and boundary conditions of the study are determined. These choices can have a big impact on which data needs to be collected, and on how the collection should be performed.

The data on processes and materials is gathered in a life cycle inventory (LCI). The source of the data can be either direct measurements or data from production, generic input from data bases, or a combination.

An assessment of the large amount of LCI data is performed through life cycle impact assessment (LCIA) methods, where the impacts are categorised. Different methods use different categorisations that focus on different impacts, for example damage to ecosystems, acidification, or global warming. Some methods only focus on a single issue.

In the interpretation phase, the results of the assessment are evaluated based on the objectives determine in the first phase. A common objective of LCAs is to find the environmental “hot spots” in the production, or to compare alternative products based on specific criteria.

2.3. Assessment of energy systems

In the assessment of renewable energy systems, one also needs to consider the avoided environmental impact by not using more polluting sources of energy. This impact depends on the amount of energy that can be generated by the system, but also on the type of energy which is replaced. Both these factors depend on local conditions, which mean that results from two different studies cannot be directly compared.

Most of the studies that were reviewed for this paper focused on the payback time for energy (EPBT) or greenhouse gas emissions (GPBT) of a specific system in years. The energy payback time is a measure of how many years of operation it takes for the system to generate the same amount of energy that was required for its production, the so-called embodied energy. The payback time therefore depends both on how and where the system was produced, as well as its energy performance during operation. An energy efficient production, high use of renewable energy, and a well-performing system lead to low values of EPBT.

A simplified calculation method for EPBT (years) is shown in Eq. (1), where CED (kWh) is the cumulative energy demand of the production, and E_{out} (kWh/year) is the annual energy output of the system. A more detailed calculation will also include energy use for operation and maintenance, as well as degradation of the modules.

$$EPBT = \frac{CED}{E_{out}} \tag{1}$$

A weakness of the EPBT is that it does not take into account the expected lifetime of the system and its components, which means that the EPBT can be longer than time the system is expected to operate. Another factor that can be used to avoid this is the energy return on (energy) investment (EROI), which can be calculated from the EPBT according to Eq. (2), where L (years) is the expected lifetime of the system [5]. If the value of EROI is lower than 1, it does not have a net energy output during its lifetime.

$$EROI = \frac{L}{EPBT} \tag{2}$$

A complicating factor in the case of PV/T systems is that the output is distributed over two energy carriers (electricity and heat). This means that it is necessary to use some form of conversion factors or method to be able to compare the two. Common factors are primary energy, exergy or CO_2 emissions.

3. Results

3.1. Overview

Several research groups have studied the environmental impact of PV/T systems, although the number of published studies is small compared to that of PV systems. An overview of the publications is presented below and a summary of some of some key parameters are shown in Table 1.

Not all of the studies follow the LCA methodology, as described by ISO [4], or use only parts of it. Two commonly used impact factors are the global warming potential at 100 years (GWP100), as defined by IPCC [6], and the cumulative energy demand (CED) or primary energy resources (PER). Some of the research groups have used the LCA software SimaPro [7] to perform their analyses.

The embodied energy demand of the installations in the publications was given based on the functional unit. It has here been recalculated to a common unit (kWh/m^2 installation) to enable comparison. The GWP100 is likewise recalculated to a common unit (kg CO_2 eq/m^2 installation). The values are shown in Table 1.

All studies included the balance of system (BOS) in the calculations. The term BOS refers to all components, in addition to the solar modules, that are necessary for the system to function, such as inverter, storage tank, and mounting rails. The studies differ in what is included in the BOS, and how often (if ever) the components are replaced. The EPBT was in the range 0.8–14.33 years and the GPBT 0.8–4.0 years.

The expected lifetime is also a factor that differs between the studies. Most publications report an expected lifetime of 15–30 years, but some also report expected lifetimes of up to 45 years [8]. However, this difference does not have an impact on the calculations of EPBD and GPBT, since the payback times in all of the cases are much shorter than the expected lifetimes.

The EROI was not given in the publications, but has been calculated here and is shown in Table 1. The calculations are performed with the average of the lifetimes given in the publication, if no more specific data is given. The calculated values of EROI ranges from 1.4 for the a-Si modules in the study by Crawford et al. [9] to 34.1 for the HIT modules in the study by Kamthania and Tiwari [10].

ISO [4] describes the functional unit as the "quantification of the identified functions (performance and characteristics) of the product". All inputs and outputs relates to the functional unit, which ensures that the results can be compared. The choice of functional unit varies significantly between the studies. Some use 1 m^2 module area [8], 1 m^2 roof area [11], 1 kW_p installation [12], or the whole PV/system [13]. In other cases, no functional unit is specified.

3.2. PV/T systems with liquid heat carrier

Tripanagnostopoulos et al. [13] conducted experimental studies on water-cooled PV/T modules at University of Patras in Greece. Modules with and without glazing, working at different operating temperatures were compared. A reference PV system was used, and the effect of adding stationary aluminium reflectors to all systems was analysed. An LCA was performed to verify the benefit of using heat removal. The energy payback time was calculated based on the energy source that is being replaced (electricity or natural gas). The shortest EPBT was found to be for glazed PV/T modules at the lowest studied operating temperature (25 °C), replacing electricity (European grid mix). The EPBT of this system was 0.8 years, a 70% reduction compared to the reference PV module (2.9 years). A system with unglazed modules at the same conditions had an EPBT of 0.9 years. For an operational temperature of 45 °C, which was the highest temperature studied, the

Table 1
Key findings in the reviewed publications. (Data in *italics* is calculated based on data given in the publications).

Publication	PV/T technology	System description	PV efficiency [%]	Location of system	Embodied energy [kWh/m^2]	Embodied emissions [kg CO_2eq/m^2]	EPBT [years]	*EROI [dimensionless]*	GPBT [years]
Tripanagnostopoulos, et al. [13]	PV/T-liquid, glazed and unglazed	Optimally inclined (38°) on flat and tilted roof	*10.6–12.6*	Patras, Greece	*1281* (glazed module)*	*396 (glazed module)**	0.8–4.1	*4.9–25.0*	0.8–2.2
Battisti and Corrado [12]	PV/T-air	On flat and tilted roof, also building integrated	10.7	Rome, Italy	*1442*	*451*	1.7–2.8	*8.0–13.2*	1.6–2.8
Tripanagnostopoulos, et al. [15]	PV/T-air, glazed and unglazed	Optimally inclined (38°) on flat and tilted roof	*10.6–12.6*	Patras, Greece	*1074–1194**	*343-377**	0.9–2.0	*15.0–33.3*	1.3–2.2
Crawford et al. [9]	PV/T-air	Building integrated	Not mentioned	New, South Wales, Australia	*6570–8064 (c-Si) 4575–4738 (a-Si)*	–	6–14 (c-Si) 4–9 (a-Si)	*1.4–3.3 (c-Si) 2.2–5.0 (a-Si)*	–
Tiwari et al. [8]	PV/T-liquid	Open field and roof-top. Optimal inclination. Battery included.	11	New Dehli and Leh, India	*1380–2078*	–	11.4–14.33	*2.4–6.6*	–
Chow and Ji [14]	PV/T-liquid	Free-standing at optimal angle and façade integrated	13	Hong Kong	*1303–1726*	*387–513*	2.8–3.8	*5.9–8.0*	3.2–4
Kamthania and Tiwari [10]	PV/T-air (9 different PV technologies)	Semi-transparent façade integrated.	5–17 (different technologies)	Srinagar, India	*603–1772*	–	0.86–2.37 (energy) 3.19–9.28 (exergy)	*3.7–34.1*	–
Agrawal and Tiwari [16]	PV/T-air	Free-standing, inclination 30°	Not mentioned	New Dehli, India	*1235*	–	1.7 (energy) 7.88 (exergy)	*3.8–16.7*	–

* Reflectors not included in embodied energy and emissions figures.

EPBT was 2.2 and 3.6 years respectively. Interestingly, the study also found that even though the aluminium reflectors added to the total embodied energy of the system, the energy and emissions payback time was decreased by 6.9% and 7.4% respectively.

Tiwari et al. [8] calculated the embodied energy, EPBT, yield factor, and embodied CO_2 emissions of PV/T-liquid systems in two locations in India (New Dehli and Leh). The impact of BOS, mounting system (in-roof or open-field), degradation, and component replacements were studied. They found that the EBPT ranged from 5.33 years without BOS, to 14.33 years with BOS, degradation and replacements. The highest value (14.33 years) was for a non-integrated system with degradation of the modules and replacement of the battery bank every fifth year, which appears to be a quite pessimistic scenario. The EBPT was nevertheless found to be lower than for a pure PV system. The embodied GHG emissions were calculated for 1 m^2 per year, a unit which is not easily comparable to other publications. The embodied emissions ranged from 21.26 kg CO_2 eq/m^2 year to 38.76 kg CO_2 eq/m^2 year.

Chow and Ji [14] studied two PV/T-liquid systems in Hong Kong, of which one was optimally inclined and free-standing, and one was integrated into a façade. Both systems worked with the thermosiphon principle and included a water storage tank at the upper part of the installation. A thorough inventory of the systems was performed. Data for the inventory was taken from other publications and the Hong Kong Government Electrical and Mechanical Service Department (EMSD). Payback times for cost, energy and greenhouse gas emissions (CPBT, EPBT and GPBT) were calculated for the two systems. The EPBT was calculated to 2.8 years for the free-standing system and 3.8 years for the façade integrated system. The corresponding GPBT were 3.2 and 4.0 years, respectively.

3.3. PV/T with air as heat carrier

A thorough investigation of a PV module with air heat recovery was performed by Battisti and Corrado [12] in Italy, where the heat recovery was introduced as a step to improve PV performance. They calculated the cumulative energy demand (CED), global warming potential (GWP100) using SimaPro 5.1 and Ecoindicator'95 impact assessment method. Both primary data from producers and generic data were used. The production of PV modules was found to account for the major part of the energy demand, but the mounting structure also accounted for around 6% of the CED. The energy and greenhouse gas payback times (EPBT and GPBT) were calculated based on energy replaced. The EPBT and GPBT were 1.7–2.8 and 1.6–2.8 years, respectively. The corresponding numbers for a standard PV module was 3.3 and 4.1 years.

In a later study by Tripanagnostopoulos et al. [15], the environmental impact of PV/T-air collectors are studied in a similar manner to the PV/T-liquid collectors [13]. The study includes glazed and unglazed PV/T-air modules, also with the inclusion of aluminium diffuse reflectors. The analysed systems are installed in Greece, either mounted at optimal tilt angle on a flat roof, or integrated into a tilted roof with the same angle. The EPBT was 1.0–2.0 years for the unglazed systems, and 0.9–1.9 for the glazed systems, compared to 2.9–3.2 years for the reference PV system. The GPBT is 1.3–2.3 for the unglazed system, 1.2–2.2 years for the glazed system, and 2.7–3.1 years for the reference PV systems. The authors found that the payback times were shorted for the PV/T-liquid systems compared to the PV/T-air systems, depending on the lower thermal efficiency of the latter. However, all of the PV/T systems achieved lower payback times than the reference PV systems, proving the benefit of the hybrid technology.

Crawford et al. [9] studied building integrated crystalline (c-Si) and amorphous silicon (a-Si) systems with a heat recovery unit, and compared it to a c-Si system without heat recovery. The heat recovery unit, which was attached to the backside of the modules, was made of a black-painted and insulated plywood duct, with a fan forcing air through. The authors used a hybrid LCA approach, which combined process based analysis with input–output (I–O) analysis, arguing that this would give a more comprehensive embodied energy assessment. The embodied energy and energy payback time of the systems were calculated. It was found that the EPBT ranged from 6 to 14 years for the c-Si modules with heat recovery, and 4–9 years for the a-Si modules. Without heat recovery, the EBPT ranged between 12 and 16.5 years, proving that there was a significant benefit of installing a heat recovery unit. The large span in EPBT was due to the fact that low and high values of the embodied energy from silicon production were used, as well as two different thermal energy output scenarios (electricity and gas).

Kamthania and Tiwari [10] studied the energy metrics, including embodied energy demand and energy payback time, of a semi-transparent double pass PV/T façade with air as heat carrier. Three different system configurations were considered, where the PV/T modules were connected either in series, parallel, or a combination of the two. The performance of 9 different PV technologies was studied, including both crystalline silicon and thin film alternatives such as CIS, CIGS and CdTe. The embodied energy for each of the systems were calculated, and it was found that the use of crystalline silicon cells resulted in the highest embodied energy, while CIGS cells resulted in the lowest. The energy payback time ranged between 0.86 years for the CIGS system to 2.37 years for the crystalline silicon system. The EPBT based on exergy calculations ranged from 3.19 to 9.28 years.

Agrawal and Tiwari [16] conducted an “enviroeconomic” study of PV/T-air modules, where also earned carbon credits were included as a factor. The embodied energy of the collector is calculated based on a component breakup with quantities and energy densities; however, no source was given for the energy densities. The energy payback time is calculated to 1.8 years based on annual thermal energy gain and 7.88 years based on annual exergy gain. The output is assumed to replace electricity from coal.

3.4. Comparing electricity and heat

A complication factor in the case of PV/T systems is that the output is distributed over two energy carriers (electricity and heat). This means that it is necessary to use some form of conversion factors or method to be able to compare the two.

The reviewed publications have solved this issue in different ways, although most have evaluated the output based on the type of energy which is replaced. The electricity is usually assumed to replace grid electricity on the location of the installation. The thermal energy output is evaluated based on the source of energy that would otherwise be used for heating. One research group also converted the output to exergy [10,16].

The grid electricity has different environmental impact, or emission factors, in different countries and regions. The grid emissions factor is most often expressed in CO_2 eq/kWh. It is evident that an installation in a location with a more polluting grid has a larger positive environmental impact than an installation in a location with a “greener” grid.

Tripanagnostopoulos et al. [13] assumed that the electricity from the solar energy system replaces electricity with a European grid mix (0.6 CO_2 eq/kWh). The thermal energy is assumed to replace either natural gas or an electric boiler, with the emission factors 0.3 and 0.6 CO_2 eq/kWh respectively. They thus concluded that the benefit was largest when the systems replaced an electric

boiler. For their later study of PV/T air collectors [15], the authors included three scenarios for the thermal output: 12 months use for space heating, 6 months use for space heating, and finally 6 months use for space heating and 6 months use for pre-heating of domestic hot water. They found that the benefit was larger the longer the thermal output was used, and that the third scenario, with both space and water heating, was an interesting alternative for domestic applications.

Crawford et al. [9] also assumed that thermal energy would replace either electricity or natural gas. Primary energy factors natural gas (1.4) and the electricity grid (3.1) and New South Wales, Australia were used. The authors also used efficiency factors for of 0.7 and 1.0, respectively. Consequently, the benefit from replacing electricity was found to be larger than replacing gas.

Kamthania and Tiwari [10] converted high grade electricity output to low grade thermal output, by dividing it with the conversion coefficient for a thermal power plant in India (0.38). The EBPT was then calculated based on this overall thermal performance of the system. They also performed similar calculations based on exergy, in which case the EPBTs were found to be significantly longer.

Agrawal and Tiwari [16] also calculated the EPBT based on overall thermal energy and exergy, and also found longer payback times based on exergy. They assumed that output replaced electricity from coal, which has a GHG emission factor of 0.96 kg CO_2 eq/kWh, but with transmission losses (40%) and efficiency losses in equipment (20%) it was assumed to be 2.0 kg CO_2 eq/kWh.

Battisti and Corrado [12] used the Italian grid mix, which has an emission factor of 0.8 kg CO_2 eq/kWh. They also introduce a "use coefficient", C_u, to account for the different values of thermal energy when used for different purposes. Thermal energy replacing energy for DHW preparation (coefficient 0.6) was calculated to be more valuable than thermal energy replacing space heating (coefficient 0.2).

Chow and Ji [14] assumed that heat and electricity replace town gas (0.2 kg CO_2 eq/kWh) and electricity from the grid (0.7 kg CO_2 eq/kWh), respectively. A heat-to-electricity factor of 0.3 is used in the computation.

4. Discussion

The number of studies on the environmental impact of PV/T modules and systems is still small. It is therefore difficult to draw any general conclusions. However, all of the studies presented here have found that the energy and emissions payback times are much shorter than the expected lifetime of the modules, which is to say that the installations "make sense" environmentally.

Some of the publications follow the standard procedure for LCA, as described by ISO, but there are also some where the choice of method is less transparent. Some studies are also missing references for the LCI data sources. This makes it difficult to compare the results of the studies, and to evaluate the transferability of the results.

All of the studies calculate the EPBT of the system, and some also calculated the GPBT. Payback times are very useful for evaluating the environmental soundness of an installation. They do not, however, say anything about how much renewable energy the system will generate during its lifetime. A system with a low embodied energy but short expected lifetime may for example have a short EPBT, but a low total energy output. A system with a higher value on embodied energy and a longer EPBT may have a higher total renewable energy during its lifetime.

The value of EPBT ranges from 0.8 to 14.33 years in the reviewed studies. However, most of the studies seem to agree on an EPBT of around 1–4 years. The GPBT is calculated in fewer studies, and ranges from 0.8 to 4 years. It is difficult to establish the main reason for these differences in EPBT. On the whole, LCA studies are sensitive to the calculation method and the choices and assumptions made by the individual LCA practitioner. The EPBT of solar energy systems is sensitive to, among other factors, the boundary for the calculation, assumptions about the production of components, energy and emission factors, components included in the BOS, maintenance and replacement schemes, energy output, and how thermal and electric output is compared.

The lifetime of the modules are also an important factor. The expected lifetime of solar energy systems in general is uncertain. Most PV producers today give an energy performance warranty of 25 years, but it is expected that the actual lifetime can be longer. The guidelines for life cycle assessments of PV systems recommend to use a lifetime of 30 years for mature technologies in calculations [17]. Of the PV/T producers on the market today, several give a product warranty of 5–10 years, and an energy performance warranty of 20–25 years (see for example [18–22]). Unglazed PV/T modules can be kept cooler than standard PV modules, which could result in a longer lifetime. The analysed systems are located in Asia, Australia and Southern Europe. The irradiation (when given) is around 1200–1650 kWh per year. None of the studies analysed systems in areas with lower levels of irradiation or colder climates. Installation in colder climates could mean that the benefit of PV/T compared to PV is smaller, since over-heating of the modules is less of a problem. The temperature of the thermal output would also be lower. On the other hand, the period with space heating demand is longer which could make the thermal output more useful. However, there are other aspects that may decrease the lifetime of the modules, such as larger temperature fluctuations and higher module temperatures for glazed PV/T modules, the use of hydronic components, and in general more complex installations than for PV or solar thermal.

The energy output of the systems, which is a very important parameter in the calculation of payback times, was sometimes approximated or calculated in a simplified way. Several of the studies were, however, based on measurements, or a combination of measurements and calculations.

To evaluate the possibility of saving materials by installing PV/T systems instead of separate PV and solar thermal systems, it is necessary to have more studies that compare the installations. A few of the studies used a PV reference system, and in all of those the use of heat recovery for PV (i.e. the use of PV/T technology) resulted in an environmental benefit. Tripanagnostopoulos et al. [13] found that the best PV/T system had a 70% reduction in EPBT compared to the reference PV system, and Battisti and Corrado [12] found a reduction of around 50%.

Most of the analysed systems are at least partly custom-made, and no study describing the industrial manufacturing of PV/T modules was found. Future studies should also address the industrial production of PV/T modules. Compared to the market for PV modules and solar thermal collectors, the market for PV/T modules is still small, but the number of producers and installed systems are growing. The cost of PV/T systems are not the focus of this paper, but is of course an important factor for the future development of the technology and the market. PV systems are now reaching grid parity in many countries, and it is reported that the economic return on investment (ROI) is shorter for PV/T modules compared to PV systems [20]. However, the economic benefit also depends on whether the low temperature heat can be made use of. In the last few years, a number of larger projects have been built, especially in combination with ground source heat pumps [23]. This appears to be a suitable use of PV/T modules, since the thermal output can be used to increase the performance

of the heat pump, and in some cases also for seasonal thermal energy storage in the ground.

5. Conclusions

A review of published data on environmental assessments of PV/T modules and system has been presented. It was found that the energy payback time (EPBT) ranged from 0.8 to 14.33 years, although most studies found that the EPBT was around 1–4 years. The greenhouse gas payback time (GPBT), which was calculated in fewer studies, ranged from 0.8 to 4 years. The EPBT of solar energy systems is sensitive to, among other factors, the boundary for the calculation, assumptions about the production of components, energy and emission factors, components included in the BOS, maintenance and replacement schemes, energy output, and how thermal and electric output is compared. A general conclusion is that the payback time for both energy and greenhouse gas emissions of the PV/T systems are much shorter than their expected lifetime and that PV/T installations "make sense" environmentally. However, due to the unclear method and lack of sources in some of the publications, it is sometimes hard to evaluate the transferability of the results.

Acknowledgements

This publication was created as part of the Joint Research Centre in Sustainable Energy between Shanghai Jiao Tong University and the Norwegian University of Science and Technology (JRC SJTU-NTNU). The Joint Research Centre is funded by the Research Council of Norway, project number 221 657.

References

[1] Zhang X, Zhao X, Smith S, Xu J, Yu X. Review of R&D progress and practical application of the solar photovoltaic/thermal (PV/T) technologies. Renew Sustain Energy Rev 2012;16:599–617.
[2] Tyagi VV, Kaushik SC, Tyagi SK. Advancement in solar photovoltaic/thermal (PV/T) hybrid collector technology. Renew Sustain Energy Rev 2012;16:1383–98.
[3] Chow TT, Tiwari GN, Menezo C. Hybrid solar: a review on photovoltaic and thermal power integration. Int J Photoenergy 2012;2012.
[4] Environmental management – life cycle assessment – principles and framework; 2006.
[5] Raugei M, Fullana-i-Palmer P, Fthenakis V. The energy return on energy investment (EROI) of photovoltaics: methodology and comparisons with fossil fuel life cycles. Energy Policy 2012;45:576–82.
[6] IPCC. Climate Change 2013: The Physical Science Basis. Contribution of Working Group I to the Fifth Assessment Report of the Intergovernmental Panel on Climate Change. Cambridge, United Kingdom and New York, NY, USA: Cambridge University Press; 2013.
[7] PRé Consultant. The Netherlands: Simapro 7.3 Amersfoort; 2013.
[8] Tiwari A, Raman V, Tiwari GN. Embodied energy analysis of hybrid photovoltaic thermal (PV/T) water collector. Int J Ambient Energy 2007;28:181–8.
[9] Crawford RH, Treloar GJ, Fuller RJ, Bazilian M. Life-cycle energy analysis of building integrated photovoltaic systems (BiPVs) with heat recovery unit. Renew Sustain Energy Rev 2006;10:559–75.
[10] Kamthania D, Tiwari GN. Energy metrics analysis of semi-transparent hybrid PVT double pass facade considering various silicon and non-silicon based PV module Hyphen is accepted. Solar Energy 2014;100:124–40.
[11] Carnevale E, Lombardi L, Zanchi L. Life cycle assessment of solar energy systems: comparison of photovoltaic and water thermal heater at domestic scale. Energy 2014;77:434–46.
[12] Battisti R, Corrado A. Evaluation of technical improvements of photovoltaic systems through life cycle assessment methodology. Energy 2005;30:952–67.
[13] Tripanagnostopoulos Y, Souliotis M, Battisti R, Corrado A. Energy, cost and LCA results of PV and hybrid PV/T solar systems. Prog Photovolt: Res Appl 2005;13:235–50.
[14] Chow TT, Ji J. Environmental life-cycle analysis of hybrid solar photovoltaic/thermal systems for use in Hong Kong. Int J Photoenergy 2012;2012.
[15] Tripanagnostopoulos Y, Souliotis M, Battisti R, Corrado A. Performance, cost and life-cycle assessment study of hybrid PVT/AIR solar systems. Prog Photovolt: Res Appl 2006;14:65–76.
[16] Agrawal S, Tiwari GN. Enviroeconomic analysis and energy matrices of glazed hybrid photovoltaic thermal module air collector. Solar Energy 2013;92:139–46.
[17] Fthenakis V, Frischknecht R, Raugei M, Kim HC, Alsema E, Held M, de Wild-Scholten M. Methodology Guidelines on Life-Cycle Assessment of Photovoltaic Electricity. 2nd ed.2011.
[18] Meyer Burger Group, Hybrid – the intelligent combination of solar thermal energy and photovoltaics (product datasheet), ⟨http://energysystems.meyerburger.com/en/products/hybrid/⟩; 2014.
[19] Solarzentrum Allgäu, Wiosun PV – Therm (product datasheet), ⟨http://www.solarzentrum-wiosun.com/products/pv-therm/principle-infos⟩; 2014.
[20] Solimpeks Energy Corp. Volther hybrid collectors (product datasheet), ⟨http://www.solimpeks.com/pv-t-hybrid-solar-collectors/⟩; 2014.
[21] PA-ID GmbH, 2Power (product datasheet), ⟨http://www.2power.de/files/paid/uploads/downloads/2Power%20Modul.pdf⟩; 2014.
[22] Hörmann, Solarhybrid by Hörmann (product datasheet), ⟨http://hoermann-solarhybrid.de/beispiel-seite/produkte/kollektorfamilie/⟩; 2013.
[23] Good C, Chen J, Dai Y, Hestnes AG. Hybrid photovoltaic–thermal systems in buildings – a review. Energy Proc 2015;70:683–90.

Paper V

Good, C., Kristjansdottir, T. F., Houlihan Wiberg, A., Georges, L., & Hestnes, A. G. (2015). *Influence of PV technology and system design on the emission balance of a net zero emission building concept.* Solar Energy, 130, 89-100.
doi:http://dx.doi.org/10.1016/j.solener.2016.01.038.

Previously presented at Eurosun 2014, Aix-les-Bains, France, with the title “A comparative study of different PV installations for a Norwegian net zero emission building concept”.

Available online at www.sciencedirect.com

ScienceDirect

Solar Energy 130 (2016) 89–100

SOLAR ENERGY

www.elsevier.com/locate/solener

Influence of PV technology and system design on the emission balance of a net zero emission building concept

Clara Good [a,*], Torhildur Kristjansdottír [a], Aoife Houlihan Wiberg [a], Laurent Georges [b], Anne Grete Hestnes [a]

[a] Norwegian University of Science and Technology (NTNU), Department of Architectural Design, History and Technology, Trondheim, Norway
[b] Norwegian University of Science and Technology (NTNU), Department of Energy and Process Engineering, Trondheim, Norway

Received 25 September 2015; received in revised form 7 January 2016; accepted 14 January 2016

Communicated by: Associate Editor D. Yogi Goswami

Abstract

This paper presents an analysis of how the design of a photovoltaic (PV) system influences the greenhouse gas emission balance in a net zero emission building (nZEB). In a zero emission building, the emissions associated both with the energy required in the operation of the building (operational emissions) and the energy used to produce the building materials (embodied emissions) are offset by renewable energy generated on-site (avoided emissions). The analysis is applied to a nZEB concept for a single-family building, developed by the Norwegian Research Centre on Zero Emission Buildings. Previous analyses have shown that the installation of a PV system accounts for a significant share of the embodied emissions of a nZEB. The objective of this paper is to assess how the PV system design choices influence the embodied and avoided emissions, in order to determine how the environmental impact can be minimised. Four different PV technologies (Si-mono, poly-Si and CIS, and high-efficiency Si-mono) in four different system designs for flat roofs are evaluated using two different grid emission factors. The installations are compared by means of net avoided emissions, greenhouse gas payback time (GPBT), greenhouse gas return on investment (GROI), and finally the net emission balance of the building. The results show that the system with the largest area of high-efficiency Si-mono modules achieves the best lifetime emission balance, but that the greenhouse gas return on investment is highest for the optimally oriented CIS modules.

Keywords: Net zero emission buildings; Embodied emissions; PV system design; Net zero emission balance; Greenhouse gas return on investment (GROI); Greenhouse gas payback time (GPBT)

1. Introduction and background

1.1. Zero emission buildings

Buildings account for about a third of the global energy use and greenhouse gas (GHG)[1] emissions (International Energy Agency, 2013). To reduce this contribution, the environmental performance of buildings needs to be drastically improved. In the European Union, the revised directive on Energy Performance of Buildings (EPBD) requires of the member states that by 2020 all new buildings should be "nearly zero energy buildings". These are described as buildings with a very high energy performance where "the nearly zero or very low amount of energy required should be covered to a very significant extent by energy from renewable sources, including energy from renewable sources produced on-site or nearby" (European Parliament, 2010).

* Corresponding author.
[1] *Abbreviations:* GHG: greenhouse gas, nZEB: net zero emission building, ZEB Centre: the Research Center on Zero Emission Buildings (www.zeb.no), DHW: domestic hot water, BOS: balance of system, LCA: life cycle assessments, GPBT: greenhouse gas payback time, GROI: greenhouse gas return on investment.

http://dx.doi.org/10.1016/j.solener.2016.01.038
0038-092X/

Nomenclature

A_{fl}	heated floor area, m^2
E_{net}	net emission balance of building, kg CO_2eq
E_{netPV}	net emission balance of PV modules, kg CO_2eq
$E_{embodied}$	embodied emissions, kg CO_2eq
$E_{embodied,PV}$	embodied emissions of PV modules, kg CO_2eq
$E_{avoided}$	avoided emissions due to use of renewable energy from PV, kg CO_2eq
$E_{avoided,year}$	avoided emissions due to use of renewable energy from PV, average for 30 year module lifetime, kg CO_2eq/year
N_{PV}	lifetime of PV modules, years
N	lifetime of building, years
$GBPT$	greenhouse gas payback time, years
$GROI$	greenhouse gas return on investment, years

There are a number of definitions of net zero energy and net zero emission buildings (nZEB) Marszal et al., 2011. The main difference between a net zero *energy* building and a net zero *emission* building is the weighting system used. The word *net* indicates that energy can be exported from and imported to the building, and that the net emission balance is calculated over a specific period of time, usually a year. In practice, this usually means that the building is connected to the electricity grid.

In the analysis presented in this paper, we follow the definition framework developed by Sartori et al. (2012), and use the load/generation balance weighted by GHG emissions, measured in units of carbon dioxide equivalents (kg CO_2 eq). A schematic drawing of the framework, including the use of system boundaries and weighting systems, is shown in Fig. 1.

Depending on the definition, the load side of the net zero emission balance includes GHG emissions due to the *operation* of the building, but also GHG emissions which are emitted during the different lifecycle stages, the latter of which is defined as the *embodied* emissions. Embodied GHG emissions is a method of accounting for the amount of greenhouse gases (regardless of their type and source) emitted during one or more life cycle stages of a given product, other than the ones related to its operation (Lützkendorf, 2016). The emissions are calculated and expressed as CO_2 equivalents. These include production of the materials and components (A1-3), transport to site (A4) and construction (A5), maintenance phase (B1-7) including replacement of new materials over the lifetime of the building (B4), 'end-of-life' of the building (C1-4) and next stage product (D) including reuse, recycling (EN 15978, 2011), (not shown in Fig. 1). The embodied and operational emissions can be seen as a loan, which is paid back by the renewable energy generated on-site, here referred to as *avoided* emissions.

The Norwegian Research Centre on Zero Emission Buildings (the ZEB Centre) has defined five ambition levels for nZEBs, namely ZEB-O (operation only), ZEB-O÷EQ (operation, excluding equipment), ZEB-OM (operation and materials), and the strictest level ZEB-COM (construction, operation and materials) (Dokka et al., 2013). In the

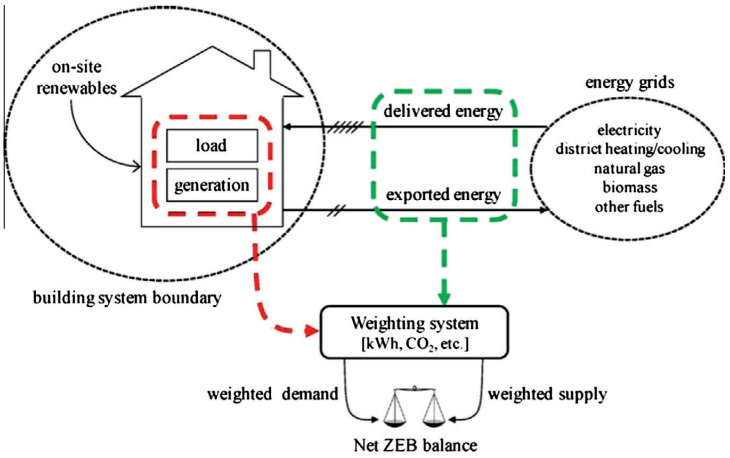

Fig. 1. Schematic drawing of the connection between buildings and energy grids, showing relevant terminology, boundary conditions and weighting systems. Figure from Sartori et al. (2012), used with permission.

analysis presented here, the ambition level is ZEB-OM. The impact of embodied emissions is distributed over the lifetime of the building, which is assumed to be 60 years in line with the work in the ZEB Centre. The normalization unit used in the calculations is therefore heated floor area per year of the building lifetime (m^2 A_{fl}/year).

1.2. Grid emission factors

The electricity generation in Norway is based almost entirely on hydro power. The Norwegian grid is, however, connected to both the Scandinavian grid and the European grid through both import and export. The import/export balance of Norway depends largely on how much hydropower is available, as well as the temperature during winter. Norway is a net exporter of electricity most years. Between 2003 and 2012, the average was an electricity export of 3.8 TWh per year (Statnett, Key Figures 1974–2012) The intra-annual import and export profile reflects the dependence on hydropower, which means that the import is most likely to occur in the first quarter of the year, when the level in the hydro power reservoirs are low, but a heating demand is still present (Statnett, Import and Export, 2015). The emission factor of the imported power depends on the source of the marginal power, i.e. the power that is used to balance a power system in case of increased demand. The source of the marginal power varies over the year, and depends on the power situation in the rest of Europe. Nevertheless, the current grid emission factor in Norway is very low compared to other European countries, around 0.04 kg CO_2 eq/kW h according to figures from Ecoinvent 3.1 (Swiss Centre for Life Cycle Inventories, 2014).

Since the emissions are calculated over the 60-year lifetime of the building, future developments need to be accounted for. Several scenarios for the future grid in Europe were developed in the ZEB Centre by Graabak et al. (2014), and the influence on zero emission buildings was analysed by Georges et al. (2015) in a European and Norwegian context. The most ambitious scenario they analysed was the so-called ZEB ultra-green scenario, in which it is assumed that GHG emissions of the European grid will be reduced by 90% by 2050 in line with EU long term political goals (European Commission, 2012; ECF, 2010). Emissions related to marginal power are included in the calculated grid emission factor. In the current grid, the marginal power is mostly from fossil fuels (coal, gas and lignite). In the ZEB ultra-green scenario, the renewable energy in the grid is assumed to increase steadily, which means that the emissions from marginal power will decrease over time. All in all this leads to an average grid emission factor of 0.132 kg CO_2eq/kW h over 60 years (Graabak et al., 2014). The current EU grid was estimated to have an emission factor of 0.361 kg CO_2eq/kW h. Both these two factors assume a strong interconnection between the Norwegian and European grids and are both used in the analysis in this paper.

1.3. Photovoltaic modules and systems

To reach net zero energy or emission balance, the use of active solar energy solutions is often necessary to provide electricity and heating. Heating can be generated directly in solar thermal collectors, or by using solar electricity to run a heat pump. Electricity is generated using photovoltaic (PV) modules.

Mono-crystalline silicon (Si-mono) and polycrystalline silicon (Si-poly) PV modules together account for about 85% of the PV market (EPIA, 2014). These are mature and robust technologies, with efficiencies of commercially available modules of about 11–22%. Technology developments and increased efficiency have made thin film modules, including amorphous silicon, CdTe (Cadmium Telluride), CIS/CIGS (Cadmium Indium (Gallium) Selenide) and organic solar cells, a viable alternative to crystalline silicon. Efficiencies range from 5% to 13% (EPIA, 2014). Thin film modules can be produced on different substrates, can be made flexible, and can be less sensitive to shading and overheating.

During their operation, PV systems generate nearly emission-free electricity, but the production of the modules is associated with a significant amount of embodied emissions. A thorough overview of life cycle assessments (LCA) of several PV technologies was published by Frischknecht et al. (2015a). In terms of embodied emissions, Si-mono and Si-poly modules have the highest impact, which to a large extent is due to production of high-purity silicon. The technological development in the PV industry has been substantial in the last decades, and the efficiencies of PV modules have increased. As Frischknecht et al. (2015a) point out, the publicly available data on PV module production does not always mirror the current situation. As an example, a typical crystalline solar cell is now significantly thinner than a decade ago, and the process chain for silicon for the solar industry has become more efficient (Peng et al., 2013). For crystalline silicon modules, there is a 30–40% decrease in greenhouse gas emissions reported from 2006 to 2009, and a corresponding decrease of 30% for CdTe thin film (Frischknecht et al., 2015a).

In addition, the production of PV modules has to a large extent moved from Europe to Asia in the last decade. The influence of the country of production on the embodied emissions of PV modules has been studied by Yue et al. (2014), who found that crystalline silicon PV modules produced in China had a 28–48% higher primary energy demand compared to modules produced in Europe.

1.4. Scope of the paper

This paper presents a study of how the emissions balance of a building is influenced by the design of the PV system. A nZEB residential building model, developed by the ZEB Centre and further described in Section 2.1, is used as a case study. In the analysis of the building model by

Houlihan Wiberg et al. (2014), it was found that the PV modules accounted for 29% of the embodied emissions from the materials – a significant amount. The work presented here aims to analyse if and how this share can be decreased. The objective is to find a balance between high energy output and a low environmental impact. The focus in this study is only on the greenhouse gas emissions contribution to the global warming potential at 100 years (GWP100), as defined by the IPCC (IPCC, 2013). Four different PV technologies (Si-mono, poly-Si, CIS, and high-efficiency Si-mono), four installation designs, and two grid mixes are evaluated in terms of embodied emissions and energy performance. The emissions balance, greenhouse gas payback time (GBPT), and greenhouse gas return on investment (GROI) of the building are calculated for each of the alternative systems.

2. Method

2.1. The case building

In practice, only a coherent set of measures can lead to the achievement of a net zero emission balance for a building. The need to study the influence of these measures has led the ZEB Centre to investigate a number of nZEB models. The building models are based on current available technology, and thus reflect today's practices in the construction sector. The models are designed using the nZEB definition by Dokka et al. (2013). A detailed calculation of the embodied emissions of the materials in the building was performed in order to identify the key materials and components that contribute the most to the embodied greenhouse gas emissions (Houlihan Wiberg et al., 2014).

The analysis presented in this paper is based on the ZEB model for a single-family residential house (Fig. 2) which is further described in Houlihan Wiberg et al. (2014). It is a two-storey detached house with a heated floor area, A_{fl}, of 160 m^2, located in Oslo in Southern Norway. The concept is solar-based: a well-insulated building envelope is combined with solar façade-mounted thermal collectors and an air-to-water heat pump to cover the heating needs, while a roof-mounted and grid-connected photovoltaic (PV) system generates enough electricity to reach the zero energy balance. The heating system is connected to a combined tank which provides both domestic hot water (DHW) and space heating. This means that the only form of delivered energy to the building is electricity. The total annual energy demand of the building is simulated to 70 kW h/m^2 and the total annual electricity use to 39 kW h/m^2 (Houlihan Wiberg et al., 2014).

The operational and avoided emissions are calculated based on the energy that is used at the location of the building (and which is replaced by the on-site generation), i.e. the grid electricity. Symmetric factors for import and export are used. The distribution of operational emissions of the building, amounting to a total of 5.1 kg CO_2 eq/m^2 A_{fl} year calculated using the ZEB ultra-green grid emission factor, is shown in Fig. 3. Using the current EU grid emission factor, the operational emissions are 13.9 CO_2 eq/m^2 A_{fl} year.

The embodied emissions of materials, excluding the PV system, were calculated to 5.0 kg CO_2 eq/m^2 A_{fl} year when divided over the 60 year lifetime of the building. The distribution is shown in Fig. 4. It can be noted that for the ZEB ultra-green scenario, the embodied and operational emissions are almost equal.

2.2. PV system design

The orientation of a PV system is defined by the tilt angle (the angle between the PV plane and the horizontal) and the azimuth (the orientation in the compass plane). In Oslo, the optimal tilt angle for yearly yield is around 40°. The reference building has a flat roof, where the PV modules are installed in rows. For modules installed with a high

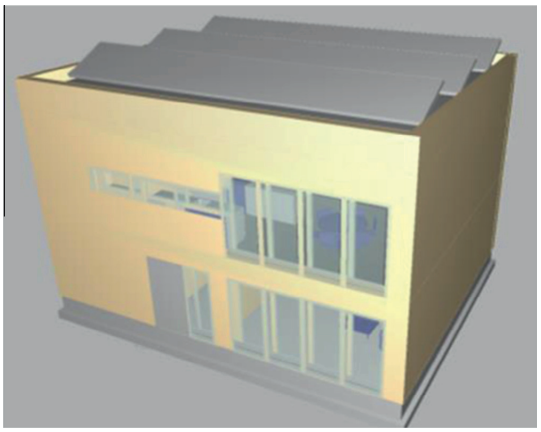

Fig. 2. The ZEB residential building model (Houlihan Wiberg et al., 2014).

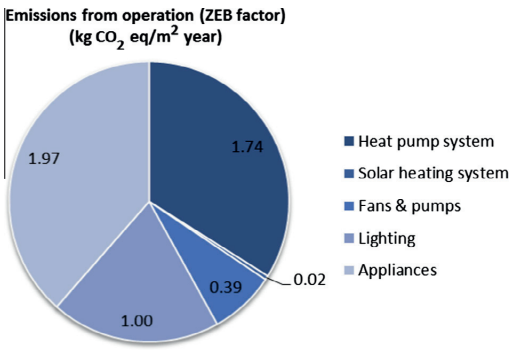

Fig. 3. The building's operational emissions calculated using the ZEB ultra-green grid emission factor (0.132 kg CO_2 eq/kW h) as simulated in Houlihan Wiberg et al. (2014).

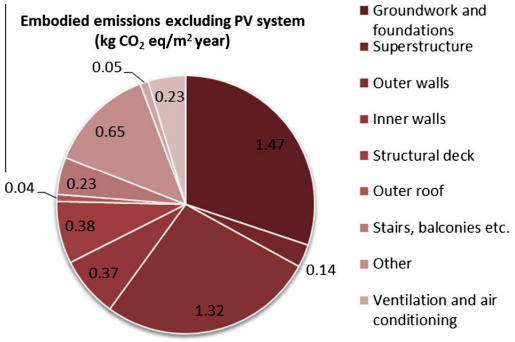

Fig. 4. The embodied emissions of the building (excluding the PV system) as calculated by Houlihan Wiberg et al. (2014).

tilt angle, a large distance between the rows is necessary to avoid self-shading. This is especially important at high latitudes with low sun angles.

There are in practice two alternative installation strategies: the modules can be mounted at the optimal tilt angle and spaced with enough distance to avoid shading, or they can be installed at a lower-than-optimal tilt angle, but closer together. In the latter case, the modules may also be installed with two orientations, which increases the number of modules that can be installed.

The roof area of 80 m^2 was set as the design boundary condition for the systems. It is assumed that the total roof area is available for PV and that there are no shading objects such as chimneys or pipes. Four alternative designs for the installation were developed, and an overview is shown in Table 1 and Fig. 5.

The rows of modules are spaced with enough distance to avoid self-shading at the sun height at noon in the middle of February (15°) or higher. Since the insolation at times with lower sun angles (November to February) accounts for only about 2–8% of the annual insolation, this is seen as a reasonable compromise.

The details of each simulated case are presented in Table 4. The rows of modules are assumed to be one module high and equally spaced over the length of the roof. As many modules as possible were designed to fit in each row. Each of the design options A–D was simulated with the four different PV technologies Si-mono, poly-Si and CIS. Due to the different dimensions and number of the modules, the size of the system are slightly different for each technology.

The crystalline silicon modules are mounted in a landscape orientation to make best use of the three bypass diodes in the modules. Shading of the lower edge, for example from snow build-up, will thereby have a limited influence on the output power. The thin film modules, on the other hand, were placed in vertical orientation since this limits the effects of shading for this technology. The details for the rest of the system design (e.g. string layout and choice of inverter) have been kept as similar as possible between the alternative designs.

The energy performance of the PV systems was evaluated using the simulation software PVsyst v5.73 (PVsyst SA, 2011) together with Meteonorm meteorological data for Oslo (Meteotest, 2009). The annual irradiation on a horizontal surface in Oslo is around 1000 kW h/m^2.

2.3. Embodied emissions of PV modules

Emissions data is extracted from the Ecoinvent database v.3.1 (Swiss Centre for Life Cycle Inventories, 2013). The selected modules are chosen to represent the 'best match' to the average in performance of each PV technology, available on the market. Average industry efficiency values from 2012 are used, as presented by de Wild-Scholten (2013). Commercial modules matching these are used in the simulation of the energy performance. The characteristics of the selected modules are shown in Table 3. As a point of comparison, the high-efficiency Si-mono module from SunPower that was used in the original study by Houlihan Wiberg et al. (2014) is also analysed. The GWP value for this module is taken from a life cycle assessment presented in Fthenakis et al. (2012).

The expected lifetime of the modules is set to 30 years, with a linear annual degradation of 0.7% in line with the value suggested for mature technologies in the Methodology Guidelines on Life-Cycle Assessment of Photovoltaic Electricity, developed by Fthenakis et al. (2011). (Since the producer warranty of the CIS modules is the same as for the silicon modules, the same degradation factor has

Table 1
Design options for the PV system on the flat roof.

Design	Azimuth of modules	Tilt angle of modules (°)	Description
A	South	40	Optimal tilt angle and orientation for Oslo. This high tilt requires large row spacing to avoid mutual shading. High energy output for each module, but a low number of modules can fit on the roof.
B	South	15	Lower tilt angle to reduce the required row spacing. Lower yield per module but more modules can fit on the roof.
C	South/North	15	A development of design B, where north-facing modules are added in the space between the south-facing modules. More modules can fit on the roof but the north-facing modules will have a lower output.
D	East/West	15	The same low tilt angle as in C, but modules oriented east/west. The advantages of low self-shading are the same as in C, but output is shifted towards autumn and spring.

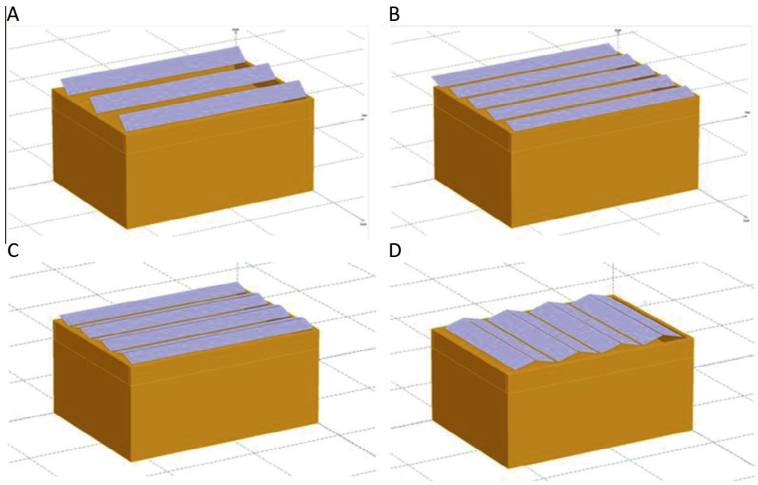

Fig. 5. Design options A to D. Images from PVsyst (PVsyst SA, 2011).

Table 2
Detailed data for the design options using different PV technologies.

Design	PV technology	Total no of modules	Total module area (m^2)	Total power (kW_p)
A	Si-mono	18	30.4	4.6
A	Si-poly	18	29.7	4.3
A	CIS	20	24.6	2.9
A	Si-mono (high-eff)	18	29.4	6.0
B	Si-mono	24	40.5	6.1
B	Si-poly	24	39.6	5.8
B	CIS	30	36.8	4.4
B	Si-mono (high-eff)	24	39.1	8.0
C	Si-mono	42	70.9	10.7
C	Si-poly	42	69.3	10.1
C	CIS	50	61.4	7.3
C	Si-mono (high-eff)	42	68.5	14.0
D	Si-mono	35	59.1	8.9
D	Si-poly	28	46.2	6.7
D	CIS	48	58.9	7.0
D	Si-mono (high-eff)	35	57.1	11.7

Table 3
Characteristics of the three PV modules used in the simulations: the module dimensions are taken from producer data sheet and the emissions data from Ecoinvent database (Swiss Centre for Life Cycle Inventories, 2013; Fthenakis et al., 2012).

PV technology	Module area (m^2)	Rated power (W_p)	Efficiency (%)	Embodied emissions per m^2 of module (kg CO_2eq/m^2)
Si-mono	1.69	255	15.1	278
Si-poly	1.65	250	14.7	213
CIS thin film	1.23	145	11.9	134
Si-mono (high-efficiency)	1.63	333	20.4	281

been used, even though it can be argued that the technology is less mature.)

The balance of system (BOS), i.e. the materials used for the supporting structures and components such as inverters, controlling units and cabling, have not been included in the emissions analysis. This simplification is supported by the results from Fthenakis et al. (2011) which showed that the modules are by far the largest emission contributors.

2.4. Replacement of PV modules

Since the lifetime of the PV modules is assumed to be 30 years – half of the expected building lifetime – the system needs to be replaced once. Since prediction about the future developments in PV module production technology is difficult, we have chosen to use a future scenario where all systems are replaced by the same types of modules after 30 years. (The design options A–D are the same for the

whole 60-year period.) The future scenario was developed by Kristjansdottir et al. (2016) based on work by Frischknecht et al. (2015b) and Fthenakis et al. (2012). The future modules are assumed to have an efficiency of 25.2%, an expected lifetime of 30 years, and degradation equal to the current SunPower modules. The emission factor is estimated to be 100 kg CO_2 eq/m^2. The energy yield of the future systems are calculated in a simplified way based on efficiency, performance ratio, and irradiation.

2.5. Net emission balance

The net emissions of the PV modules, E_{netPV} (kg CO_2 -eq) are calculated according to Eq. (1), where $E_{avoided,i}$ (kg CO_2 eq/year) are the avoided emissions due to renewable energy generation during year i, and, $E_{embodiedPV}$ (kg CO_2 eq) are the emissions embodied in the modules themselves. This is calculated over the whole lifetime, N_{PV} (years), of the modules.

$$E_{netPV} = \sum_{i}^{N_{PV}} E_{avoided,i} - E_{embodiedPV} \quad (1)$$

The net emission balance of the building, E_{net}, (kg CO_2 eq) is calculated in an analogous way according to Eq. (2), where the total embodied emissions of the building materials $E_{embodied}$ (kg CO_2 eq/year) and the operational emissions of the building are taken into account. While the factor E_{netPV} is a measure of the net emissions impact of each PV technology, the factor E_{net} describes how the different PV technologies effect the emissions balance of the building. The factor E_{net} must therefore be regarded together with information on the building energy demand.

$$E_{net} = \sum_{i}^{N} E_{avoided,i} - E_{embodied} - E_{operation} \quad (2)$$

Replacement of materials is included in the embodied emissions, and N (years) is the lifetime of the building. A net zero emission balance is reached if E_{net} is zero or larger, i.e. if the generation meets the demand. E_{net} is presented in the results section normalized per heated floor area and year (m^2 A_{fl} year).

2.6. Greenhouse gas payback time and greenhouse gas return on investment

The greenhouse gas payback time (GPBT) is the number of years of operation it takes the PV modules to generate enough renewable electricity to offset the emissions caused by their production (Reich-Weiser et al., 2008). GPBT is calculated as shown in Eq. (3), where $E_{embodiedPV}$ (kg CO_2 eq) is the total embodied emissions of the technology and $E_{avoided,year}$ (kg CO_2 eq/year) is the emissions that are avoided per year due to the replacement of grid electricity (the average value over the 30 year lifetime of the modules is used here).

$$GPBT = \frac{E_{embodiedPV}}{E_{avoided,year}} \quad (3)$$

The impact of different technologies and products can also be assessed using the greenhouse gas return on investment (GROI), first introduced by Reich-Weiser et al. (2008). GROI is calculated as the lifetime of the technology divided by the GPBT. The GROI is a dimensionless number, analogous to the metrics economic return on investment (ROI) and energy return on investment (EROI). A GROI below 1 indicates that the technology does not bring about a net reduction in emissions. Neither GPBT nor GROI is a measure of the energy generated by the PV modules in absolute terms; a high GROI can either be the effect of a low embodied emissions or a high energy output.

It should be noted that the factors E_{net} refers to a particular building, the GBPT and GROI only concern the PV modules, and are therefore independent of the building energy demand.

3. Results

3.1. Energy yield

The annual simulated energy output of the systems is shown in Fig. 6, together with the annual electricity need of the building. Only the modules used during the first 30 years are shown. The Si-mono modules (high-efficiency and average) have the highest yield for all design options. Design C has the highest energy yield for all module types, which is a direct reflection of the size of the systems (see Table 2). All module technologies in the C and D designs generated more electricity than the annual electricity need of the building.

The influence of orientation and tilt angle is shown in Fig. 7 using Si-mono modules as an example (the trend is the same for all technologies). The modules installed at 40° and south facing (optimal angle at the location) have around 40% higher yield than the modules installed at 15° tilt and north facing.

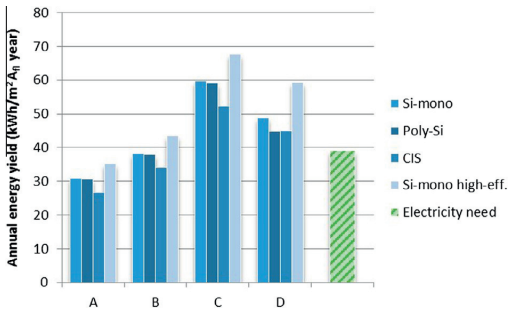

Fig. 6. Annual simulated energy yield per heated floor area for different systems. The annual electricity demand of the building is shown for comparison.

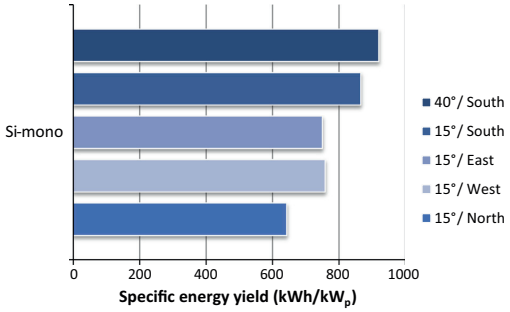

Fig. 7. Specific energy yield (kW h/kW$_p$) for Si-mono modules installed at different orientation and tilt angles.

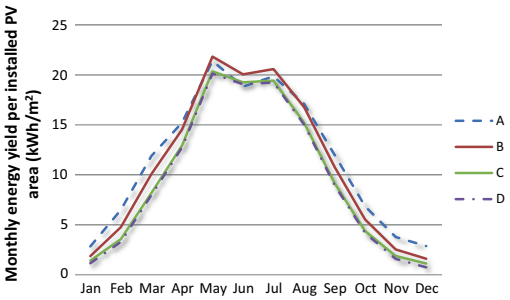

Fig. 8. Monthly yield per installed PV area (kW h/m^2) for the Si-mono modules in the four different design options.

The monthly energy yield of the four system options are shown in Fig. 8, and are normalized per installed PV area. The Si-mono modules are used as an example. The summer peak is very prominent for all design options, but it is highest for option B with only south-facing modules at 15°. The optimally inclined modules have a lower yield in the summer, and a higher yield during autumn to spring. The north/south facing option C, and east/west facing option D have the lowest yield per installed area for all months.

3.2. Embodied and avoided emissions

The embodied emissions of the different PV installations are shown in Fig. 9, for both the original and future modules. The embodied emissions of design C are highest, since this is the largest system by area. The embodied emissions of both types of Si-mono modules are significantly higher than those of CIS modules, while Si-poly modules lies somewhere in between.

The net avoided emissions, as calculated in Eq. (1) are shown in Fig. 10 over the full 60-year building lifetime. In this graph, each design and module type includes both the original and future modules. The net avoided emissions are largest for system C with both types of Si-mono modules, i.e. the largest system with the most efficient modules. For all module types, it is lowest for the optimally inclined

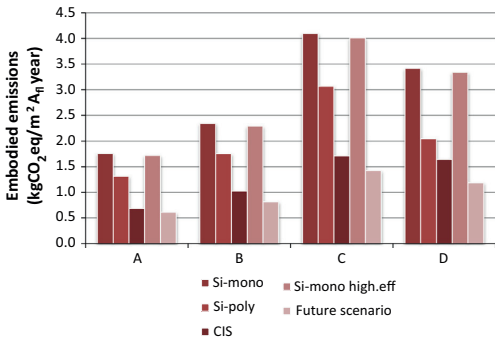

Fig. 9. Embodied emissions of the different PV modules for the functional unit 1 square metre heated floor area per year (kg CO_{2eq}/m^2 A_{fl} year). The embodied emissions of the original and future modules are shown separately.

system A, which is also the smallest installation. The net avoided emissions are also significantly higher when calculated with the current EU grid factor, since the replaced energy in this case would have been the cause of higher emissions.

The emissions rate (kgCO_{2eq}/kW h) is calculated based on embodied emissions and energy yield of the systems. This number is directly comparable to the electricity grid emission factor. The emissions rate of the systems are 0.045–0.055 kgCO_{2eq}/kW h for the Si-mono modules, 0.036–0.044 kgCO_{2eq}/kW h for the Si-poly modules, 0.030–0.037 kgCO_{2eq}/kW h for the CIS modules and 0.034–0.042 for the mono-Si high-efficiency modules.

3.3. Greenhouse gas payback time and greenhouse gas return on investment

The GPBT for all systems are well below the lifetime of the modules. In the ZEB ultra-green grid, the GPBT of the systems range from 10 years (CIS, design A) to 20.4 years (Si-mono, design D). The larger systems (C and D) have longer GPBT than the smaller systems (A and B). The GPBT in the current EU grid is significantly shorter; the GPBT of the systems range from 3.7 years (CIS, design A) to 7.5 years (Si-mono, design C). The future modules have GPBT of 3.7–4.5 years in the ZEB ultra-green grid and 1.3–1.7 years in the current EU grid.

The GROI of the systems are shown in Fig. 11. The GROI is generally largest for the system with CIS modules, and for system A with the optimal orientation.

3.4. Net emissions balance of the building

The resulting net emissions balance (ZEB-OM ambition level), E_{net}, for the complete building is calculated for each of the PV system alternatives, using Eq. (2). As shown in Table 4, four systems reach a balance when the current EU grid factor is used: the Si-mono, Si-poly and Si-mono

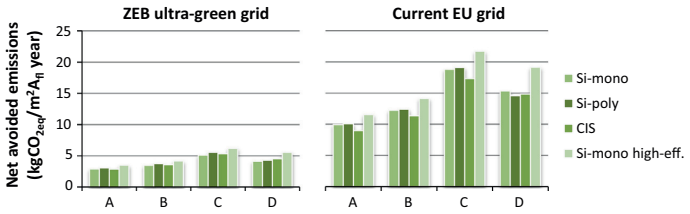

Fig. 10. Net avoided emissions of the different PV installations for the functional unit 1 square metre heated floor area per year (kg CO_{2eq}/m^2 A_{fl} year), calculated using the ZEB grid factor and the EU grid factor. The original and future modules are included in each design.

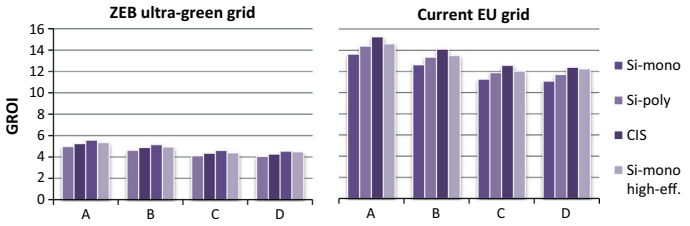

Fig. 11. The GROI of the PV installations, calculated for ZEB grid factor and EU grid factor.

high-efficiency modules in design C, as well as the Si-mono high-efficiency modules in design D. None of the systems reach a net zero emission balance if the ZEB ultra-green grid factor is used.

A simplified calculation was performed to determine the PV module areas that would have been required to reach net zero emission balance. To reach a net zero emission balance with design option D in the ZEB ultra-green grid scenario, the required module area ranges from 85 m^2 for the mono-Si high-efficiency modules to 104 m^2 for the CIS modules, The lowest *module* areas (68–84 m^2) are required for design option A, due to the better specific yield of the modules, but on a flat roof this solution would require a much larger *roof* area to avoid self-shading.

The value of E_{net} is a function of the embodied emissions of the PV system as well as the energy yield. It also depends strongly on the operational emissions and the grid emission factor. Two examples of this dependence, system C with Si-mono modules and CIS modules, are shown in more detail in Fig. 12. While nZEB-OM level is only reached for the system with Si-mono modules in the current EU grid (lower right), it can be noted that nZEB-O level, which includes only operational emissions, is reached for all the systems shown in Fig. 12.

The PV modules in system A accounted for 11% (CIS), 16% (Si-poly) and 19% (Si-mono, both types) of the total embodied emissions of the building, while the modules in system C accounted for 24%, 31% and 35% respectively. That is, the system that led to the largest net avoided emissions itself accounted for about a third of the embodied emissions of the building.

4. Discussion

The results of the analysis presented here give a composite answer to the question of which system technology and design has the lowest environmental impact in terms of greenhouse gas emissions. It is concluded that there is no connection between having a short payback time in terms of emissions and reaching a net zero emission balance.

Table 4
The net emissions balance E_{net} (ZEB-OM ambition level) for each of the buildings over the full 60 year lifetime of the building. The colour scale from red to green indicates the worst to the best system in terms of net emission balance.

	E_{net} (kg CO_2eq/m^2 A_{fl} year)							
	ZEB ultra-green grid				Current EU grid			
	Si-mono	Si-poly	CIS	Si-mono high-eff.	Si-mono	Si-poly	CIS	Si-mono high-eff.
A	-7.1	-6.9	-7.1	-6.5	-8.9	-8.7	-9.8	-7.3
B	-6.5	-6.3	-6.4	-5.8	-6.6	-6.4	-7.5	-4.7
C	-4.9	-4.4	-4.6	-3.8	0.0	0.3	-1.5	2.9
D	-5.8	-5.7	-5.5	-4.4	-3.5	-4.3	-4.0	0.3

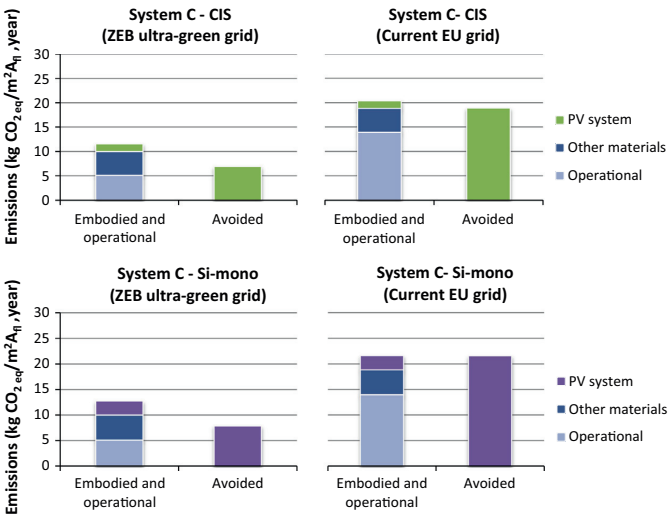

Fig. 12. The net emission balance for buildings with two of the PV technologies, CIS (top row) and Si-mono (bottom row). The operational and avoided emissions are calculated with the ZEB ultra-green grid emission factor (left column) and with the current EU grid emission factor (right column).

The emission rate and the greenhouse gas payback time (GPBT) are lowest, and greenhouse gas return on investment (GROI) highest, for the thin film modules. However, the modules that contribute the most to the net emissions balance of the building are the high efficiency Si-mono modules, even though they are associated with the highest embodied emissions and GPBT.

The optimally inclined design A had the highest performance in terms of kW h/kW$_p$ for all the modules, as well as the lowest emission rate and GPBT. Nevertheless, design C, with the largest number of modules, resulted in the highest net avoided emissions. As a total system, design C for both types of Si-mono modules has the highest total yield. However, the benefit of increasing the systems' size by mounting modules with north-facing orientation, as is done in design C, can be questioned. The yield of the north-facing modules in this system was only around 70% of the optimally inclined ones and the GPBT of these modules were up to 23.9 years for the Si-mono technology with ZEB ultra-green grid mix.

About half of the PV system combinations reach the ZEB-O level, but only the largest installations reach the ZEB-OM ambition level, showing that this is very demanding to achieve. The systems with high-efficiency modules reach ZEB-O in design B, C and D, but not in design A.

The analysis presented in this paper involves a number of simplifications, generalisations and uncertainties. The embodied emissions of the PV modules (except the Si-mono high-efficiency modules) use generic data from the Ecoinvent database (Swiss Centre for Life Cycle Inventories, 2013). Some of the data is relatively old, in some cases dating from 2001. As mentioned in Section 1.3, there has been a substantial change in the PV industry in this time, and the validity of the data can therefore be questioned.

Another uncertainty that has a large influence on the results is the choice of electricity grid factor for the location of the installation. The net positive effect of installing a PV system in terms of reduced CO_{2eq} emissions depends to a high degree on the electricity it replaces. An installation in a location where the grid mix has a large share of fossil energy leads to a larger reduction than the same system with amore renewable energy mix. Due to the changes in the sun path over the year, the difference between summer and winter yield of PV systems is significant at high latitude locations such as Norway, as shown in Fig. 8. On an annual scale, the yield is also mismatched with the energy demand, which is higher in the winter. The design of the PV system can be used to mitigate this to some degree, as different orientations will favour energy output during different parts of the year. As Fig. 8 shows, the higher tilt angles decrease the summer yield, but increase the yield during the rest of the year. To avoid a large mismatch during summer, it could be feasible to install PV systems vertically on building facades.

As described in Section 1.2, the import/export balance of the Norwegian power system varies over the year, as do the emissions related to marginal power. The amount of the avoided emissions from solar electricity is in reality not constant over the year, which means that the load matching of the PV yield and the building energy need will influence the amount of avoided emissions. The intra-annual variability of the grid factor was not considered in this study, but should be included in future analyses.

In addition to the analysis of global warming potential, as presented here, a full LCA would also take into account

other environmental impacts, such as the use of toxic materials. We are also excluding the BOS from the study. Other publications have reported that the BOS has a minor impact of the life cycle emissions of a PV system compared to the modules themselves, but a preliminary analyses by Kristjansdottir et al. (2016) show that this is highly dependent on the type of installation used. In addition to the emission data, there are of course also uncertainties related to the energy performance simulations.

Finally, the importance of reaching a zero emission balance for a single building can be questioned. As this analysis has shown, a relatively large PV installation is required for a single building to reach net zero emission balance, which leads to periods of large export and import to the electricity grid. This, in turn, may require new or improved grid infrastructure. It may be more efficient, as well as cheaper, to install grid connected renewable energy sources at a local or regional level. Wind power plants, for example, are significantly more efficient on a larger scale than at individual buildings. On a larger scale, an increased share of renewable energy sources has been shown to increase the system stability of the grid (Sovacool, 2009). Recently, much of the research focus on zero emission concepts has shifted towards zero emission neighbourhoods, where the combination of buildings with different energy demand profiles can result in a more balanced energy demand on a neighbourhood scale. Furthermore, the optimum between on-site, nearby and off-site renewables is still an open question for the Norwegian research community.

5. Conclusions

An analysis of different PV installations for a Norwegian nZEB concept building has been presented. Four different PV technologies (Si-mono, Si-poly, CIS and Si-mono high-efficiency) and four design options have been analysed based on net avoided emissions, emission rate, greenhouse gas emission payback time (GPBT), greenhouse gas return on investment (GROI), and finally net emission balance of the whole building. Two grid emission factors were used: one assuming a significant de-carbonization of the EU grid here referred to as the ZEB ultra-green scenario with 0.132 $kgCO_{2eq}$/kW h, and the current EU grid emission factor of 0.361 $kgCO_{2eq}$/kW h.

The systems in design A, with optimally inclined and oriented modules (40° south-facing), had the lowest emission rate and GBPT, and the highest GROI for all module types. Nevertheless, only the largest systems reached a net zero emission balance with ambition level nZEB-OM (system designs C and in one case D). These systems also had the highest amount of embodied emissions (up to 35% of the total embodied emissions of the building), and the lowest energy yield per module. The calculations with two grid emission factors also showed that the value of a PV installation is more evident if the grid electricity it replaces is more carbon-intensive. None of the systems reached a zero emission balance when using the ZEB ultra-green grid emission factor.

Acknowledgements

This work has been supported by the Research Council of Norway through the *Joint Research Centre for Sustainable Energy* between the Norwegian University of Science and Technology (NTNU) and Shanghai Jiao Tong University (SJTU).

References

Dokka, T.H., Sartori, I., Tyholt, M., Lien, K., Byskov Lindberg, K., 2013. A Norwegian Zero Emission Building Definition. In: Passivhus Norden 2013. Gothenburg, Sweden.

ECF, 2010. Roadmap 2050: A Practical Guide to a Prosperous, Low-Carbon Europe, European Climate Foundation.

EN 15978, 2011. Sustainability of construction works. Assessment of Environmental Performance of Buildings. Calculation Method.

EPIA, 2014. Solar Photovoltaic Technology, EPIA – European Photovoltaic Industry Association.

European Commission, 2012. Energy Roadmap 2050, Publications Office of the European Union.

European Parliament, 2010. Directive 2010/31/EU of the European Parliament and of the Council of 19 May 2010 on the Energy Performance of Buildings, Directive 2010/31/EU. Brussels.

Frischknecht, R., Itten, R., Sinha, P., de Wild-Sholten, M., Zhang, J., Fthenakis, V., Kim, H.C., Raguei, M., Stucki, M., 2015. Life Cycle Inventories and Life Cycle Assessment of Photovoltaic Systems, second ed.

Frischknecht, R., Itten, R., Wyss, F., Blanc, I., Heath, G., Raugei, M., Sinha, P., Wade, A., 2015. Life Cycle Assessment of Future Photovoltaic Electricity Production from Residential-scale Systems Operated in Europe.

Fthenakis, V., Frischknecht, R., Raugei, M., Kim, H.C., Alsema, E., Held, M., de Wild-Scholten, M., 2011. Methodology Guidelines on Life-Cycle Assessment of Photovoltaic Electricity, second ed.

Fthenakis, V., Betita, R., Shields, M., Vinje, R., Blunden, J., 2012. Life cycle analysis of high-performance monocrystalline silicon photovoltaic systems: energy payback times and net energy production. In: 27th European Photovoltaic Solar Energy Conference and Exhibition. Frankfurt, Germany.

Georges, L., Haase, M., Houlihan Wiberg, A., Kristjansdottir, T.F., Risholt, B., 2015. Life cycle emissions analysis of two nZEB concepts. Build. Res. Inform. 43, 82–93.

Graabak, I., Bakken, B.H., Feilberg, N., 2014. Zero emission building and conversion factors between electricity consumption and emissions of greenhouse gases in a long term perspective. Environ. Clim. Technol. 13, 12–19.

Houlihan Wiberg, A., Georges, L., Dokka, T.H., Haase, M., Time, B., Lien, A.G., Maltha, S., 2014. A net zero emission concept analysis of a single-family house. Energy Build. 74, 101–110.

International Energy Agency, 2013. Transition to Sustainable Buildings – Strategies and Opportunities to 2050. Directorate of Sustainable Energy Policy and Technology (SPT). Paris, France.

IPCC, 2013. Climate change 2013: the physical science basis. Contribution of Working Group I to the Fifth Assessment Report of the Intergovernmental Panel on Climate Change. Cambridge University Press, Cambridge, United Kingdom and New York, NY, USA.

Kristjansdottir, T.F., Good, C.S., Inman, M.R., Dahl Schlanbusch, R., Andresen, I., 2016. Embodied greenhouse gas emissions from PV systems in Norwegian residential Zero Emission Pilot Buildings. Submitted Sol. Energy (revision submitted 04.02.2016).

Lützkendorf, M.B., 2016. Evaluation of Embodied Energy and CO2eq for Building Construction – Discussion report v 1.6, International Energy Agency Energy Conservation in Buildings and Community Systems Programme (IEA EBC) Annex 57: Evaluation of Embodied Energy and CO2eq for Building Construction, Karlsruhe Institute of Technology – KIT.

Marszal, A.J., Heiselberg, P., Bourrelle, J.S., Musall, E., Voss, K., Sartori, I., Napolitano, A., 2011. Zero energy building – a review of definitions and calculation methodologies. Energy Build. 43, 971–979.

Meteotest, 2009. Meteonorm Database.

Peng, J., Lu, L., Yang, H., 2013. Review on life cycle assessment of energy payback and greenhouse gas emission of solar photovoltaic systems. Renew. Sustain. Energy Rev. 19, 255–274.

PVsyst SA, 2011. PV-syst 5.73, Photovoltaic System Software A. Mermoud (Ed.), University of Geneva.

Reich-Weiser, C., Dornfeld, D., Horne, S., 2008. Greenhouse Gas Return on Investment: A New Metric for Energy Technology. UC Berkeley: Laboratory for Manufacturing and Sustainability.

Sartori, I., Napolitano, A., Voss, K., 2012. Net zero energy buildings: a consistent definition framework. Energy Build. 48, 220–232.

Sovacool, B.K., 2009. The intermittency of wind, solar, and renewable electricity generators: technical barrier or rhetorical excuse? Utilities Policy 17, 288–296.

Statnett, Import and Export, 2015. S.M.A. Operations (Ed.), Data From the Power System, Statnett. <http://www.statnett.no/en/Market-and-operations/Data-from-the-power-system/Import-and-export/>.

Statnett, Key Figures 1974–2012, 2015. S.M.A. Operations (Ed.), Data From the Power System, Statnett. <http://www.statnett.no/en/Market-and-operations/Data-from-the-power-system/Key-figures-1974-20121/>.

Swiss Centre for Life Cycle Inventories, 2013. Ecoinvent database v 2.2.

Swiss Centre for Life Cycle Inventories, 2014. Ecoinvent database v 3.1.

de Wild-Scholten, M.J., 2013. Energy payback time and carbon footprint of commercial photovoltaic systems. Sol. Energy Mater. Sol. Cells 119, 296–305.

Yue, D., You, F., Darling, S.B., 2014. Domestic and overseas manufacturing scenarios of silicon-based photovoltaics: life cycle energy and environmental comparative analysis. Sol. Energy 105, 669–678.

Paper VI

Kristjansdottir, T.F., Good, C., Inman, M.R., Dahl Schlanbusch, R., Andresen, I (2016).
Embodied greenhouse gas emissions from PV systems in Norwegian residential Zero Emission Pilot Buildings. Solar Energy, 133, 155-171.
doi:http://dx.doi.org/10.1016/j.solener.2016.03.063

Available online at www.sciencedirect.com

ScienceDirect

Solar Energy 133 (2016) 155–171

SOLAR ENERGY

www.elsevier.com/locate/solener

Embodied greenhouse gas emissions from PV systems in Norwegian residential Zero Emission Pilot Buildings

Torhildur Fjola Kristjansdottir [a,*], Clara Stina Good [a], Marianne Rose Inman [a,b], Reidun Dahl Schlanbusch [b], Inger Andresen [a]

[a] *Norwegian University of Science and Technology, Department for Architectural Design, History and Technology, Alfred Getz vei 3, 7465 Trondheim, Norway*

[b] *SINTEF Building and Infrastructure, Forskningsveien 3b, 0314 Oslo, Norway*

Received 25 September 2015; received in revised form 22 March 2016; accepted 28 March 2016

Communicated by: Associate Editor Ruzhu Wang

Abstract

Greenhouse gas (GHG) emissions from the combustion of fossil energy need to be reduced to combat global climate change. For zero energy and Zero Emission Buildings (ZEB), photovoltaic solar energy systems are often installed. When the goal is to build a life cycle Zero Emission Building, all emissions come under scrutiny. Emissions from photovoltaic (PV) energy systems in Zero Emission Buildings have been shown to have a relative large share of material emissions. In this paper, we compare GHG emissions per kW h of electricity and greenhouse gas emission payback times (GPBT) for three residential PV systems in Zero Emission Pilot Buildings in Norway. All the buildings have roof mounted PV systems with different design solutions. The objective is to analyse the emission loads and GPBT of these three systems to facilitate for more informed choices of energy systems for Zero Emission Buildings. The results show that the total embodied emissions allocated per square meter of module area are around 150–350 kg CO_2 eq/m^2 for the three different systems. Emissions from the mounting systems vary from 10 to 25 kg CO_2 eq/m^2 depending on the material types and quantities used. When modules replace other roofing materials, such as roof tiles, mounting emissions were reduced by approximately 60%. GHG emissions per kW h electricity produced were in the range of 30–120 g CO_2 eq/kW h for the different systems. The system with the lowest emissions was the largest system, which had a simple mounting structure and modules with reused cells. It was found that the GPBT was strongly dependent on the scenario used for electricity grid emissions. By applying a dynamic emission payback scenario with an optimistic reduction of emissions from the European electricity grid, the GPBT was 3–8 years for the different systems. When comparing the emissions with current Norwegian hydropower emissions, of around 20 g CO_2 eq/kW h, it was found that all of the PV system's emissions were higher. When compared to a mainly fossil fuel based grid, all the PV system's emissions are low. This study highlights the importance of reliable emission documentation for PV modules and their mounting structures on the market.

Keywords: Zero Emission Buildings; Building integrated photovoltaics; Embodied emissions; GPBT; PV system design

1. Introduction

The building industry accounts for approximately one third of global energy use (IEA, 2013) and one fifth of global greenhouse gas emissions (IPCC, 2007). In order to reduce these emissions the concepts of zero energy and

* Corresponding author at: Norwegian University of Science and Technology, Research Centre for Zero Emission Buildings, Alfred Getz vei 3, 7465 Trondheim, Norway. Tel.: +354 6922202.
E-mail address: torhildur.kristjansdottir@ntnu.no (T.F. Kristjansdottir).

http://dx.doi.org/10.1016/j.solener.2016.03.063
0038-092X/

Zero Emission Buildings have emerged. The revised directive on energy performance of buildings requires that all new buildings should be 'nearly zero energy buildings' by 2020 (European Parliament, 2010). According to Peterson et al. (2015) zero energy building is defined as "An energy-efficient building where, on a source energy basis, the actual annual delivered energy is less than or equal to the on-site renewable exported energy". Photovoltaic solar energy systems are the most common energy source installed in zero energy buildings (Voss and Musall, 2011). Dokka et al. (2013) presents a definition for Norwegian zero emission greenhouse gas buildings. The concept of a Zero Emission Building is similar to zero energy buildings, except it uses emissions of CO_2 equivalents as the balancing indicator instead of primary energy (Sartori et al., 2012). A zero greenhouse gas building (Zero Emission Building – ZEB) can also be referred to as a zero carbon building, ZCB (Hui, 2010). The definition of Zero Emission Buildings (ZEB) presented by Dokka et al. (2013) includes different ambition levels depending on which emissions are included and compensated for. Two fundamental levels are the "ZEB-O" level, which aims to balance out all operational emissions (O) from energy use, and the "ZEB-OM" level, which aims to compensate for both operational emissions (O) and material (M) emissions. Material emissions can also be referred to as embodied emissions. A life cycle zero energy concept has also been introduced by Ramesh et al. (2010) and Cellura et al. (2014). The relative share of embodied energy compared to operational energy is higher in zero energy buildings compared to conventional buildings (Cabeza et al., 2014) (Chau et al., 2015). Life cycle GHG analysis of two Norwegian ZEB concept buildings aiming for the ZEB-OM level is presented in Georges et al. (2015). In order to take the first steps from theoretical concept buildings to real-life pilot buildings, three residential Zero Emission Pilot Buildings have been built in Norway. These are the Skarpnes case study with a ZEB-O ambition level, and the Multikomfort and Living Lab buildings both with ZEB-OM ambition levels. Previously, material emission accounting for both of the ZEB-OM pilot buildings have been performed (Kristjansdottir et al., 2016; Inman and Wiberg, 2015). The studies showed that the PV systems were a large contributor to embodied emissions for both cases, confirming the results from the concept studies (Good et al., 2016; Wiberg et al., 2014; Georges et al., 2015). In these analyses the PV system emission accounting were simplified. Since the PV systems contribute largely to the material emissions in Norwegian ZEBs, it is important to know more about these systems and different emission loads. Can these emissions be reduced? What are the emissions per kW h produced? What are the building integration benefits? And what is their greenhouse gas payback time (GPBT) in years?

The objective of this study is to analyse greenhouse gas emissions from these three PV systems installed in Norwegian ZEB pilot buildings. Further, the goal is to look into their GPBT with different electricity grid emission scenarios. Increased knowledge on emission profiles for different PV systems suitable for Norwegian dwellings will facilitate more informed choices on energy systems for Zero Emission Buildings. The PV systems installed differ in terms of type of modules used, the roof mounting system, geographical location and design. In Norway, there is limited experience with photovoltaics, and there are no standardised solutions for integrating PV modules into roofs. In general, learning from PV pilot systems with regards to mounting solutions, module choices and emissions pay back times, can improve future installations. To follow, we provide an overview of the status of life cycle assessments of PV systems, and provide an introduction to roof integrated PV systems. We then provide a description of the applied method and present the three case studies. Subsequently, we present the results, and discuss and interpret our approach. Finally, we present some concluding remarks.

1.1. Life cycle assessment

Life cycle assessment is divided into four main steps: goal and scope definition, inventory analysis, impact assessment, and interpretation. Life cycle assessments often include a sensitivity analysis of important parameters (ISO, 2006). The basic steps of a life cycle assessment for a photovoltaic system are presented in Fthenakis and Kim (2011). The raw material inputs and manufacturing of PV modules have been well documented through various life cycle assessments (Alsema and de Wild-Scholten, 2006; Jungbluth, 2005; Jungbluth et al., 2009, 2012; Fthenakis et al., 2011; NREL, 2012). However, according to Peng et al. (2013), life cycle assessments of installed/operating PV systems are limited. In order to increase the comparability, transparency and credibility of the life cycle assessment of photovoltaic electricity, methodological guidelines have been developed by Fthenakis et al. (2011). Fthenakis and Kim (2011) conclude that the emissions and energy payback times of PV modules are heavily dependent on the type of electricity used to produce the modules. The global PV market share is dominated by China and Taiwan (ISE, 2014). A comparative study of the carbon footprint of PV module production in China and Europe was carried out by Yue et al. (2014). The study revealed that modules produced in China have almost double the emissions compared to modules produced in Europe, with emissions of around 72 g CO_2 eq/kW h and 37 g CO_2 eq/kW h respectively (for mono-Si modules). This difference is mostly due to the fact that the emission intensity of electricity production in China is significantly higher than in Europe. Yue et al. (2014) apply irradiation levels of 1700 kW h/m^2 y and a performance ratio of 0.75. In contrast, documentation of Norwegian produced PV modules has shown that there is a significant benefit from using renewable hydropower in the production of silicon solar modules (Glöckner and de Wild-Scholten, 2012). Prospective studies of the life cycle primary energy use of PV modules have been presented in Frischknecht et al.

(2015), Bergesen et al. (2014) and Mann et al. (2014). These studies highlight the expected reduction of material use, as well as expected increases in the efficiencies of PV modules.

1.2. Integrated roof mounting solutions for PV modules

PV systems may be integrated into building facades or roofs, or may be roof mounted. The three cases studied herein, all have roof mounted PV modules. In building integrated photovoltaic (BIPV) systems, the PV modules are used as part of the building envelope or any other architectural element that is necessary for the proper functioning of the building (SUPSI, 2015). Hence, the PV modules are replacing traditional parts of the building envelope, e.g. the roofing. A BIPV module can therefore not be removed without damaging the physical functions of the building envelope. Integrated systems present possible cost and material savings, as the modules are serving dual purposes (Jelle et al., 2012). Other roof mounting solutions on the market includes semi-integrated PV systems, sometimes referred to as in-roof systems. These solutions are designed to mount PV modules in line with the roof surface, in order to be visibly integrated in the existing roof.

2. Materials and methods

The life cycle approach used is an attributional approach, focuses on the documentation of greenhouse gas emission burdens from the different life cycles of the PV system. The environmental impact category assessed is global warming potential (GWP) and is based on the IPCC GWP (2007) and IPCC (2013) 100-year method, measured in kg CO_2 equivalents (IPCC, 2007, 2013). This assessment follows the methodological guidelines developed by Fthenakis et al. (2011) for the selection of functional unit and service lifetimes. The module degradation is calculated using values given by the producers.

2.1. Goal, scope and functional unit

The goal of the assessment is to analyse and compare the different systems with respect to the GHG emission burden per kW h of produced electricity and the greenhouse gas payback time (GPBT) in years. The functional unit is "an averaged kW h of electricity produced per square meter of module area from the systems over a period of 30 years." Life cycle stages include: production of raw materials, manufacture of components, transport to the building site, manufacture of replaced components and simulated energy production with degradation over the service lifetime. Emissions associated with energy used during the installation of the systems are not included, as these emissions are considered to be similar across the different systems. The embodied emissions are calculated according to Eq. (1):

$$CO_2\ eq_{embodied} = CO_2\ eq_{modules} + CO_2\ eq_{mounting} + CO_2\ eq_{electric} + CO_2\ eq_{transport} \quad (1)$$

Here, the parameter $CO_2\ eq_{embodied}$ includes the embodied emissions that have gone into the production of the PV modules, the mounting structure, the electric installations (e.g. inverter and cabling) and transport. The transport scenario includes transport to the building site. Fig. 1 presents the scope of the analysis. The scope is divided into two main phases based on an estimates service lifetime of 30 years for the PV modules. The first phase, the initial 30-year scenario analysis is based on specific information from the case studies, and then a simplified generic future scenario is used for the replaced system in 30 years time. The end of life stage is not included, as it does not affect the emissions occurring in the next 30 years. In addition, waste treatment of PV modules in the future is highly uncertain.

2.2. GHG payback time

The term GHG payback time (GPBT) is defined as the number of years it takes for an energy generation system to "pay back" its embodied emissions through renewable energy generation (Reich-Weiser et al., 2008). It is calculated according to Eq. (2), whereby ($CO_2\ eq_{avoided(year)}$) (kg CO_2 eq) are the emissions avoided per year due to the production of electricity from the installation. $CO_2\ eq_{avoided(year)}$ is calculated by multiplying the annual production with the average emissions per kW h per year from the local grid.

$$GPBT = \frac{CO_2\ eq_{embodied}}{CO_2\ eq_{avoided(year)}} \quad (2)$$

2.3. Case descriptions

The three analysed PV installations in Norway are shown in Fig. 2. The three buildings are pilot studies within the Norwegian Research Centre on Zero Emission Buildings. All the buildings have low consumption of energy for space heating due to highly insulated envelopes, and a high heat recovery rate in the ventilation systems. The energy target set for the PV systems studied states that they should provide enough electricity on an average annual basis to cover all electricity consumption of the buildings. Details on the energy concepts for the three case studies can be found in Dokka et al. (2015), Goia et al. (2015) and Nord et al. (2016). For the Multikomfort building and the Living Laboratory, the ambition was set to a ZEB-OM level, whereby the PV systems were dimensioned to provide electricity to compensate for the electricity use from operation, and the embodied emissions from materials over the 60 year service lifetime of the building. We do not include the entire ZEB-OM balance calculations here, but focus only on the PV systems performances. Selected

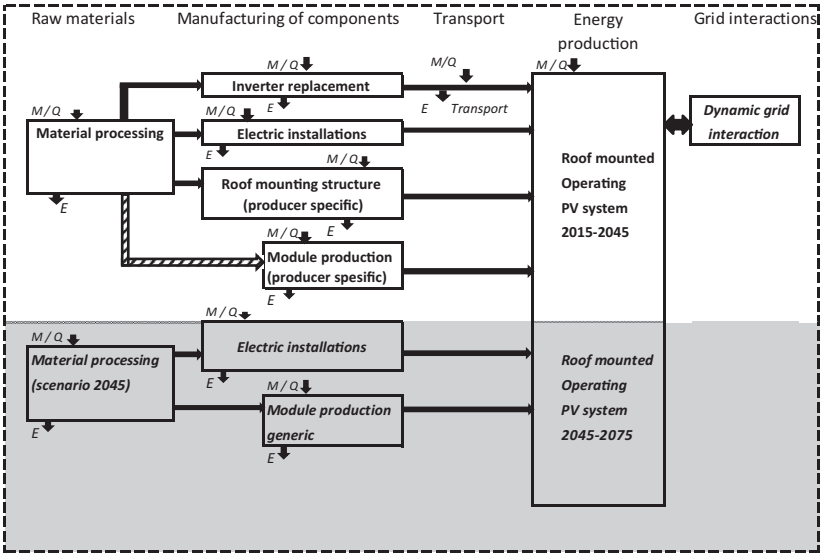

Fig. 1. Scope of the analysis, the boxes illustrate what is included in the analysis, M refers to materials, Q refers to energy, and E refers to emissions. The white area refers to the initial specific comparison applied for the first 30 years of the life time, whilst the grey area refers to a simplified generic scenario applied for the last 30 years of the life time.

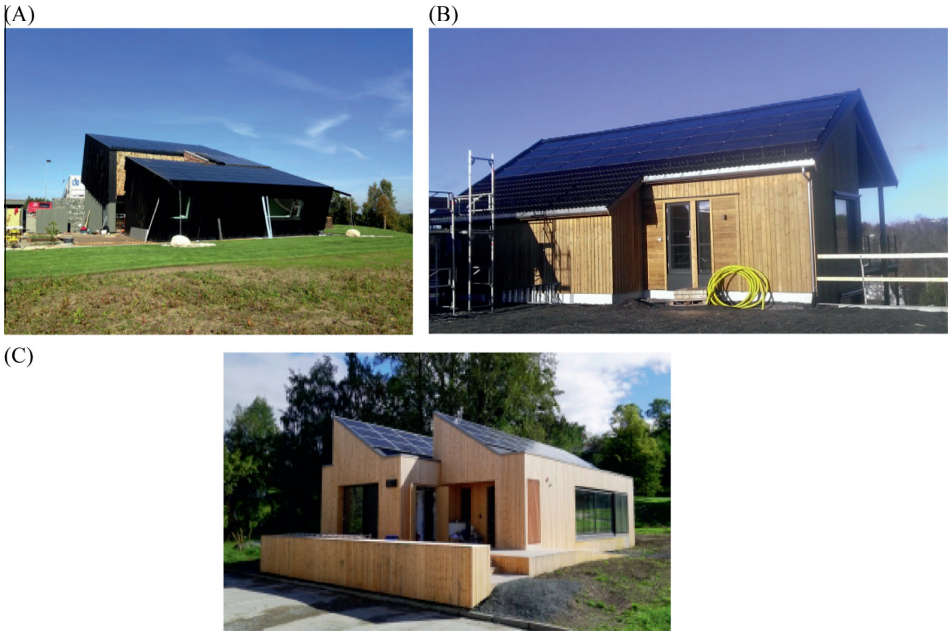

Fig. 2. The roof mounted PV system design of the pilot buildings: (A) Multikomfort (Kristian Edwards, Snøhetta), (B) Skarpnes (Skanska), and (C) Living Laboratory (Katrine Peck Sze Lim).

information for the PV systems for each of the buildings is provided in Table 1. Table 2 shows details of the installed PV systems. The three case studies represent three different roof mounting systems for the fixing of PV modules.

2.3.1. Case A: Multikomfort

The Multikomfort case study is shown in Fig. 2A. It is a two-story residential building completed in 2014. It was built as a demonstration building for energy solutions for

Table 1
Building specifications.

Description	Unit	A – Multikomfort	B – Skarpnes	C – Living Laboratory
Location	–	Larvik (59°12′N, 10°15′E)	Arendal (58°25′N, 08°43′E)	Trondheim (63°25′N 10°24′E)
Annual average ambient temperature	°C	8	8	5.7
Annual irradiation with optimal tilt angle*	kW h/m^2	1182	1182	1120
Annual irradiation on the tilted plane*	kW h/m^2	1057	1060	1091
Loss at current angle compared to optimal	kW h/m^2	11%	10%	3%
Year of construction	year	2014	2015	2015
Heated floor area	m^2	202	154	102
Available roof area	m^2	155	106	108
Roof orientation		−45 (south-east)	51 (south-west)	0 (south)
Roof tilt	°	19	32	30
Ratio roof/floor area	m^2/m^2	0.77	0.69	1.06

* Irradiation data from PVGIS (Institute for Energy – Renewable Energy Unit).

Table 2
Details of the three PV installations.

Description	Unit	A – Multikomfort	B – Skarpnes	C – Living Lab
Manufacturer	–	Innotech Solar (ITS)	Sunpower	REC
Type of module	–	Design Black 250	SPR-230NE-BLK-D	REC260PE
Country of PV module production		Sweden (modules) and Germany (cells)	The Philippines	Singapore
Cell technology	–	Poly-Si	Mono-Si (back-contacted)	Poly-Si
Rated power per module	Wp	250	230	260
Efficiency at STC[a]	%	15.5	18.5	15.8
Module size	m^2	1.65 (1.665 × 0.991)	1.24 (1.559 × 0.798)	1.65 (1.665 × 0.991)
Weight	kg	19	15	18
Number of modules	–	91	32	48
Total module area	m^2	150	40	79
Total rated power	kWp	22.75	7.36	12.48
Total weight of modules	kg	1729	480	864
Inverter		Schneider Electric	1 x SMA Sunny Tripower 7000TL	2 x SMA Sunny Boy 5000TL 21-MS Basic
Number of strings		4	2	4
PV/inverter power ratio		1.15	1.05	1.36
Type of mounting system		BAPV	BIPV	In roof (semi integrated)
Mounting system manufacturer		K2 Systems	Schweizer/Schweizer	Renusol/InterSole SE
Place of mounting frame production		Leonberg, Germany	Chemnitz, Germany	Cologne, Germany
Battery storage		24, 42.3 kg Norbat, CFPV 2 V 600 Ah, OpzV GEL, (China)	No storage	No storage

[a] STC – standard test conditions: 1000 W/m^2, cell temperature 25 °C and AM 1.5 spectrum.

plus energy buildings. The design of the house is based on Saint-Gobain's Multi-Comfort concept (Saint-Gobain, 2015). The focus of the concept is both on comfort issues such as indoor air quality and daylight, as well as environmental performance. The photovoltaic modules are from Innotech Solar (ITS) (EcoPlus) and were chosen due to their low carbon profile (Innotech Solar, 2015; ITS, 2012; de Wild-Scholten, 2013). The PV system consists of 91 installed ITS modules. The PV system is grid connected and mounted in a landscape orientation. There are no shading objects in the immediate surroundings of the building. Energy storage is included in the form of a battery bank, with the aim to increase the economic output of the PV system. Previous LCA studies have documented that batteries used in photovoltaic systems may contribute significantly to GHG emissions. This is mainly due to the manufacturing processes used, and the short lifetime of batteries (Beccali et al., 2012, 2014). In order to compare the three case studies upon the same technological basis it was decided to exclude the batteries used in the Multikomfort house from the system boundary. A section of the roof construction for the Multikomfort building is shown in Fig. 3A and site pictures of the installation and battery bank are shown in Fig. 3B and C. The PV modules are not integrated in the roof, but are instead mounted on top of bitumen felt. Both the PV modules and the mounting structure can be removed without any impact on the physical functions of the roof. The roof mounting system is named K2 systems (Systems, 2015).

2.3.2. Case B: Skarpnes

The Skarpnes case study is shown in Fig. 2B. It is a two storey single residential building available on the normal

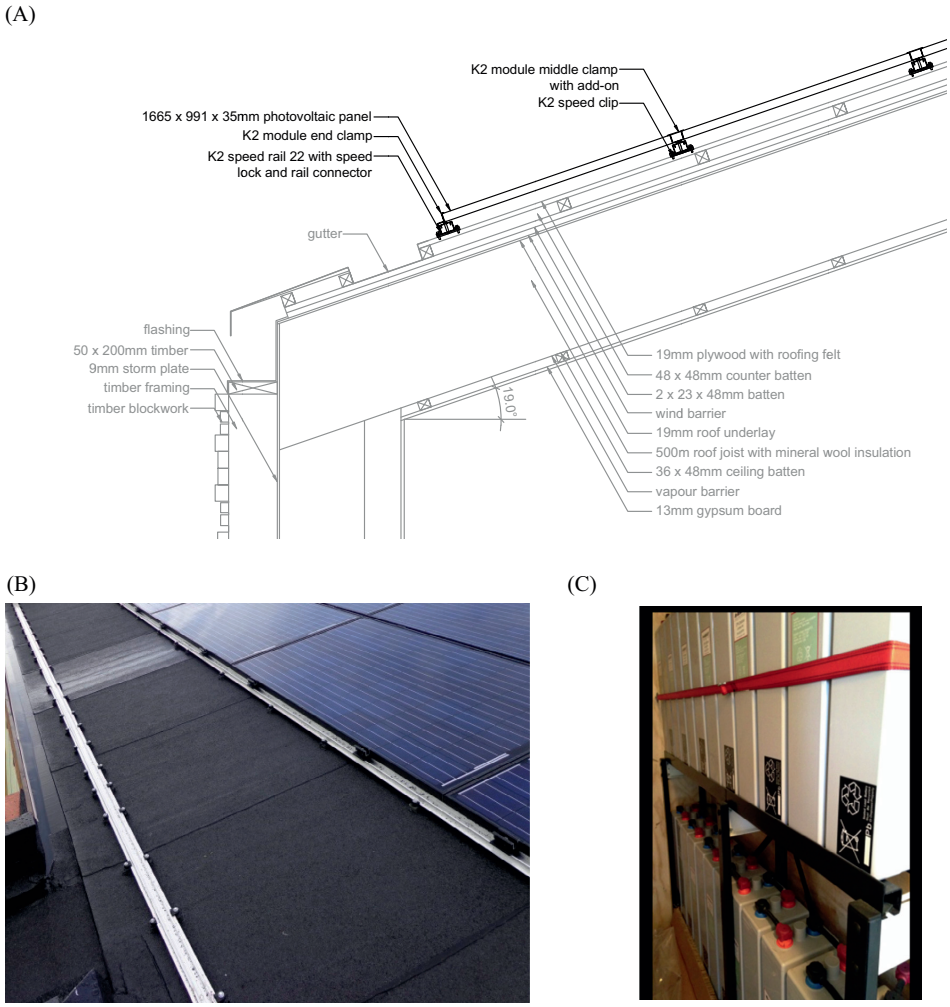

Fig. 3. (A) Section of the roof construction adapted from Snøhetta architects), (B) picture of the roof installation, and (C) battery ban.

housing market. Skanska is responsible for the energy concept of the building. The building is located in the first zero energy neighbourhood in Norway. The PV system consists of 32 high efficiency modules from SunPower. The modules are mounted in a landscape orientation in four rows on the south-facing part of the pitched roof. The PV array is connected in two strings to one inverter from SMA which is communicating with the grid. There are no shading objects in the immediate surroundings of the building. The installation is a fully building integrated PV system (BIPV). The mounting solution used is Solrif®XL from Schweizer (Schweizer, 2015). The BIPV installation on the Skarpnes building does not cover the full area of the roof, but is integrated in the upper part of the south facing side. The rest of the roof is covered with traditional roof tiles. Hence, the modules are substituting roof tiles in the areas they cover. A section of the roof solution is shown in Fig. 4A, and site photographs are given in Fig. 4B and C.

2.3.3. Case C: Living Lab

The Living Lab building is shown in Fig. 2C. The building is located on campus at the Norwegian University of Science and Technology (NTNU) in Trondheim. The purpose of the building is to be a "living laboratory" whereby the performance of the building and its technology is observed and measured, whilst the building is in operation (i.e. when inhabited). The roof of the Living Lab has a saw-tooth shape, and the PV installation is divided between the two tilted roof areas (see Fig. 2C), each with 24 PV modules from REC Corp (REC, 2013). The PV installation is

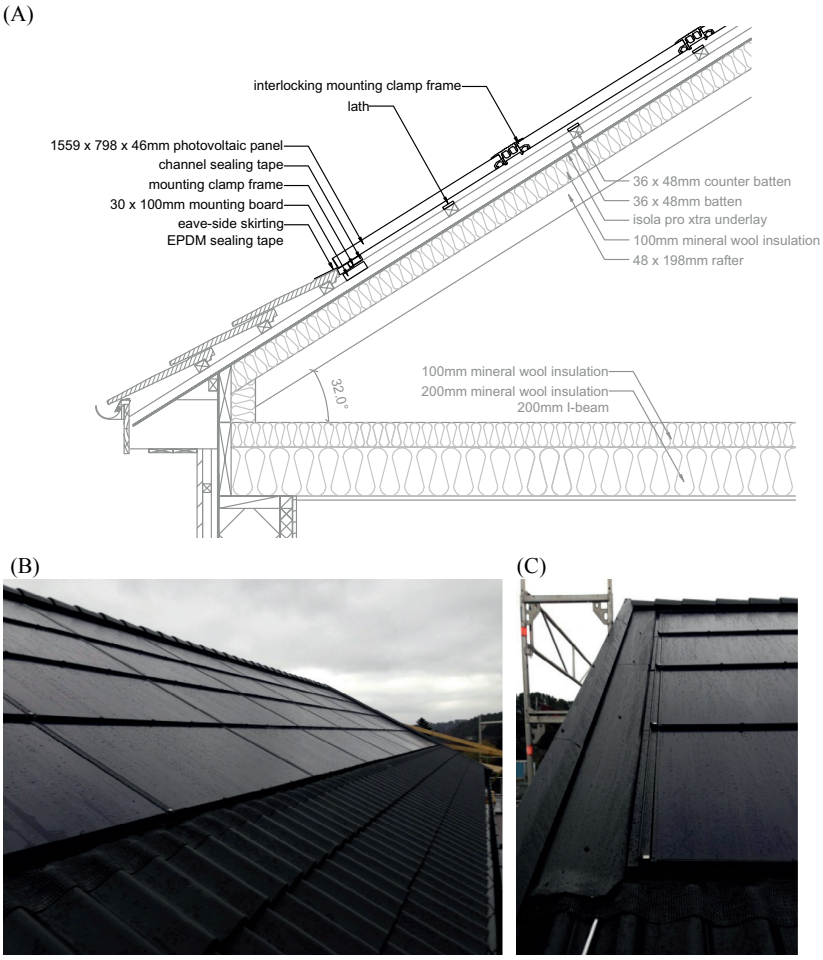

Fig. 4. (A) Section of the roof construction adapted from Roald Rasmussen at Skanska), (B) picture of the roof installation, and (C) end profil.

south facing with a 30° inclination. The southern-most roof shades the lower part of the northern-most roof during a relatively large part of the year. To minimize the impact of shading as much as possible, the modules are divided into two module strings (one upper and one lower). The module strings are connected to two inverters from SMA which feed into the grid. The roof construction of the Living Lab is shown in Fig. 5A, and site pictures are shown in Fig. 5B and C. The mounting structure replaces the roofing, but the modules, which are mounted on top of a solid board, can be removed without any impact to the building physics. The system applied is from Renusol Solar Mounting Systems (Renusole, 2015). The mounting structure has a 10-year product warranty and an expected reference service lifetime of more than 30 years (Solbes, 2013; Renusol, 2010a, 2010b).

2.4. Inventory assessment

The inventory is based on specific data gathered on the installed PV systems. The inventory includes simulations of operational energy performance, module emissions (with frames), the mounting structures, transport, the inverter and other electrical installations (cabling, etc.). The background data is obtained from Ecoinvent v.2.2 and v.3.1 (Frischknecht et al., 2007; Weidema et al., 2013). The life cycle analysis tool SimaPro v.8.0.5 (Pre Consultants, 2012) has been applied to access and analyse the Ecoinvent data. Benefits from the reuse or recycling of components are not included. The inventory for the electrical installations is based on specific details relating to the size of the system and weight of the inverters with background data from Ecoinvent.

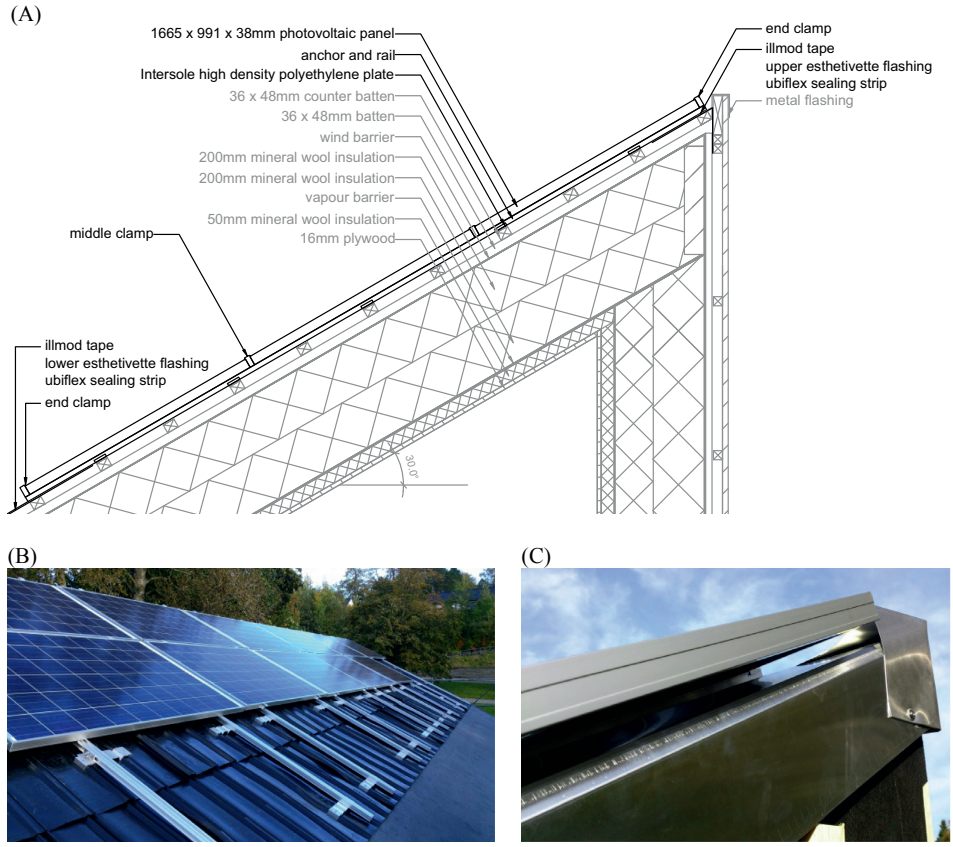

Fig. 5. (A) Section of the roof construction adapted from Luca Finocchiaro), (B) photograph of the roof installation, and (C) end profil.

2.4.1. Energy performance of PV systems

The energy performance of the three PV systems is evaluated through simulations, using the tool PVsyst (PVSYST SA, 2011). Site-specific Meteonorm data (Meteotest, 2009) has been used. Annual total solar irradiation for the given locations is given in Table 1. The performance ratio (PR) is defined as the ratio between the final system yield (Yf) divided by the reference yield (Yr) given by Eq. (3):

$$\mathrm{PR} = \frac{\mathrm{Yf}}{\mathrm{Yr}} \tag{3}$$

whereby, Yf is the ratio of the net energy output and the nominal power of the installed array and Yr is the ratio between the total in-plane irradiance and the PV reference irradiance (1000 W/m^2).

The performance ratio takes into account array and system losses, such as losses due to shadows, the inverter and wiring (Marion et al., 2005) (PVSYST SA, 2011). The performance ratio of these three systems was around 0.8, depending on the actual system design in each case. Losses due to snow coverage of the PV modules represent an area of high uncertainty. Snow coverage and the possibility of snow clearing depend not only on the location, but also the orientation, maintenance, type of modules, glazing and frame (Andrews et al., 2013). It is assumed that the modules are covered by 20% snow, between November and February, for all three cases. This assumption is based on discussions with PV consultants and installers in Norway.

Internal energy consumption of the inverters is considered negligible. None of the systems are optimally oriented for their location, which would be around 40–45° and south facing (annual optimisation). The losses in available irradiation, due to non-optimal orientation (not including shading losses), are largest for Multikomfort with around 12%, followed by 9% for Skarpnes and 3% for the Living Lab. Module degradation has been included in accordance with the warranty specified by the producers, as shown in Table 3. However, we apply a service lifetime of 30 years to all of the modules according to Fthenakis et al. (2011). The linear degradation is assumed to extend beyond the 25-year warranty period.

The energy output with degradation accounted for, E' (kW h/m^2, year), is calculated according to Eq. (4) where

Table 3
Product and power warranties of the three types of PV modules (Innotech Solar, 2013, SunPower Corp, 2012, REC Group, 2013).

Module	ITS	SunPower	REC
Product warranty	12 years	25 years	10 years
Performance, warranty, initial degradation	At least 97% of initial power after the first year	At least 95% of initial power for the first 5 years	At least 97% of initial power after the first year
Performance, warranty, annual degradation	No more than 0.7% (at least 80.2% after 25 years)	No more than 0.4% per year (at least 87% after 25 years)	No more than 0.7% (at least 80.2% after 25 years)

E (kW h) is the first year energy yield, d_{int} (–) is the initial degradation, d_{lin} (–) is the linear degradation, A_{PV} (m^2) is the module area, t_{int} (years) is the time of initial degradation, and t (years) is the module lifetime.

$$E' = \frac{E \cdot d_{int}}{A_{PV} \cdot t} \cdot \frac{1 - d_{lin}^{t - t_{int}}}{1 - d_{lin}} \quad (4)$$

PV module efficiency is dependent on the operating temperatures, decreasing with increased temperatures (Green, 1992). In a building integrated PV system, it is more difficult to assure good ventilation of the modules, resulting in higher temperatures than in free standing systems. This factor is taken into account in the simulations, whereby the Skarpnes system is considered fully integrated, the multi-comfort and Living Lab systems are building adapted and semi-integrated respectively, and therefore have some degree of ventilation. The rear ventilation of the modules is taken into account by changing the thermal loss factor in the simulation program. The fully integrated system was simulated with a thermal loss factor of 15 W/m^2 K, and the semi-integrated and building adapted systems were simulated with a thermal loss factor of 20 W/m^2 K, as per the recommendations in the program (PVSYST SA, 2011). When calculating the CO_2 avoided in the GPBT, we apply the dynamic production profiles per year, including the degradation of the modules. The PV energy performance, in the replacement scenario, is assessed in a simplified way, due to the large uncertainties in future module performance.

2.4.2. Module emissions

PV module emissions are sensitive to the local energy source at the production site of the main material inputs (Fthenakis and Kim, 2011; Yue et al., 2014). It is assumed likely that single-Si module production emissions are within the range of 100–300 kg CO_2 eq/m^2 based on previous analyses (Jungbluth et al., 2012; Frischknecht et al., 2015; Fthenakis et al., 2011; Fthenakis and Kim, 2011). Life cycle emissions from the SunPower modules have been thoroughly documented in Fthenakis et al. (2012). According to that previous study, the SunPower life cycle emissions are 281 kg CO_2 eq/m^2 based on Philippine production, which is to the authors' knowledge the case for the modules used in Skarpnes. According to ITS, the emissions from the ITS modules are 80% lower than that from conventional crystalline modules, due to the optimisation process of unused cells from other manufacturers (ITS, 2012). Emissions from the ITS modules have been documented with a simplified carbon footprint analysis by de Wild-Scholten (2013), a study that is not comparable to a complete LCA study. Thus, we use module emissions data from the Ecoinvent database to resemble the ITS modules: "Photovoltaic panel, multi-Si, at plant/RER/I." We make the following adjustment in the Ecoinvent process to resemble the use of secondary cells in the ITS modules: "50% reduction in the use of primary cells for the baseline scenario, based on ITS (2012), de Wild-Scholten (2013) and Ecoinvent (2013)." We apply emission data based on the Ecoinvent database directly for the REC module (photovoltaic panel, multi-Si, at plant/RER/I) with 210 kg CO_2 eq/m^2 (Ecoinvent, 2013). REC was unable to provide specific emission data for their modules. Since the modules are the largest fraction of the PV system inventory, we have carried out a sensitivity analysis based on assumptions for "best case" and "worst case" scenarios for module emissions. The sensitivity analysis for the SunPower modules is based on differences in production locations as presented in the paper by Fthenakis et al. (2012). The "best case" is based on Norwegian production and the "worst case" is based on Malaysian production, whilst the baseline is Philippine production. The sensitivity for the REC modules is based on a Monte Carlo analysis performed in SimaPro v.8.0.5 of the Ecoinvent data, resulting in a normal distribution with a standard deviation (SD) of 16.8 kg CO_2 eq/m^2 (Ecoinvent, 2013; Pre Consultants, 2012). The "best case" is −2× SD, the "worst case" +2× SD, whilst the mean value is the baseline scenario. Finally, the sensitivity for the ITS modules is based on different assumptions of the amount of primary cells used. The "best case" is based on a scenario were 75% of the cells are reused, whilst the baseline assumes 50% reused cells, and the "worst case" assumes that no cells are reused. The ITS scenarios are inspired by the production methods of the ITS modules (ITS, 2012; de Wild-Scholten, 2013). The sensitivities are given in Table 4.

Table 4
Module emission scenarios.

Module	Best case (kg CO_2 eq/m^2)	Baseline (kg CO_2 eq/m^2)	Worst case (kg CO_2 eq/m^2)
SunPower	200	281	307
ITS	89	130	210
REC	176	210	244

2.4.3. Mounting structures

All materials used for the sake of mounting the PV modules have been included. The mounting material inventory is given in Table 5. The PV roof mounting structures consist of rails, clamps, sealing materials and other components. In some cases, for their installation in or onto the roof, additional timber battens were necessary, and flashings were required for the edges of the roof, for reasons of building physics and/or aesthetics. Material quantities for the Schweizer system were obtained directly from Jungbluth et al. (2007). For the Living Laboratory and Multikomfort case studies, the inventory was gathered from technical datasheets for the system and system descriptions. Aluminium is used in all three of the mounting structures, because of the lack of specific information concerning the type and location of aluminium used, we have included a sensitivity analysis for aluminium emissions based on the Ecoinvent database: "best case" 1.4 kg CO_2 eq/kg (secondary), "baseline" 8.4 kg CO_2 eq/kg (production mix) and "worst case" 22.8 kg CO_2 eq/kg (alloy based on Chinese electricity).

2.4.4. Transport

To calculate transport emissions of the components used, the production factory has been located using product information from the manufacturer and factory inspection certificates. The online route explorer tool SeaRates (2015) has been used to calculate distances. Three transport scenarios have been modelled: "best case" by ship, "baseline" by ship and truck and "worst case" only by trucks. Transport emission data is based on Ecoinvent EURO 5 truck (Ecoinvent, 2013) and Ecoinvent Transoceanic Ship.

2.4.5. Electricity grid factor scenario

To calculate the greenhouse gas payback time (GPBT) in years, a reference value for the local grid is necessary to calculate the avoided emissions. Future dynamic grid emission scenarios are complex and we apply annual averages in our analysis. Currently around 97% of the electricity production in Norway stems from hydropower (NVE, 2013). The emissions of CO_2 eq/kW h from Norwegian Hydropower have been calculated to be around 20 g CO_2 eq/kW h (low voltage) by Ecoinvent (2010). Fig. 6 shows the average monthly power balance for Norway, (production/consumption) based on hourly production and consumption statistics from 2006 to 2014 (Statnett, 2015). From these statistics we see that Norway is normally exporting electricity. However, Norway has been, on average, sensitive to the import of electricity during the spring months. Norway is connected to the European electricity grid and the transfer capacity between Norway and Europe will increase in the near future (Statnett, 2013). Graabak and Feilberg (2011) and Graabak et al. (2014) previously developed scenarios for emission profiles in 2010, 2020, 2030, 2040 and 2050, for the emissions of electricity production in Europe. One of the scenarios developed is the "ultra-green" scenario, which assumes the European electricity grid in 2050 will be nearly emission free. In this scenario, it is assumed that Norway is fully integrated with the European electricity grid. Initial emissions for this scenario are documented as 361 g CO_2 eq/kW h. We have interpolated the hourly profiles of the ultra-green scenario for each year towards 2050; the results are shown in Fig. 7. From this figure we

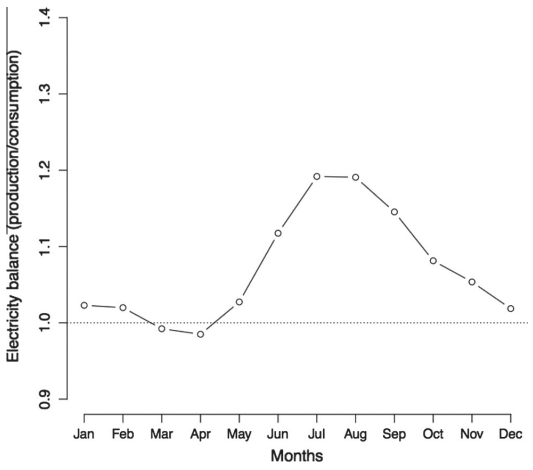

Fig. 6. Average monthly power balance for Norway, 2006–2015 (import lower than 1, export higher than 1).

Table 5
Material inventory for the roof mounting structures, given per m^2 of PV.

Material	Unit	A – Multikomfort	B – Skarpnes	C – Living Lab
Aluminium	kg	1.02	2.1	2.12
Glass fibre reinforced polyamide	kg	0.06	n/a	n/a
Polyethylene	kg	n/a	1.08	2.84
Polyurethane foam	kg	n/a	0.68	0.28
Rubber	kg	n/a	1.2	n/a
Sealing tape (alu PE)	kg	n/a	n/a	1.34
Steel	kg	0.07	0.19	n/a
Zinc plated steel	kg	0.05	n/a	n/a
Wood	m^3	n/a	0.004	0.002

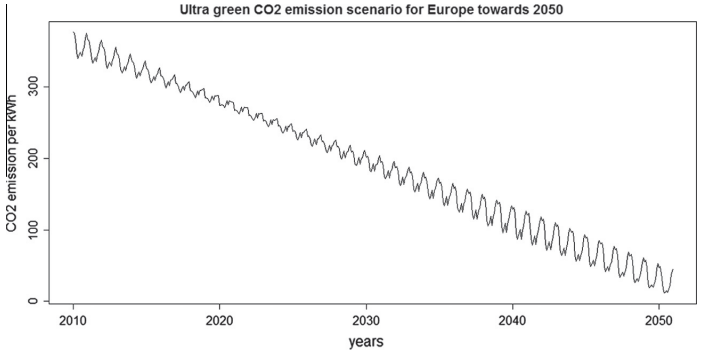

Fig. 7. Ultra-green scenario for emissions per kW h electricity in Europe towards 2050 (Graabak and Feilberg, 2011).

see seasonal variations due to the dynamics of electricity production and consumptions patterns modelled in the scenario by Graabak and Feilberg (2011). We also see the decreasing trend towards 2050. We apply this future scenario for our baseline GPBT calculations, starting from year 2015. Graabak and Feilberg (2011) also developed a simplified "worst case" scenario, the "red" scenario, with low emission reductions due to a higher demand and lower increase in renewable energy production. The "red" scenario estimates emissions from the grid to be 224 g CO_2 eq/kW h in 2050, in contrast to the ultra-green scenario which predicts an optimistic 30 g average.

Dokka et al. (2013) present a Norwegian "ZEB emission factor" that is based on averaged emissions from the "ultra-green" scenario towards 2050, resulting in emissions of 132 g CO_2 eq/kW h. For the sensitivity assessment, we include the ZEB emission factor and the "red" scenario.

2.5. System replacement scenario 2045

Within the PV industry there is a continuous development for new technologies and material use, as well as efficiencies for PV modules (NREL, 2016). For our case studies the building service lifetime is estimated to be 60 years, thus the PV system needs to be replaced once. To increase our long term perspective we include a replacement scenario for the Skarpnes system. We assume that the replaced technology for the PV modules is the same, mono-Si. Frischknecht et al. (2015) developed scenarios for life cycle emissions from future mono-Si and CdTe modules. They developed three different scenarios: "business as usual", "realistic improvement" and "optimistic improvement". The efficiency of the replaced single-Si modules is expected to be 22.9%, 25.2% and 27.6% in the different scenarios, respectively. We have chosen the realistic improvement scenario and set the module efficiency to 25.2%. The embodied emissions per m^2 of module are expected to decrease by 65%, based on Frischknecht et al. (2015). It is assumed that future modules will be produced in Asia, with initial emissions resembling the Malaysian production of SunPower modules (300 kg CO_2 eq/m^2), as documented by Fthenakis et al. (2012). This estimates replacement module emissions at 100 kg CO_2 eq/m^2. It is assumed that there are no emissions from mounting structures; the PV modules are fully integrated. Transport distances are assumed to be the same. It is assumed that the inverter, electrical installations and transport emissions are also reduced by 65%, (Frischknecht et al., 2015). The degradation profile is based on data from SunPower (SunPower Corp, 2012). The production yield calculations are further based on irradiation and efficiency. For the future scenario we calculate greenhouse gas emissions per kW h produced, and the GPBT with the ZEB-factor and "red" scenario.

3. Results

3.1. Production yield

In Fig. 8, the simulated production yield from the different systems is shown, in terms of both the annual energy production per module area, and per floor area of the

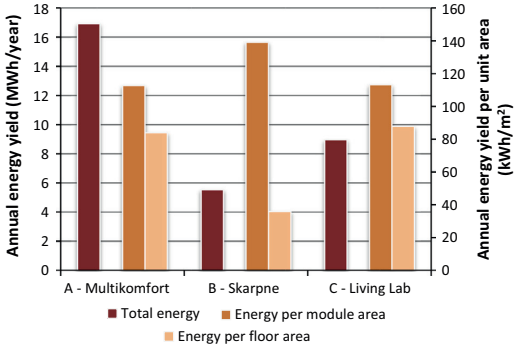

Fig. 8. Simulation results for the total annual the energy yield per year (left axis) is shown together with the annual yield normalised per square meter module area and per square meter heated floor area (right axis).

buildings. The figure also shows the total annual power yield from the systems. The yield from the Multikomfort system is the highest, since this is the largest system.

The normalised values for Multikomfort and the Living Laboratory are approximately equal, both with respect to energy yield per square meter module area and heated floor area. The irradiation (see Table 1) is slightly higher for the Living Lab than Multikomfort, but the Living Lab's system is also significantly influenced by self-shading, resulting in a similar energy output between the two buildings. Skarpnes has a smaller production in relation to heated floor area, but a higher energy production performance per square meter due to the higher efficiency of the mono-Si modules. The monthly energy yield for the first year of the three systems is shown in Fig. 9. The Skarpnes system has the highest specific output during the whole year. The energy yield from Multikomfort is slightly higher during the autumn months compared to the Living Lab, due to the difference in tilt angles.

3.2. Emissions from mounting structures

The emission loads for the different mounting structures are shown in Fig. 10 for the baseline aluminium scenario.

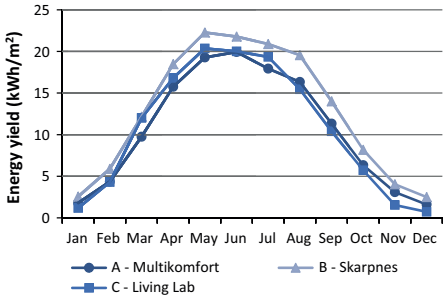

Fig. 9. Simulations results for the monthly yield for the first year energy per square meter module area.

The K2 System applied in the Multikomfort building, has less than half of the emissions compared to the Schweizer and the Renusol systems. Between Schweizer and Renusol, the difference is less significant. The Living Lab and Skarpnes mounting systems have a larger material demand, which drives up emissions compared to the simpler K2 BAPV system. BIPV systems reduce the demand for traditional roofing material, because the system replaces the roofing materials in the areas where the PV is installed. The avoided emissions associated with this will depend on the type of roofing avoided. In the Skarpnes case, cement roof tiles are used. By applying the emission factor for roof tiles from Ecoinvent, 13 kg CO_2 eq/m^2, (Ecoinvent, 2010) the Skarpnes mounting structure emissions are reduced by around 60%. The emissions for the Living Lab are reduced by approximately 3 kg CO_2 eq/m^2 due to the avoidance of bitumen felt (Ecoinvent, 2010), but still has the largest amount of GHG emissions compared to the two other cases.

3.3. Emissions per square meter module area and kW h

In Fig. 11, we present the results for the total embodied emissions allocated per square meter module area, including the sensitivity scenarios for module, transport and mounting aluminium emissions. The module emissions are the largest contributor, followed by the mounting structures and inverters. Total embodied emissions for the baseline scenario are around 150 kg CO_2 eq/m^2 for Multikomfort, 350 kg CO_2 eq/m^2 for Skarpnes and around 280 kg CO_2 eq/m^2 for the Living Lab.

From this figure, we see that the GHG emissions per kW h for the different systems range from around 30 to 120 g CO_2 eq/kW h. Emissions per kW h produced are lowest for Multikomfort. Emissions per kW h for Skarpnes and the Living Lab cases are similar. The sensitivity assessment shows that there can be a significant difference between system emissions per kW h. With emissions ranging from around 50 g to 120 g for the Skarpnes system,

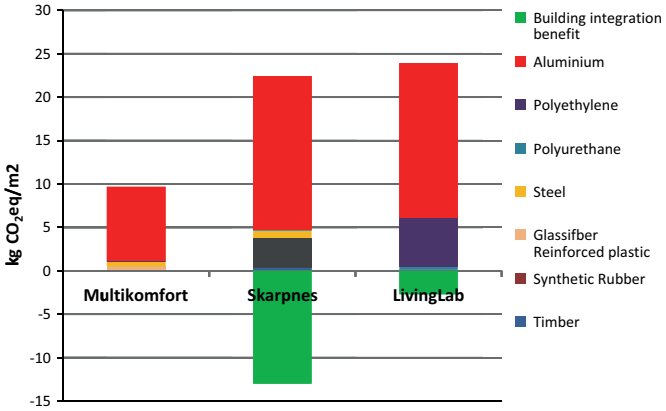

Fig. 10. Emissions in kg CO_2 eq/m^2 for the different materials for the roof mounting structures and building integration benefits.

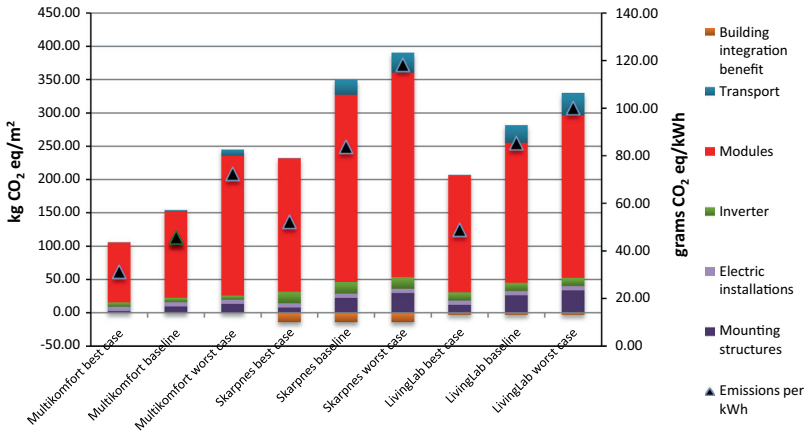

Fig. 11. Emissions loads from the systems in kg CO_2 eq/m^2 and GHG emissions per kW h produced over the service lifetime of 30 years, including best, baseline and worst case scenarios.

30–70 g for the Multikomfort system and 50–100 g for the Living Lab.

3.4. Greenhouse gas payback time (GPBT)

In Fig. 12, we show the dynamics of the emission payback scenario per square meter of module area for the different systems. The production profiles and cumulated avoided emissions are very similar for the Living Lab and Multikomfort systems, giving similar efficiencies. For the baseline scenario, embodied emissions and the "ultra-green" electricity emission scenario have payback times of around 3, 7 and 8 years for the Multikomfort, Living Lab and Skarpnes respectively. We also see from Fig. 12 that Skarpnes gives larger emissions avoided per year due to higher module efficiency. When applying the "red" scenario; the GPBT is reduced to around 6 years for both the Living Lab and Skarpnes. With the current averaged Norwegian ZEB factor of 132 g CO_2 eq/kW h, the GPBT increases to 8, 15 and 18 years respectively.

For the replacement scenario from 2045 to 2075, the emissions per kW h are around 20 g CO_2 eq/kW h for the Skarpnes system, with annual production yields of around 220 kW h/m^2. In the "ultra-green" emission scenario, the

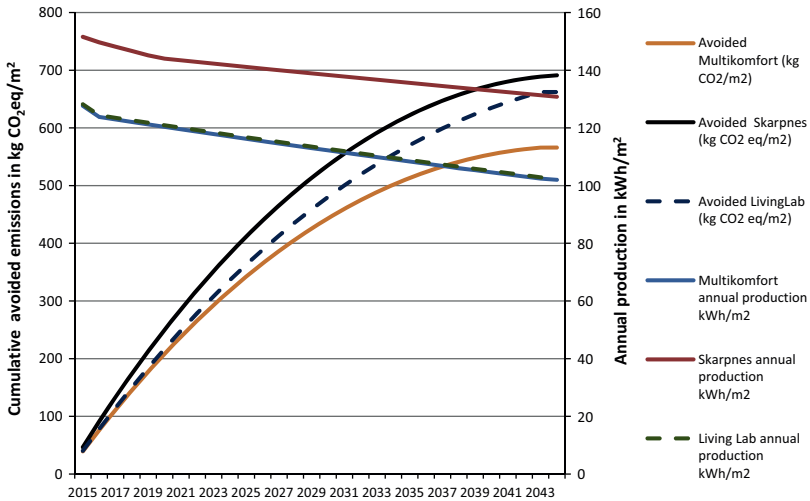

Fig. 12. Annual average productions with degradation and corresponding cumulative avoided emissions based on the "ultra-green" scenario. (For interpretation of the references to colour in this figure legend, the reader is referred to the web version of this article.)

emissions are not payed back, but for the "red" scenario emissions are payed back within two years. When using the ZEB emission factor emissions are payed back within three years.

4. Discussion

From our analysis, we see that the life cycle emissions from the PV systems analysed have lower emissions compared to fossil fuels, thus confirming previous studies (NREL, 2013). We also see that there are significant differences between the systems, with respect to emissions from the modules and mounting structures. However, we also saw a wide range of emission loads within the best and worst case scenarios, thus it is challenging to make any decisive comparative conclusions. The GPBT varies significantly according to which scenario is applied, according to the avoided emissions in the grid. In the "ultra-green" scenario we saw that it takes 8 years to payback emissions from the Skarpnes system, but in the "red" scenario we saw a GPBT of 6 years for the same system. The simplified, static ZEB emission factor scenario gave us a GPBT of up to 15 years. Emissions can be paid back if PV system emissions are lower than the grid emissions. If we consider only an isolated Norwegian hydropower grid, which would have emissions of approximately 20 g CO_2 eq/kW h, (Ecoinvent, 2010) then the PV systems emissions are not payed back. This uncertainty emphasises the need for careful consideration, between the grid interaction and related system boundaries, when choosing energy systems for buildings. Even though module emissions represent the largest fraction of emissions from PV systems, the mounting structures also contribute significantly. From our analysis we saw that with proper integration of PV systems, we can reduce the use of roofing materials, and thus reduce building material emissions. With large-scale implementation of solar home systems, mounting emissions become more significant, even though they seem small when viewed on an individual building basis. Therefore, minimizing mounting structure emissions with proper integration is beneficial. Based on our simplified future emission scenario, emissions from electricity, from PV systems are likely to be significantly reduced. At the same time, a payback calculation becomes more irrelevant in a scenario where the grid becomes nearly emission free.

Emissions from the SunPower modules have been thoroughly documented, whilst for the REC modules, emission data was not available. For the Multikomfort case, emissions from the module scenarios were low, due to the use of reused cells in the ITS modules. The allocation procedures for emission burdens, when using secondary or waste material, can be challenging. We therefore made a simplification, in that there were no emission loads from the reused cells, which is debatable. Comparing different life cycle studies is challenging, as different methods and reporting formats are used by different authors, thus reducing comparability. When installing a PV system, it is preferable to have proper knowledge of the emission burdens of the installed modules. In some cases, we encountered difficulties in gaining specific data from producers, a challenge that may be resolved in the future. According to Fraunhofer (2012) the end of life benefits of recycling, especially glass and aluminium can have significant influence on the overall life cycle impact of PV modules. These potential benefits have not been included.

With regards to the battery storage, the Multikomfort system is more self-sufficient and possibly gains a better economic output. We have not included the impact from the batteries. This is an aspect that requires further investigation. We have limited our analysis to GHG emissions, mainly due to the fact that the pilot case studies have focused on a zero emission GHG balance. Looking also into the primary energy balance of the different systems would be of interest. Nevertheless, previous studies have shown that cumulative energy demand and greenhouse gas emissions often correlate (Huijbregts et al., 2006).

Service lifetime is an important parameter for emission burden accounting; in a scenario with a shorter service lifetime, emissions per kW h are increased. The replacement of possible defect modules has not been taken into account, which is also an aspect that could increase service lifetime emissions.

Currently, there is a lack of guidelines for good BIPV practice in Norway. In cold climates, shading caused by snow, needs to be considered. How much this influences a system is difficult to know, without site-specific measurement. None of the systems are optimally oriented for their location, which would be around 40–45° and south facing (annual optimisation). Optimal orientation would have resulted in lower emissions per kW h.

From historical statistics of the Norwegian export profile for electricity, it can be argued that producing electricity in the spring months gives an extra benefit for the Norwegian electricity grid. Production in the summer months is considered to have a lesser value, as it could lead to lower prices. With the high availability of hydropower in Norway, one could argue that PV system installations are not necessary. As a result, PV systems should be prioritised in areas with higher solar irradiation and electricity grids based on fossil energy. In contrast, a large fraction of Europe's electricity is produced from fossil fuels, emphasising a general need for the increased electricity production from renewable energy sources, and therein PV systems (Eurostat, 2015).

From the "ultra-green" emission scenario in Fig. 7, and the Norwegian export–import sensitivity analysis in Fig. 6, we get a picture of the seasonal grid production and emission sensitivities. Essentially, the emissions are higher in the winter and lower in the summer. As an area for further study, it would be interesting to include a month-by-month emission payback profile of the systems, combining energy demand and generation on an hourly basis. There are plans to measure the energy outputs of the systems, which will bring insight into the real operational performance of the PV systems in a Norwegian context.

5. Conclusions

We have looked at the emissions of GHG and GPBT for three different PV systems installed in Norwegian Zero Emission Buildings for an estimated service lifetime of 30 years. These systems are referred to as the Multikomfort, Skarpnes and Living Lab. We have included a simplified future scenario, whereby one of the PV systems is replaced after 30 years. Total embodied emissions, allocated per square meter of module area, for the baseline scenario are around 150 kg CO_2 eq/m^2 for Multikomfort, 350 kg CO_2 eq/m^2 for Skarpnes and around 280 kg CO_2 eq/m^2 for the Living Lab. The simplest mounting system showed emission of around 10 kg CO_2/m^2, whilst the other, more complex systems showed emissions from around 20 to 25 kg CO_2 eq/m^2. A building integration benefit, where roof tiles were replaced with PV modules, reduced mounting system emissions by around 60%. We also see that module emissions have the largest proportion of emissions from the three different systems, stressing the need for reliable data on PV module production. Emissions per kW h produced, showed that the lowest emissions originated from the Multikomfort system which had approximately 45 g CO_2 eq/kW h, and around 80–85 g for the other two systems. Emissions from the Multikomfort system are lowest, due to the use of reused cells in the modules, combined with the large dimension of the system, and the simple roof mounting structure. The sensitivity analysis showed that there are large variations in emissions, with the total span from around 30 to 120 g CO_2 eq/kW h. The GPBT is very sensitive to the grid scenario for emissions. The baseline scenario "ultra-green", showed emission payback times of 3, 7 and 8 years respectively. The GBPT is decreased to around 6 years, if the "red" scenario for emissions from the grid is used for the Living Lab and Skarpnes cases. A constant emission factor, namely the Norwegian "ZEB factor" of 132 g CO_2 eq/kW h showed payback times of 8, 15 and 18 years for the three systems. If we assume Norwegian hydropower emissions of 20 g CO_2 eq/kW h, as an average for local grid emissions, then the modules do not payback emissions within their 30 year service lifetime. Furthermore, when looking 30 years into the future, the emissions from the Skarpnes system are likely to be reduced from around 80 to 20 g CO_2 eq/kW h.

Acknowledgements

The authors gratefully acknowledge the support from the Research Council of Norway, several partners through the Research Centre on Zero Emission Buildings (ZEB) and the research project Building Integrated Photovoltaics for Norway (BIPV Norway). Special thanks to Harald Amundsen, Project Manager at Brødrene Dahl in Norway who provided details on the Multikomfort PV system. Also thanks to Roald Rasmussen at Skanska in Norway for providing details on the Skarpnes PV system.

References

Alsema, E., de Wild-Scholten, M., 2006. Environmental impacts of crystalline silicon photovoltaic module production. In: 13th CIRP International Conference on Life cycle Engineering, Leuven, Belgium.

Andrews, R.W., Pollard, A., Pearce, J.M., 2013. The effects of snowfall on solar photovoltaic performance. Sol. Energy 92, 84–97.

Beccali, M., Cellura, M., Finocchiaro, P., Guarino, F., Longo, S., Nocke, B., 2012. Life cycle assessment performance comparison of small solar thermal cooling systems with conventional plants assisted with photovoltaics. Energy Procedia 30, 893–903.

Beccali, M., Cellura, M., Finocchiaro, P., Guarino, F., Longo, S., Nocke, B., 2014. Life cycle performance assessment of small solar thermal cooling systems and conventional plants assisted with photovoltaics. Sol. Energy 104, 93–102.

Bergesen, J.D., Heath, G.A., Gibon, T., Suh, S., 2014. Thin-film photovoltaic power generation offers decreasing greenhouse gas emissions and increasing environmental co-benefits in the long term. Environ. Sci. Technol. 48, 9834–9843.

Reich-Weiser, C., Dornfeld, D., Horne, S., 2008. Greenhouse gas return on investment: a new metric for energy technology. Green Manuf. Sustain. Manuf. Partnersh.

Cabeza, L.F., Rincón, L., Vilariño, V., Pérez, G., Castell, A., 2014. Life cycle assessment (LCA) and life cycle energy analysis (LCEA) of buildings and the building sector: a review. Renew. Sustain. Energy Rev. 29, 394–416.

Cellura, M., Guarino, F., Longo, S., Mistretta, M., 2014. Energy life-cycle approach in net zero energy buildings balance: operation and embodied energy of an Italian case study. Energy Build. 72, 371–381.

Chau, C., Leung, T., Ng, W., 2015. A review on life cycle assessment, life cycle energy assessment and life cycle carbon emissions assessment on buildings. Appl. Energy 143, 395–413.

de Wild-Scholten, M., 2013. Certificate of Simplified Carbon Foot Print of Innotech Solar PV Modules. SmartGreenScans.

Dokka, T.H., Berggren, B., Lassen, N., 2015. Comparison of Five Zero and Plus Energy Projects in Sweden and Norway. A Technical Review. Passivhus Norden, Sustainable Cities and Buildings, Cobenhagen, Denmark.

Dokka, T.H., Sartori, I., Tyholt, M., Lien, K., Byskov Lindberg, K., 2013. A Norwegian Zero Emission Building Definition. Passivhus Norden, Gothenburg, Sweden.

Ecoinvent, 2010. Ecoincent Database v. 2.2. Swiss Centre for Life Cycle Inventories, Zürich, Switzerland. <www.ecoinvent.org>.

Ecoinvent, 2013. Ecoinvent Database Version 3.1. In: Centre, E. (Ed.). Zurich, Switzerland. <www.ecoinvent.org>.

European Parliament, 2010. Directive 2010/31/EU of the European Parliament and of the Council of 19 May 2010 on the Energy Performance of Buildings. Directive 2010/31/EU. Brussels.

Eurostat, 2015. Environmental Data Centre on Natural Resources. European Commision. <http://ec.europa.eu/eurostat/web/environmental-data-centre-on-natural-resources/natural-resources/energy-resources>.

Fraunhofer, 2012. Executive Summary: Life Cycle Assessment (LCA) screening of the Maltha recycling process for Si-PV modules. IPB Department Life Cycle Engineering (GaBi).

Frischknecht, R., Itten, R., Wyss, F., Blanc, I., Heath, G., Raugei, M., Sinha, P., Wade, A., 2015. Life cycle assessment of future photovoltaic electricity production from residential-scale systems operated in Europe. Subtask 2.0 "LCA", IEA-PVPS Task 12.

Frischknecht, R., Jungbluth, N., Althaus, H.J., Doka, G., Heck, T., Hellweg, S., Hischier, R., Nemecek, T., Rebitzer, G., Spielmann, M., Wernet, G., 2007. Overview and Methodology Ecoinvent Report No. 1. Swiss Centre for Life Cycle Inventories, Dübendorf.

Fthenakis, V., Betita, R., Shields, M., Vinje, R., Blunden, J., 2012. Life cycle analysis of high-performance monocrystalline silicon photovoltaic systems: energy payback times and net energy production

value. In: 27th European Photovoltaic Solar Energy Conference and Exhibition.
Fthenakis, V., Frischknecht, R., Raugei, M., Kim, H., Alsema, E., Held, M., de Wild-Scholten, M., 2011. Methodology Guidelines on Life Cycle Assessment of Photovoltaic Electricity: IEA PVPS Task 12. International Energy Agency.
Fthenakis, V.M., Kim, H.C., 2011. Photovoltaics: life-cycle analyses. Sol. Energy 85, 1609–1628.
Georges, L., Haase, M., Wiberg, A. Houlihan, Kristjansdottir, T., Risholt, B., 2015. Life cycle emissions analysis of two nZEB concepts. Build. Res. Inf. 43, 82–93.
Glöckner, R., de Wild-Scholten, M., 2012. Energy payback time and carbon footprint of Elkem Solar Silicon®. In: EU PVSEC Proceedings. Frankfurt, Germany.
Goia, F., Finocchiaro, L., Gustavsen, A., 2015. The ZEB Living Laboratory at the Norwegian University of Science and Technology: A Zero Emission House for Engineering and Social Science Experiments. Passivhus Norden Conference, Sustainable Cities and Buildings, Cobenhagen, Denmark.
Good, C., Kristjansdottír, T., Wiberg, A. Houlihan, Georges, L., Hestnes, A.G., 2016. Influence of PV technology and system design on the emission balance of a net zero emission building concept. Sol. Energy 130, 89–100.
Graabak, I., Bakken, B.H., Feilberg, N., 2014. Zero emission building and conversion factors between electricity consumption and emissions of greenhouse gases in a long term perspective. Environ. Clim. Technol. 13, 12–19.
Graabak, I., Feilberg, N., 2011. CO_2 emission in different scenarios of electricity generation in Europe (Technical Report). SINTEF Energy Research.
Green, M.A., 1992. Solar Cells: Operating Principles, Technology and System Applications. University of New South Wales, Kensington.
Hui, S.C., 2010. Zero energy and zero carbon buildings: myths and facts. In: Proceedings of the International Conference on Intelligent Systems: Intelligent Infrastructure and Buildings, pp. 15–25.
Huijbregts, M.A.J., Rombouts, L., Hellweg, S., Frischknecht, R., Hendriks, J., van de Meent, D., 2006. Is cumulative fossil energy demand a useful indicator for the environmental performance of products? Environ. Sci. Technol. 40, 641–648.
IEA, 2013. IEA Online Data Services. Available at: <http://data.iea.org/ieastore/statslisting.asp>.
Inman, M., Wiberg, A. Houlihan, 2015. Life Cycle GHG Emissions of Material Use in the Living Laboratory Norway. SINTEF Building and Infrastructure.
Innotech Solar, 2013. Warranty Conditions. Innotech Solar. August 2013.
Innotech Solar, 2015. Green Energy (Online). Innotech Solar webpage. Available: <http://www.innotechsolar.com/en/company/green-energy.html> (accessed 27 May 2015).
Institute for Energy – Renewable Energy Unit, 2013. Photovoltaic Geographical Information System (PVGIS) (Online). European Commission, Joint Research Centre (accessed 31 January 2013).
IPCC, 2007. In: Solomon, S., Qin, D., Manning, M., Marquis, M., Averyt, K.B., Tignor, M., Miller, J. (Eds.), Climate Change, 2007. The Physical Science Basis, Fourth Assessment Report of the Intergovernmental Panel on Climate Change (IPCC). Cambridge University Press, Cambridge (United Kingdom).
IPCC, 2013. In: Stochker, T.F., Qin, D., Plattner, G.-K., Tignor, M., Allen, S.K., Boschung, J., Nauels, A., Xia, Y., Bex, V., Midgley, P.M. (Eds.), Climate Change 2013: The Physical Science Basis. Contribution of Working Group I to the Fifth Assessment Report of the Intergovernmental Panel on Climate Change.
ISE, 2014. Photovoltaics Report. Technical Report MSU-CSE-00-2. Institute for Solar Energy Systems, Freiburg, Germany.
ISO, 2006. Environmental Management – Life Cycle Assessment – Principles and Framework. International Organization for Standardization.
ITS, 2012. CO_2 Study on ITS-Modules: 80% lower CO_2 Emissions. Innotech Solar.
Jelle, B.P., Breivik, C., Røkenes, H. Drolsum, 2012. Building integrated photovoltaic products: a state-of-the-art review and future research opportunities. Sol. Energy Mater. Sol. Cells 100, 69–96.
Jungbluth, N., 2005. Life cycle assessment of crystalline photovoltaics in the swiss ecoinvent database. Prog. Photovoltaics Res. Appl. 13, 429–446.
Jungbluth, N., Stucki, M., Flury, K., Frischknecht, R., Büsser, S., 2012. Life Cycle Inventories of Photovoltaics. ESU-Services Ltd on behalf of the Swiss Federal Office of Energy SFO.
Jungbluth, N., Stucki, M., Frischknecht, R., 2009. Photovoltaics, Contribution to Ecoinvent Version 2.1. Technical Report Ecoinvent Report No 6-XII. Swiss Centre for Life Cycle Inventories, Dubendorf, Switzerland.
Jungbluth, N., Tuchschmid, M., Dones, R., 2007. Photovoltaics. Sachbilanzen von Energiesystemen: Grundlagen für den ökologischen Vergleich von Energiesystemen und den Einbezug von Energiesystemen in Ökobilanzen für die Schweiz. Ecoinvent report No. 6-XII. Swiss Centre for Life Cycle Inventories, Dübendorf, CH.
Kristjansdottir, T., Andresen, I., Amundsen, H., Good, C., 2016. Design phase calculation of greenhouse gas emissions for a Zero emission residential pilot building. SBE 16 – International Conference on Sustainable Built Environment, Hamburg, Germany.
Mann, S.A., de Wild-Scholten, M.J., Fthenakis, V.M., van Sark, W.G.J. H.M., Sinke, W.C., 2014. The energy payback time of advanced crystalline silicon PV modules in 2020: a prospective study. Prog. Photovoltaics Res. Appl. 22, 1180–1194.
Marion, B., Adelstein, J., Boyle, K., Hayden, H., Hammond, B., Fletcher, T., Canada, B., Narang, D., Shugar, D., Wenger, H., Kimber, A., Mitchell, L., Rich, G., Townsend, G., 2005. Performance parameters for grid-connected PV systems. IEEE Photovoltaics Specialists Conference and Exhibition Lake Buena Vista. National Renewable Energy Laboratory, Florida.
Meteotest, 2009. Meteonorm Database.
Nord, N., Qvistgaard, L.H., Cao, G., 2016. Identifying key design parameters of the integrated energy system for a residential zero emission building in Norway. Renewable Energy 87, 1076–1087.
NREL, 2012. Life cycle greenhouse gas emissions from solar photovoltaics. Technical Report NREL/FS-6A20-56487. National Renewable Energy Laboratory, Denver, Colorado, US.
NREL, 2013. Life Cycle Greenhouse Gas Emissions from Electricity Generation. National Renewable Energy Laboratory, Denver, Colarado.
NREL, 2016. Research Cell Efficiency Records. National Center for Photovoltaics at the National Renewable Energy Laboratory, U.S Department of Energy.
NVE, 2013. Production and Consumption of Electric Energy in 2012 Energy in Norway. Norwegian Water Resources and Energy Directorate. <http://www.nve.no/Global/Energi/Analyser/Energi%20i%20Norge%20folder/FOLDE2013.pdf>.
Peng, J., Lu, L., Yang, H., 2013. Review on life cycle assessment of energy payback and greenhouse gas emission of solar photovoltaic systems. Renew. Sustain. Energy Rev. 19, 255–274.
Peterson, K., Torcellini, P., Grant, R., Taylor, C., Punjabi, S., Diamond, R., Colker, R., Moy, G., Kennett, E., 2015. A Common Definition for Zero Energy Buildings. U.S Department of energy, Energy Efficiency and Renewable Energy.
Pre Consultants, 2012. SimaPro Version 8.0.5. Netherland.
PVSYST SA, 2011. In: Mermoud, A. (Ed.), PV-Syst 5.73. Photovoltaic System Software, Geneva, U.O. (5.73).
Ramesh, T., Prakash, R., Shukla, K., 2010. Life cycle energy analysis of buildings: an overview. Energy Build. 42, 1592–1600.
REC, 2013. High performance solar modules REC peak energy series. In: Group, R. (Ed.). <www.recgroup.com>.
REC Group, 2013. Real Life, Real Security (Warranty Factsheet). REC Group.
Renusol, 2010a. Renusol Solar Mounting Systems: Installation Guide Intersole SE, Germany.

Renusol, 2010b. Renusol Solar Mounting Systems: Intersole SE In-Roof System.

Renusole, 2015. Renusole Solar Mounting systems, Installation Manual Intersole SE and Picture Manual Intersole SE (Online). <http://www.renusol.com/en/download.html> (accessed June 2015).

Saint-Gobain, 2015. Saint-Gobain Multi-Comfort Concept (Online). <http://www.isover.co.uk/saint-gobain-multi-comfort> (accessed January 2015).

Sartori, I., Napolitano, A., Voss, K., 2012. Net zero energy buildings: a consistent definition framework. Energy Build. 48, 220–232.

Schweizer, 2015. Installation Manual Solrif® XL/D (Online). <https://www.schweizer-metallbau.ch/en/produkte/photovoltaik-systems/technical-documents.html> (accessed June 2015).

SeaRates, 2015. SeaRates LP. <www.Searates.com>.

Solbes, 2013. ZEB Living Lab Takintegrert PV-system. Tilbud for leveranse og installasjon. (Roof integrated PV system, offer on deliverables and installations).

Statnett, 2013. National plan for the next generation main grid. Statnett. <http://www.statnett.no/Global/Dokumenter/Prosjekter/Nettutviklingsplan%202013/Statnett-Nettutviklingsplan2013-engelsk_03korr.pdf>.

Statnett, 2015. Power Situation (Online). <http://www.statnett.no/Drift-og-marked/Kraftmarkedet/Kraftsituasjonen/>.

SunPower Corp, 2012. SunPower Limited Product and Power Warranty for PV Modules. SunPower Corp.

SUPSI, 2015. Building Integrated Photovoltaic Systems (Online). The University of Applied Sciences and Arts of Southern Switzerland. <http://www.bipv.ch/index.php/en/about-en-top> (accessed June 2015).

Systems, K., 2015. Brochure material, installation manual and image brochure (Online). <http://www.k2-systems.uk.com/downloads/product-information.html> (accessed June 2015).

Voss, K., Musall, E., 2011. Net Zero Energy Buildings, Germany.

Weidema, B.P., Bauer, C., Hischier, R., Mutel, C., Nemecek, T., Reinhard, J., Vadenbo, C., Wernet, G., 2013. Data Quality Guideline for the Ecoinvent Database Version 3. Swiss Centre for Life Cycle Inventories, St. Gallen.

Wiberg, A.H., Georges, L., Dokka, T.H., Haase, M., Time, B., Lien, A. G., Mellegård, S., Maltha, M., 2014. A net zero emission concept analysis of a single-family house. Energy Build. 74, 101–110.

de Wild-Scholten, M., 2013. Certificate of Simplified Carbon Foot Print of Innotech Solar PV Modules. SmartGreenScans.

Yue, D., You, F., Darling, S.B., 2014. Domestic and overseas manufacturing scenarios of silicon-based photovoltaics: life cycle energy and environmental comparative analysis. Sol. Energy 105, 669–678.